THE EFFECTS OF SUCROSE AND SORBITOL ON CEMENT HYDRATION — APPLICATIONS TO CEMENT-STABILIZATION OF METAL WASTE

By

LINGHONG ZHANG

A thesis

presented to Lakehead University

in fulfillment of the

thesis requirement for the degree of

Masters of Science

in

Environmental Engineering

Thunder Bay, Ontario, Canada, 2007

ProQuest Number: 10611948

ProQuest 10611948

ABSTRACT

Cement-based stabilization/solidification (S/S) is a widely used technique to treat industrial wastes containing toxic metal ions before land disposal. To prevent the fast setting of the treated waste during its transportation from the treatment plant to the disposal site, small amounts of sucrose or sorbitol can be added to slow down the speed of cement setting, thus adding flexibility to the handling of the treated waste. However, sucrose and sorbitol may also affect the leachability of the metal ions present in the treated waste because of their ability to alter the microstructure of hydrated cement pastes.

In the first stage of this research, various types of cements (pure tricalcium silicate [C_3S], white Portland cement [WPC] and ordinary Portland cement [OPC]), which represent systems of increasing compositional complexity, were investigated to better understand the contribution of individual cement components to the properties of hydrated pastes. The degree of hydration was measured as a function of curing time by SEM grey level analysis and loss-on-ignition testing. The hydration rate was found to decrease as C_3S > WPC > OPC, correlating with the relative content of C_3S and tricalcium aluminate (C_3A). The fraction of non-evaporable water in fully hydrated OPC and WPC was $0.234_9 \pm 0.005_7$ and $0.208_6 \pm 0.003_2$, respectively. The microstructure of hydrated C_3S was characterized by two prominent features: 1) large zones of unhydrated C_3S particles embedded in dense calcium hydroxide (CH); and 2) porous zones in which calcium silicate hydrate (CSH) was the only hydration product. CH-rich zones were also observed in hydrated OPC and WPC, but they were smaller and became less distinct as

hydration progressed. No large porous zones were present in hydrated OPC and WPC, which exhibited much lower overall porosity than C_3S.

In the second stage of this research, the effects of a small amount of sucrose (0.037 or 0.15 wt%) or sorbitol (0.40 wt%) on the hydration and microstructure OPC, WPC and C_3S were investigated as a function of curing time. For the above concentrations of sucrose or sorbitol, the retardation period was longer in OPC (3-7 days) than in WPC (1-3 days). Calcium hydroxide appeared before CSH at the earliest stages of hydration, and eventually formed into dense CH-rich islands that contained unhydrated grains of C_3S. These islands were especially prominent in the hydrated C_3S. The delaying effects with the above concentrations of sucrose or sorbitol were only temporary, except for 0.15% sucrose, which seemed to inhibit the hydration of C_3S permanently. Due to adsorption on C_3A, the same addition of sucrose caused less retardation on OPC and WPC than on C_3S. By contrast, sorbitol had a more consistent impact on all the samples. After 56 days of curing, OPC and WPC consistently exceeded 77% degree of hydration and 27.6 MPa (4000 psi) unconfined compressive strength. OPC which contained 0.40 wt% sorbitol had significantly higher strength and degree of hydration than all other OPC samples at 56 days.

In the last stage of this research, the effects of sucrose or sorbitol addition on the hydration, unconfined compressive strength and leachability of Portland cement pastes containing 1% Pb and 1% Zn were studied as a function of time. Whereas Pb and Zn were found to shorten the time to achieve maximum hydration of Portland cement, the combination of these metals with 0.15 wt% sucrose or 0.40 wt% sorbitol retarded the setting of cement by at least 7 days and 28 days, respectively, without affecting the

strength at 56 days. The leachability of Pb and Zn evaluated by the TCLP 1311 protocol at 56 and 71 days was slightly reduced or unchanged by the addition of sucrose or sorbitol. SEM-EDS and XRD analyses revealed that ettringite precipitation was favored whereas the formation of CSH gel, which accounts for most of the strength of hydrated cement, was delayed in cement pastes containing both metals and sucrose or sorbitol. These results indicate that controlled additions of sucrose or sorbitol can add flexibility to the handling of cement-treated metal waste, particularly when it needs to be transported between the treatment plant and the disposal site, without affecting its long term performance.

ACKNOWLEDGEMENTS

TABLE OF CONTENTS

LIST OF TABLES

LIST OF FIGURES

CHAPTER 1

INTRODUCTION

1.1. Background

Stabilization/solidification (S/S) is a widely used technique to treat industrial

wastes containing toxic metal ions before land disposal [1-3][1]. Stabilization refers to the

process of converting hazardous contaminants into less soluble, less mobile, and less

toxic forms through chemical reactions. Solidification focuses on improving the physical

stability of the treated wastes, such as by increasing compressive strength and decreasing

permeability [2, 3]. Ordinary Portland cement (OPC) is often employed as the

solidification medium owing to its wide availability, high strength, and well documented

performance [2]. Cement-based S/S can be applied to the treatment of natrojarosite

sludge produced by zinc refineries [4], mine tailings for making pastes backfill [5] and

some brownfield sites, such as former wood preserving facilities, manufactured gas plants,

and electric generating stations [6]. Sometimes, the treated wastes need to be transported

from the treatment plant to the disposal site at some distance. During the transportation

(e.g., by truck), the normal setting process of cement can be too rapid and cause

operational difficulties. In these situations, controlling the setting rate with chemical

retarders, such as sugars and sugar derivatives, is desirable. On the other hand, sugars and

sugar derivatives may also influence the microstructure of the treated waste and the

leachability of metals bound to the cement matrix.

---

[1] References appear at the end of each chapter.

This Chapter begins with some basic information on Portland cement, including its composition, its hydration reactions and products, the comparison of different types of Portland cement, and the mechanisms by which toxic metal wastes can be immobilized in Portland cement matrix. Next, a brief review of the current state of knowledge on how sugars and sugar derivatives interfere with cement hydration reactions is presented, and various other admixtures to cement-based S/S process are mentioned. This is followed by an identification of knowledge gaps and research opportunities. Lastly, the research objectives and the organization of the thesis are presented.

1.1.1. Composition of Ordinary Portland Cement Clinker

OPC is a basic construction material that is widely used in the daily life of human beings. It has five main components: tricalcium silicate (C_3S); dicalcium silicate (C_2S); tricalcium aluminate (C_3A); tetracalcium aluminoferrite (C_4AF); and gypsum ($C\bar{S}H_2$). The typical composition of OPC is listed in Table 1-1. Minor constituents of Portland cement include magnesia, free lime, and alkalis [7-10].

Table 1-1 Typical composition of ordinary Portland cement [9]

	Chemical Formula	Shorthand Notation	Weight Percentage
Tricalcium silicate	$3CaO \cdot SiO_2$	C_3S	40-63
Dicalcium silicate	$2CaO \cdot SiO_2$	C_2S	9-31
Tricalcium aluminate	$3CaO \cdot Al_2O_3$	C_3A	6-14
Tetracalcium aluminoferrite	$4CaO \cdot Al_2O_3 \cdot Fe_2O_3$	C_4AF	5-13
Gypsum	$CaSO_4 \cdot 2H_2O$	$C\bar{S}H_2$	2-10 [11]

1.1.2. Hydration of Portland Cement

C_3S and C_2S react exothermically with water to form calcium hydroxide (CH) and calcium silicate hydrate (CSH). CH crystallizes in the free pore spaces; it has definite $Ca(OH)_2$ stoichiometry, but its crystal morphology varies with the available space, admixtures and temperature [10, 12, 13]. By comparison, CSH is an amorphous gel and does not have a fixed composition. It is the main product of cement hydration, making up one-half to two-thirds of the volume of the hydrated paste, and thus provides most of the product's strength [10]. The specific surface area of CSH, measured by physical adsorption of water vapour on freeze-dried CSH paste, ranges from 250 to 450 m^2/g, which is three orders of magnitude higher than that of unhydrated cement [10]. Due to its large surface area, CSH has the potential to adsorb toxic metal ions present in the waste [14]. In addition, coprecipitation [15] and the formation of metallosilicates [16-18] can also take place on CSH. Although C_3S and C_2S react with water to form the same hydration products, C_2S hydrates more slowly and thus contributes more to long-term strength development [7-10].

Figure 1-1 depicts the rate of heat evolution during the hydration of C_3S. As the heat generation is proportional to the amount of reaction, this calorimetric curve shows the various stages in the hydration of C_3S [10]. Stage 1 is the period of rapid heat evolution during which calcium and hydroxide ions are rapidly dissolved from the surface of C_3S grains, resulting in a highly alkaline solution. A pseudo-C_3S structure, deficient in calcium with partially hydrolyzed orthosilicate groups, forms an outer layer around the unhydrated C_3S [19]. Stage 2 is the dormant period in which hydration

becomes self-retarding and slows down. Thin films of CSH form around the C_3S particles, probably owing to polymerization of the hydrolyzed silicate groups and the rearrangement of the "hydrated" layer [19]. Once the concentrations of calcium and hydroxide ions reach critical values, CH crystallizes from solution and CSH precipitates at the surface of C_3S grains. This is Stage 3: the acceleration period. As more and more hydration products form, they accumulate around the unhydrated grains and act as barriers that hinder the contact between C_3S and water. Hydration becomes a diffusion-controlled process, thus leading to Stage 4: the deceleration period. In Stage 5, hydration continues at a very slow rate and is accompanied by an extremely low rate of heat generation.
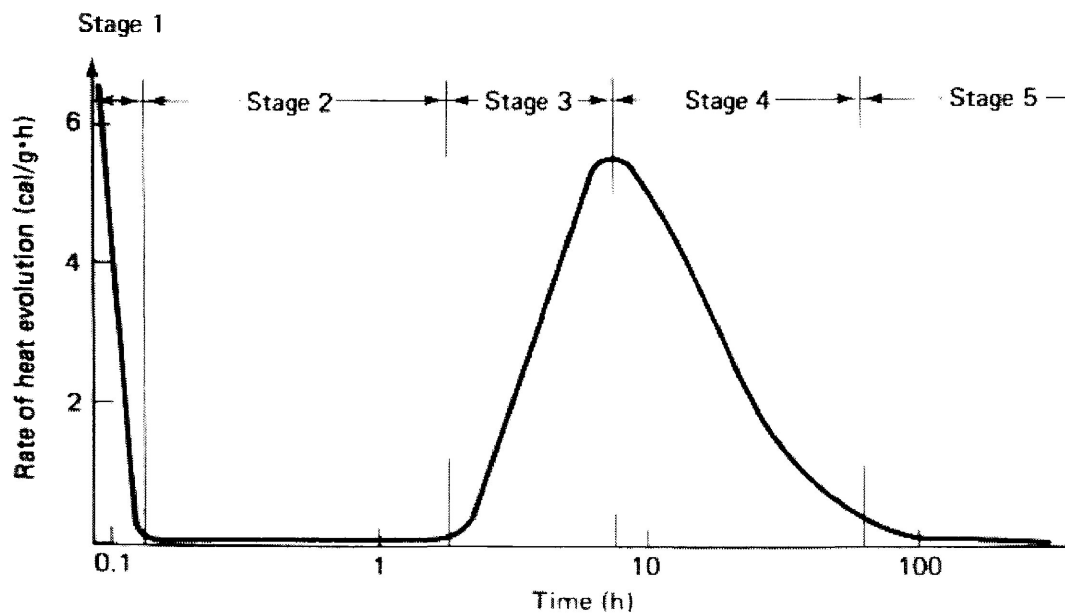
Figure 1-1 Rate of heat evolution during the hydration of tricalcium silicate [7, 10].

Tricalcium aluminate is another important component of unhydrated cement clinker. C_3A is a reactive compound that, once contacted with water, forms calcium aluminate hydrates which, in turn, convert rapidly to hydrogarnet [10]. This series of reactions can lead to flash-setting, which is undesirable because of the loss of some early

strength [10]. To solve this problem, a small amount of gypsum is added to the OPC [7, 8, 10]. C_3A reacts with gypsum and water to form crystals of ettringite ($C_6A\bar{S}_3H_{32}$) or, if the sulfate availability is limited, monosulfate ($C_4A\bar{S}H_{12}$) [7, 8, 10]. The aluminum in these compounds is often substituted by Fe or other heteroatoms [8, 10]. Because of their definite crystal structure, ion substitution is the major mechanism for metal ion stabilization in ettringite and monosulfate [14].

The presence of tetracalcium aluminoferrite is the main reason for the grey color of OPC. C_4AF undergoes similar hydration reactions as C_3A, although they occur more slowly. The presence of C_4AF allows the clinker mixture to be liquid at peak kiln processing temperature, thus facilitating the formation of the desired silicate phases [20]. It does not contribute significantly to the overall properties of OPC [8, 10].

1.1.3. Types of Portland Cement

There are five ASTM classifications of Portland cement [21]. The corresponding chemical compositions and properties are listed in Table 1-2.

OPC is Type I, which is the general purpose cement used for most construction [10, 22]. Type III cement is similar to Type I, except for a higher C_3S content, lower C_2S content and finer particle size which, together, make it faster setting and yield higher early strength [10, 22].

Type IV Portland cement has much more C_2S than C_3S. As a result, initial heat production during hydration is low (as is, therefore, the risk of thermal cracking), and strength develops more slowly than in other cements [10, 22]. The most important feature

of Type V cement is its high resistance to sulfate attack, which results from its high ratio of C_4AF to C_3A [10, 22]. The susceptibility to sulfate attack is correlated with the C_3A content, since sulfate can convert monosulfate into secondary ettringite, which causes volume expansion, generates internal stresses, and results in cracking ultimately [10]. By comparison, Type II cement is characterized both by moderate sulfate resistance and moderate heat generation during hydration.

Table 1-2 Typical chemical composition (wt.%) and properties of Portland cement (ASTM Types I to V) [10]

Type	I	II	III	IV	V
C_3S	50	45	60	25	40
C_2S	25	30	15	50	40
C_3A	12	7	10	5	4
C_4AF	8	12	8	12	10
CSH_2	5			4	4
Fineness (Blaine, m^2/kg)	350	350	450	300	350
Compressive strength [1 day, MPa]	6.89	6.21	13.8	3.10	6.21
Heat of hydration (7 days, J/g)	330	250	500	210	250

1.1.3.1. White Portland Cement

White Portland cement (WPC) has a much lower transition metal content (iron and manganese especially) than OPC and, thus, has a brilliant white appearance that is advantageous for many decorative/reflective applications [23]. The maximum specified

iron oxide content in WPC is 0.50%, whereas in OPC it nearly always exceeds 2%. Various pigments or coloured aggregates can be added to WPC to cover a broad colour spectrum and meet with specific aesthetic requirements. WPC is employed in city streetscapes, statues, towers, bridge parapets and reflective flooring [24]. The manufacture of WPC otherwise conforms to the above ASTM standards [21], with Type I and Type III being the most common forms [25].

Table 1-3 compares the average composition of Type I WPC with that of Type I OPC. The C_2S and C_3A levels are similar. WPC contains considerably less C_4AF, however, with C_3S making up the difference in mass. Thus, the composition of WPC can be considered to be intermediate between that of OPC and pure C_3S.

1.1.4. Set-Retardation in Portland Cement by Sugars and Sugar Derivatives

Many chemical admixtures have the ability to slow down the hydration reactions [19, 26-36]. Various sugars, including glucose, lactose, maltose, cellobiose, α-methyl glucoside, sucrose, raffinose and α,α-trehalose, have known set-retardation capacity [19, 26, 29, 30, 32-35], as do the sugar-derivatives arabitol, sorbitol and xylitol [37].

Sucrose, the main component of table sugar, is one of the most effective and commonly used set-retarders; the addition of 0.075 wt % sucrose to OPC increases the induction period of the hydration process from 2.5 to 31 hours [30]. Furthermore, sucrose can alter the microstructure of hydrated OPC paste by increasing the specific surface area and modifying the pore size distribution [38]. Many studies have investigated the mechanisms of set-retardation in cement pastes containing sucrose [19, 26, 29, 30, 33, 34,

35, 39, 40]. Although the details of these mechanisms are still unknown, there is a general consensus among researchers that sucrose plays an important role in preventing the precipitation of the dissolved Ca and Si in pore solutions by poisoning the surfaces of early hydration products and/or C_3S particles [19, 26, 29, 33, 35]. The poisoning agent may be a sucrose-calcium half salt $R\text{-}O^-...Ca^+\text{-}OH$ [26, 33].

Table 1-3 Compositions of ASTM Type I Ordinary Portland cement and ASTM Type I White Portland cement [9]

Composition	OPC (Gray)	WPC (White)
Chemical content (wt%)		
SiO_2	20.5	22.7
Al_2O_3	5.4	4.1
Fe_2O_3	2.6	0.3
CaO	63.9	66.7
MgO	2.1	0.9
SO_3	3.0	2.7
Loss-on-ignition (wt%)	1.4	1.6
Na_2O eq.[a] (wt%)	0.61	0.18
Phase content (wt%)		
C_3S	54	63
C_2S	18	18
C_3A	10	10
C_4AF	8	1

[a.] Soluble alkalies, such as Na_2O and K_2O.

1.1.5. Admixtures to Cement-based S/S Processes

Various admixtures can be added to the cement matrix to improve its immobilization efficiency. For example: lime and ferrous sulfate help maintain the pH within a desirable range; carbonates, sulfides and iron compounds can transform toxic metals into less soluble precipitates; ferrous sulfate and sodium hypochlorite have the ability to reduce or oxidize metals to less toxic forms; and activated carbon and ion-exchange resins can be used to adsorb metals [2]. The addition of bagasse (sugar cane residue) has also been reported to decrease the leachability of lead in cement-treated waste by adsorption [41].

1.1.6. Identification of Knowledge Gaps and Research Opportunities

As mentioned in Section 1.2.3.1, WPC has an intermediate composition between pure C_3S and OPC. Therefore, a comparison of hydration processes among these three cements would help better understand the contribution made by individual cement components to the properties of hydrated pastes. A previous study found that WPC has a shorter initial setting time and higher compressive strength than OPC [42], but no detailed comparison of the hydration behaviour of WPC and OPC over time has been reported. Although the microstructures of hydrated OPC and pure C_3S have been investigated by other researchers [43], no such study has been done of WPC. Therefore, a comparative study of the hydration of C_3S, OPC and WPC would be worthwhile to refine our understanding of cement hydration processes.

The mechanisms underlying the retardation of cement hydration by the addition of sugars and sugar derivatives are largely unresolved and need further investigation. Since sucrose does not bind with aqueous silicon [26, 33], whereas comparatively weaker retarders such as sorbitol and arabitol [37] do bind silicon [44], they may delay cement setting in different ways. To the best of the author's knowledge, the effect of silicon binders on cement hydration has not yet been reported. Research on this topic, therefore, may lead to a deeper understanding of the interactions between cement and sugar-based retarders.

The effect of sugars and sugar derivatives on cement based stabilization/ solidification processes has not been previously investigated. The retarding influence of sugar could be advantageous when the waste-cement mixture needs to be transported long distances between the S/S treatment plant and the disposal site. In these situations, early hardening of the cement in the truck box or pipeline could result in severe operational difficulties and limited flexibility. In addition, as sucrose has been reported to modify the surface area and porosity of hydrated cement pastes [38], sucrose and perhaps other sugars or their derivatives may affect the immobilization mechanisms of contaminants such as heavy metals in the cement matrix. Research in this area will have practical value for users of cement-based stabilization/solidification processes in industry.

1.2 Research Objectives

The objectives of this research were:

Objective 1: to understand better the hydration processes of C_3S, OPC and WPC, as well as the changes in microstructure of the hydrating pastes.

Objective 2: to study the effects of sucrose and sorbitol on:

- the hydration and microstructure of C_3S

- the hydration, microstructure, and strength development of OPC and WPC

Objective 3: to investigate the effects of sucrose and sorbitol on the leachability, strength development, hydration, and microstructure of OPC-stabilized wastes containing lead and zinc nitrates.

The three objectives listed above are complementary and range from the gathering of relevant fundamental knowledge (Objectives 1 and 2) to practical applications (Objective 3). This research is part of a research effort aimed at developing superior cement matrices to immobilize toxic metal wastes.

1.3. Organization of the Thesis

This thesis is composed of five chapters. Chapter 1 provides a general introduction, describes the objectives, and presents the organization of this thesis. Chapters 2, 3 and 4 are three separate manuscripts submitted for publication in peer-

reviewed journals. Chapter 4 has already been accepted by the *Journal of Hazardous Materials*. Each manuscript addresses one of the three research objectives that were mentioned above. All the manuscripts include separate sections for relevant background information, materials and methods, results and discussion, conclusions, tables, figures, and references. Chapter 5 presents the overall conclusions and recommendations for future work.

In addition, supporting experimental data and additional results that were not included in Chapters 2-4 (due to length restrictions for publications) are compiled as 12 appendices at the end of the thesis. Briefly, these deal with the effect of particle size on loss-on-ignition data and on hydration results (Appendix A); the effect of arabitol addition on the degree of hydration of OPC (Appendix B) and on the microstructure of hydrated C_3S (Appendix C); the strength of OPC with and without adding sucrose, sorbitol or arabitol (Appendix D); the effect of elevated curing temperature (40 $^{\circ}C$) on the hydration rate and microstructure of OPC-treated heavy metal waste (Appendix E); the selection of extraction fluids for the leaching tests (Appendix F); the influence of metal addition on the hydration rate of OPC (Appendix G); the correlation between strength and degree of hydration for OPC and OPC-metal mixtures amended with sugars (Appendix H); the effect of lignosulfonate on the leachability of Pb (Appendix I); the complete leaching test results for cement-treated metal waste with and without the addition of sucrose or sorbitol (Appendix J); X-Ray diffractograms for selected OPC-metal samples with and without sucrose or sorbitol at early hydration times (Appendix K); and SEM-EDS analysis of OPC-metal samples (Appendix L). Additionally, Appendix M includes

the PDF version of Chapter 4, which has been published by the *Journal of Hazardous Materials*.

1.4. References

[1]   C. D. Hills, C. J. Sollars, R. Perry, Ordinary Portland cement based solidification of toxic wastes: The role of OPC reviewed, Cem. Concr. Res. 23 (1993) 196-212.

[2]   J. R. Conner, S. L. Hoeffner, A critical review of stabilization/solidification technology, Environ. Sci. Technol. 28 (1998), 397-462.

[3]   B. Batchelor, Overview of waste stabilization with cement, Waste Manag. 26 (2006) 689-698.

[4]   L. J. J. Catalan, E. Merlière, C. Chezick, Study of the physical and chemical mechanisms influencing the long-term environmental stability of natrojarosite waste treated by stabilization/solidification, J. Hazard. Mater. B94 (2002) 63-88.

[5]   M. Benzaazoua, J-F Fiset, B. Bussière, M. Villeneuve, B. Plante, Sludge recycling within cemented paste backfill: Study of the mechanical and leachability properties, Minerals Engineering 19 (2006) 420-432.

[6]   C. M. Wilk, Applying Solidification/stabilization treatment to brownfield projects, http://www.cement.org/bookstore/profile.asp?id=4941 (accessed July, 2007).

[7]   Introduction to cement chemistry, Lafarge Corporation, Montreal, Quebec, February 24-28, 1992.

[8]   H. F. W. Taylor, Cement Chemistry, Academic Press Inc, San Diego, CA 92101, 1990.

[9]   Design and control of concrete mixtures, 7th ed., Cement Association of Canada, 2002.

[10] S. Mindness, J. F. Young, Concrete, Prentice-Hall, Inc, Englewood Cliffs, NJ, 1981.

[11] http://en.wikipedia.org/wiki/Portland_cement (accessed July 2007).

[12] Z.-Q. Wu, J. F. Young, Formation of calcium hydroxide from aqueous suspensions of tricalcium silicate, J. Am. Ceram. Soc. 67 (1984), 48-51.

[13] R. L. Berger, J. D. McGregor, Effect of temperature and water-solid ratio on growth of $Ca(OH)_2$ crystals formed during hydration of Ca_3SiO_5, J. Am. Ceram. Soc. 56 (2) (1973) 73-79.

[14] M. L. D.Gougar, B. E. Scheetz, D. M. Roy, Ettringite and C-S-H Portland cement phases for waste ion immobilization: A review, Waste Manage. 16 (1996) 295-303.

[15] F. K. Cartledge, L. G. Butler, D. Chaiasani, H. C. Eaton, F. P. Frey, E. Herrera, M. E. Tittlebaum, S.-Y. Yang, Immobilization mechanisms in solidification/stabilization of Cd and Pb salts using Portland cement fixing agents, Environ. Sci. Technol. 24 (1990), 867-873.

[16] I. Moulin, W. E. E. Stone, J. Sanz; J. Bottero, F. Mosnier, C. Haehnel, Lead and zinc retention during hydration of tri-calcium silicate: A study by sorption isotherms and ^{29}Si nuclear magnetic resonance spectroscopy, Langmuir 15 (1999), 2829-2835.

[17] F. Ziegler, A. M. Scheidegger, C. A. Johnson, R. Dahn, E. Wieland, Sorption mechanisms of zinc to calcium silicate hydrate: X-ray absorption fine structure (XAFS) investigation, Environ. Sci. Technol. 35 (2001), 1550-1555.

[18] F. Ziegler, R. Giere, C. A. Johnson, Sorption mechanisms of zinc to calcium silicate hydrate: Sorption and microscopic investigations, Environ. Sci. Technol. 35 (2001), 4556-4561.

[19] J. F. Young, A review of the mechanisms of set-retardation in Portland cement pastes containing organic admixtures, Cem. Concr. Res. 2 (1972) 415-433.

[20] http://en.wikipedia.org/wiki/Calcium_Aluminoferrite (accessed July, 2007)

[21] Standard specification for Portland cement, ASTM C150-04a (2004).

[22] http://www.cement.org/tech/cct_cement_types.asp (accessed July, 2007).

[23] Uses of White cement for architectural, safety, and specialty application, Portland Cement Association, Concrete Technology Today 20 (1999). (http://www.cement.org/bookstore/profile.asp?itemid=PL991, accessed July, 2007).

[24] http://www.cement.org/tech/faq_white_cement.asp (accessed July, 2007).

[25] http://www.cement.org/decorative/about.asp (accessed July, 2007).

[26] J. D. Birchall and N. L. Thomas, The mechanism of retardation of setting of OPC by sugars, Br. Ceram. Proc. 35 (1984) 305-315.

[27] L. Ben-Dor, C. Heitner-Wirguin, H. Diab, The effect of ionic polymer on the hydration of C_3S, Cem. Concr. Res. 15 (1985) 681-686.

[28] L. H. Grierson, J. C. Knight, R. Maharaj, The role of calcium ions and lignosulfonate plasticizer in the hydration of cement, Cem. Concr. Res. 35 (2005) 631-636.

[29] P. F. G. Banfill and D. C. Saunders, The relationship between the sorption of organic compounds on cement and the retardation of hydration, Cem. Concr. Res. 16 (1986) 399-410.

[30]   V. S. Ramachandran, M. S. Lowery, Conduction calorimetric investigation of the

        effect of retarders on the hydration of Portland cement, Thermochim. Acta 195

        (1992) 373-387.

[31]   H. M. Jennings, H. Taleb, G. Frohnsdorff, J. R. Clifton, Interpretation of the effects

        of retarding admixtures on pastes of C_3S, C_3A plus gypsum, and Portland cement,

        The 8th International Congress on the Chemistry of Cement, Communications

        Theme 2, Volume III, 1986.

[32]   N. B. Singh, P. N. Ojha, Effect of glucose on the hydration of Portland cement, The

        7th International Congress on the Chemistry of Cement, 1980.

[33]   N. L. Thomas and J. D. Birchall, The retardation action of sugars on cement

        hydration, Cem. Concr. Res. 13 (1983) 830-842.

[34]   K. Luke, G. Luke, Effect of sucrose on retardation of Portland cement, Adv. Cem.

        Res. 12 (2000) 9-18.

[35]   M. Bishop, A. R. Barron, Cement hydration inhibition with sucrose, tartaric acid,

        and lignosulfonate: analytical and spectroscopic study, Ind. Eng. Chem, Res. 45 (21)

        (2006) 7042-7049.

[36]   N. B. Milestone, Hydration of tricalcium silicate in the presence of lignosulfonates,

        glucose, and sodium gluconate, J. Am. Ceram. Soc. 62 (1979) 321-324.

[37]   S. D. Kinrade, personal communication.

[38]   M. C. G. Juenger, H. M. Jennings, New insights into the effects of sugar on the

        hydration and microstructure of cement pastes, Cem. Concr. Res. 32 (2002) 393-

        399.

[39] B. E. I. Abdelrazig, D. G. Bonner, D. V. Nowell, J. M. Dransfield, P. J. Egan, The solution chemistry and early hydration of ordinary Portland cement pastes with and without admixtures, Thermochim. Acta 340-341 (1999) 417-430.

[40] V. K. Peterson, M. C. G. Juenger, Hydration of tricalcium silicate: Effects of $CaCl_2$ and sucrose on reaction kinetics and product formation, Chem. Mater. 18 (2006) 5798-5804.

[41] M. A. Janusa, C. A. Champagne, J. C. Fanguy, G. E. Heard, P. L. Laine, A. A. Landry, Solidification stabilization of lead with the aid of bagasse as an additive to Portland cement, Microchem. J. 65 (1998) 255-259.

[42] B. S. Hamad, Investigations of chemical and physical properties of white cement concrete, Adv. Cem Based Mater. 2 (1995) 161-167.

[43] K. O. Kjellsen, H. Justnes, Revisiting the microstructure of hydrated tricalcium silicate. A comparison to Portland cement, Cem. Concr. Composites 26 (2004) 947-956.

[44] S. D. Kinrade, J. W. Del Nin, A. S. Schach, T. A. Sloan, K.L. Wilson, C. T. G. Knight, Stable five- and six-coordinated silicate anions in aqueous solution, Science 285 (1999) 1542-1545.

CHAPTER 2

COMPARATIVE STUDY OF THE HYDRATION AND MICROSTRUCTURE OF TRICALCIUM SILICATE, ASTM TYPE I ORDINARY PORTLAND CEMENT, AND WHITE PORTLAND CEMENT

Summary: The hydration and microstructure of ASTM Type I ordinary Portland cement (OPC), white Portland cement (WPC), and tricalcium silicate (C_3S) were investigated by SEM-grey level analysis and loss-on-ignition tests as a function of curing time. The hydration rate was found to be C_3S > WPC > OPC and was correlated with the total content of C_3S and C_3A. The fraction of non-evaporable water content in fully hydrated OPC and WPC is $0.234_9 \pm 0.005_7$ and $0.208_6 \pm 0.003_2$, respectively. The microstructure of hydrated C_3S was characterized by two prominent features: 1) large zones of unhydrated C_3S particles embedded in dense calcium hydroxide (CH) and 2) porous zones in which CSH was the only hydration product. CH-rich zones were also observed in hydrated OPC and WPC but they were smaller and became less distinct as hydration progressed in these systems. No large porous zones were present in hydrated OPC and WPC, which exhibited much lower overall porosity than C_3S.

Key words: Tricalcium silicate (C_3S); Ordinary Portland cement (OPC); White Portland cement (WPC); Hydration; Microstructure

2.1. Introduction

Ordinary Portland cement (OPC) is a fundamental component of most concretes. Raw OPC has five main components: tricalcium silicate (C_3S), dicalcium silicate (C_2S), tricalcium aluminate (C_3A), tetracalcium aluminoferrite (C_4AF), and calcium sulfate (gypsum or anhydrite, 10% max). When contacted with water, C_3A reacts with sulfate coming from the dissolution of gypsum to form ettringite (AFt) and monosulfate (AFm), thus preventing flash set associated with the formation of calcium aluminate hydrates. C_3S and C_2S undergo hydration to form calcium hydroxide (CH) and calcium silicate hydrate (CSH), which is the main hydration product and the principal contributor to cement strength [1].

White Portland cement (WPC) contains significantly fewer transition metal oxides (iron, manganese, and others) than OPC and, thus, once cured, has a brilliant white appearance that is advantageous for decorative applications as well as reflective flooring and roadway infrastructure [2]. WPC has been found to have a shorter initial setting time and higher compressive strength than OPC [3]; however, no detailed comparison of the degree of hydration and microstructure of WPC and OPC over time has been reported. The microstructure of hydrated C_3S and ASTM Type V Portland cement were compared by Kjellsen and Justnes [4]. C_3S was found to hydrate into dense pockets in which C_3S grains were engulfed in large calcium hydroxide masses. By contrast, hydrated OPC had a groundmass structure having more complex features such as finely dispersed calcium hydroxide, remnant Al and Fe phases, and reduced porosity. To the best of the author's

knowledge, no detailed investigation of the microstructure of hydrated WPC pastes has been previously reported.

The objectives of the present research were to compare the hydration and microstructure of OPC, WPC, and C_3S as a function of curing time. This is done by using different analytical techniques such as loss-on-ignition measurements (i.e. destructive dehydration) and backscattered electron (BSE) microscopy incorporating grey level analysis. The results provide significant insights on how compositional differences affect cement hydration.

Degree of hydration is an important parameter to quantify the conversion from unhydrated cement to its hydration products. It can be determined indirectly by various methods. Quantitative X-ray diffraction analysis (QXRD) [5-7], ^{1}H & ^{29}Si NMR [5, 8] and grey level analysis [5, 6, 9] have been used to monitor the degree of hydration by determining the amount of unhydrated phases. The degree of hydration can also be measured by determining the amount of hydrated phases through loss-on-ignition testing [1, 7, 10-12] or isothermal conduction calorimetry [7]. In this study, both loss-on-ignition testing and grey level analysis were used to determine the degree of hydration. Loss-on-ignition testing was selected because of its simplicity, low cost, and high efficiency (many samples can be tested at the same time). Grey level analysis provides information on both the degree of hydration and the distribution of mineralogical phases in hydrated pastes, and is thus a valuable tool to investigate the microstructure of hydrated cement.

The aim of loss-on-ignition testing is to measure the amount of non-evaporable water, which is the water retained after freeze-drying or oven-drying at 105°C. The non-

evaporable water content can be easily obtained by comparing the weights of the oven-dried paste before and after dehydrating at 1005 $^{\circ}$C for two hours [1, 10, 11]. Since non-evaporable water approximately represents the structurally bound water in the hydration products, it is proportional to the fraction of cement that has reacted and can be used to estimate the degree of hydration if the non-evaporable water content in fully hydrated cement paste is known [1, 10, 12].

Scanning electron microscopy (SEM) in conjunction with image analysis is a powerful approach to study the microstructure of hydrated cement and can be used to determine degree of hydration through grey level analysis [5, 6, 9]. In a typical image of a hydrated cement paste taken by SEM in BSE mode, the main phases (C_3S, C_2S, CSH, and CH) appear in different grey levels due to their various average atomic numbers (the larger the atomic number, the higher the intensity of the electrons, and the brighter a chosen material appears). Typically, unhydrated clinkers are brighter than calcium hydroxide (lighter grey) and other hydration products including CSH and little amount of Al-containing phases (darker grey), whereas the porosity appears in black. With these distinct grey levels, BSE images can provide valuable information about hydration status, hydration products, and the phase distribution of the examined cement paste. [4, 9, 13-16]. When displayed in a grey level histogram ranging from 0 to 255 in which 0 and 255 represent black and white and other intermediate grey levels are in between, various phases appear as individual peaks and the ratio of the area under each peak over the area of the whole histogram equals to the area percentage of the corresponding phase in the whole selected BSE image. The volume fraction of a phase in hydrated cement can be equated to its area fraction by this grey level analysis [15]. Scrivener [15, 16] found that

the ratios of unhydrated phases, calcium hydroxide, and porosity calculated based on their grey levels are correlated to those determined by traditional methods. The area percentage of unhydrated phases can also be applied to calculate the degree of hydration of cement paste at a given water-to-cement ratio [5, 13].

2.2. Materials and Methods

2.2.1. Sample Preparation

ASTM C 150 Type I ordinary Portland cement (CEMEX Inc., Charlevoix, MI), ASTM C150 Type I white Portland cement (Aalborg Portland, Aalborg, Denmark) and pure tricalcium silicate (CTL Group, Skokie, IL) were used in this research. Both the OPC and WPC conform to the ASTM C150 standard for Type I cement which specifies the compositional and physical requirements including loss-on-ignition, insoluble residue, setting time, strength and air content. [17]. The manufacturers' specifications for all three cements are provided in Table 3-1. The C_3S was crystallographically-pure triclinic alite, with reported traces of Al_2O_3 and MgO, at 325 mesh. (Particles measure less than 44 μm.)

Deionised-distilled water was pre-cooled to 10 °C and then mixed with kilogram quantities of OPC and WPC at a water-to-cement mass ratio of 0.40:1[1] in a plastic bowl immersed in an ice-water bath. Temperature control was necessary with such large samples to counteract the heat generation at early times. The mixtures were stirred with a plastic spoon for about 7 min until they were homogeneous. All the samples were slurries after being mixed with water. They were then poured into either polyethylene ice cube

---

[1] This ratio was optimized in preliminary tests. It is within the range of values (0.35 to 0.50) commonly used by other researchers.

trays (WPC) or 5.08 × 10.16 cm (2×4 inch) PVC cylinders (OPC) and placed in triple-sealed, air-tight polyethylene bags to prevent carbonation and avoid the loss of humidity. They were immersed in a room temperature (20-22°C) water bath to cure. Sixteen

Table 2-1 Chemical and physical analysis and potential compound compositions of unhydrated OPC, WPC, and C_3S samples

	OPC (Gray)	WPC (White)	PureC_3S
Chemical composition (wt%)			
SiO_2	19.35	24.5	26.3
Al_2O_3	5.16	2.1	traces
Fe_2O_3	2.47	0.34	0
CaO	62.60	69.0	73.7
MgO	3.48	0.59	traces
SO_3	3.57	2.13	0
Loss-on-ignition (wt%)	1.52	0.5	na^a
Insoluble residue (wt%)	0.15	0.08	na
Alkalies as Na_2O eq. (wt%)	0.85	0.19	0
Blain fineness (m^2/kg)	378	393	na
Potential compound composition (wt.%)			
C_3S	60	74	100
C_2S	11	14	0
C_3A	10	5	0
C_4AF	8	1	0

[a.] na = not applicable

parallel test samples were prepared of each type of cement, which allowed the loss-on-ignition to be determined in triplicate after 5 different curing periods of 3, 7, 14, 28 and 56 days. A further loss-on-ignition measurement was done after 1 day curing.

SEM analyses were performed with pure C_3S at 1, 7 and 56 days of curing. Samples were placed in three separate 8 ml polyethylene plastic bottles. In each bottle, 1.20 g t C_3S was blended with 0.72 ml deionised-distilled water at a water-to-solid mass ratio of 0.60:1[2] [18]. The slurry was then mixed with a small glass stir rod for 30 seconds. In order to prevent undesirable carbonation, all the preparation steps were done in a glove box under nitrogen. Samples were sealed in plastic bottles and cured at room temperature until testing.

2.2.2. Loss-on-ignition Testing

A small portion of each OPC or WPC sample was crushed, and 1.0 to 1.5 g of the 850-2000 μm^3 fraction was oven-heated for 24 h at 105 °C to remove evaporable water and obtain the evaporable free-water mass, W_{105}. Next, the temperature was increased and maintained at 1005 °C for 2 h to determine the fully dehydrated mass, W_{1005}. The degree of hydration α_{LI} can be calculated by the equation

$$\alpha_{LI} = (W_{105} - W_{1005})/(FNEW \times W_{1005}) \qquad (2\text{-}1)$$

in which the constant FNEW is the mass fraction of non-evaporable water in fully hydrated cement [1, 11]. The FNEW has been reported to be either 0.23 [19] or 0.24 [1, 20] for OPC. However, the FNEW of white Portland cement is unknown and, without this value, equation 2-1 cannot be used to calculate the degree of hydration of WPC.

---

[2] This value was initially selected based on previous studies of C_3S by X-ray diffractometry.
[3] The particle size distribution was found not to have a significant influence on the hydration results obtained by loss-on-ignition tests. For details, please see Appendix A.

Therefore, one of the objectives of the present research was to evaluate the FNEW of WPC and compare it to the values measured for OPC.

2.2.3. SEM-EDS Analyses

After reaching the desired curing time, a small slice (*ca.* 0.5 g) was removed from the inner part of the sample, immersed for 24 h in acetone to halt hydration [21], dried at 105 °C for 15 min, and then imbedded in epoxy resin. A thin-section was cut, lapped and polished using oil-based media so as not to alter the water-soluble minerals. After carbon-coating, it was analyzed with a JEOL JSM 5900 scanning electron microscope in BSE mode to improve contrast between different mineral phases [13, 16]. The elemental composition of mineral phases was determined by X-ray energy dispersive spectrometry (EDS) using an Oxford Link ISIS system (50 s live-time). SEM-EDS analyses were carried out on days 1, 7 and 56 for all the OPC, WPC, and C_3S samples.

2.2.4. Grey Level Analysis

Grey level analysis was performed by using the Image-Pro Plus 5.0 software [22]. Each BSE image consists of 1280 $\times$ 960 pixels having grey levels ranging from 0 (black) to 256 (white). The grey levels are directly related to the atomic number of the material, and thus can be used to distinguish between mineralogical phases: unhydrated cement grains are the brightest features, CH and CSH appear as two shades of grey, whereas pore space is black. (Figure 2-1) [4]. Also, as shown in Figure 2-1, there are two types of CSH: inner CSH that forms around residual unhydrated calcium silicate and outer CSH that

forms in the pore space; both of inner and outer CSH appears in similar grey scales [13]. The identity of all the above mentioned phases was confirmed by EDS separately.
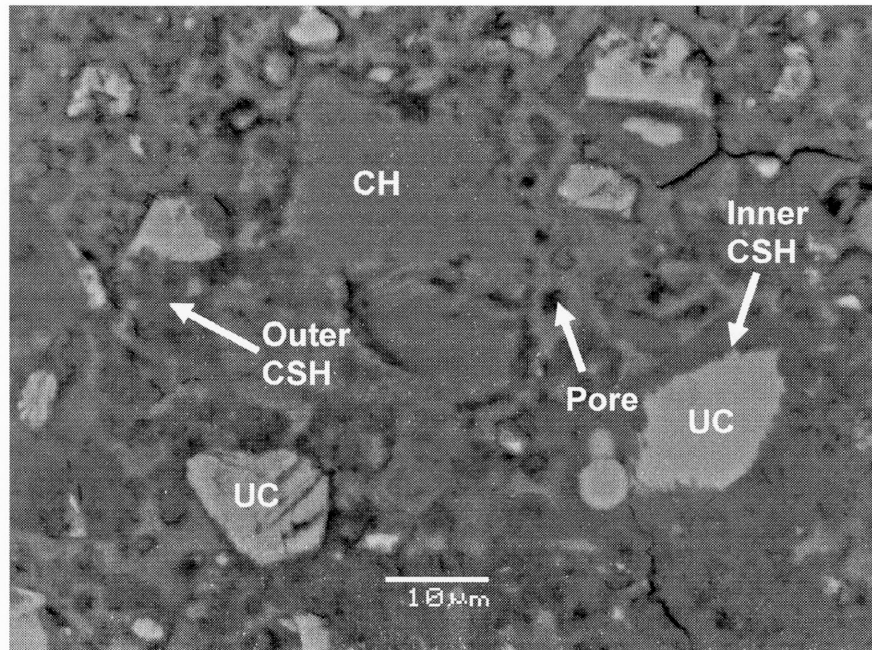
Figure 2-1 Backscattered electron image of OPC sample at day 7

(UC: unhydrated cement grains, CH: calcium hydroxide).

These phases also appear as separate peaks in grey-scale histograms (Figure 2-2). The areas under these peaks can be used to calculate the percentage of individual phases [16][4]. For each OPC and WPC sample, calculations were carried out on 10 BSE images taken at different locations in the central section, and the results were averaged to obtain a representative phase distribution [16]. Because of the heterogeneous feature of hydrated C_3S, a larger number of BSE images (15) were acquired for C_3S samples. Every BSE image covered an area of 254×190 μm at an image scale of 0.198 μm/pixel. The results of the grey level analysis were then plotted as a function of curing time (day 1, 7 and 56)

---

[4] Microcracks were included in the calculation of porosity. They may be induced by shrinkage during the curing process or by drying during the preparation of thin slices for SEM analyses.

for OPC, WPC, and C$_3$S, respectively. Additionally, grey level analyses on C$_3$S samples were also carried out on 7 fields at lower magnification (image scale of 0.657 μm /pixel with a covered area of 841 × 630 μm), 7 fields at intermediate magnification (image scale of 0.100 μm /pixel with a covered area of 128 × 96 μm) and 7 fields at higher magnification (image scale of 0.055 μm /pixel with a covered area of 71 × 53 μm).
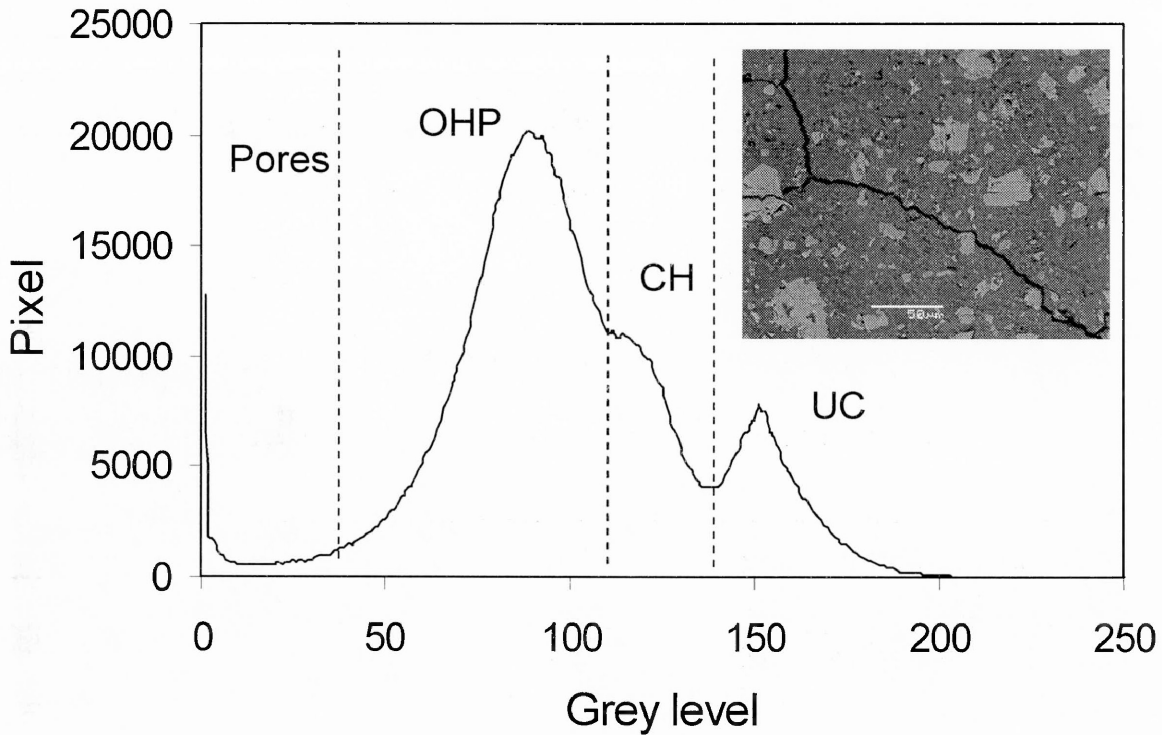
Figure 2-2 Backscattered electron image of OPC sample at day 7 and its grey level histogram (UC: unhydrated cement grains, CH: calcium hydroxide, OHP: other hydration products).

The degree of hydration α$_{GL}$ of OPC, WPC and C$_3$S can be calculated by the equation

$$\alpha_{GL} = 1 - UC/UC_0 \quad [5, 9] \qquad (2\text{-}2)$$

in which UC and UC_0 are the area fractions of unhydrated cement particles at time t and the start of the hydration process, respectively. UC can be obtained from the area percentage of the unhydrated cement shown in BSE images, while UC_0 can be evaluated from the density of unhydrated cement powder as determined by ASTM C 188-95 [23] (d_c = 3.14 g/cm^3 for OPC, d_c = 3.06 g/cm^3 for WPC, and d_c = 3.15 g/cm^3 for C$_3$S), density of water (d_w = 1.00 g/cm^3) and the corresponding water-to-cement mass ratio R (0.40 for OPC and WPC, 0.60 for C$_3$S) by Equation 2-3.

$$UC_0 = (1/d_c)/(1/d_c + R/d_w) \qquad (2\text{-}3)$$

Determining degree of hydration from grey level analysis is considerably more complex and time consuming than from loss-on-ignition data, but does not require knowledge of the FNEW. In the following section, we will show how grey level analysis and loss-on-ignition data for a few samples can be combined to evaluate the FNEW of OPC and WPC. Once the FNEW values are known, they can be used to determine the degree of hydration of a larger number of samples relatively easily using Equation 2-1 and loss-on-ignition data, thus removing the need for complex grey level analysis.

2.3. Results and Discussion

2.3.1. Degree of Hydration

Figure 2-3 illustrates the degree of hydration of OPC, WPC, and C$_3$S at days 1, 7 and 56 determined by grey level analysis. The degree of hydration was always highest for pure C$_3$S. WPC hydrated faster than OPC during the first day, and then at a similar rate between day 1 and day 7. At day 56, both types of cement reached 80% hydration. These

results suggest that the rate of hydration reaction during the first day is correlated with the total content of C_3S and C_3A in the unhydrated samples (70% in OPC, 79% in WPC, and 100% in C_3S). This is consistent with the fact that C_3S and C_3A are more reactive than C_2S and C_4AF [1]; hence the higher the C_3S and C_3A content, the faster the initial hydration rate. The larger hydration rate of OPC by comparison with WPC at later times (after day 7) can be explained by the higher combined contents of C_2S and C_4AF in OPC (19% in OPC versus 15% in WPC), which hydrate more slowly than C_3A and C_3S [1].
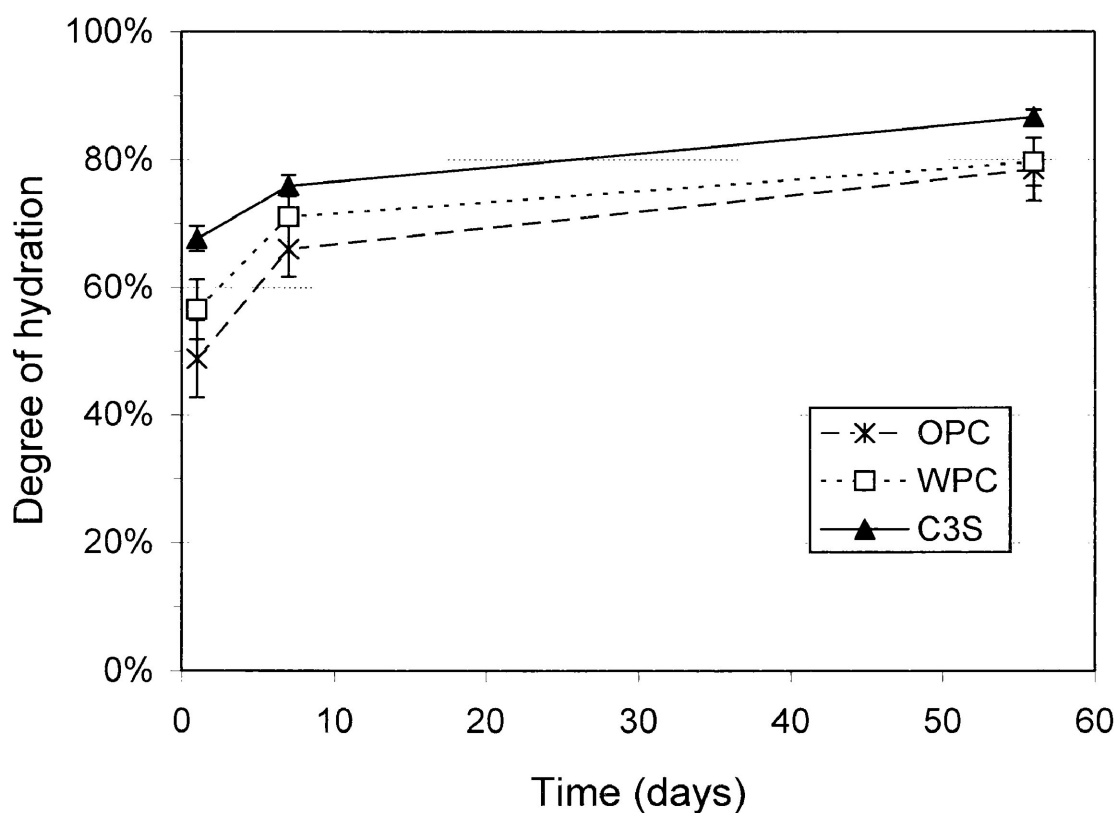
Figure 2-3 Degree of hydration of OPC, WPC, and pure C_3S determined by grey level analysis. Error bars correspond to the standard deviations over 15 measurements for C_3S and 10 measurements for OPC and WPC.

Figure 2-4a and 2-4b show the degree of hydration determined by grey level analysis versus the ratio $(W_{105} - W_{1005})/W_{1005}$ for OPC and WPC, respectively. Samples

aged 1, 7 and 56 days were used to construct these plots. To include more data points with intermediate degree of hydration, samples containing 0.40 wt% sorbitol as well as 0.037 wt% and 0.15 wt% sucrose (cement retarders [24, 25]) were also analyzed. Standard errors on the degree of hydration obtained by grey level analysis (error bars in the Y direction) are much higher than standard errors on the ratio $(W_{105} - W_{1005})/W_{1005}$ (error bars in the X direction). This is likely caused by the heterogeneous distribution of unhydrated phases in BSE images (i.e., there is significant variability in the amount of unhydrated phases present in each image). According to Equation 2-1, the data points are expected to plot linearly with a slope equal to the $FNEW^{-1}$. The values of FNEW for OPC and WPC, including standard errors, obtained by linear regression are $0.234_9 \pm 0.005_7$ for OPC and $0.208_6 \pm 0.003_2$ for WPC. The FNEW of OPC compares well with previously reported values of either 0.23 [19] or 0.24 [1, 20].

Now that the numerical values for FNEW have been determined for the specific OPC and WPC cement samples used in this work, the degrees of hydration at 1, 3, 7, 14, 28, and 56 days can be calculated from loss-on-ignition tests. Figure 2-5 depicts the degree of hydration as a function of time for OPC and WPC. The curing of OPC and WPC proceeded in two stages: a period of rapid hydration lasting about 3 days, followed by a slower reaction period. WPC hydrated faster than OPC during the first day, and then both materials hydrated at a similar rate (parallel curves) until day 14. Between days 14 and 56, OPC hydrated at a faster rate than WPC. On day 56, both OPC and WPC had the same degree of hydration of 80%. These results are in accordance with those obtained from grey level analysis (Figure 2-3).
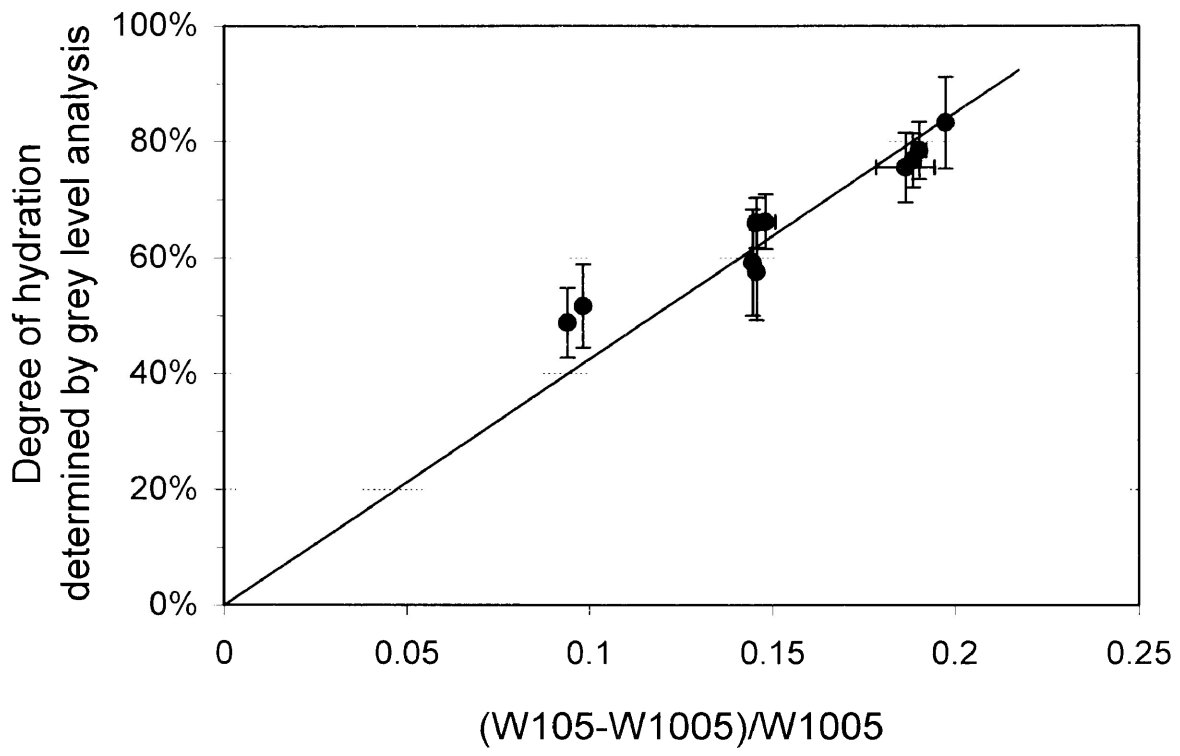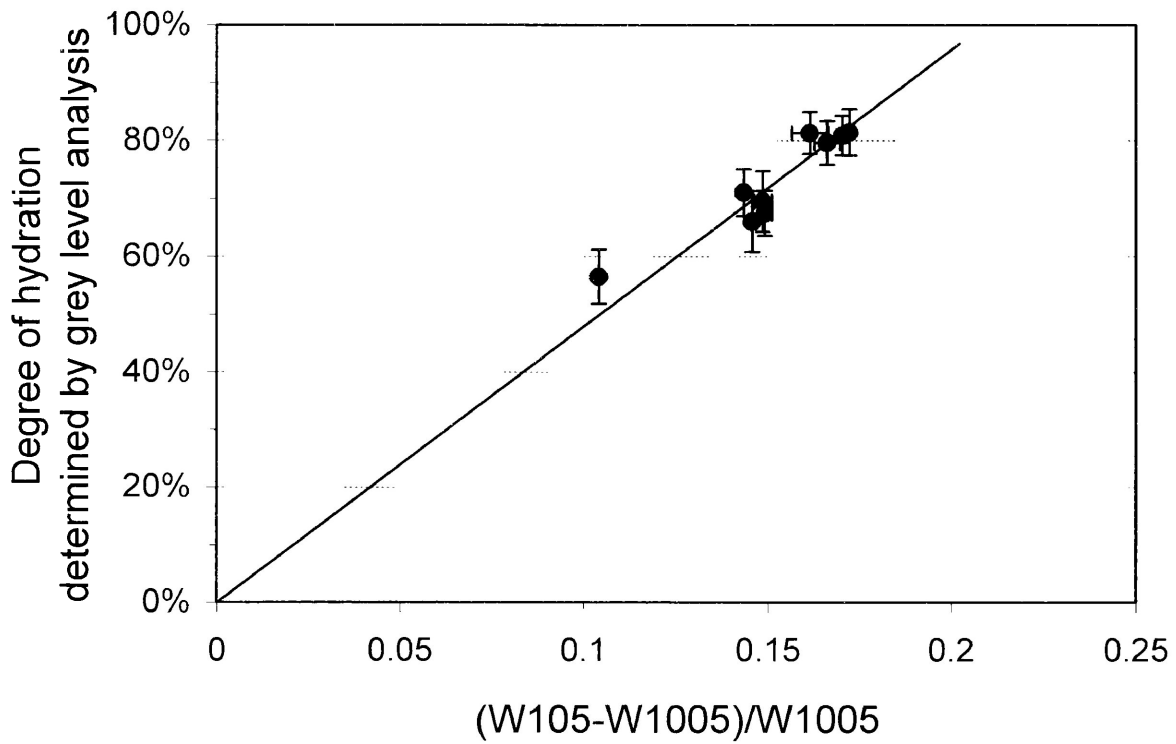
Figure 2-4 Degree of hydration obtained by grey level analysis for (a) OPC and (b) WPC

versus the ratio $(W_{105}-W_{1005})/W_{1005}$ from loss-on-ignition testing.
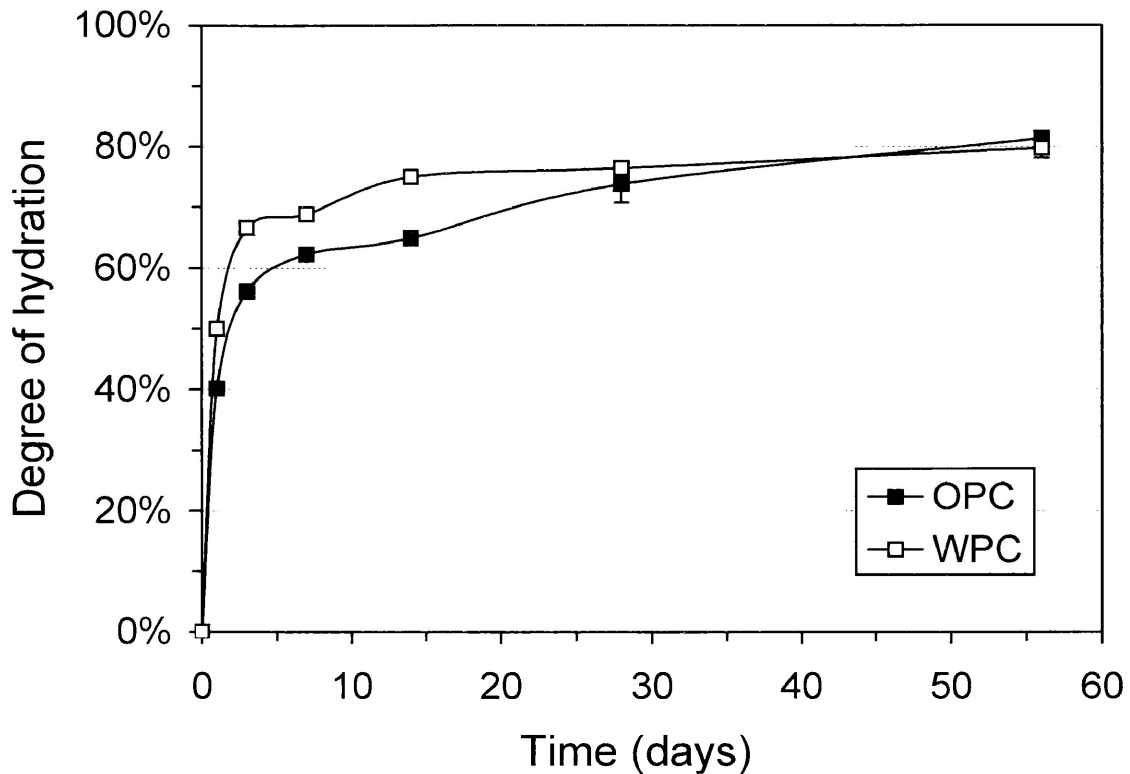
Figure 2-5 Degree of hydration of OPC and WPC determined by loss-on-ignition tests. Error bars correspond to the standard deviation over 3 measurements. In many cases, the error bars are too short to be seen.

2.3.2. Microstructure

2.3.2.1. Pure C_3S

The microstructure of hydrating pure tricalcium silicate at days 1, 7 and 56 is shown in Figures 2-6 to 2-8. Islands consisting of bright unhydrated C_3S grains embedded in a dense calcium hydroxide matrix (light grey) are clearly visible on BSE micrographs taken at a large image scale 0.657 µm /pixel (Figures 2-6a, 2-7a, and 2-8a). The identity of the two main phases in the islands (unhydrated C_3S and CH) was ascertained by EDS analyses carried out at a smaller image scale of 0.055 µm /pixel

(Figures 2-6b, 2-7b, and 2-8b). The islands have dimensions ranging from tens to several hundred microns and are surrounded by a more porous matrix consisting mostly of unhydrated C_3S and calcium-silicate-hydrate (CSH) gel (Figures 2-6c, 2-7c, and 2-8c, image scale: 0.100 μm /pixel). These observations are similar to those by Kjellsen and Justnes who used a lower water-to-solid ratio (0.40 versus 0.60 in this study) [4].

The contribution of CH-rich islands to the total sample area increased from $30._9 \pm 4._5$ % at day 1 to $42._2 \pm 4._2$ % at day 7 (Table 2-2). This increase coincided with growth and amalgamation of individual islands (compare Figures 2-6a and 2-7a). However, CH-rich islands stopped growing after day 7, and their contribution to the total area at day 56 ($39._3 \pm 2._6$ %) was not statistically different from that at day 7. Berger and Mcgregor [26] proposed that the formation of calcium hydroxide deposits is favoured on the surfaces of C_3S particles acting as ideal nucleation sites because of the nearby high concentration of Ca^{2+} ions and the higher temperature at the liquid-solid surface, caused by the exothermic dissolution of C_3S, which lowers the solubility of CH. By contrast, our observations of the growth of CH-rich islands combined with the paucity of CH in the porous areas until at least day 7, indicate that the precipitation of calcium as calcium hydroxide is not uniformly distributed on the surfaces of all C_3S grains but rather occurs preferentially at the interfaces between a few CH-rich islands and the surrounding porous regions.

In the porous areas surrounding the CH-rich islands, CSH is the main hydration product and forms rims around residual C_3S cores (Figures 2-6c, 2-7c, and 2-8c). As hydration progresses, these residual C_3S cores shrink and eventually disappear completely while the thickness of the CSH rims increases. The amount of porosity (i.e.,

the number of black pixels) in the porous areas decreases with curing time, due to

precipitation of mostly CSH but also some CH in these areas.
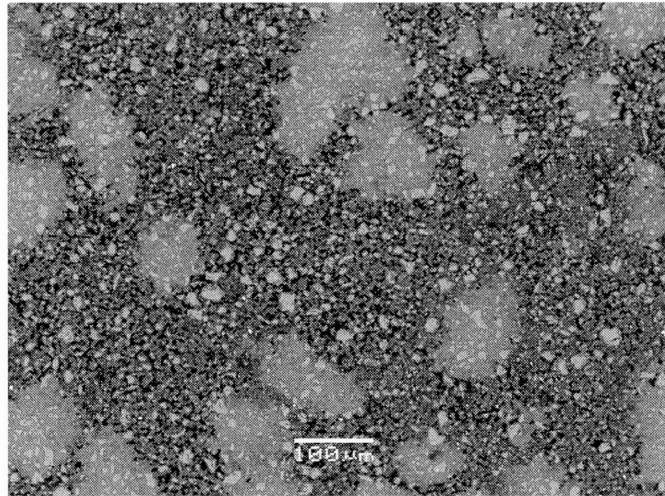
(a)
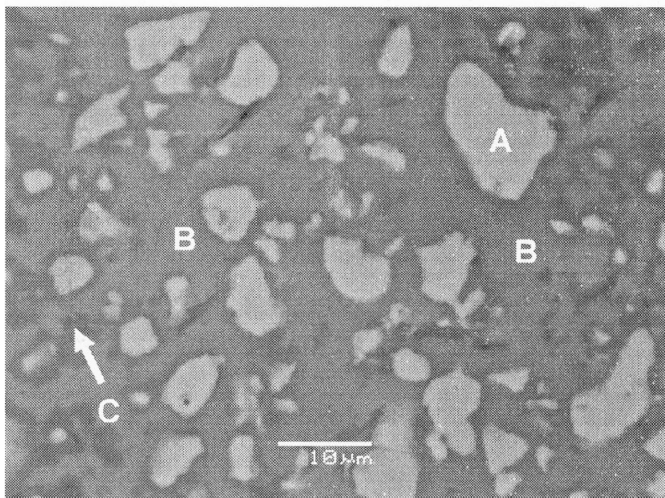
(b)
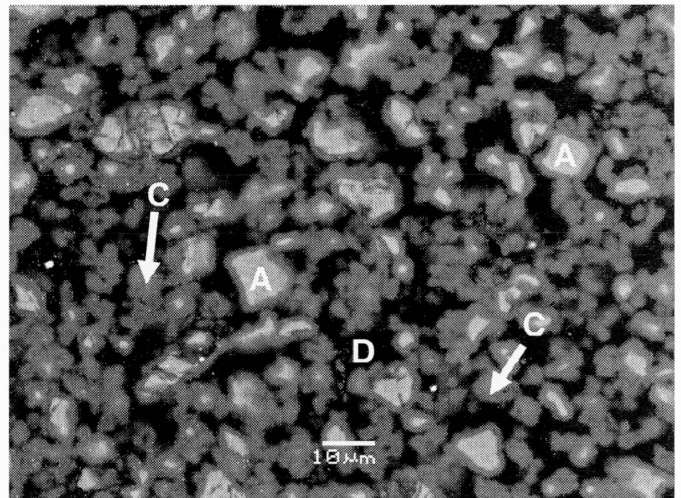
(c)

Figure 2-6 Backscattered electron images of C_3S sample at day 1. (a) overall view,

(b) CH-rich island, and (c) porous area showing (A) C_3S, (B) CH, (C) CSH, and (D)

pores.
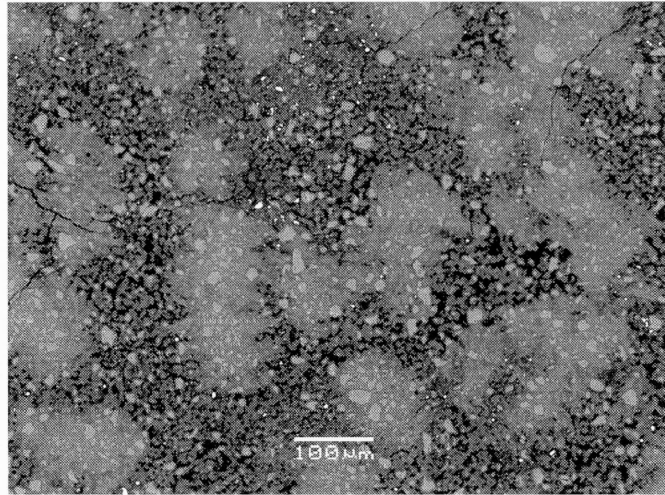
(a)
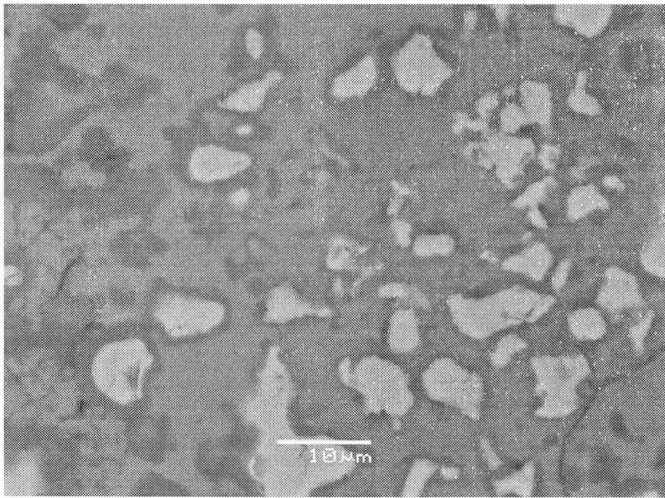
(b)
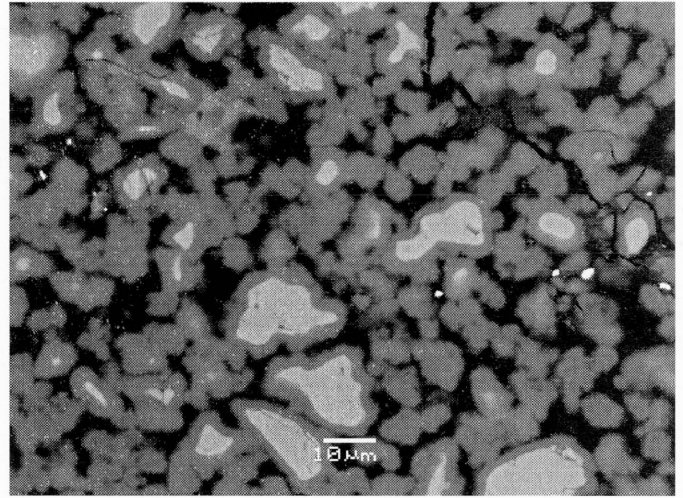
(c)

Figure 2-7 Backscattered electron images of C_3S sample at day 7.

(a) overall view, (b) CH-rich island, and (c) porous area.
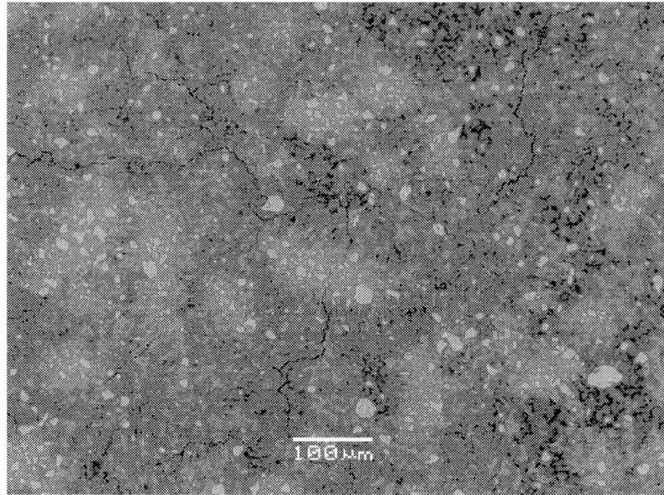
(a)
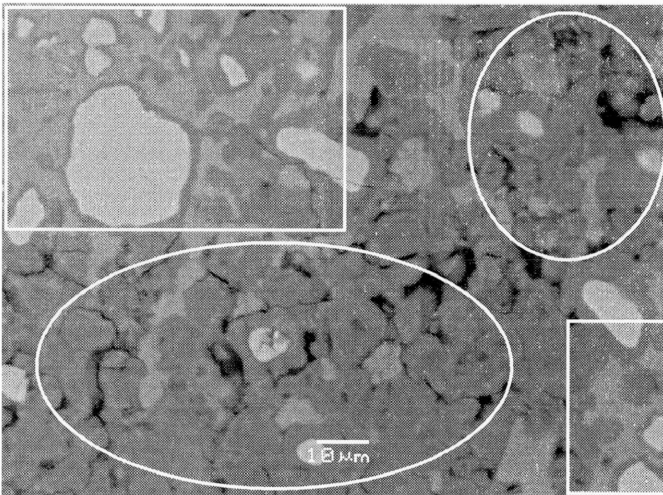
(b)
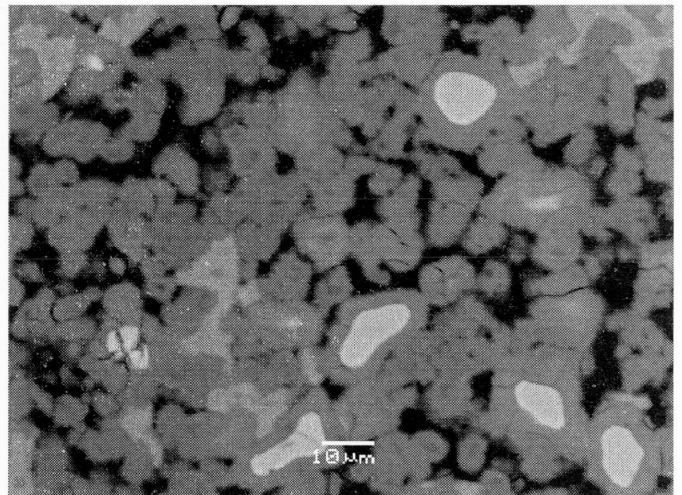
(c)

Figure 2-8 Backscattered electron images of C_3S sample at day 56. (a) overall view,

(b) CH-rich island (in rectangle) and porous area (in ellipse), and (c) porous area.

Table 2-2 Area percentages of the CH-rich islands in C_3S samples

at days 1, 7 and 56

Day	Area percentage (%)	Standard deviation (%)
1	30.$_9$	4.$_5$
	42.$_2$	4.$_2$
56	39.$_3$	2.$_6$

Note: All values in this table were calculated from the results of grey level analysis on 7 individual BSE images taken throughout a sample cross section. Each BSE image covered an area of 841 × 630 μm at an image scale of 0.657 μm /pixel. On each image, the boundaries of all the CH-rich islands were traced by hand, and the Image-Pro Plus 5.0 software was used to calculate the ratio of islands to total area.

Table 2-3 shows the distribution of individual phases in the islands and porous areas after 1, 7 and 56 days of curing. The composition of the CH-rich islands remained stable from day 1 to day 7. It consisted of approximately 20% unhydrated C_3S, 63% CH, 16% CSH, and 0.3% pores. All percentages refer to area or volume. The thick deposits of CH in the islands shielded the unhydrated C_3S from contact with pore water, thus considerably slowing down the hydration of C_3S in the islands. Therefore, the formation of CH-rich islands had a negative impact on the degree of hydration of C_3S pastes. However, slow diffusion of water toward the C_3S grains in the CH-rich islands caused a progressive hydration of these grains and the amount of CSH in the islands to increase from 18% on day 7 to 30% on day 56. It is also clear that the growth of CH-rich islands between day 1 and day 7 (see Table 2-2) is fed by the dissolution of C_3S from the porous areas, which releases calcium in solution. The calcium then diffuses toward the islands

where it precipitates as calcium hydroxide. The interruption in the growth of CH-rich islands after day 7, which was mentioned earlier (see Table 2-2) may be caused by the increased difficulty for Ca ions to diffuse towards the islands as the amount of pore space decreases significantly in the porous regions from 41% on day 7 to 19% on day 56.

Table 2-3 Phase distribution in CH-rich islands and porous areas of C_3S samples

Phases	Day 1		Day 7		Day 56	
	Island area percentage (%)	Porous area percentage (%)	Island area percentage (%)	Porous area percentage (%)	Island area percentage (%)	Porous area percentage (%)
C_3S	$20._8\pm2._7$	$8._4\pm1._6$	$19._7\pm6._6$	$6._3\pm1._5$	$15._0\pm4._0$	$2._4\pm1._6$
CH	$63._2\pm2._8$	na	$62._1\pm5._9$	na	$54._5\pm3._5$	$11._1\pm4._3$
CSH	$15._5\pm3._2$	$51._1\pm2._8$	$17._7\pm3._6$	$51._6\pm3._7$	$29._9\pm4._1$	$67._4\pm5._9$
pore	$0.3_2\pm0.2_3$	$40._2\pm2._7$	$0.3_6\pm0.2_5$	$41._5\pm4._5$	$0.6_0\pm0.8_7$	$19._0\pm8._6$

Note: All values in this table were calculated from the results of grey level analysis on 7 individual BSE images taken in CH-rich islands and 7 individual BSE images taken in porous areas. Each BSE image taken in the CH-rich islands covered an area of 71×53 μm at an image scale of 0.055 μm / pixel. Each BSE image taken in the porous areas covered an area of 127×96 μm at an image scale of 0.100 μm / pixel.

The percentage of unhydrated C_3S in the porous areas was much lower than in the CH-rich islands and decreased with curing time (from roughly 8% at day 1 to 2% at day 56). As shown in Table 2-3, there was almost no CH detected from day 1 to day 7 in the porous areas, and only a small amount formed between day 7 and day 56 (11%).

Figure 2-9 depicts the overall phase distributions (with no differentiation between CH-rich islands and porous areas) in hydrated C_3S samples at days 1, 7 and 56. The large standard errors are attributable to the heterogeneity of the images (i.e., some images contain more CH-rich islands while others have more porous areas). The ongoing decrease in amount of unhydrated C_3S between day 1 and day 56 reflects the progression in degree of hydration and coincides with a corresponding ongoing increase in amount of CSH and decrease in pore space. It is interesting to note, however, that although the amount of calcium hydroxide increased between day 1 and day 7 (at 97.7% confidence level determined by the Student t-test), it remained stable between day 7 and day 56 (within statistical uncertainty). This finding is consistent with the earlier result that CH-rich islands grew between day 1 and day 7 but remained stable in size between day 7 and day 56 (Table 2-2). This result is important because it suggests that the overall stoichiometry of the C_3S hydration reaction is not constant over time: initially the hydration of C_3S produces both CH (which accumulates in the CH-rich islands) and CSH (mostly in the porous regions) but at later times, the production of CH almost comes to a halt while the formation of CSH continues in the porous regions.
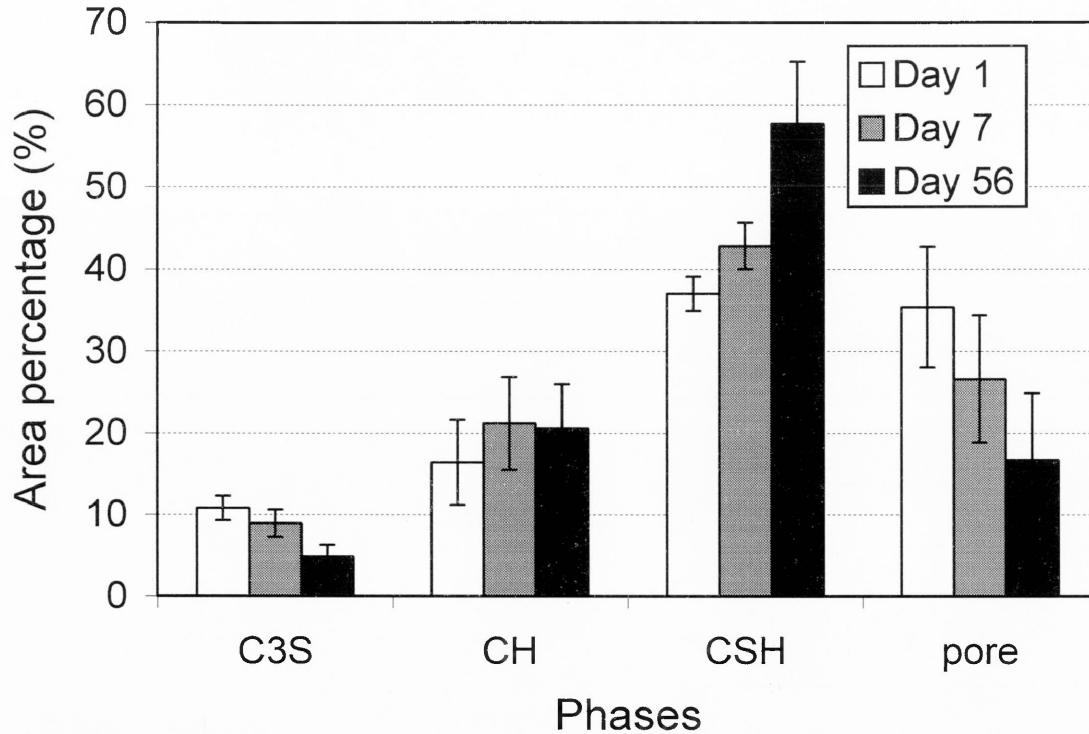
Figure 2-9 Overall phase distributions of C_3S samples at days 1, 7 and 56 (CH: calcium

hydroxide). The bar heights were obtained by averaging the results of grey level analysis

on 15 different BSE images each covering an area of 254×190 μm at an image scale of

0.198 μm / pixel. Standard deviations appear as error bars.

2.3.2.2. OPC

CH-rich islands encompassing unhydrated C_3S grains and containing little CSH

are visible in BSE micrographs of OPC samples (Figure 2-10a), but their sizes usually

remain below 100 microns, which is smaller than their counterpart in C_3S samples.

Another important difference with C_3S samples is that even at day 1, CH along with CSH

precipitate in large quantities in the regions surrounding the islands (Figure 2-10b). As a

result, the porosity of the regions surrounding the CH-rich islands is much smaller than in C_3S samples of equal age.

(a)   (b)
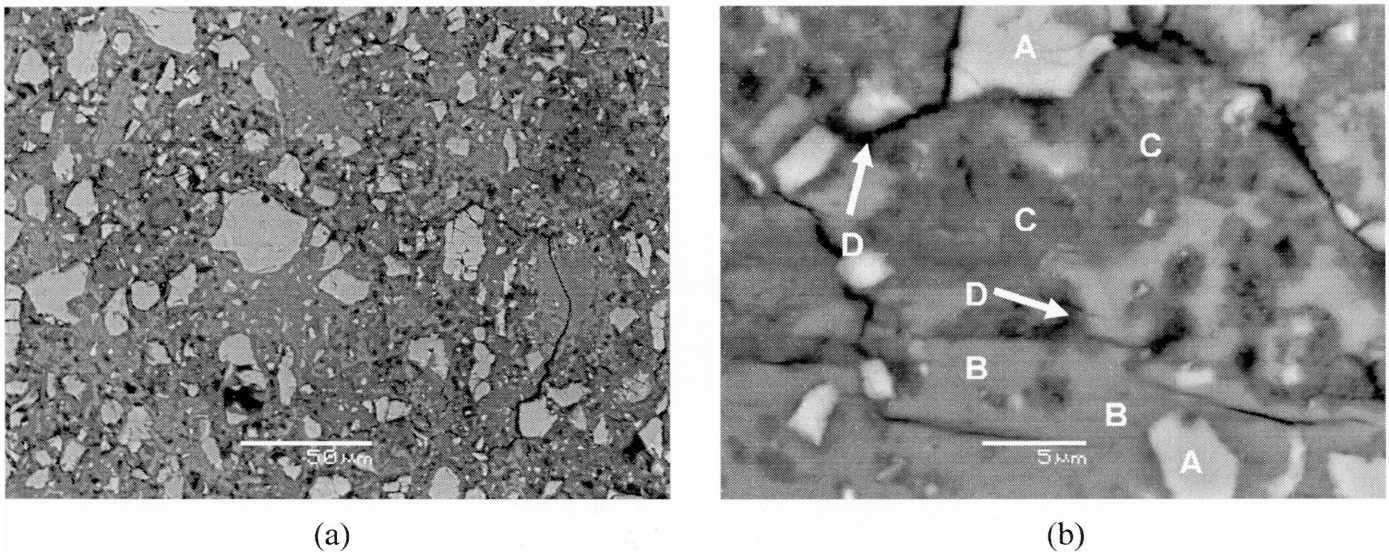
Figure 2-10 Backscattered electron images of OPC sample at day 1. (a) Overall view and (b) transition between CH-rich islands at the bottom and surrounding area at the top showing (A) unhydrated phases, (B) CH, (C) OHP (other hydration product, which is mainly CSH), and (D) porosity.

The differences in the precipitation behaviour of CH at early curing times between OPC and C_3S samples may be explained by a combination of factors. The dissolution of free calcium oxide, sodium oxide, and potassium oxide present in OPC results in a higher pH and larger OH^- concentrations in the pore water of OPC compared to that of C_3S [4]. Because of the common ion effect (OH^-), the solubility of CH is lower in OPC, which probably results in a larger number of CH nucleation centres in OPC compared to C_3S. In C_3S, the lower number of nucleation centres favours the growth of large CH-rich islands, whereas the large number of nucleation centres in OPC explains the more uniform precipitation of CH throughout the entire sample and limits the size to

which the CH-rich islands can grow. Moreover, the diffusion of dissolved Ca towards the CH-rich islands, which is required for their growth, is hindered in OPC by the presence of CH and additional hydration products (such as ettringite and monosulfate) in the pore space surrounding the islands. By contrast, the large open spaces in the porous regions of the C_3S samples (see Figures 2-6c and 2-7c) facilitate the diffusive transport of Ca towards the CH-rich islands, thus favouring their growth.

Another difference between C_3S and OPC samples is the much greater abundance of separated hydration shells (Hadley grains) [4, 13, 14, 16, 27, 28] in the OPC sample at early times (Figure 2-11). Separated hydration shells have been linked to the formation of an amorphous hydration product of C_3A and gypsum on the surface of cement grains, which may inhibit the precipitation of CSH directly on the grain surface [13]. Big cement grains tend to be surrounded by a thin CSH shell, whereas the cores of small grains eventually disappear, leaving hollowed hydration shells. Interestingly, some separated hydration shells were also observed, although less frequently, in the C_3S samples (Figure 2-12) in spite of the fact that C_3A and gypsum were absent from these samples. This observation is also consistent with previous findings [4].

As curing time increased, the distinction between CH-rich islands and the rest of the sample progressively disappeared as a result of the following transformations: large C_3S grains originally embedded in CH-rich islands partially hydrated and became covered by shells of smooth-textured CSH, small C_3S grains were completely converted to CSH, and the pore space in the surrounding regions was gradually filled with irregularly textured CSH (Figure 2-13). The hydration of C_3S grains contained in the

early CH-rich islands proceeded faster for OPC than for pure C_3S, probably because the islands were smaller in OPC than in C_3S.
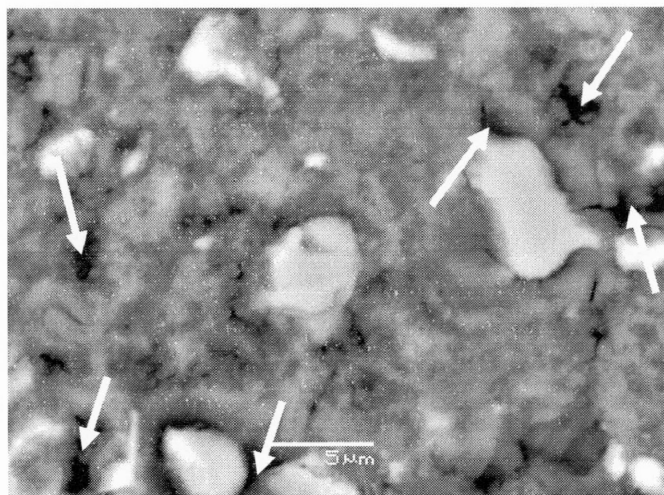
Figure 2-11 Backscattered electron image of OPC samples at day 1 showing abundant separated hydration shells (indicated by arrows).
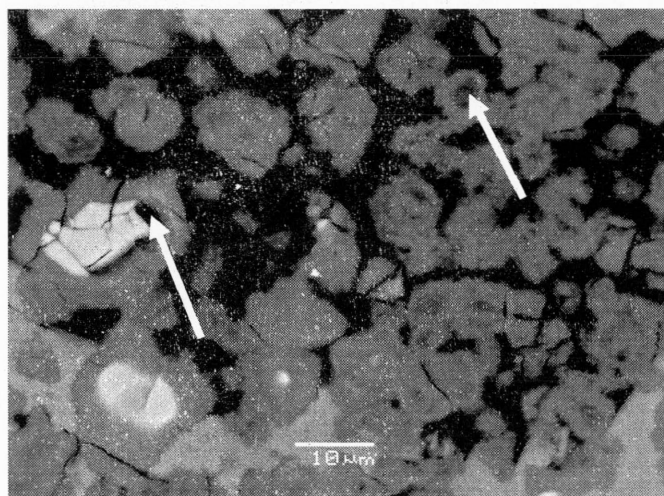
Figure 2-12 Backscattered electron image of C_3S samples at day 56 showing the existence of some separated hydration shells (indicated by arrows).
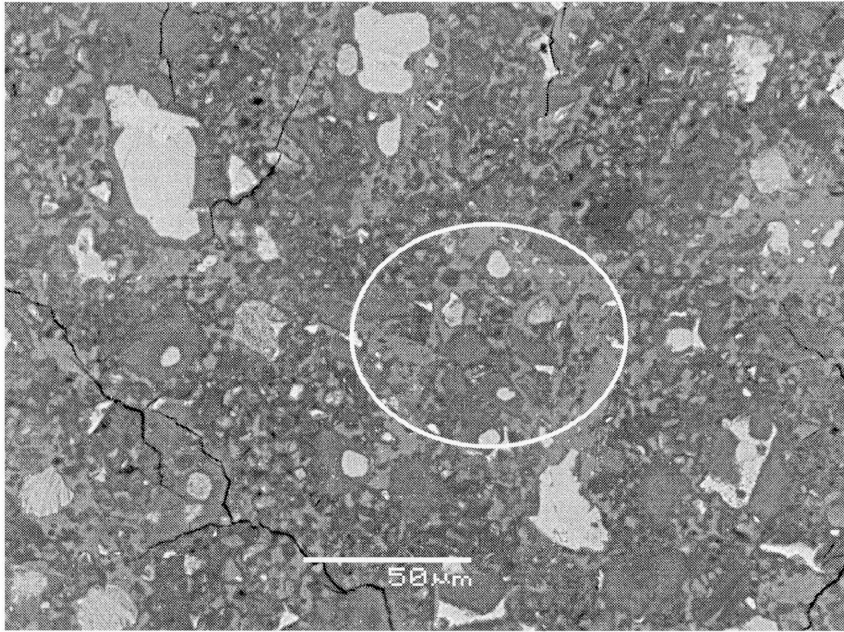
Figure 2-13 Backscattered electron image of OPC sample at day 56 showing the initially formed CH island in circle.

Figure 2-14 shows the phase distribution in hydrated OPC sample after 1, 7 and 56 days of curing. The phase named OHP (other hydration products) is mainly composed of CSH with minor components such as ettringite and monosulfate, which are usually intermingled with CSH [14]. The amount of unhydrated cement (UC) and the porosity decreased from day 1 to day 56, whereas the amount of CSH increased. The amount of CH remained approximately constant (within statistical error) between day 1 and day 56, thus indicating that very little CH if any was formed after day 1. These results are generally similar to those obtained in pure C_3S samples (Figure 2-9), except that the porosity is much lower in OPC than in pure C_3S (by 5 times or more) at each curing time. The lower porosity in OPC is attributable to a combination of the lower water-to-cement

ratio (0.4 in OPC versus 0.6 in pure C_3S) and the abundant precipitation of CH in the pores surrounding the CH-rich islands in OPC.
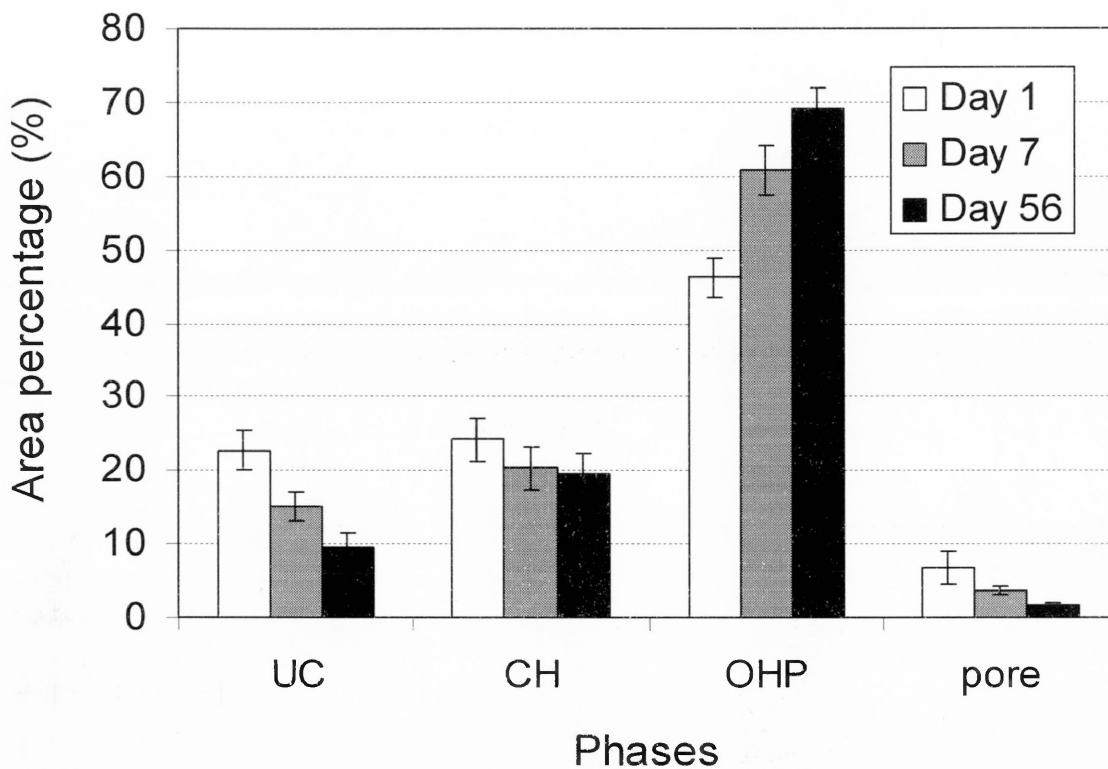
Figure 2-14 Overall phase distributions of OPC samples at day 1, 7 and 56 (UC: unhydrated cement, CH: calcium hydroxide, and OHP: other hydration products). The bar heights were obtained by averaging the results of grey level analysis on 10 different BSE images each covering an area of 254×190 μm at an image scale of 0.198 μm / pixel. Standard deviations appear as error bars.

2.3.2.3. WPC

The microstructure in WPC was generally similar to that of OPC of the same age. CH-rich islands were visible BSE images of WPC at day 1, but the C_3S grains embedded in these islands appeared to have thicker rims of CSH than those in the OPC samples

(Figure 2-15a). This is consistent with the larger degree of hydration measured for WPC samples at day 1 (Figure 2-3). At longer curing times, CH-rich islands were no longer distinguishable in either WPC or OPC images (Figure 2-15 b). Separated hydration shells were also abundant in WPC samples at day 1. The phase distributions of WPC samples (Figure 2-16) were generally similar (within statistical variability) to those of OPC samples of the same age. Comparing the phase distributions of WPC samples (Figure 2-16) and OPC samples (Figure 2-14) shows that the OHP content was higher in OPC (69.2 $\pm$ 2.7%) than in WPC (63.8 $\pm$ 2.3%) at day 56. By contrast, the CH content was lower in OPC (19.4 $\pm$ 3.0%) than in WPC (23.1 $\pm$ 2.7 %). Both differences are significant at a confidence level higher than 99.9% by Student's T-tests. These differences may explain why the measured FNEW value for WPC (0.209 $\pm$ 0.003) is lower than that for OPC (0.235 $\pm$ 0.006), since the water/calcium mole ratio is 2.3 in CSH [29] but only 1.0 in CH.
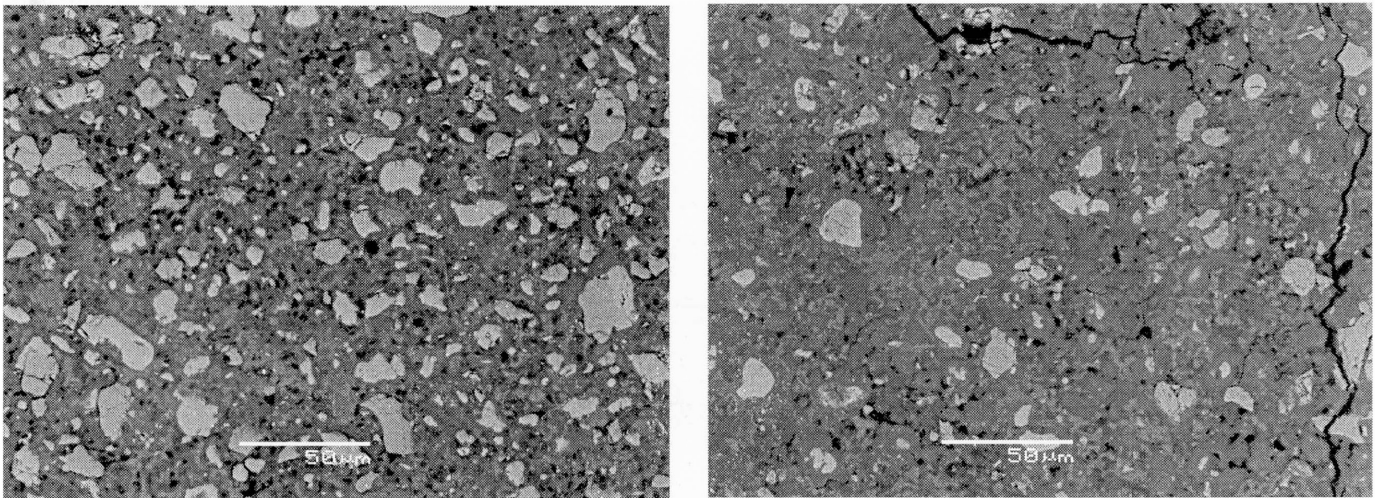
| (a) | (b) |

Figure 2-15 Backscattered electron images of WPC samples at (a) day 1 and (b) day 56.
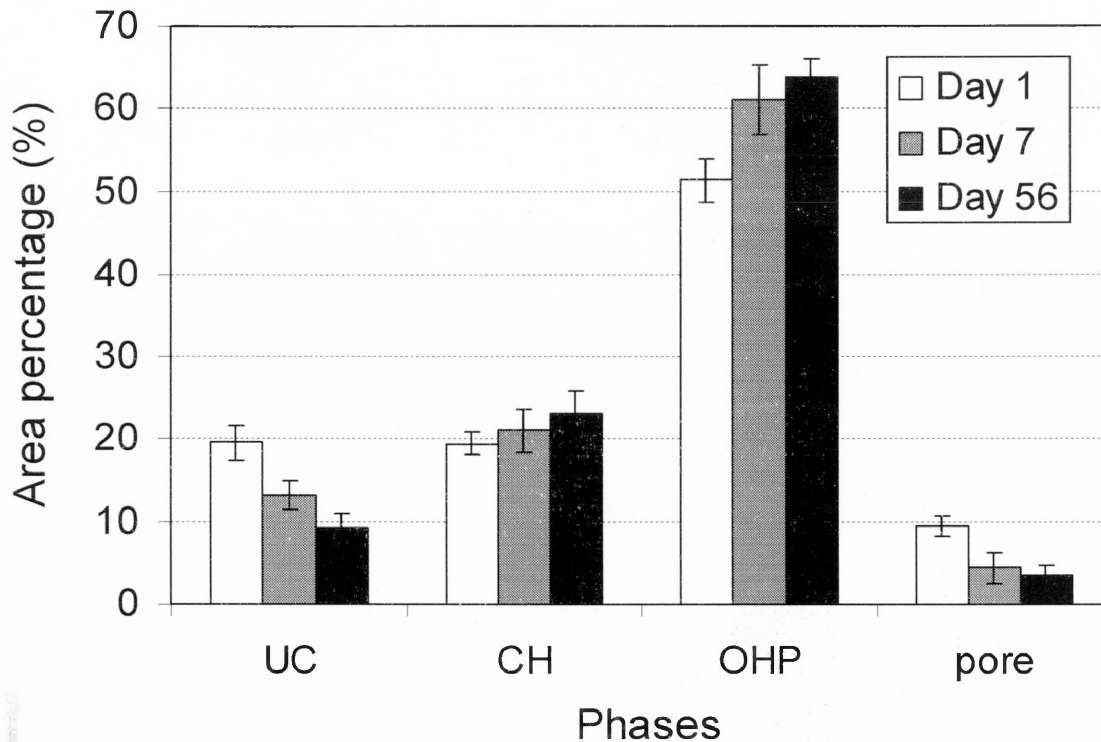
Figure 2-16 Overall phase distributions of WPC samples at day 1, 7 and 56 (UC: unhydrated cement, CH: calcium hydroxide, and OHP: other hydration products). The bar heights were obtained by averaging the results of grey level analysis on 10 different BSE images each covering an area of 254×190 μm at an image scale of 0.198 μm / pixel. Standard deviations appear as error bars.

2.4. Conclusions

1. The ratios of non-evaporable water content in fully hydrated OPC and WPC are 0.235 ± 0.006 and 0.209 ± 0.003, respectively.

2. C_3S has a higher degree of hydration than OPC and WPC at any given time. WPC hydrates faster than OPC during the first day, but both reach the same degree of

hydration (80%) at day 56. The early rate of hydration is positively correlated with the C_3S and C_3A contents.

3. Pure C_3S hydrates by forming dense CH-rich islands containing a large proportion of unhydrated C_3S grains surrounded by porous regions mainly composed of residual C_3S particles and CSH.

4. The amount of CH-rich islands in C_3S increases from day 1 to day 7 but reaches a plateau at around day 7. Precipitation of CSH and some CH in the porous regions accounts for the increase in sample hydration after day 7.

5. OPC samples contain CH-rich islands at day 1, but these islands are much smaller that in pure C_3S samples. As curing time increases, the distinction between CH-rich islands and the rest of the sample progressively disappears as a result of the hydration of the large C_3S grains originally embedded in CH-rich islands and the precipitation of irregularly textured CSH in the porous regions.

6. The evolution of the microstructure of WPC during hydration is similar to that of OPC, except that C_3S grains embedded in CH islands in WPC samples have thicker CSH rims than those in OPC samples, consistent with the larger degree of hydration of WPC at early times.

7. Separated hydration shells (Hadley grains) are more prevalent in OPC and WPC than in pure C_3S.

8. The overall hydration stoichiometries for C_3S, OPC and WPC are not constant over time: initially the hydration reactions produce both CH and CSH, but at later times the production of CH almost ceases while the formation of CSH continues.

2.5. Acknowledgement

2.6. References

[1] S. Mindness, J. F. Young, Concrete, Prentice-Hall, Inc, Englewood Cliffs, NJ, 1981.

[2] Portland cement association, http://www.cement.org/decorative/overview.asp (accessed in July, 2007).

[3] B.S. Hamad, Investigations of chemical and physical properties of white cement concrete, Advn Cem Bas Mat 2 (1995) 161-167.

[4] K. O. Kjellsen, H. Justnes, Revisiting the microstructure of hydrated tricalcium silicate-a comparison to Portland cement, Cem. Concr. Composites 26 (2006) 947-956.

[5] K. O. Kjellsen, L. Fjällberg, Measurements of the degree of hydration of cement paste by SEM, ^{29}Si NMR and XRD methods, Workshop on water in cement paste & concrete hydration and pore structure, Skagen, Denmark 7.& 8. October 1999.

[6] J. E. Ash, M. G. Hall, J. I. Langford, M. Mellas, Estimations of degree of hydration of Portland cement pastes, Cem. Concr. Res. 23 (1993), 399-406.

[7] L. J. Parrott, M. Geiker, W. A. Gutteridge, D. Killoh, Monitoring Portland cement hydration: comparison of methods, Cem. Concr. Res. 20 (1990) 919-926.

[8] J. Greener, H. Peemoeller, C. Choi, R. Holly, E. J. Reardon, C. M. Hansson, M. M. Pintar, Monitoring of hydration of white cement paste with proton NMR spin-spin relaxation, J. Am. Ceram. Soc. 83 (2000) 623-627.

[9] S. Igarashi, M. Kawamura, A. Watanabe, Analysis of cement pastes and mortars by a combination of backscatter-based SEM image analysis and calculations based on the Powers model, Cem. Concr. Composites 26 (2004) 977-985.

[10] L. E. Copeland and J. C. Hayes, Determination of non-evaporable water in hardened Portland-cement paste, ASTM bulletin, 1953.

[11] M. C. G. Juenger, H. M. Jennings, Examining the relationship between the microstructure of calcium silicate hdyrate and drying shrinkage of cement pastes, Cem. Concr. Res. 32 (2002) 289-296.

[12] L. J. Parrott, M. Geiker, W. A. Gutteridge, D. Killoh, Monitoring Portland cement hydration: comparison of methods, Cem. Concr. Res. 20 (1990) 919-926.

[13] K. L. Scrivener, Backscattered electron imaging of cementitious microstructures: understanding and quantification, Cem. Concr. Composites 26 (2004) 935-945.

[14] S. Diamond, The microstructure of cement paste and concrete-a visual primer, Cem. Concr. Res. 26 (2004) 919-933.

[15] K. L. Scrivener, Microscopy methods in cement and concrete science, World Cement Research and Development, Sept 1997, 92-112.

[16] K. L. Scrivener, H. H. Patel, P. L. Pratt, L. J. Parrott, Analysis of phases in cement paste using backscattered electron images, methanol adsorption and thermogravimetric analysis, Mater. Res. Soc. Symp. Proc. 85 (1987) 67-76.

[17] ASTM C150-04a, Standard specification for Portland cement (2004).

[18] N. B. Milestone, Hydration of tricalcium silicate in the presence of lignosulfonates, glucose, and sodium gluconate, J. Am. Ceram. Soc. 62 (1979) 321-324.

[19] H. F. W. Taylor, Cement Chemistry, Academic Press Inc, San Diego, CA 92101, 1990.

[20] Design and control of concrete mixtures, seventh Canadian edition, Cement association of Canada, 2002.

[21] K. O. Kjellsen, R. J. Detwiler, O. E. Gjorv, Backscattered electron image analysis of cement paste specimens: specimen preparation and analytical methods, Cem. Concr. Res. 21 (1991) 388-390.

[22] Image-Pro Plus Version 5.0, Copyright 1993, 2003 Media Cybernetics, Inc.

[23] Standard test method for density of hydraulic cement, ASTM C 188-95, re-approved 2003.

[24] J. D. Birchall and N. L. Thomas, The mechanism of retardation of setting of OPC by sugars, Br. Ceram. Proc. 35 (1984) 305-315.

[25] http://www.freshpatents.com/Use-of-particular-polysaccharides-as-admixtures-for-mineral-materials-dt20060316ptan20060054062.php?type=description (accessed July, 2007).

[26] R. L. Berger and J. D. Mcgregor, Effect of temperature and water-solid ratio on growth of calcium hydroxide crystals formed during hydration of C_3S, J. Am. Ceram. Soc. 56 (1973) 73-79.

[27] D. W. Hadley, The nature of the paste-aggregate interface, Ph.D. thesis, Purdue University, 1972.

[28] D. W. Hadley, W. L. Dolch, S. Diamond, On the occurrence of hollow-shell

hydration grains in hydrated cement paste, Cem. Concr. Res. 30 (2000) 1-6.

[29] J. F. Young, W. Hansen, W., Volume Relationships for CSH Formation Based on

Hydration Stoichiometry, Materials Research Society Symp. Proc. 85 (1987) 313-

322.

CHAPTER 3

EFFECT OF SUCROSE AND SORBITOL ON THE HYDRATION AND MICROSTRUCTURE OF ASTM TYPE I ORDINARY PORTLAND CEMENT, WHITE PORTLAND CEMENT, AND TRICALCIUM SILICATE

Summary: The effect of a small amount of sucrose (0.037 or 0.15 wt%) or sorbitol (0.40 wt%) on the hydration and microstructure of ASTM Type I ordinary Portland cement (OPC), white Portland cement (WPC) and tricalcium silicate (C_3S) were investigated by loss-on-ignition tests and scanning electron microscopy (SEM) as a function of curing time. For a given concentration of sucrose or sorbitol, the retardation period was longer in OPC (3-7 days) than in WPC (1-3 days). Calcium hydroxide (CH) precipitated first and before calcium silicate hydrate (CSH) in un-set samples, and later formed dense CH-rich islands that shielded unhydrated C_3S grains. These islands persisted in all the set samples, but they were more prominent in pure C_3S than in OPC or WPC. There is a range of sucrose and sorbitol concentrations in which the effects of these compounds on both the hydration rate and microstructure are only temporary. This range is lower for C_3S than for OPC and WPC when sucrose is added. Sucrose affected the initial hydration and microstructure of C_3S much more than that of OPC and WPC. By contrast, sorbitol had a more consistent effect on all the samples and less impact on the initial hydration and microstructure of pure C_3S than sucrose. All the OPC and WPC samples reached degrees of hydration higher than 77% and strengths higher than 27.6 MPa (4000 psi) after 56 days. OPC containing 0.40 wt%

sorbitol had significantly higher strength and degree of hydration than the other samples at 56 days.

3.1. Introduction

Ordinary Portland cement (OPC) is a fundamental component of most concretes. Raw OPC has five main components: tricalcium silicate (C_3S); dicalcium silicate (C_2S); tricalcium aluminate (C_3A); tetracalcium aluminoferrite (C_4AF); and calcium sulfate (gypsum or anhydrite). Once contacted with water, C_3A reacts with sulfate coming from the dissolution of gypsum to form ettringite (AFt) and monosulfate (AFm), thus preventing the flash set produced by the formation of calcium aluminate hydrates. C_3S and C_2S undergo hydration to form calcium hydroxide (CH) and calcium silicate hydrate (CSH), which are the main hydration products and the principal contributors to cement strength. C_3S is more reactive and has a higher exothermic heat of formation than C_2S. As a result, C_3S and C_2S are largely responsible for the early and late stages, respectively, of hydration and strength development [1, 2]. White Portland cement (WPC) contains significantly fewer transition metal oxides (iron, manganese and others) than OPC and thus, once cured, has a brilliant white appearance that is advantageous for decorative applications as well as reflective flooring and roadway infrastructure [3].

For certain applications such as transporting cement-stabilized waste long distances by truck, the normal setting process could be too rapid and cause operational difficulties. In these situations, controlling the setting rate with chemical retarders is desirable. Many chemical admixtures have the ability to slow down the cement hydration reactions [4-15]. Among commonly used retarders, sucrose (table sugar) is one of the most effective; the addition of 0.075 wt % sucrose to OPC increases the induction period of hydration from 2.5 to 31 hours [9]. Many studies have investigated the mechanisms of set-retardation in cement pastes containing sucrose [4, 7, 8, 9, 12, 13, 14, 16, 17]. Although the details of these mechanisms are still unknown, it is generally recognized that sucrose plays an important role in preventing the precipitation of Ca and Si present in pore solution by poisoning the growth surface of early hydration products or the surface of C_3S particles [4, 7, 8, 12, 14]. It has been proposed [4, 12] that the poisoning agent is a sucrose-calcium half salt [R-O$^-$...Ca$^+$-OH] that adsorbs onto growing CH nuclei via its pendant Ca(OH)$^+$ group, thus inhibiting further deposition of calcium and hydroxide ions. The precipitation of CSH gel, which relies on the deposition of silica on an existing CH lattice, could be similarly inhibited by poisoning of the CH surface. In addition to retarding the setting of cement, sucrose may alter the microstructure of hydrated OPC paste by increasing the specific surface area and modifying the pore size distribution [18].

Sucrose does not bind significantly with silicon in solution [4, 12], but sorbitol, which is a sugar alcohol and a weaker retarder [19], can react with silicon to form stable five- or six-coordinated silicon polyolate complexes in high pH surroundings [20]. To the best of the author's knowledge, no investigation has been reported previously of the effects of silicon binders on the hydration and microstructure of cement. Sorbitol is usually

employed as a water-reducing plasticizer (superplasticizer) in cement admixtures [19, 21]; that is, it decreases the water needed to make the cement workable which, in turn, enhances its strength [22]. Sorbitol has been reported to prevent the nucleation and linear growth of ettringite owing to chelation of calcium and possibly aluminium ions that are incorporated into the crystal, thus shielding ettringite from further growth [21]. However, even if sorbitol-calcium complexes may exist, the interaction between sorbitol and calcium ions is very weak (pK_{a1} = 13.6) [23].

The objectives of this research were to explore the effects of a small addition of sucrose or sorbitol on the degree of hydration and microstructure of ASTM Type I OPC and WPC as a function of time[1]. To facilitate the interpretation of the results, the microstructure of a much simpler system — pure tricalcium silicate (C_3S) — was also investigated for comparison. Because the composition of WPC is intermediate between that of C_3S and OPC (Table 3-1), these three systems provide increasing degrees of compositional complexity, with pure C_3S and OPC being the least and most complex, respectively.

3.2. Materials and methods

3.2.1. Sample Preparation

ASTM C 150 Type I ordinary Portland cement (CEMEX Inc., Charlevoix, MI), ASTM C150 Type I white Portland cement (Aalborg Portland, Aalborg, Denmark), and pure tricalcium silicate (CTL Group, Skokie, IL) were used in this research. Both the OPC

---

[1] The effects of arabitol (a silicon binder) on the hydration of OPC and on the microstructure of C_3S were also investigated; the results are displayed in Appendices B and C.

and WPC conform to the ASTM C150 standard for Type I cement which specifies

compositional and physical requirements, including loss-on-ignition, insoluble residue,

setting time, strength and air content [24]. The manufacturers' specifications for all three

cements are provided in Table 3-1. The C_3S was crystallographically-pure triclinic alite,

with reported traces of Al_2O_3 and MgO, at 325 mesh. (Particles measure less than 44 μm.)

Table 3-1 Chemical and physical analysis and potential compound compositions of

unhydrated OPC, WPC, and C_3S samples

	OPC (Gray)	WPC (White)	PureC₃S
Chemical composition (wt%)			
SiO_2	19.35	24.5	26.3
Al_2O_3	5.16	2.1	traces
Fe_2O_3	2.47	0.34	0
CaO	62.60	69.0	73.7
MgO	3.48	0.59	traces
SO_3	3.57	2.13	0
Loss-on-ignition (wt%)	1.52	0.5	na^a
Insoluble residue (wt%)	0.15	0.08	na
Alkalies as Na_2O eq. (wt%)	0.85	0.19	0
Blain fineness (m^2/kg)	378	393	na
Potential compound composition (wt.%)			
C_3S	60	74	100
C_2S	11	14	0
C_3A	10	5	0
C_4AF	8	1	0

a. *na* = not applicable

Reagent grade sucrose and sorbitol were dissolved in deionised water at concentrations ranging between 0 and 10 g/L. The solutions were pre-cooled to 10 °C and then mixed with kilogram quantities of OPC and WPC at a water-to-cement mass ratio of 0.40:1 in a plastic bowl immersed in an ice-water bath. (Temperature control was necessary with such large samples to counteract the heat generation at early times. Some mixtures – most notably those containing sorbitol – released more heat than others.) The mixtures were stirred with a plastic spoon for about 7 min until they were homogeneous. All the samples were slurries after being mixed with water, especially those with the addition of sorbitol. They were then poured into either polyethylene ice cube trays (WPC) or 5.08 × 10.16 cm (2×4 inch) PVC cylinders (WPC and OPC). The cylinders were filled in two successive layers, and each layer was tamped 50 times to minimize the entrapment of air bubbles. Next, the samples were placed in triple-sealed air-tight polyethylene bags, and immersed in a water bath at room temperature (20-22 °C) to cure. WPC samples cured in ice trays were used for loss-on-ignition testing after 1, 3, 7, 14 and 28 days of curing. All tests were carried out in triplicate, except at day 1. WPC cylinder samples were used for seven replicate strength tests and three replicate loss-on-ignition tests at 56 days of curing. OPC samples were used for triplicate loss-on-ignition tests at day 3, 7, 14, 28 and 56, triplicate strength tests at day 56, and a further loss-on-ignition test at day 1.

Due to low material availability, much smaller quantities were used of C_3S. Samples were placed in separate 8 ml polyethylene plastic bottles. In each bottle, 1.20 g C_3S was blended with 0.72 ml deionised-distilled water at a water-to-solid mass ratio of 0.60:1 [15]. The slurry was then mixed with a small glass stir rod for 30 seconds. In order

to prevent carbonation, all the preparation steps were done in a glove box under nitrogen. Samples were sealed in plastic bottles and cured at room temperature until testing.

Table 3-2 shows the composition of all the samples. The letters "O", "W", and "C" in the batch names represent OPC, WPC, and C_3S, respectively. Sucrose and sorbitol contents ranged from 0 to 0.40 wt%.

Table 3-2 Sample compositions

Batch name	Binder	Sorbitol/sucrose content (wt% of cement)
O_Control	OPC	0
O_Sorbitol	OPC	0.40
O_Sucrose low	OPC	0.037
O_Sucrose high	OPC	0.15
W_Control	WPC	0
W_Sorbitol	WPC	0.40
W_Sucrose low	WPC	0.037
W_Sucrose high	WPC	0.15
C_Control	C_3S	0
C_Sorbitol	C_3S	0.40
C_Sucrose low	C_3S	0.037
C_Sucrose high	C_3S	0.15

3.2.2. Loss-on-ignition Testing

Loss-on-ignition testing was performed to determine the degree of hydration of OPC and WPC samples. A small portion of each sample was crushed, and 1.0 to 1.5 g of

the 850-2000 μm fraction was oven-heated for 24 h at 105 °C to remove evaporable water and obtain the evaporable water-free mass, W_{105}. Next, the temperature was increased and maintained at 1005 °C for 2 h to determine the fully dehydrated mass, W_{1005}. The degree of hydration α_{LI} was calculated as follows [1, 25],

$$\alpha_{LI} = (W_{105} - W_{1005})/(cW_{1005}) \qquad (3\text{-}1)$$

in which the constant c is the fraction of non-evaporable water content in fully hydrated cement. The value of c was determined to be 0.234_9 for OPC and 0.208_6 for WPC (Chapter 2).

3.2.3. Strength Testing

Strength tests were carried out after the OPC and WPC samples had been cured for 56 days. Immediately after they were removed from the moulds, sample cylinders were capped top and bottom with sulfur according to ASTM C617-98 [26], and the unconfined compressive strength was measured according to ASTM C109 [27][2].

3.2.4. SEM-EDS Analyses

After reaching the desired curing time, a small slice (*ca.* 0.5 g) was removed from the inner part of the sample, immersed for 24 h in acetone to halt hydration [28], dried at 105 °C for 15 min, and then imbedded in epoxy resin. A thin-section was cut, lapped, and polished using oil-based media so as not to alter the water-soluble minerals. After carbon-

---

[2] Considering the large number of samples and the elevated cost of the cubic moulds, PVC cylinders were selected for curing samples for strength testing. Preliminary test results demonstrated that after capping the cylindrical samples with sulfur, the standard errors for both shapes of samples were comparable.

coating, it was analyzed with a JEOL JSM 5900 scanning electron microscope in backscattered electron (BSE) mode to improve contrast between different mineral phases [29, 30]. The elemental composition of the phases was determined by X-ray energy dispersive spectrometry (EDS) using an Oxford Link ISIS system (50 s live-time). SEM-EDS analyses were carried out on days 1, 7 and 56 for all the OPC, WPC and C_3S samples.

3.3. Results

3.3.1. Degree of Hydration

3.3.1.1. Ordinary Portland Cement (OPC)

Figure 3-1 depicts the effects of sucrose and sorbitol on the degree of hydration of OPC as a function of time, determined by loss-on-ignition testing. The addition of 0.037 wt% sucrose (O_Sucrose low) did not significantly retard the hydration of OPC. A higher amount of sucrose (O_Sucrose high) only led to a temporary retardation period of less than 7 days. At day 56, there was no statistically significant difference between the degree of hydration of O_Sucrose high ($80.2_9 \pm 0.8_3$ %) and O_Control ($81.0_1 \pm 0.8_2$%). Adding 0.40 wt% sorbitol (O_Sorbitol) also caused a retardation of OPC hydration before day 7 and acceleration between day 7 and day 14. At day 56, O_Sorbitol had a higher degree of hydration ($84.1_0 \pm 0.4_1$ %) than O_Control ($81.0_1 \pm 0.8_2$ %) with a confidence level of 99% by Student's T-test.
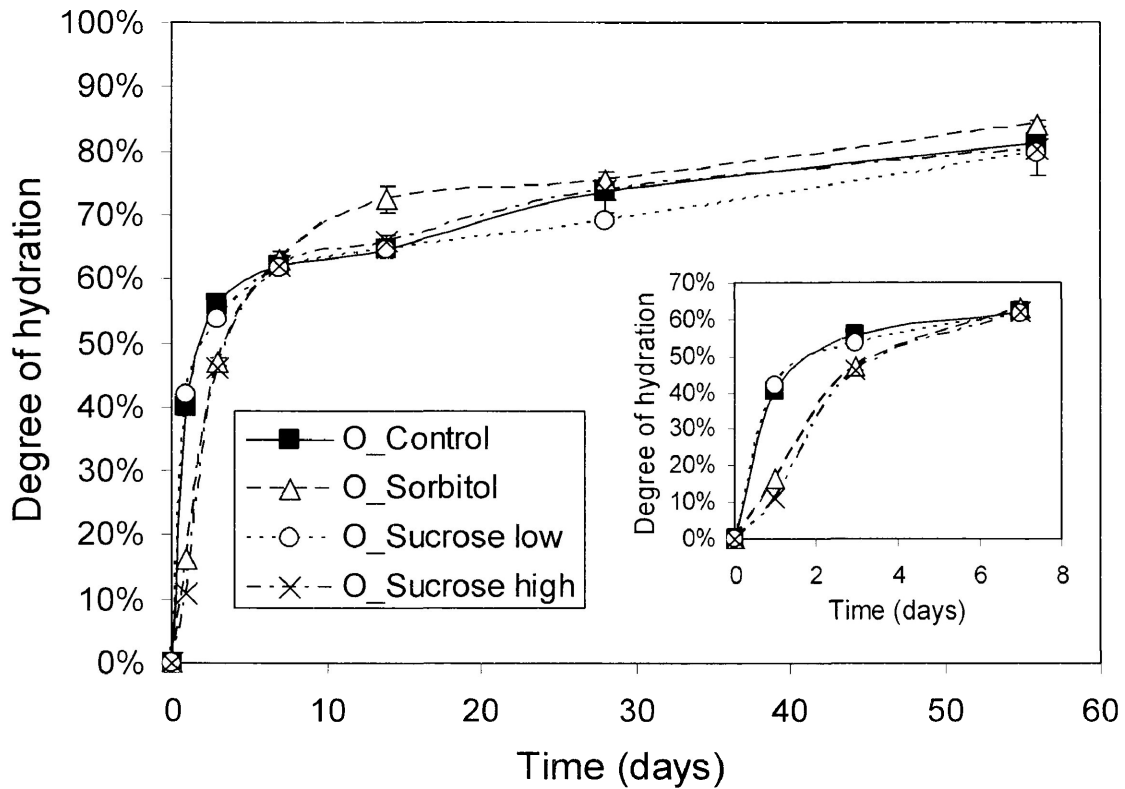
Figure 3-1 Effect of sucrose and sorbitol on the degree of hydration of OPC. The expanded

graph shows the details for the first 8 days. Error bars correspond to standard deviations

over three measurements. In many cases, the error bars are too short to be seen.

3.3.1.2. White Portland Cement (WPC)

The effects of sucrose and sorbitol on the degree of hydration of WPC as a function

of time, determined by loss-on-ignition testing, are shown in Figure 3-2. The retardation

effect was more short-lived in WPC (less than 3 days) than in OPC when either high

sucrose or sorbitol was added. (Compare the expanded graphs in Figures 3-1 and 3-2).

However, low sucrose delayed the hydration of WPC, but not that of OPC. At day 1, high

sucrose did not decrease the hydration degree of WPC (32.0_9 %) as much as that of OPC

(10.9_0%). The addition of sorbitol, however, affected the hydration of both cements

similarly (OPC, $16.3_4\%$; WPC, $17.0_8\%$). The degree of hydration at day 3 in all the WPC

samples was nearly 65%, which was higher than that measured in any OPC sample.
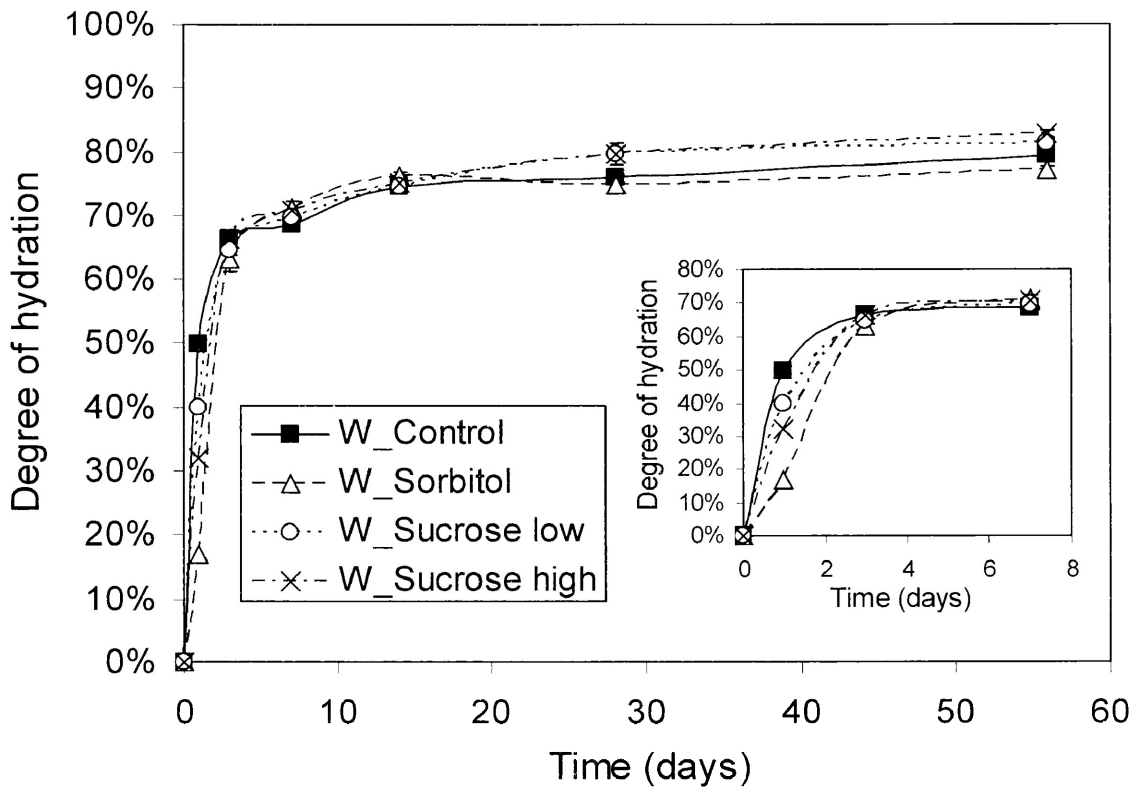
Figure 3-2 Effect of sucrose and sorbitol on the degree of hydration of WPC. The expanded

graph shows the details for the first 8 days. Error bars correspond to standard deviations

over three measurements. In many cases, the error bars are too short to be seen.

After 14 days of curing, all WPC samples reached approx. 74% degree of hydration.

At that time, the two sucrose samples were slightly more hydrated than the Control and

Sorbitol samples (at more than 80% confidence level by Student T-test).

Comparison of the 56-day hydration data for OPC and WPC (Figures 3-1 and 3-2)

shows that O_Control and W_Control both attained roughly 80% degree of hydration.

However, O_Sorbitol hydrated significantly more than W_ Sorbitol (84.1_0 versus $77.4_0\%$ at

a 96% confidence level). By contrast, O_Sucrose high hydrated less than the W_Sucrose high (80.2$_9$ versus 82.9$_7$% at a 98% confidence level), while the difference between O_Sucrose low and W_Sucrose low is not statistically significant.

3.3.2. Strength

Figures 3-3 and 3-4 depict the average 56-day strength of OPC and WPC with and without adding sucrose or sorbitol[3]. Strength data are closely correlated to hydration data. Adding 0.40 wt% sorbitol increased the strength of OPC at day 56 at 81% confidence level by Student T-test. This result reflects the fact that the degree of hydration of O_Sorbitol was higher than that of O_Control after 56 days curing, and it is also consistent with previous research [19] showing that sorbitol improves the 28-day strength of OPC. By contrast, low and high sucrose decreased the 56-day strength only slightly.
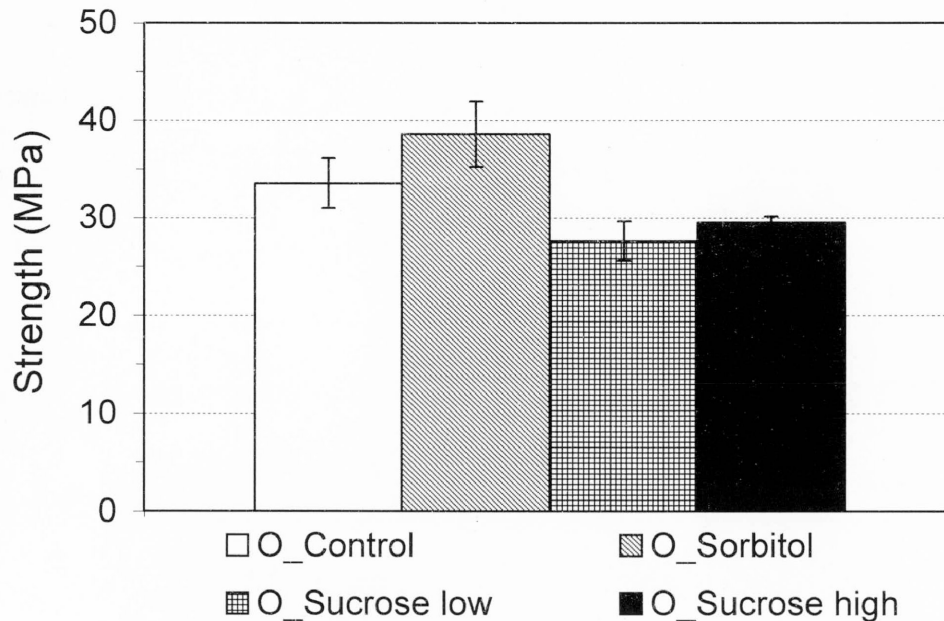
Figure 3-3 Effect of sucrose and sorbitol on the strength of OPC at day 56. Error bars correspond to the standard deviations over three measurements.

---

[3] The compressive strength of OPC samples with and without the addition of sucrose, sorbitol and arabitol was also tested at days 3, 7, 14 and 28. Please see Appendix D for additional strength results for OPC.

The effect of sorbitol or sucrose addition on the 56-day strength of WPC samples is shown in Figure 3-4. These effects are generally different in WPC and OPC samples. Although W_Sucrose high exhibited a somewhat higher strength than W_Control at the 82% confidence level, neither W_ Sorbitol nor W_Sucrose low differed significantly from W_Control in their 56-day strength.

Similar to the hydration data, the strengths of O_Control and W_Control at day 56 were comparable when considering experimental uncertainty. In addition, O_Sorbitol (38.6 MPa or 5594 psi) was much stronger than W_Sorbitol (29.0 MPa or 4208 psi) at a 99.99% confidence level, while O_Sucrose was weaker than W_Sucrose (at a 95% and 87% confidence levels for Sucrose low and Sucrose high, respectively). Both results are consistent with the corresponding degree of hydration data.
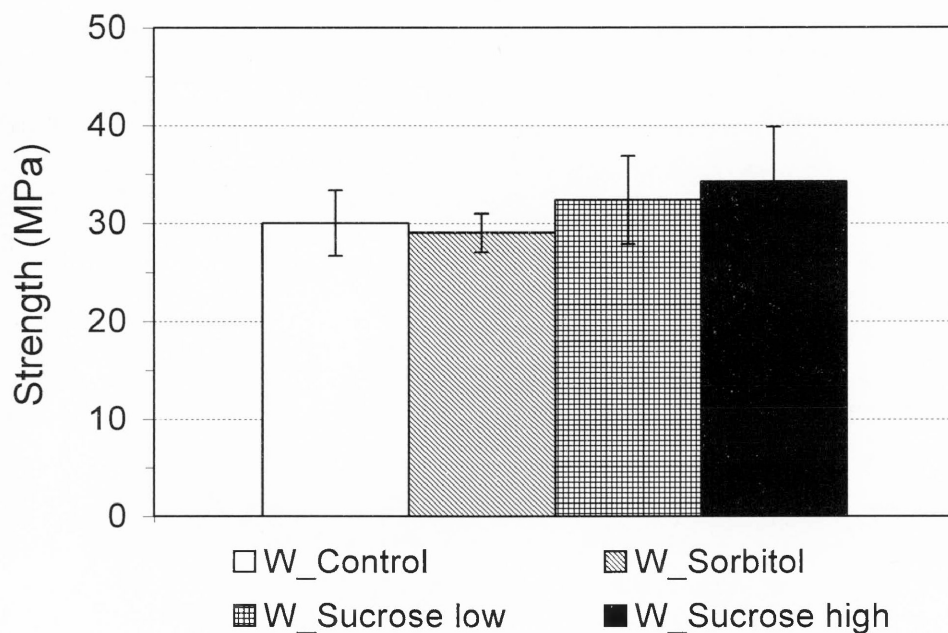
Figure 3-4 Effect of sucrose and sorbitol on the strength of WPC at day 56. Error bars correspond to the standard deviations over seven measurements.

3.3.3. Microstructure

As hydrated C_3S samples have the simplest composition, their microstructure will be presented first and then compared with that of OPC and WPC.

3.3.3.1. C_3S

The status (set or not set) of C_3S samples and the distribution of hydration products with and without the addition of sucrose or sorbitol after 1, 7 and 56 days of curing are summarized in Table 3-3.

Table 3-3 Status and distribution of hydration products for C_3S samples at days 1, 7, and 56

Sample	Day 1	Day 7	Day 56
C_ Control	Set; CH-rich islands and porous areas; diameter of CH-rich islands is 100~150 μm [Figure 3-5]	Set; CH-rich islands and porous areas; diameter of CH-rich islands is ~200 μm [Figure 3-6]	Set; CH-rich islands surrounded by CSH-rich regions and some remaining porous areas [Figure 3-7]
C_ Sucrose low	Not set; no hydration products [Figure 3-8]	Set; CH-rich islands and porous areas; diameter of CH-rich islands is 100~200 μm (similar to Figure 3-8)	Set; CH-rich islands surrounded by CSH-rich regions and some remaining porous areas (similar to Figure 3-8)
C_ Sucrose high	Not set; no hydration products (similar to Figure 3-8)	Not set; no hydration products (similar to Figure 3-8)	Not set; no hydration products (similar to Figure 3-8)
C_ Sorbitol	Not set; some CH [Figure 3-9]	Set; CH-rich islands and porous areas; diameter of CH-rich islands is 300~400 μm [Figure 3-10]	Set; CH-rich islands surrounded by CSH-rich regions [Figure 3-11]

Figure 3-5 shows typical BSE images of the C_Control sample at day 1 at different magnifications. Dense CH-rich islands consisting of bright unhydrated C_3S grains embedded in a dense calcium hydroxide matrix (light grey) are surrounded by a more porous matrix consisting mostly of unhydrated C_3S and CSH gel. These observations are similar to those by Kjellsen and Justnes [31] who used a lower water-to-solid ratio (0.40 versus 0.60 in this study). The CH-rich islands grew from day 1 to day 7 up to approximately 200 µm (Figure 3-6) without significant modification in their composition (See Chapter 2), but stopped growing thereafter. Precipitation of further CSH and some CH in the porous areas led to a significant decrease in the porosity of these areas and to bridging of CH-rich islands by day 56 (Figure 3-7).

The addition of 0.037 wt% sucrose (C_Sucrose low) delayed the hydration of C_3S, and no hydration product was visible at day 1 in BSE images (Figure 3-8). The effect of sucrose had disappeared by day 7, as indicated by the similarity of the BSE images for C_Sucrose low and C_Control. At day 56, the porous areas in C_Sucrose low were also mostly filled-in by CSH precipitates. Nevertheless, when 0.15 wt% sucrose was added (C_Sucrose high), the hydration process was drastically delayed such that no hydration product was observed during 56 days of curing.

The hydration of C_Sorbitol was also retarded but, by contrast with the sucrose samples, a small amount of elongated calcium hydroxide crystals was found at day 1 (Figure 3-9). These CH crystals formed within unhydrated C_3S clusters and were the precursors of the CH-rich dense areas. Despite the initial delay, C-Sorbitol contained larger CH-rich islands (300-400 µm) at day 7 than C_Control and C_Sucrose low (Figure 3-10).

At day 56, all the previous porous areas were mostly filled-in by CSH precipitates (Figure 3-11). The size of the CH-rich islands at day 56 in C_Sorbitol remained larger than in C_Control and C_Sucrose of the same age. Furthermore, the amount of unhydrated C_3S remaining in the CH-rich regions was higher for C_Sorbitol than for C_Sucrose low and C_Control. (Compare Figure 3-11 with Figure 3-7.) The large CH-rich regions probably impeded the diffusion of water to the embedded C_3S.
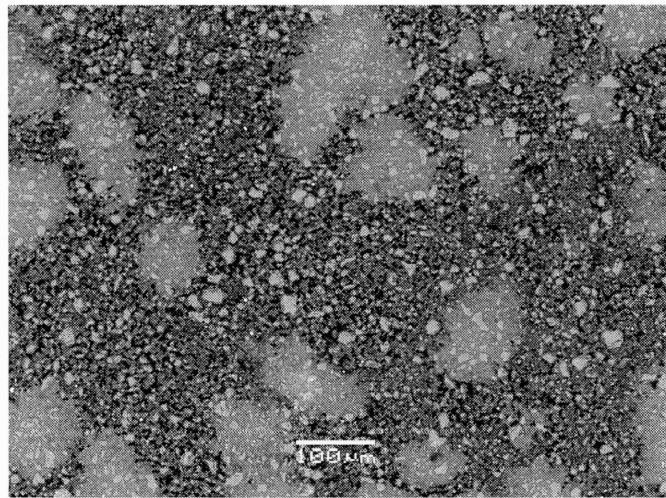
(a)
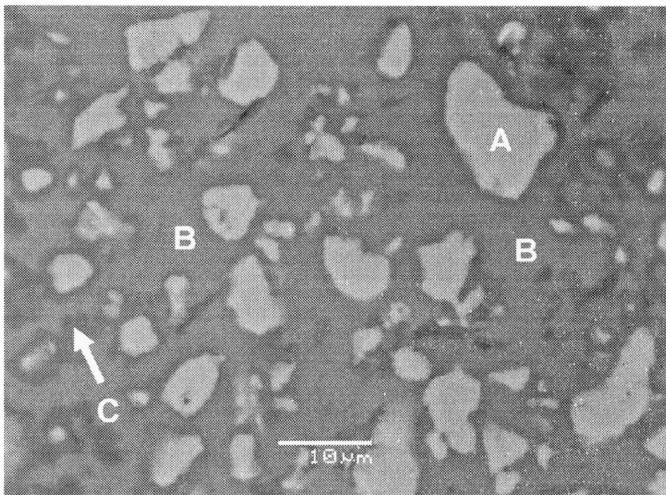
(b)
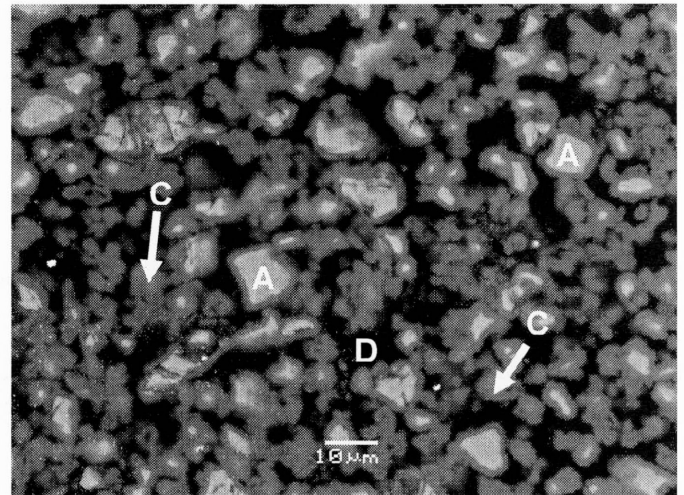
(c)

Figure 3-5 Backscattered electron images of C_Control at day 1: (a) overall view; (b) dense CH-rich islands; and (c) porous area, showing (A) C_3S, (B) CH, (C) CSH and (D) pores.

Figure 3-6 Backscattered electron image of C_Control at day 7.

Figure 3-7 Backscattered electron image of C_Control at day 56.

Figure 3-8 Backscattered electron image of C_Sucrose low at day 1. The bright particles are unhydrated C_3S.
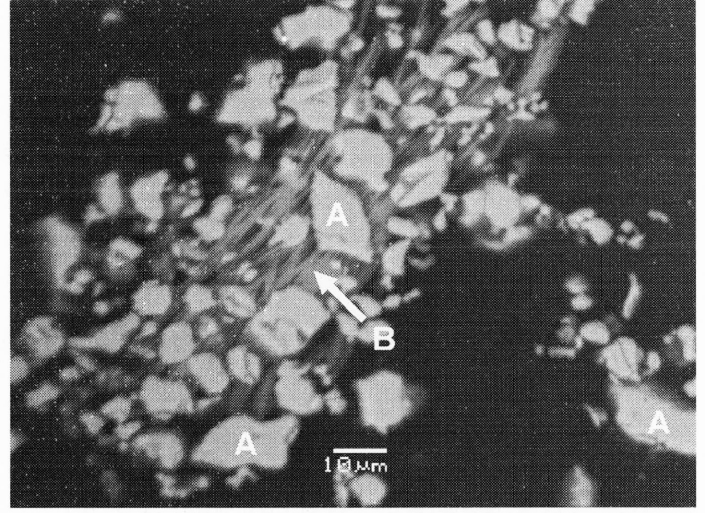
Figure 3-9 Backscattered electron image of C_Sorbitol at day 1, showing (A) C_3S and (B) CH.

Figure 3-10 Backscattered electron image of C_Sorbitol at day 7.
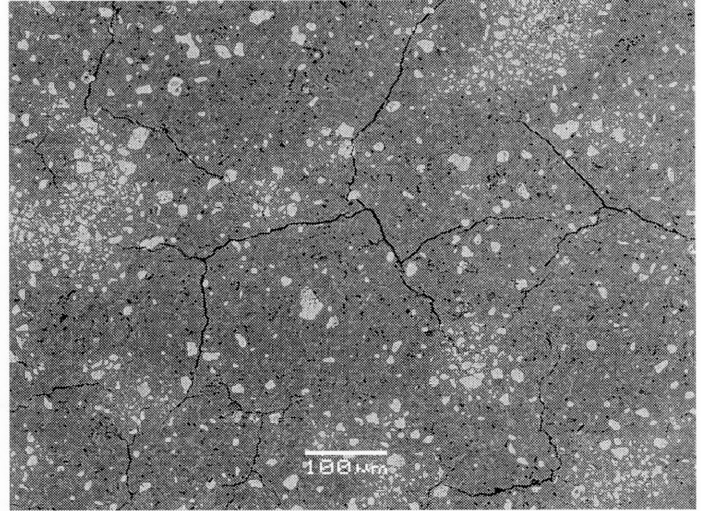
Figure 3-11 Backscattered electron image of C_Sorbitol sample at day 56.

3.3.3.2. OPC

Table 3-4 shows the status (set or not set) of OPC samples and the distribution of hydration products, with and without the addition of sucrose or sorbitol, after 1, 7 and 56 days of curing. The microstructure of O_Control has been fully described in Chapter 2. In brief, when compared to C_Control, the O_Control sample has smaller and less distinct CH-rich islands, reduced porosity, and more complex and dispersed precipitation of CH, CSH, and other hydration products such as ettringite and monosulfate (Figure 3-12). The differences in the microstructure of these two systems are likely attributable to the presence of alkalis (free calcium oxide, sodium oxide, and potassium oxide) that may affect the nucleation rate of CH and other components such as Al and Fe phases in OPC (Chapter 2). As hydration progressed in OPC, the rims of CSH covering large C_3S grains became thicker, smaller C_3S grains were completely converted to CSH, and the pore space was

gradually filled with irregularly textured CSH and freshly formed CH (Figures 3-13 and 3-14).

The addition of 0.037 wt% sucrose to OPC (O_Sucrose low) neither delayed its hydration nor affected the microstructure at day 1. However, when 0.15 wt% sucrose or 0.40 wt% sorbitol was added, the formation of CSH was delayed but small amounts of calcium hydroxide precipitated. The CH appeared either as large elongated crystals in O_Sucrose high (Figure 3-15) or as masses of smaller crystals in O_Sorbitol (Figures 3-16), which were likely the precursors of the CH-rich islands. After day 7, sorbitol and sucrose ceased to affect the development of the OPC microstructure, and BSE images of O_Control, O_Sorbitol, and O_Sucrose high became indistinguishable.

(a)   (b)
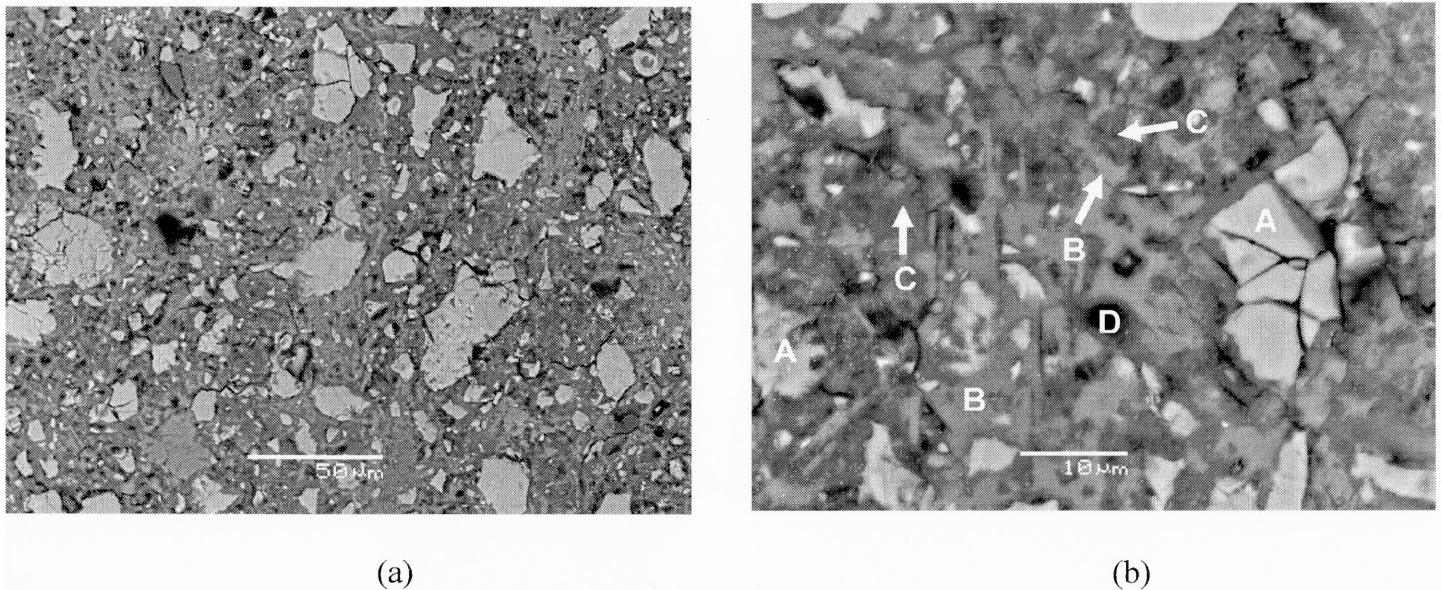
Figure 3-12 Backscattered electron images of O_Control at day 1 with (a) low and (b)

high magnification, showing

(A) unhydrated cement grains, (B) CH, (C) CSH and (D) pore.

Table 3-4 Status and distribution of hydration products for OPC samples at days 1, 7 and 56

Sample	Day 1	Day 7	Day 56
Control	Set; small CH-rich islands (< 100 μm); thin rims of CSH on C$_3$S grains; complex precipitation of CSH, CH, and other hydration products in the pore space [Figure 3-12]	Set; thicker CSH rims on C$_3$S grains and reduced porosity (by comparison with day 1) [Figure 3-13]	Set; very thick CSH rims on remaining C$_3$S grains; complex precipitation of CSH, CH, and other hydration products in the pore space; almost no porosity [Figure 3-14]
Sucrose - low	Set; similar to Control at day 1 [similar to Figure 12]	Set; similar to Control at day 7 [similar to Figure 3-13]	Set; similar to Control at day 56 [similar to Figure 3-14]
Sucrose- high	Not set; some CH crystals [Figure 3-15]	Set; similar to Control at day 7 [similar to Figure 3-13]	Set; similar to Control at day 56 [similar to Figure 3-14]
Sorbitol	Not set; some CH crystals [Figure 3-16]	Set; similar to Control at day 7 [similar to Figure 3-13]	Set; similar to Control at day 56 [similar to Figure 3-14]
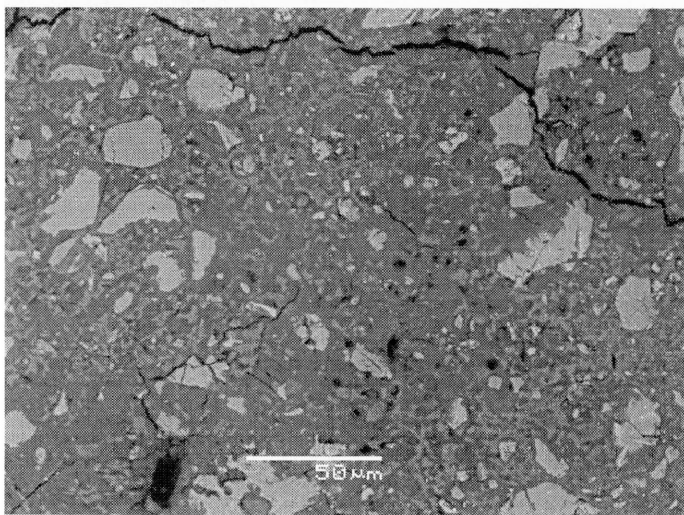
Figure 3-13 Backscattered electron image of

O_Control at day 7.
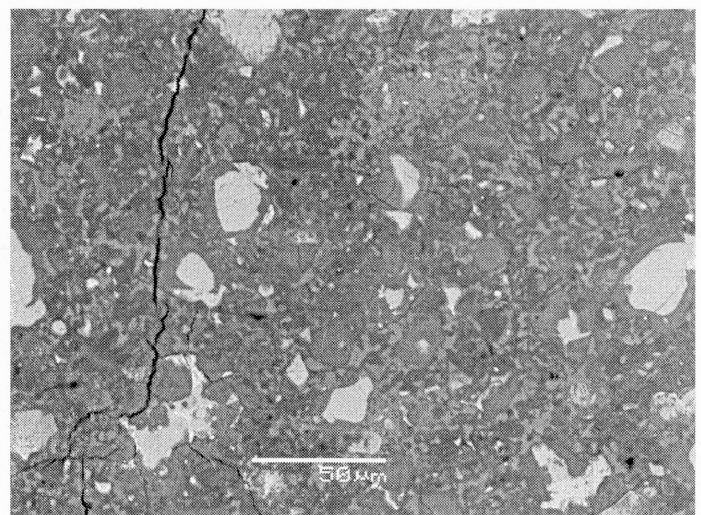
Figure 3-14 Backscattered electron image of

O_Control at day 56.
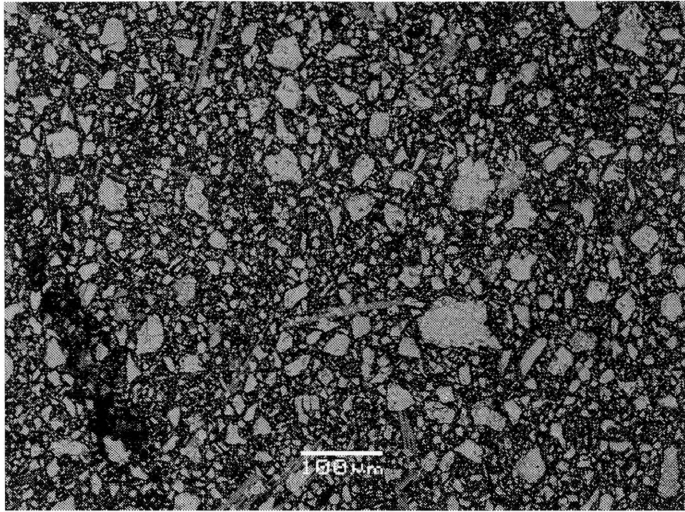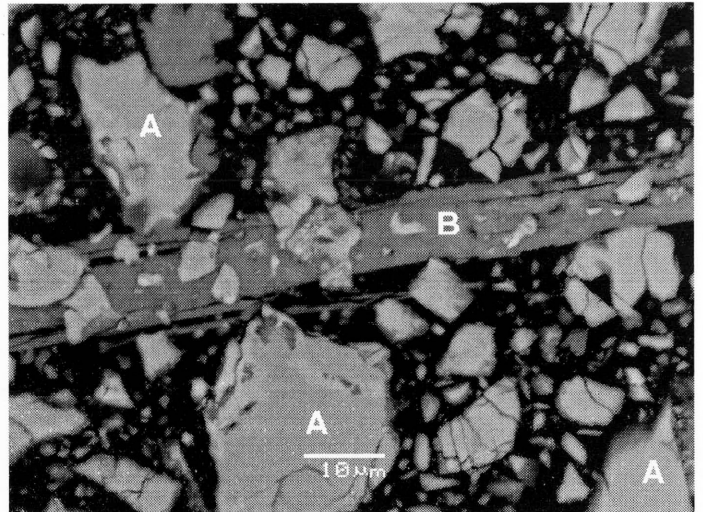
(a)   (b)

Figure 3-15 Backscattered electron images of O_Sucrose high sample at day 1 with (a)

low and (b) high magnification, showing (A) unhydrated cement grains and (B) CH.
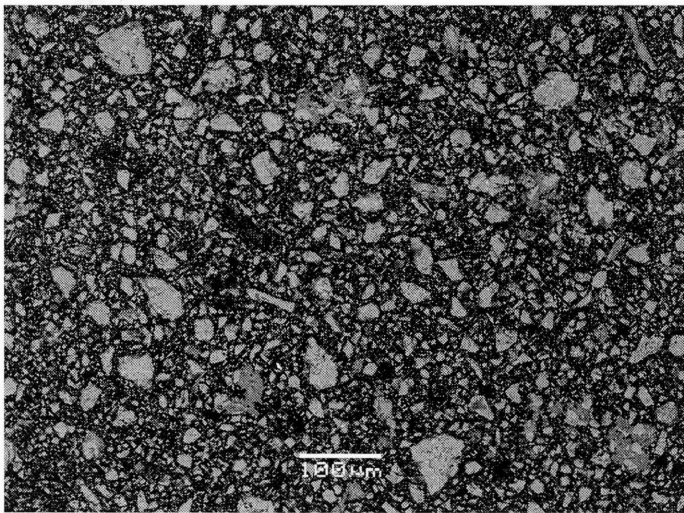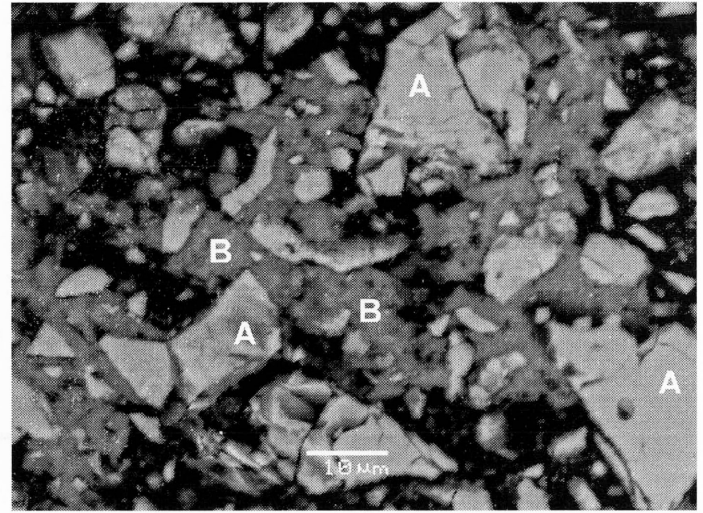
(a)   (b)

Figure 3-16 Backscattered electron images of O_Sorbitol at day 1 with (a) low and (b)

high magnification, showing (A) unhydrated cement grains and (B) CH.

3.3.3.3. WPC

The microstructure of W_Control and O_Control samples at the same age are similar (Figures 3-17 to 3-19). Adding 0.037 wt% sucrose did not significantly alter the microstructure of WPC at day 1 (Figure 3-20). Although addition of 0.15 wt% sucrose or

(a)   (b)
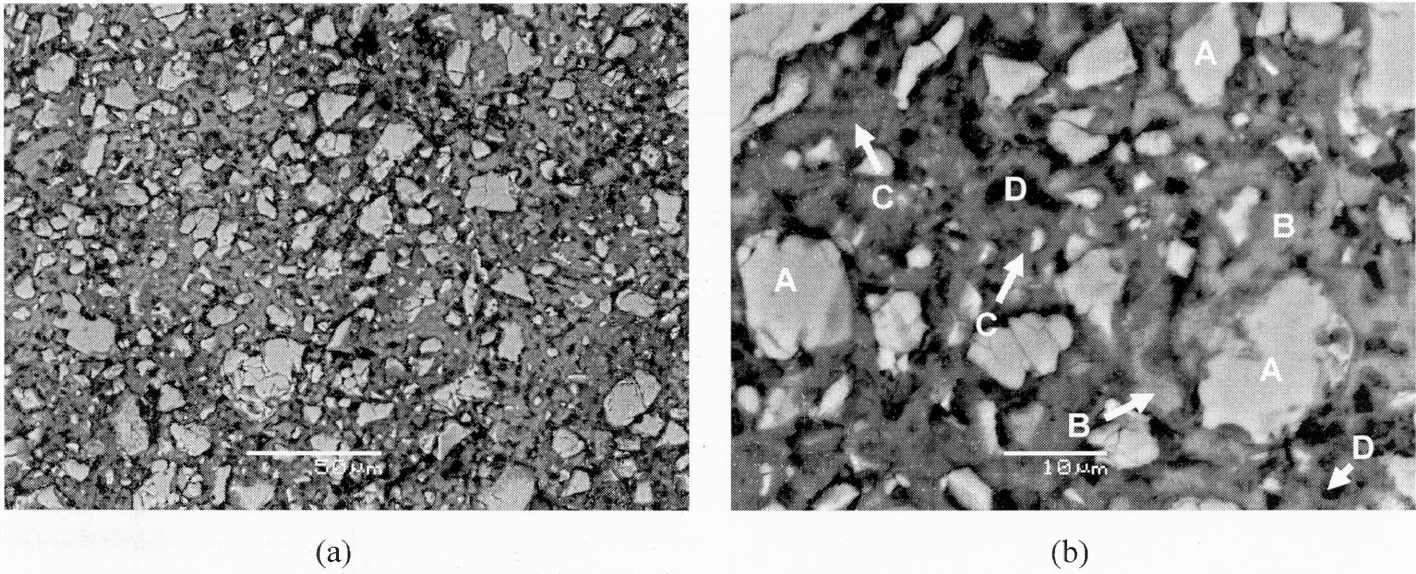
Figure 3-17 Backscattered electron images of W_Control at day 1 with (a) low and (b) high

magnification, showing (A) unhydrated cement grains, (B) CH, (C) CSH and (D) pore.

0.40 wt% sorbitol delayed the precipitation of CSH, some calcium hydroxide was present at day 1 (Figures 3-21 and 3-22). The amount of CH formed at day 1 with 0.15 wt% sucrose was significantly larger in WPC than in OPC. (Compare Figures 3-15a and 3-21a.) No difference was observed when sorbitol was added, however. This is consistent with the fact that the degree of hydration at day 1 was much higher in W_Sucrose high (32%) than in O_Sucrose high (11%), whereas O_Sorbitol and W_Sorbitol had similar degrees of hydration (17%). (See Figures 3-1 and 3-2.) After 1 day, neither sucrose nor sorbitol had a significant effect on the microstructure of WPC. Despite the slight differences between the

microstructure of WPC and OPC, the overall trends of WPC samples with various additives and different curing time were similar to their equivalent OPC counterparts. Thus, the status and microstructure WPC samplse can also be read from Table 3-4.
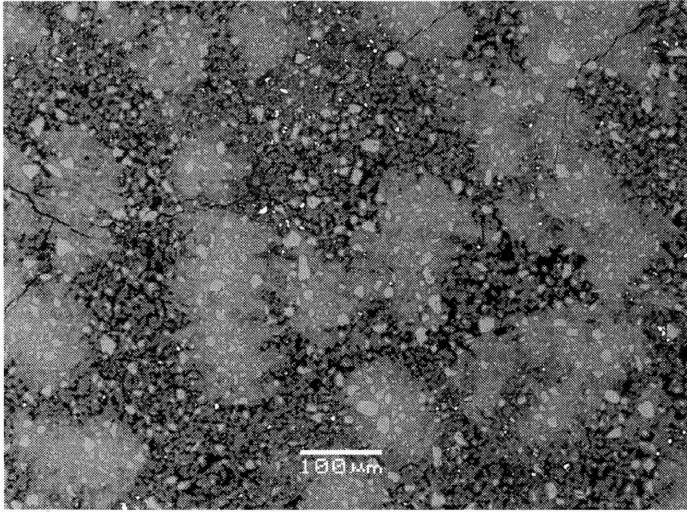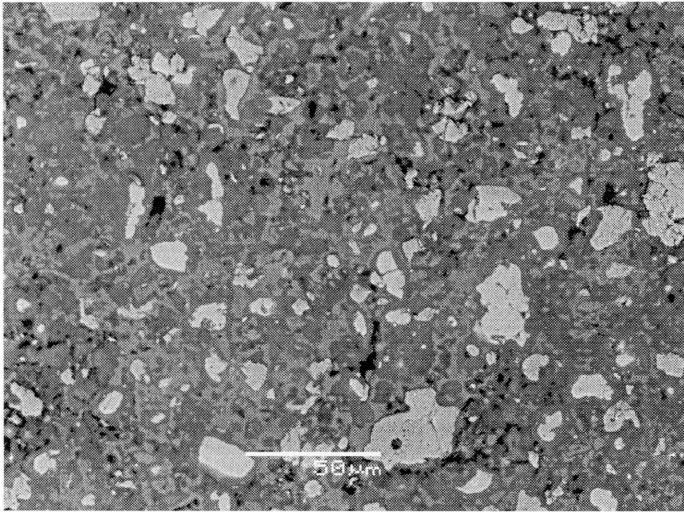

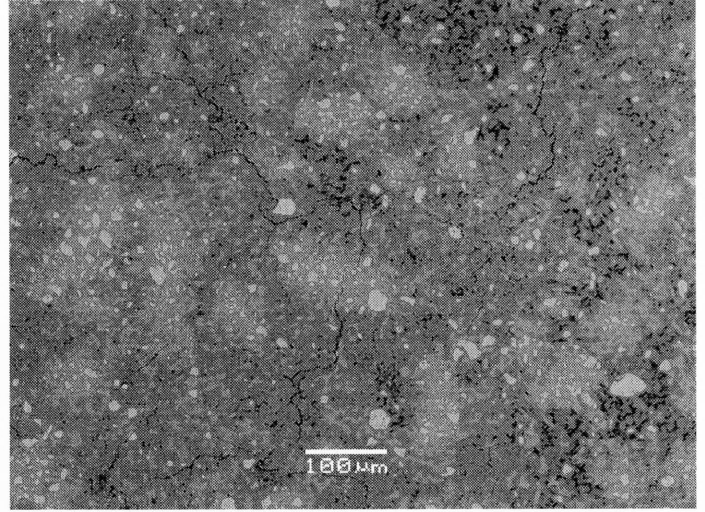Figure 3-18 Backscattered electron image of W_Control at day 7.
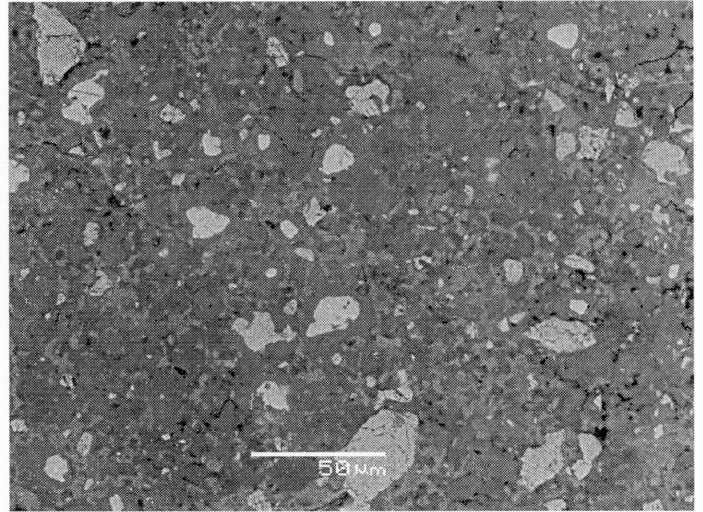
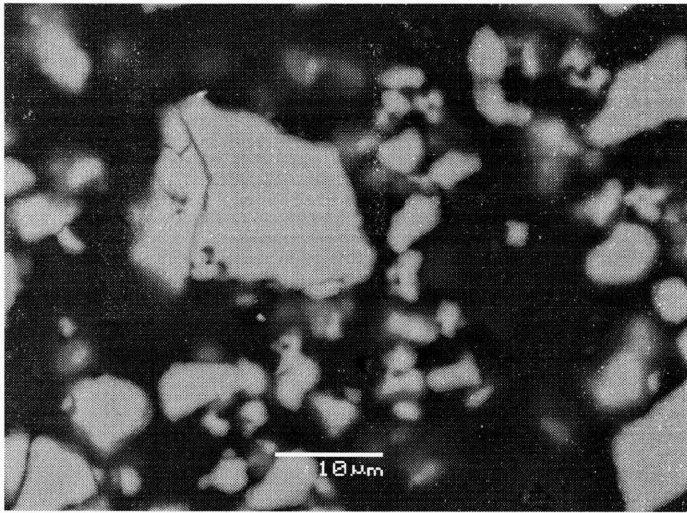Figure 3-19 Backscattered electron image of W_Control at day 56.

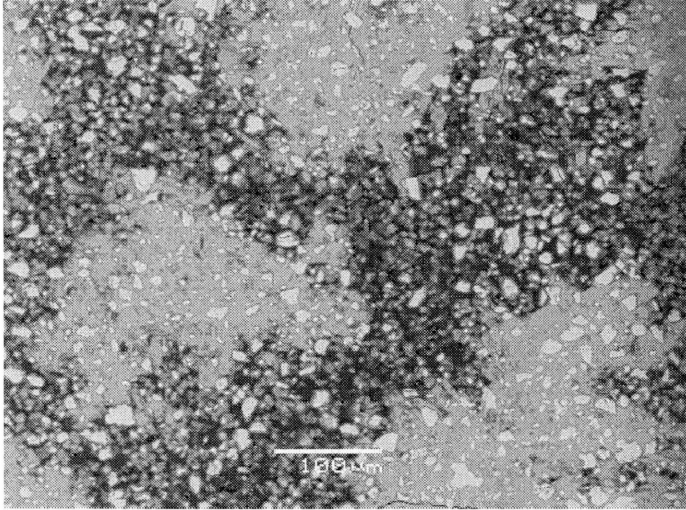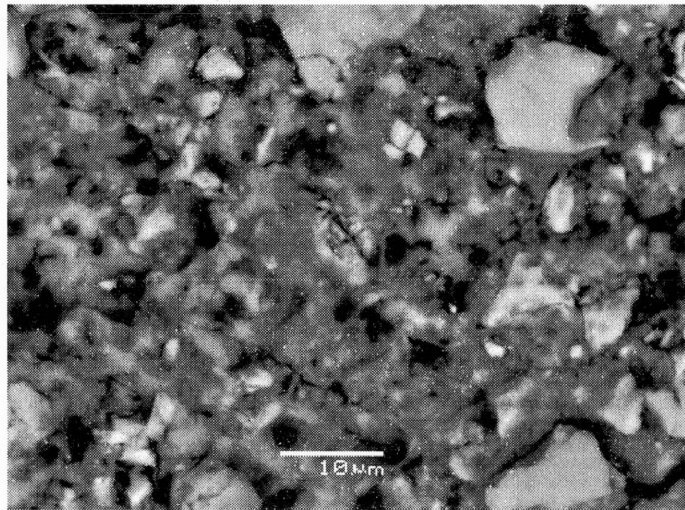Figure 3-20 Backscattered electron image of W_Sucrose low at day 1.
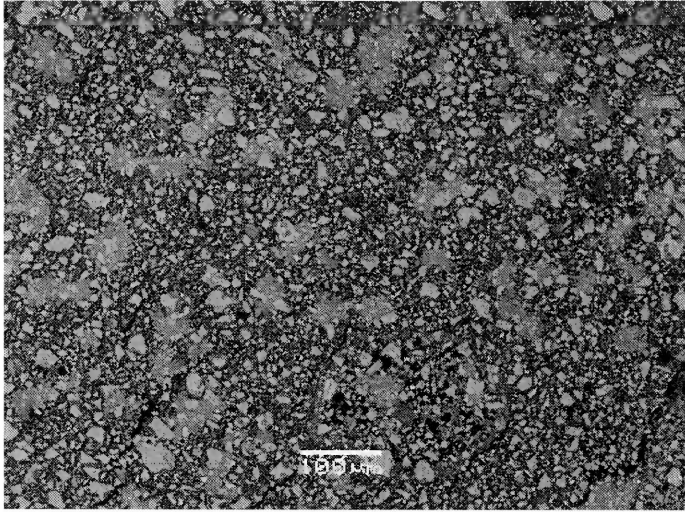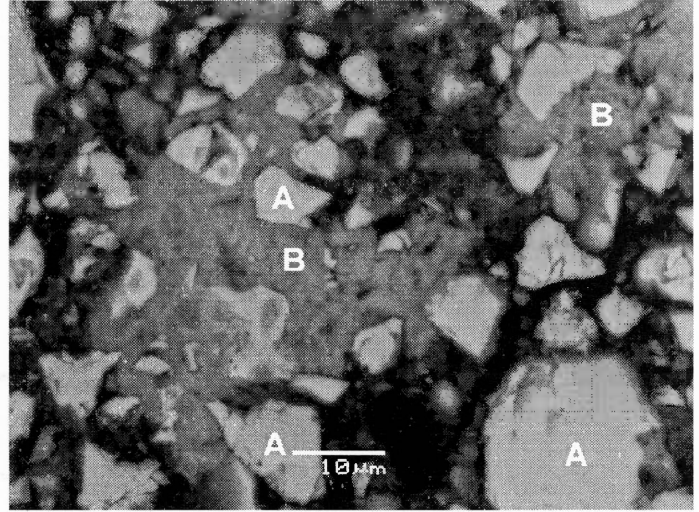
(a)	(b)

Figure 3-21 Backscattered electron images of W_Sucrose high at day 1 with (a) low and

(b) high magnification, showing (A) unhydrated cement grains and (B) CH.
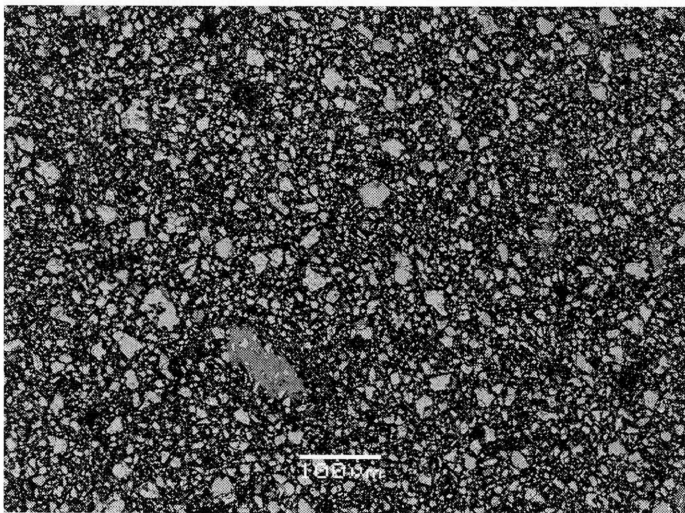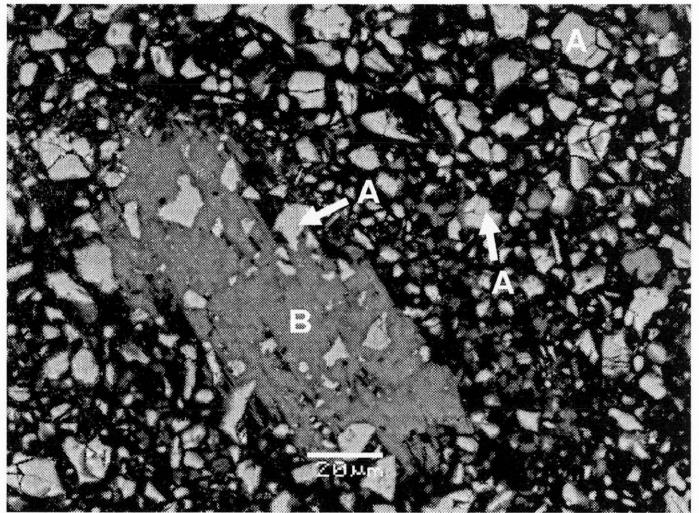
(a)	(b)

Figure 3-22 Backscattered electron images of W_Sorbitol at day 1 with (a) low and (b)

high magnification, showing (A) unhydrated cement grains and (B) CH.

3.4. Discussion

The above results show that sorbitol or sucrose at suitable concentrations can be effectively used to delay the hydration of OPC, WPC and pure C_3S. The retardation effect was more severe on the precipitation of CSH than on that of CH. In all the systems where hydration was delayed, CH precipitated before CSH, and the early CH was the precursor of CH-rich islands that were later observed in the set samples.

OPC, WPC and C_3S were affected differently by sucrose, especially during the early stages of hydration. Addition of 0.037 wt% sucrose completely prevented the formation of hydration products in C_3S at day 1, but did not significantly affect the microstructure of WPC or OPC. Increasing the concentration of sucrose to 0.15 wt% temporarily delayed the hydration of OPC and WPC (up to seven days), but prevented the precipitation of hydration products in C_3S throughout the whole test period (56 days). Furthermore, addition of 0.15wt% sucrose affected OPC more than WPC: after 1 day, the degree of hydration was significantly higher for WPC than for OPC, and more CH had precipitated in WPC than in OPC. The smaller effect of sucrose on OPC and WPC than on C_3S may be explained by the adsorption of sucrose onto the aluminium phases, especially unhydrated C_3A, which reduces the amount of free sucrose available to react with cement [7, 9, 10, 13].

The effect of sorbitol on C_3S, OPC and WPC samples was more consistent than that of sucrose. At day 1, addition of 0.40 wt.% sorbitol prevented C_3S, OPC and WPC from setting, but all three samples contained some CH precipitates. OPC and WPC samples

containing sorbitol had similar degrees of hydration at day 1. By day 7, sorbitol no longer had a visible effect on the microstructure of C_3S, OPC and WPC.

The results indicate that there is a range in sucrose and sorbitol concentrations in which the effects of these compounds on both the hydration rate and microstructure are only temporary. With sucrose, this range is lower for C_3S than for OPC and WPC. It is well established that sucrose enhances the solubility of Ca, Si, Al, and Fe initially in the aqueous phase [4, 12], probably as a result of the poisoning of growth surfaces on CH by a sucrose-calcium half salt [4, 12] or another poisoning agent such as surface-bound oligomeric calcium alkoxides [14]. As the concentration of ions in solution increases, the opportunity for these ions to precipitate by forming new nucleation sites rather than attaching to the poisoned nuclei also increases [18]. Although these new sites can also be poisoned by sucrose, as more and more new ones form, the "retardation barrier" can be overcome suddenly once there are more nucleation sites present than available sugar. This theory may explain why samples containing sucrose, although they were initially delayed, eventually hydrated fast enough to catch up with the control samples and achieve similar strengths, although they were initially delayed. In addition, this theory also explains why, if too much sucrose is added, the hydration is forever prevented by an "unconquerable barrier" [18].

Until now, no specific retardation mechanism has been proposed for sorbitol. However, unlike sucrose, sorbitol is able to form $[HOSi(R_{sor})_2]^-$ and $[Si(R_{sor})_3]^{2-}$ complexes with aqueous silicon in alkaline media [20]. These anionic complexes may play a role in delaying the hydration of cement, possibly through $Ca(OH)^+$ association. Moreover, it is tempting to speculate that the enhancement in strength and final degree of hydration of

OPC that resulted from 0.40% sorbitol addition was caused by the formation of sorbitol-silicate cross-links in the solid cement matrix.

3.5. Conclusions

Sucrose and sorbitol delayed the hydration of C_3S, OPC and WPC by interfering with the precipitation of CSH and CH at early curing times. The delaying effect of sucrose and sorbitol only lasted a few days, except for the combination of C_3S with 0.15 wt% sucrose, which did not set even after 56 days. For a given concentration of sucrose or sorbitol, the retardation period was longer in OPC (3-7 days) than in WPC (1-3 days). Calcium hydroxide appeared before CSH at the earliest stages of hydration, and eventually formed into dense CH-rich islands that contained unhydrated grains of C_3S. These islands persisted in the paste microstructure even after CSH had started precipitating and the samples had set, but they were more prominent in pure C_3S than in OPC or WPC. Sucrose affected the initial hydration and microstructure of C_3S much more than that of OPC and WPC. By contrast, sorbitol had a more consistent effect on all the samples, and its impact on the initial hydration and microstructure of pure C_3S was less severe than that of sucrose. After 56 days, all the OPC and WPC samples reached degrees of hydration close to 80% and strengths between 27.6 and 34.5 MPa (4000 and 5000 psi), except, that is, for OPC with 0.40 wt% sorbitol which had significantly higher strength and degree of hydration.

3.6. Acknowledgement

3.7. References

[1]   S. Mindness, J. F. Young, Concrete, Prentice-Hall, Inc, Englewood Cliffs, NJ, 1981.

[2]   H. F. W. Taylor, Cement Chemistry, Academic Press Inc, San Diego, CA 92101, 1990.

[3]   Portland cement association, http://www.cement.org/decorative/overview.asp (accessed in July, 2007).

[4]   J. D. Birchall, N. L. Thomas, The mechanism of retardation of setting of OPC by sugars, Br. Ceram. Proc. 35 (1984) 305-315.

[5]   L. Ben-Dor, C. Heitner-Wirguin, H. Diab, The effect of ionic polymer on the hydration of C_3S, Cem. Concr. Res. 15 (1985) 681-686.

[6]   L. H. Grierson, J. C. Knight, R. Maharaj, The role of calcium ions and lignosulfonate plasticizer in the hydration of cement, Cem. Concr. Res. 35 (2005) 631-636.

[7]   J. F. Young, A review of the mechanisms of set-retardation in portland cement pastes containing organic admixtures, Cem. Concr. Res. 2 (1972) 415-433.

[8]   P. F. G. Banfill and D. C. Saunders, The relationship between the sorption of organic compounds on cement and the retardation of hydration, Cem. Concr. Res. 16 (1986) 399-410.

[9]   V. S. Ramachandran, M. S. Lowery, Conduction calorimetric investigation of the effect of retarders on the hydration of Portland cement, Thermochim. Acta 195 (1992) 373-387.

[10] H. M. Jennings, H. Taleb, G. Frohnsdorff, J. R. Clifton, Interpretation of the effects of retarding admixtures on pastes of C_3S, C_3A plus gypsum, and Portland cement,

The 8th International Congress on the Chemistry of Cement, Communications Theme 2, Volume III, 1986.

[11] N. B. Singh, P. N. Ojha, Effect of glucose on the hydration of Portland cement, The 7th International Congress on the Chemistry of Cement, 1980.

[12] N. L. Thomas, J. D. Birchall, The retardation action of sugars on cement hydration, Cem. Concr. Res. 13 (1983) 830-842.

[13] K. Luke, G. Luke, Effect of sucrose on retardation of Portland cement, Adv. Cem. Res. 12 (2000) 9-18.

[14] M. Bishop, A. R. Barron, Cement hydration inhibition with sucrose, tartaric acid, and lignosulfonate: analytical and spectroscopic study, Ind. Eng. Chem. Res. 45 (2006) 7042-7049.

[15] N. B. Milestone, Hydration of tricalcium silicate in the presence of lignosulfonates, glucose, and sodium gluconate, J. Am. Ceram. Soc. 62 (1979) 321-324.

[16] B. E. I. Abdelrazig, D. G. Bonner, D. V. Nowell, J. M. Dransfield, P. J. Egan, The solution chemistry and early hydration of ordinary Portland cement pastes with and without admixtures, Thermochim. Acta 340-341 (1999) 417-430.

[17] V. K. Peterson, M. C. G. Juenger, Hydration of tricalcium silicate: effects of $CaCl_2$ and sucrose on reaction kinetics and product formation, Chem. Mater. 18 (2006) 5798-5804.

[18] M. C. G. Juenger, H. M. Jennings, New insights into the effects of sugar on the hydration and microstructure of cement pastes, Cem. Concr. Res. 32 (2002) 393-399.

[19] Patent: Use of particular polysaccharides as admixtures for mineral materials, http://www.freshpatents.com/Use-of-particular-polysaccharides-as-admixtures-for-

mineral-materials-dt20060316ptan20060054062.php?type=description (accessed in July, 2007).

[20] S. D. Kinrade, J. W. Del Nin, A. S. Schach, T. A. Sloan, K.L. Wilson, C. T. G. Knight, Stable five- and six-coordinated silicate anions in aqueous solution, Science 285 (1999) 1542-1545.

[21] A. M. Cody, H. Lee, R. D. Cody, P. G. Spry, The effects of chemical environment on the nucleation, growth, and stability of ettringite $[Ca_3Al(OH)_6]_2(SO_4)_3 \cdot 26H_2O$, Cem. Concr. Res. 34 (2004) 869-881.

[22] http://en.wikipedia.org/wiki/Plasticizer (accessed July 2007).

[23] J. K. Beattie, M. T. Kelso, Equilibrium and dynamics of the binding of calcium ion to sorbitol (D-glucitol), Austr. J. Chem. 34 (1981) 2563 – 2568.

[24] Standard specification for Portland cement, ASTM C150-04a (2004).

[25] M. C. G. Juenger, H. M. Jennings, Examining the relationship between the microstructure of calcium silicate hydrate and drying shrinkage of cement pastes, Cem. Concr. Res. 32 (2002) 289-296.

[26] Standard practice for capping cylindrical concrete specimens, ASTM C617-98 (2003).

[27] Standard test method for compressive strength of hydraulic cement mortars (using 2-in. or [50-mm] cube specimens), ASTM C109/C109M-98 (1998).

[28] K. O. Kjellsen, R. J. Detwiler, O. E. Gjorv, Backscattered electron image analysis of cement paste specimens: specimen preparation and analytical methods, Cem. Concr. Res. 21(2/3) (1991), 388-390.

[29] K. L. Scrivener, Backscattered electron imaging of cementitious microstructures: understanding and quantification, Cem. Concr. Composites 26 (2004) 935-945.

[30] K. L. Scrivener, H. H. Patel, P. L. Pratt and L. J. Parrott, Analysis of phases in

cement paste using backscattered electron images, methanol adsorption and

thermogravimetric analysis, Mater. Res. Soc. Symp. Proc. 85 (1987) 67-76.

[31] K. O. Kjellsen, H. Justnes, Revisiting the microstructure of hydrated tricalcium

silicate - a comparison to Portland cement, Cem. Concr. Composites 26 (2006) 947-

956.

CHAPTER 4

EFFECTS OF SUCROSE AND SORBITOL ON CEMENT-BASED STABILIZATION/SOLIDIFICATION OF TOXIC METAL WASTE[1]

Summary: The effects of sucrose or sorbitol addition on the hydration, unconfined compressive strength and leachability of Portland cement pastes containing 1% Pb and 1% Zn were studied as a function of time. Whereas Pb and Zn were found to shorten the time to achieve maximum hydration of Portland cement, the combination of these metals with 0.15 wt% sucrose or 0.40 wt% sorbitol retarded the setting of cement by at least 7 days and 28 days, respectively, without affecting the strength at 56 days. The leachability of Pb and Zn evaluated by the TCLP 1311 protocol at 56 and 71 days was slightly reduced or unchanged by the addition of sucrose or sorbitol. SEM-EDS and XRD analyses revealed that ettringite precipitation was favored whereas the formation of CSH gel, which accounts for most of the strength of hydrated cement, was delayed in cement pastes containing both metals and sucrose or sorbitol. These results indicate that controlled additions of sucrose or sorbitol can add flexibility to the handling of cement-treated metal waste, particularly when it needs to be transported by truck or pipeline between the treatment plant and the disposal site, without affecting its long term performance.

4.1. Introduction

Stabilization/solidification (S/S) is a widely used technique for immobilizing toxic metal ions in industrial waste prior to landfilling. The binder of choice is most often Portland cement, owing to its ready availability, high strength and amply documented performance [1]. The main components of Portland cement are tricalcium silicate (C_3S), dicalcium silicate (C_2S), tricalcium aluminate (C_3A), tetracalcium aluminoferrite (C_4AF) and calcium sulfate (gypsum or anhydrite, 10% max). During cement hydration, C_3A reacts with sulfate ions coming from the dissolution of calcium sulfate to form crystals of ettringite (AFt) and monosulfate (AFm), thus preventing the flash set of Portland cement. C_3S and C_2S undergo hydration to form calcium hydroxide (CH) and calcium silicate hydrate (CSH), which is the principal contributor to cement strength. [2] The CSH plays a key role in immobilizing adventitious metal ions by means of physical adsorption [3], coprecipitation [4] and formation of metallosilicates [5-7]. Further metal uptake is provided via ion substitution in ettringite crystals [3].

Sugars and their derivatives are found in many industrial wastes and byproducts, either as individual molecules or as the repeating units in long-chain compounds. For example, wood sugars and oligosaccharides mixed with lignosulfonates are byproducts from the manufacture of pulp and paper. They are widely used as retarders to control the setting of cement [8-13]. There has been no study published, however, on the effects of sugars as additives in cement-based S/S processes. The retarding influence of sugars could be advantageous when the waste-cement mixture needs to be transported for some distance between the S/S treatment plant and the disposal site. In these situations, early hardening of

the cement in the truck box or pipeline could result in severe operational difficulties and limited flexibility. In the present research, a sugar (sucrose) and a sugar alcohol (sorbitol) were investigated. Both additives are highly resistant to alkali attack but differ in their affinity toward silicon: sorbitol is a silicon binder [14], whereas sucrose is not [8, 12]. As a result, these two additives are expected to interfere differently with the cement hydration reactions. Sucrose is one of the most effective and commonly used retarders for cement setting. The addition of 0.075 wt % sucrose increases the induction period of the hydration process from 2.5 to 31 hours [11]. Moreover, sucrose has been shown to enhance the specific surface area of hydrated cement pastes by increasing the number of small (1-2 nm) pores at the expense of medium-sized (4-20 nm) pores [15]. Sorbitol is often employed as a water-reducing plasticizer (superplasticizer) in cement admixtures, that is, it decreases the water needed to make the cement workable which, in turn, enhances its strength [16, 17].

The objective of this study was to explore the effects of small additions of sucrose or sorbitol on metal leachability and strength development for specimens of metal waste treated by cement-based stabilization/solidification. Synthetic Pb and Zn waste solutions were used because both metals are common to industrial waste streams and have been identified as priority metallic pollutants by the US Environmental Protection Agency [18]. To aid in the interpretation of the results, the degree of cement hydration and the microstructure of the treated waste matrix were also assessed as a function of time.

4.2. Materials and Methods

4.2.1. Sample Preparation

Synthetic waste solutions containing 25.0 g/L of each Pb and Zn were prepared by dissolving 40.0 g $Pb(NO_3)_2$ and 114 g $Zn(NO_3)_2 \cdot 6H_2O$ per litre of distilled-deionized water. Sucrose and sorbitol were dissolved in these solutions at concentrations ranging between 0 and 10 g/L; equivalent metal-free solutions were also prepared. The solutions were pre-cooled to 10 °C and then mixed with normal Portland cement Type 10 (ASTM Type I) at a liquid-to-cement ratio of 0.40:1 in a plastic bowl over an ice-water bath. (Temperature control was necessary because certain mixtures – most notably those containing sorbitol – released more heat than others.) The mixtures were stirred with a plastic spoon until they were homogeneous, *i.e.*, for about 7 min or, in the case of those which contained synthetic waste, about 12 min because of their higher viscosity. They were then poured into cylindrical PVC molds measuring 5.08 cm (2 inches) in diameter and 10.16 cm (4 inches) in height. To minimize the entrapment of air bubbles, the cylinders were filled in two successive layers and each layer tamped 50 times. Cylinders were placed in triple-sealed, air-tight polyethylene bags and immersed in a room temperature (20-22 °C) water bath to cure[2].

Table 4-1 provides the compositions of all sample mixtures. The Pb and Zn concentrations were each either 0 or 1.00 wt% of cement (*i.e.*, 0.01 g of metal per gram of

---

[2] Samples were cured in sealed bags for eliminating the diffusion of metals from the samples to the water. The effects of higher curing temperature (40°C) on the leachability, degree of hydration and microstructure of OPC-sugar-treated wastes were also investigated; the results are displayed in Appendix E. These samples were cured in an environmental chamber at a temperature of 40 °C and humidity of 99 %.

cement). Sucrose and sorbitol ranged from 0 to 0.40 wt%. Two types of control sample

were prepared. The first ("Control") consisted only of hydrated Portland cement; the

second ("Control M") additionally contained Pb and Zn but no sorbitol or sucrose. At least

12 test cylinders were prepared of each mixture, which allowed the strength, leachability

and loss-on-ignition to be determined in triplicate after 4 different curing periods: 7, 14,

28, and 56 days. Additional tests were performed for the metal-free mixtures after curing 1

day (loss-on-ignition) and 3 days (loss-on-ignition and strength), and for the waste-

containing mixtures after 71 days (leachability).

Table 4-1 Sample compositions

Batch name	Pb content (wt% of cement)	Zn content (wt% of cement)	Sorbitol/sucrose content (wt% of cement)
Control	0	0	0
Sorbitol	0	0	0.40
Sucrose-low	0	0	0.15
Control M	1.00	1.00	0
Sorbitol M	1.00	1.00	0.40
Sucrose-low M	1.00	1.00	0.15
Sucrose-high M	1.00	1.00	0.38

4.2.2. Strength Testing

Immediately after they were removed from the molds, sample cylinders were

capped top and bottom with sulfur according to ASTM C617-98 [19] and the unconfined

compressive strength was measured according to ASTM C109 [20].

4.2.3. Loss-on-ignition Testing

A small portion of each sample was crushed and *ca.* 1.5 g of the 850-2000 μm fraction oven-heated for 24 h at 105 °C to find the evaporable water-free weight, W_{105}, and again for 2 h at 1005 °C to determine the fully dehydrated weight, W_{1005}. The degree of hydration α_{LI} is given by the equation

$$\alpha_{LI} = (W_{105} - W_{1005})/(0.24W_{1005}) \qquad (4\text{-}1)$$

in which 0.24 is the reported fraction of non-evaporable water in fully hydrated Portland cement [2, 21].

4.2.4. Standard Leaching Procedure

The mobility of Pb and Zn in treated waste samples was determined using the regulatory Toxicity Characteristic Leaching Procedure (TCLP) [22]. 20.0 g of sample with particle size 425-850 μm was combined with 400 mL 0.100 M acetic acid (pH 2.88)[3] in a 500 mL polypropylene bottle and rotated end-over-end at 30 rpm for 18 h at room temperature. The extract was passed through a 0.7 μm borosilicate microfiber filter, and its pH measured using a Metrohm 6.0233.100 combination glass electrode. It was then acidified to pH 2 with concentrated nitric acid and analyzed by inductively coupled plasma-atomic emission spectroscopy (ICP-AES) using a Varian Vista Pro ICAP Radial spectrometer. The detection limits for Pb and Zn were 0.025 and 0.05 mg/L, respectively.

---

[3] This extraction fluid has an initial acidity of 2 Eq H$^+$/kg solid. The corresponding final pH of the liquid after the leaching test is approx. 12.29. For different extraction fluids with various initial acidities, the final pH is different. Please see Appendix F for details on the relationship between the initial acidity and the final pH of the extraction fluid after 18h of leaching test.

Although the TCLP is a static batch test and does not simulate actual field conditions, it remains the standard regulatory method for monitoring the performance of full-scale cement-based stabilization/solidification operations in North America and for laboratory studies of the leaching behavior of cement-stabilized waste.

4.2.5. Microstructure Analyses

After reaching the desired curing time, a small slice (*ca.* 0.5 g) was removed from the inner part of the sample cylinder, immersed for 24 h in acetone to halt hydration [23], dried at 105 °C for 15 min, and then imbedded in epoxy resin. An oriented thin-section was cut, lapped and polished using oil-based media so as not to alter the water-soluble minerals. After carbon-coating, it was analyzed with a JEOL JSM 5900 scanning electron microscope in backscattered electron (BSE) mode to improve contrast between different mineral phases [24, 25]. The elemental composition of mineral phases was determined by X-ray energy dispersive spectrometry (EDS) using an Oxford Link ISIS system (120 s live-time) calibrated with corundum for Al, barium sulfate for S and O, orthoclase for Si and K, periclase for Mg, wollastonite for Ca, and jadeite for Na. Pure metal standards were used to calibrate Fe, Pb and Zn. SEM-EDS analyses were carried out on days 7, 28 and 56 for the samples containing Pb and Zn. The metal-free samples were analyzed on days 1, 7 and 56.

4.2.6. Grey Level Analyses

Each BSE image consists of 1280 × 960 pixels having grey levels ranging from 0 (black) to 256 (white). The grey levels are directly related to the atomic number of the

material, and thus can be used to distinguish between mineralogical phases: unhydrated cement grains are the brightest features, CH and other hydration products (abbreviated OHP, mainly composed of CSH) appear as two shades of grey, whereas pore space is black. These phases also appear as separate peaks in grey-scale histograms (Figure 4-1), and the areas under these peaks can be used to calculate the percentage of individual phases [25, 26]. For each sample, calculations were carried out on 15 adjacent BSE images and the results were averaged to obtain a representative phase distribution. Each image measured 254×190 µm, yielding a resolution of 0.198 µm/pixel. The degree of hydration of a sample can also be calculated from the results of grey level analyses [27]:
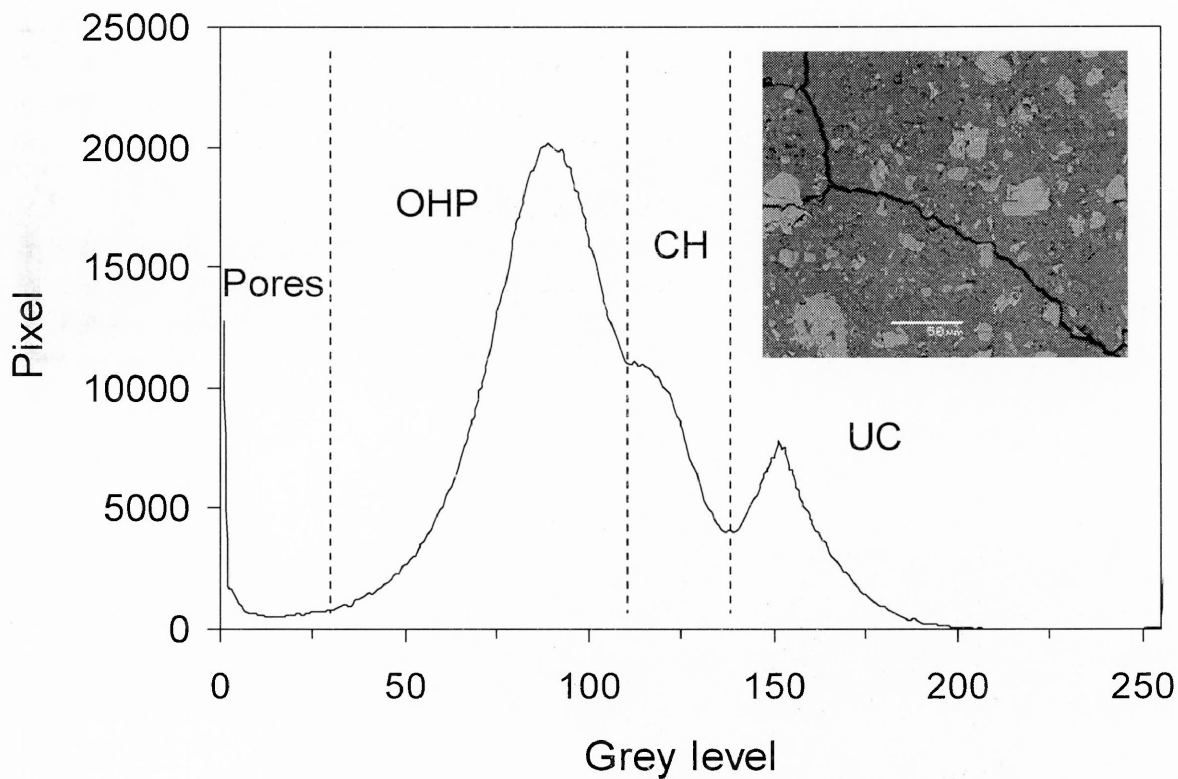
Figure 4-1 Backscattered electron image of Control sample at day 7 and its grey level histogram obtained with the Image-Pro Plus 5.0 software (UC: Unhydrated cement grains, OHP: other hydration products).

$$\gamma_{GL} = 1 - UC/UC_0 \qquad\qquad (4\text{-}2)$$

in which UC and UC_0 are the area fractions of unhydrated cement particles at time t and the start of the hydration process, respectively. The value of UC_0 can be evaluated from the densities of Portland cement ($d_c = 3.14$ g/cm^3) and water ($d_w = 1.00$ g/cm^3) and the water-to-cement mass ratio ($R = 0.40$).

$$UC_0 = (1/d_c)/(1/d_c + R/d_w)$$

4.2.7. XRD Analyses

The mineralogy of the metal-containing samples at day 7 was characterized by X-ray diffractometry using a Philips PW 1050-3710 diffractometer with Cu-Kα radiation. Scans were carried out in the range $5° < 2\theta < 75°$ with a $0.04°$ step interval and a counting time of 2 s per step.

4.3. Results and Discussion

4.3.1. Degree of Hydration

Figure 4-2 depicts degree of hydration as a function of time for pure cement (Control) and cement containing 1% Pb and 1% Zn (Control M). The curing of metal-free cement proceeded in two stages – a period of rapid hydration lasting about 3 days, followed by a slower reaction period exhibiting zeroth-order kinetics – and required 56 days to reach the maximum hydration level of 80%. The addition of Pb and Zn greatly accelerated the

overall curing process[4], with maximum hydration being achieved in only 7 days. It would

appear that added metal ions somehow interfere with the mechanistic step(s) responsible for

terminating stage-1 of the hydration process. By contrast, previous studies of cement

hydration in the presence of lead and zinc found that both metals retarded cement hydration.

These studies, however, are not directly comparable to the present one because they were

carried out with much larger metal concentrations [28, 29] or were limited to early curing

times of less than 17 hours [30]. The retardation effect of Pb at early times has been

explained by the rapid precipitation of colloidal lead hydroxide, sulfate, or hydroxysulfate

as a protective membrane around unhydrated cement particles [29, 30]. At high

concentrations, Zn may precipitate as low permeability $CaZn_2(OH)_6 \cdot H_2O$ around

unhydrated calcium silicate particles. [28].

Figure 4-3 reveals that, unlike added metal ions, sucrose and sorbitol did not

radically alter the two-stage reaction profile that characterizes the hydration of pure

Portland cement. However, the onset of stage-1 hydration was delayed by about 2 days in

cements containing 0.15 wt% sucrose (Sucrose-low) or 0.40 wt% sorbitol (Sorbitol). Also,

the sorbitol-containing mixture was slightly more hydrated after 7 days than either of the

other two. The mechanisms by which certain sugars and sugar derivatives retard the

hydration of cement are not fully understood. In the "half-salt" theory proposed by Thomas

and Birchall [8, 12], calcium ions react with sucrose in alkaline solution to form a soluble

sucrose-calcium salt complex $Ca(OH)^+ \ldots R_{suc}$ (pK_{a1} of sucrose = 12.6). The pendant

---

[4] This result was also corroborated by several additional tests on different batches of samples. For details, please see Appendix G.
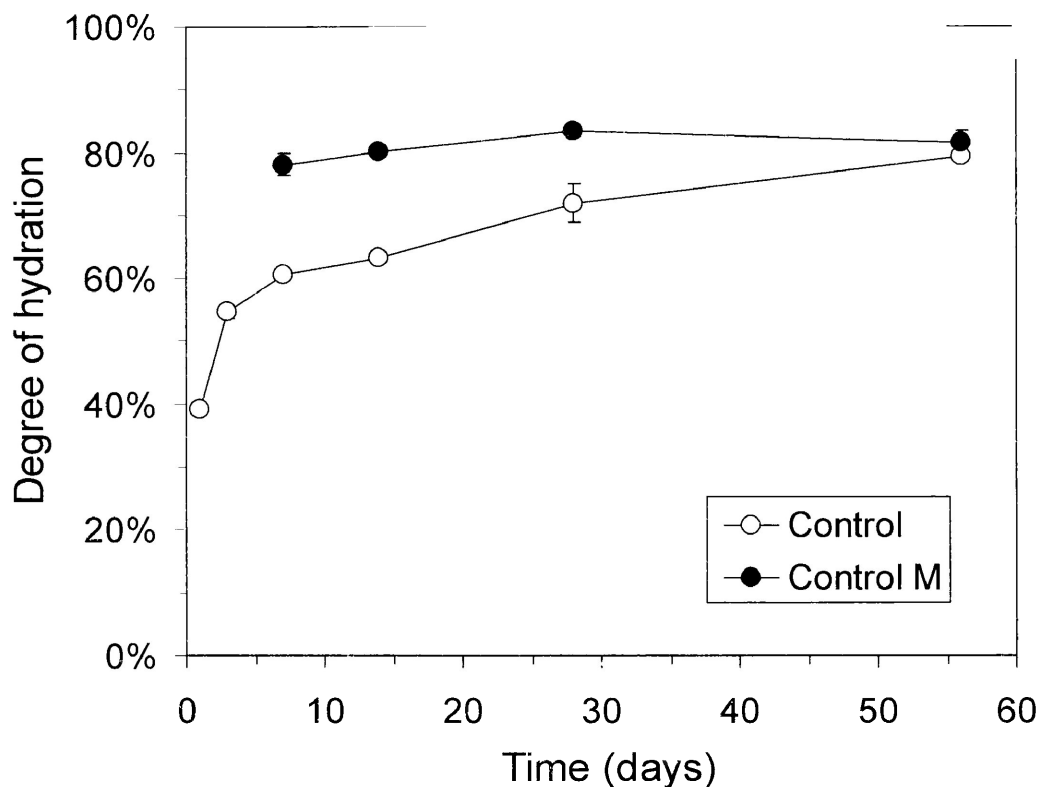
Figure 4-2 Effect of 1% Pb + 1% Zn addition on cement hydration rate. Error bars correspond to the standard deviations over 3 measurements.

$Ca(OH)^+$ group in the half-salt is thought to adsorb onto growing calcium hydroxide (CH) nuclei and thus inhibit further precipitation of calcium and hydroxide ions on the poisoned surface. The precipitation of CSH gel, which relies on the deposition of silica on an existing CH lattice, is thought to be similarly inhibited by poisoning of the CH surface. Although published evidence supporting the existence of aqueous calcium-sucrose complexes is limited, Pannetier et al. [31] report formation of stable $Ca(OH)R_{suc}$ species in dilute alkaline solution and polymeric $[Ca(OH)R_{suc}]_n$ as the concentrations are increased. By contrast, no specific retardation mechanism has been proposed for sorbitol which, at best, interacts weakly with calcium ions (pK_{a1} = 13.6) [32]. Unlike sucrose, however,

sorbitol is able to form $[HOSi(R_{sor})_2]^-$ and $[Si(R_{sor})_3]^{2-}$ complexes with aqueous silicon in

high pH surroundings [14]. These anionic complexes may play a role in delaying the

hydration of cement (possibly through $Ca(OH)^+$ association) and contribute to the

enhancement observed in the strength and final degree of hydration of cement mixtures

containing sorbitol by crosslinking in the solid cement matrix.

Figure 4-3 Effect of sorbitol or sucrose addition on cement hydration rate.

When added together with the metal ions, sucrose and sorbitol countered the

accelerating influence of Pb and Zn on cement hydration, as demonstrated in Figure 4-4.

Surprisingly, they were more effective at inhibiting hydration for the cement containing Pb

and Zn than for pure cement. Addition of 0.15 wt% sucrose (Sucrose-low M) or 0.40 wt%

sorbitol (Sorbitol M) limited the degree of hydration to 35% for at least 7 or 28 days,

respectively. Thereafter, the reaction quickly went to completion (80% degree of hydration), that is, without going through stage-2 hydration. Addition of 0.38 wt% sucrose (Sucrose-high M) maintained hydration at 35-40% through the entire 56 day experiment.
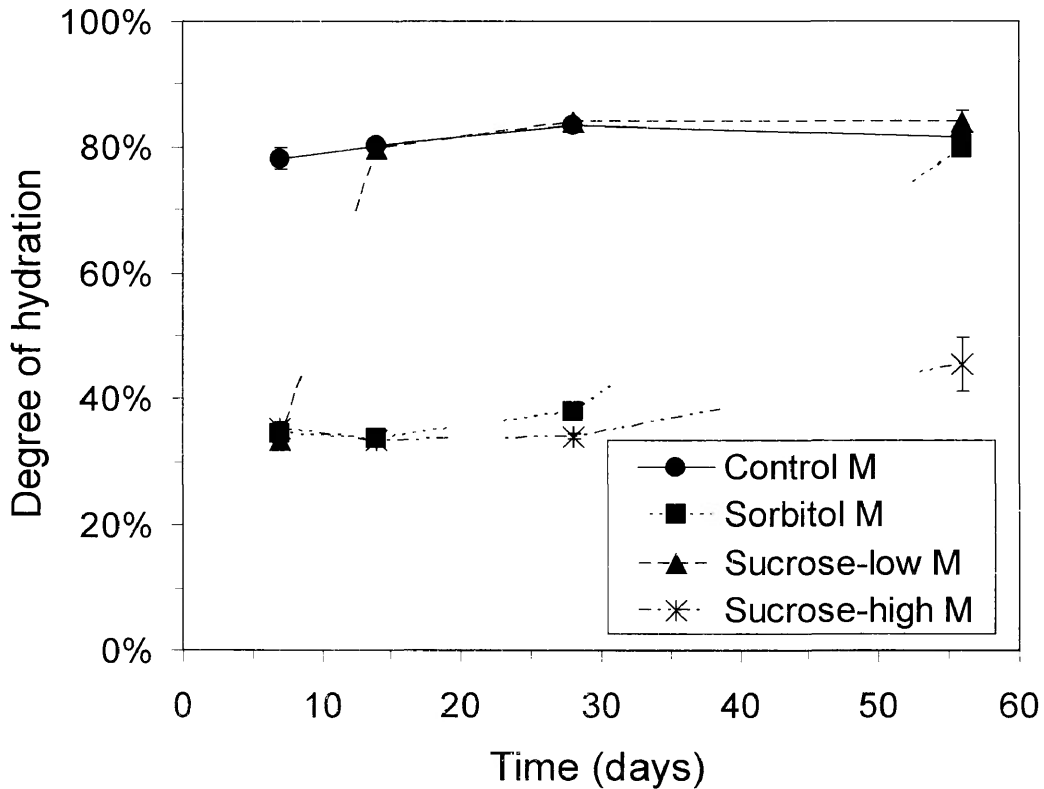
Figure 4-4 Effect of sorbitol or sucrose addition on cement hydration rate in samples containing 1% Pb + 1% Zn.

4.3.2. Grey Level Analyses

Grey level analyses were carried out on Control and Control M samples at 7 days. The percentage of unhydrated cement was lower in the Control M sample ($10._2 \pm 1._9$%) than in the Control sample ($15._1 \pm 2._6$%) at a confidence level of 99.997% (Student t-test). The degrees of hydration calculated from grey level analysis using equation 4-2 ($\alpha_{GL} = 65._9 \pm 5._9$% for the Control sample and $77._0 \pm 4._3$% for the Control M sample) are consistent

with those independently calculated by loss-on-ignition using equation 4-1 ($\alpha_{LI} = 60._7 \pm 0._7$

% for the Control sample and $78._1 \pm 1._7$% for the Control M sample, see Figure 4-2).

Hence, both methods of measuring degree of hydration show that the presence of 1% Pb

and 1% Zn improves hydration at 7 days. By contrast, grey level analyses reported by Ouki

and Hills [26] found that the addition of 1% Pb or 1% Zn *decreased* hydration of Portland

cement at 29 days by 29% and 11%, respectively.

4.3.3. Strength Tests

Table 4-2 indicates the setting status (unset, set, or partially set) of all the samples at

various stages of curing. Several of the samples (*e.g.*, samples containing both metals and

sorbitol at day 1 and day 7) were poorly solidified and friable when removed from the

molds, exhibiting less than 2.76 MPa (400 psi) compressive strength and under 35% degree

of hydration. Hence, they were deemed to be unset. By contrast, cement was considered to

be set when compressive strength exceeded 13.8 MPa (2000 psi) and the degree of

hydration was over 45%. Two samples (Sorbitol M at day 28 and Sucrose-high M at day 56)

were deemed to be only partly set. They consisted of millimetre-sized pebbles of cured

cement within a poorly consolidated matrix, while exhibiting less than 2.76 MPa (400 psi)

compressive strength and 35-45% hydration.

Comparison between Figures 4-5 to 4-7 and Figures 4-2 to 4-4 reveals that the

evolution of compressive strength correlates closely with that of the degree of hydration[5].

Pure cement (Control) reached a maximum strength of *ca.* 34.5 MPa (5000 psi)

---

[5] The relationship between strength and degree of hydration is further illustrated in Appendix H.

after 14 days (Figure 4-5). The addition of 1% Pb and 1% Zn (Control M) resulted in higher strength at day 7 compared to pure cement (86% confidence, based on Student t-test). This result reflects the higher degree of hydration for the Control M sample compared with the Control sample at day 7, and is also in accordance with the findings of Tashiro et al. [33] who reported increased strength for cement containing between 0.5% and 5% $PbO \cdot Pb(OH)_2$ or 0.5% $Zn(OH)_2$ at 3 days and 28 days. In the present study, however, there was statistically no difference between the strengths observed for pure and metal-containing cement from day 14 onwards.

Table 4-2 Summary of sample setting status and main hydration products found by SEM-EDS [a]

Sample	Day 1	Day 7	Day 28	Day 56
Control	CH, CSH	CH, CSH	na	CH, CSH
Control M	na	CH, CSH, ettringite [b]	CH, CSH, ettringite [b]	CH, CSH, ettringite [b]
Sorbitol	CH	CH, CSH	na	CH, CSH
Sucrose-low	CH	CH, CSH	na	CH, CSH
Sorbitol M	na	ettringite, CH [b], CSH [b]	ettringite, CH, CSH	ettringite, CH, CSH
Sucrose-low M	na	ettringite, CSH [b]	ettringite, CH, CSH	ettringite, CH, CSH
Sucrose-high M	na	ettringite	ettringite, CH	ettringite, CH, CSH

[a] Shading indicates that the cement was not set. Light shading indicates that the cement was partially set. No shading indicates that the cement was set. CH = calcium hydroxide. CSH = calcium silicate hydrate. na = not analyzed. [b] Only a small amount of this phase was detected.

Figure 4-5 Effect of 1% Pb and 1% Zn addition on cement strength. Error bars correspond to the standard deviations over 3 measurements.

The effect of low sucrose and sorbitol addition on the compressive strength of metal-free cement is shown in Figure 4-6. Strength was reduced at day 3 for samples containing 0.15 wt% sucrose or 0.40 wt% sorbitol, but caught up with that of pure cement by day 7. At day 56, the sample containing sorbitol was slightly stronger (81% confidence level), which confirms previous reports that sorbitol improves the strength of OPC after 28 days [16]. These results parallel the influence that sucrose and sorbitol had on the degree of hydration (Figure 4-3).
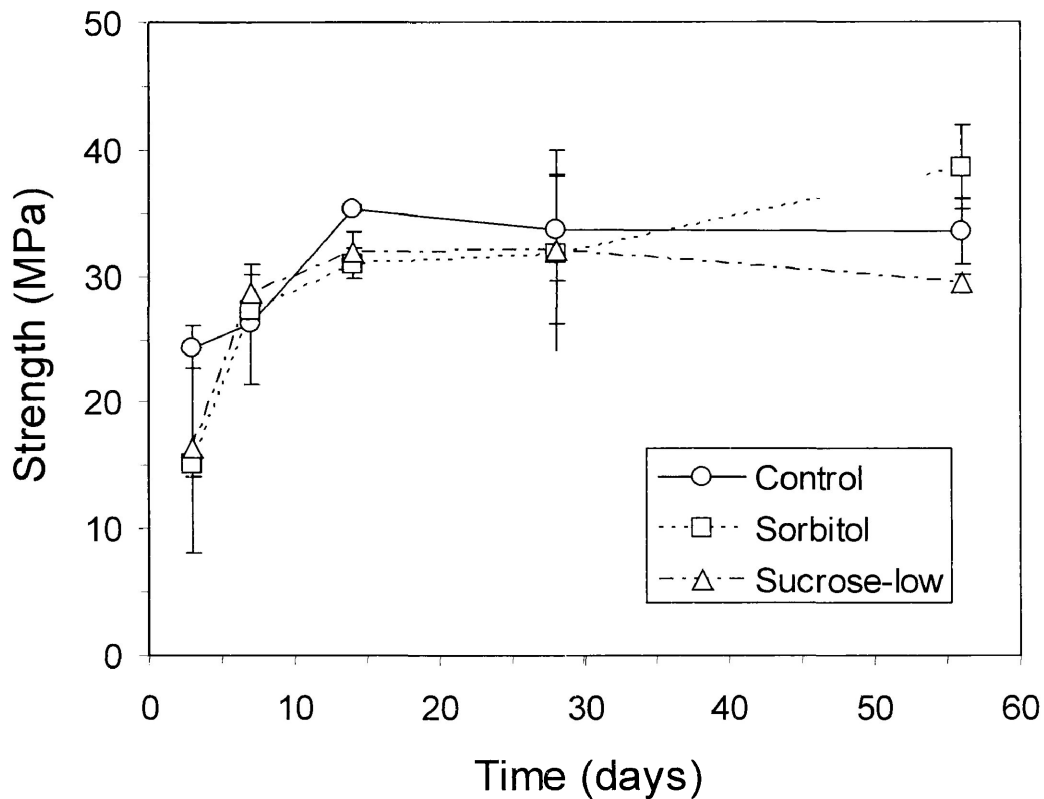
Figure 4-6 Effect of sorbitol or sucrose addition on the development of cement strength.

Similarly, the influence of added sucrose or sorbitol on the strength of cement

containing Pb and Zn (Figure 4-7) parallels their effect on the hydration of these samples

(Figure 4-4). The addition of 0.15 wt.% sucrose (Sucrose-low M) or 0.4 wt% sorbitol

(Sorbitol M) delayed cement setting for at least 7 and 28 days, respectively, with the

strength of these samples rising to that of Control M immediately thereafter. These findings

have practical importance because they demonstrate that controlled addition of sucrose or

sorbitol can delay the setting of S/S-treated metal waste for several days, thus adding

flexibility for transportation to the final disposal site without negatively impacting the final

product strength. However, excessive sucrose addition (Sucrose-high M; 0.38 wt%) delays

setting beyond 56 days with unknown effects on final strength.
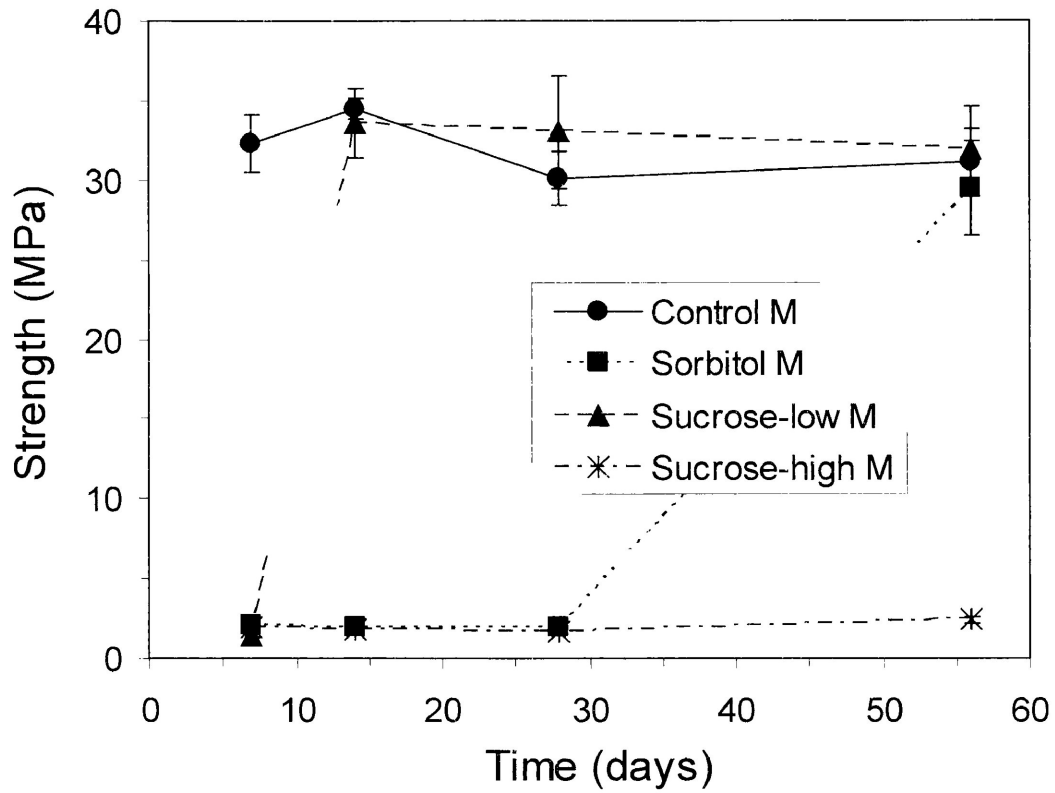
Figure 4-7 Effect of sorbitol or sucrose addition on strength of samples

containing 1% Pb + 1% Zn.

4.3.4. Leaching Tests[6]

Figure 4-8 shows the average concentrations and standard deviations of dissolved

Pb in the TCLP extracts at day 56 and day 71[7] for the Control M, Sucrose-low M, and

Sorbitol M samples, all of which were fully set by this time. The leachability of Pb from the

cement containing sorbitol decreased between the two curing periods, but remained

constant within experimental uncertainty for the other samples. On day 71, the average

---

[6] Preliminary results on the effect of lignosulfonate acid (a byproduct of the pulp and paper industry) on the leachability of Pb in cement-treated waste are shown in Appendix I.

[7] Leaching test results at days 7, 14 and 28 are shown in Appendix J.

leachability of Pb for the control sample was 0.52 ± 0.04 mg/L. Sucrose or sorbitol

addition significantly inhibited lead leachability, the final values being 0.30 ± 0.09 mg/L for

0.40 wt% sorbitol (leaching inhibited with 96% confidence) and $0.3_9 \pm 0.1_1$ mg/L for 0.15%

sucrose (84% confidence). It is worth noting that differences in leachability were not

caused by pH variations in the TCLP extracts; the final extract pH after 18 h agitation was

12.4 for all the samples.
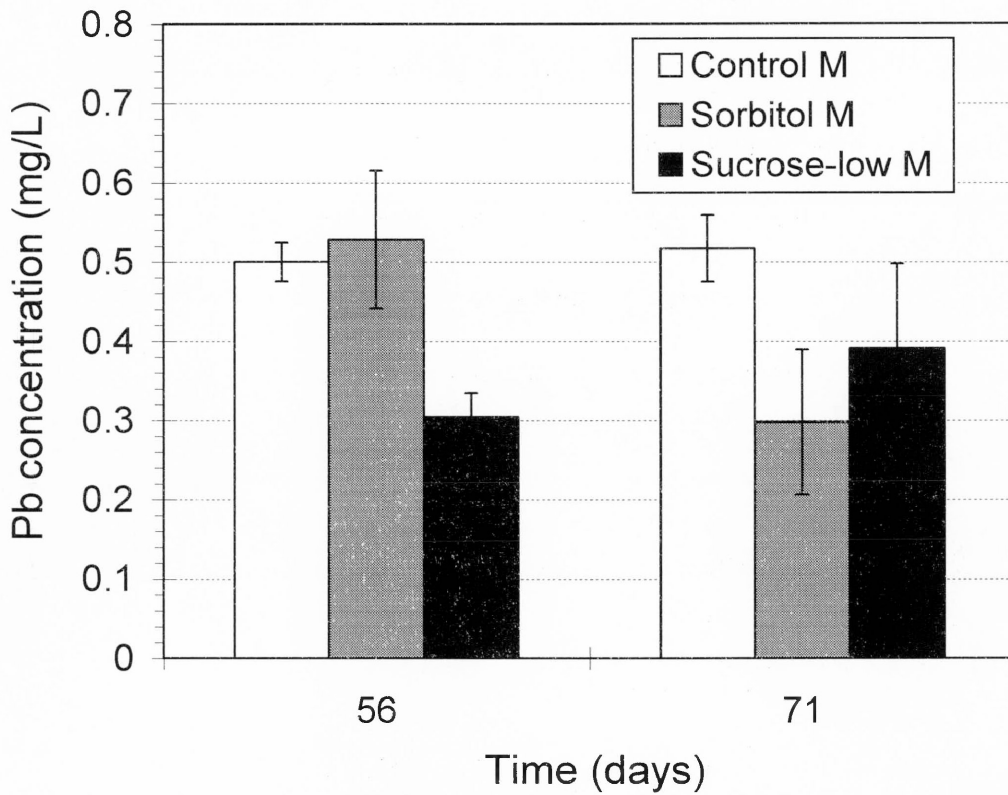
Figure 4-8 Dissolved concentration of Pb in TCLP extracts. Error bars correspond to the

standard deviations over 3 measurements.

Figure 4-9 shows the concentration of Zn in the TCLP extracts. Between 56 and 71

days, the zinc leachability decreased for the control and sorbitol-containing samples (93%

and 84% confidence, respectively) but did not significantly change for the sample

containing sucrose. Unlike the results obtained for lead, the addition of sucrose or sorbitol

to cement had no significant effect on Zn leachability by day 71.
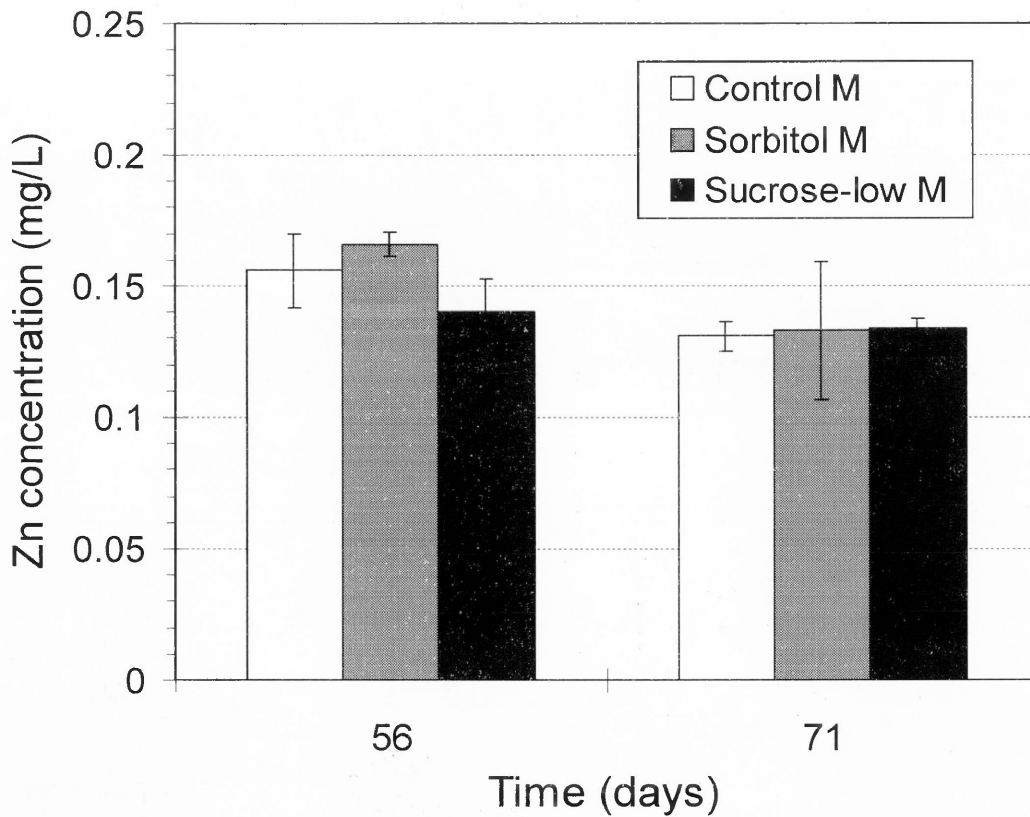
Figure 4-9 Dissolved concentration of Zn in TCLP extracts.

4.3.5. Microstructure Analyses

Table 4-2 lists the hydration products identified in each cement sample at different

curing times and indicates whether or not the samples were set.

In agreement with previous studies [24], calcium hydroxide and CSH were the main

hydration products of pure Portland cement (Control). Cement containing 1% Pb and 1%

Zn (Control M) had the same microstructure as metal-free cement (Figure 4-10). Shells of
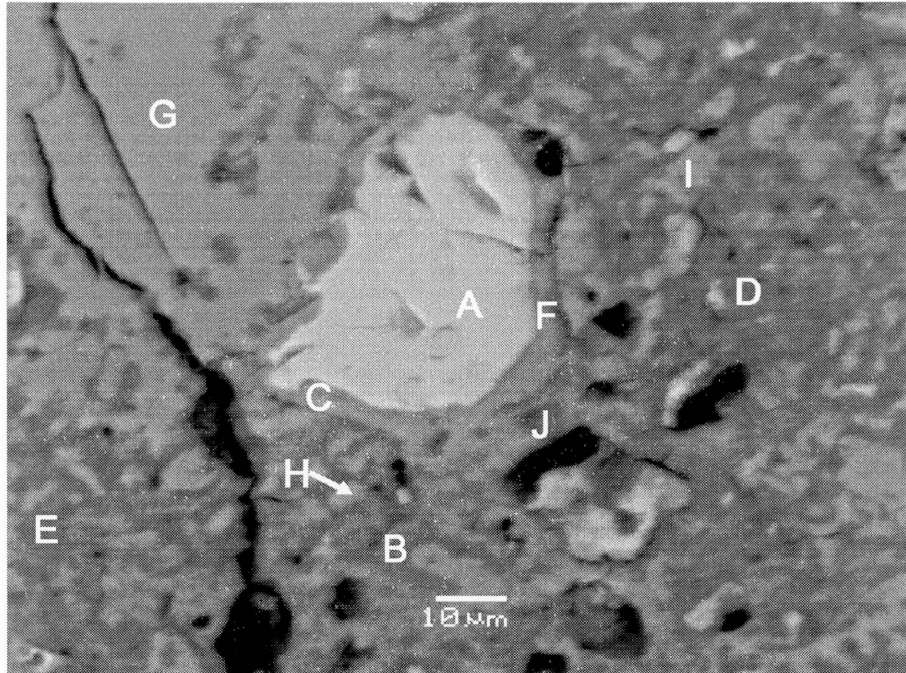
Figure 4-10 Backscattered electron images of Control M sample (1% Pb + 1% Zn) at day 56 showing (A) C_3S, (C and F) inner CSH, (B, D, and E)outer CSH, (G, H and I) CH and (J) ettringite.

smooth-textured CSH surrounded unhydrated cement grains (C_3S primarily), while irregularly textured CSH occupied much of the void space that was originally filled with water. These two different CSH phases respectively correspond to what Diamond [34] terms "inner" and "outer" CSH. Small amounts of the Ca-Al-hydroxysulfate phases ettringite and monosulfate were disseminated throughout the sample and also might have been intermixed within the CSH as is suggested by the small amounts of Al and S detected in that phase (typically less than 2 atom %). Taylor [35] reports that Ca-Al-hydroxysulfate can intermix with CSH at the micrometer to single-layer scale which is too small to be resolved by SEM-EDS. Lead and zinc were mostly present in CSH at concentrations

between 0.9 and 1.8 wt %. Ettringite and calcium hydroxide have much lower Pb and Zn concentrations (typically less than 0.8 wt %).

The addition of sorbitol or sucrose to metal-free cement delayed CSH formation. At day 1, CH was the only hydration product detected in the Sucrose-low and Sorbitol samples (Figure 4-11). From day 7 onwards, however, these samples contained both CSH and CH.

(a)   (b)
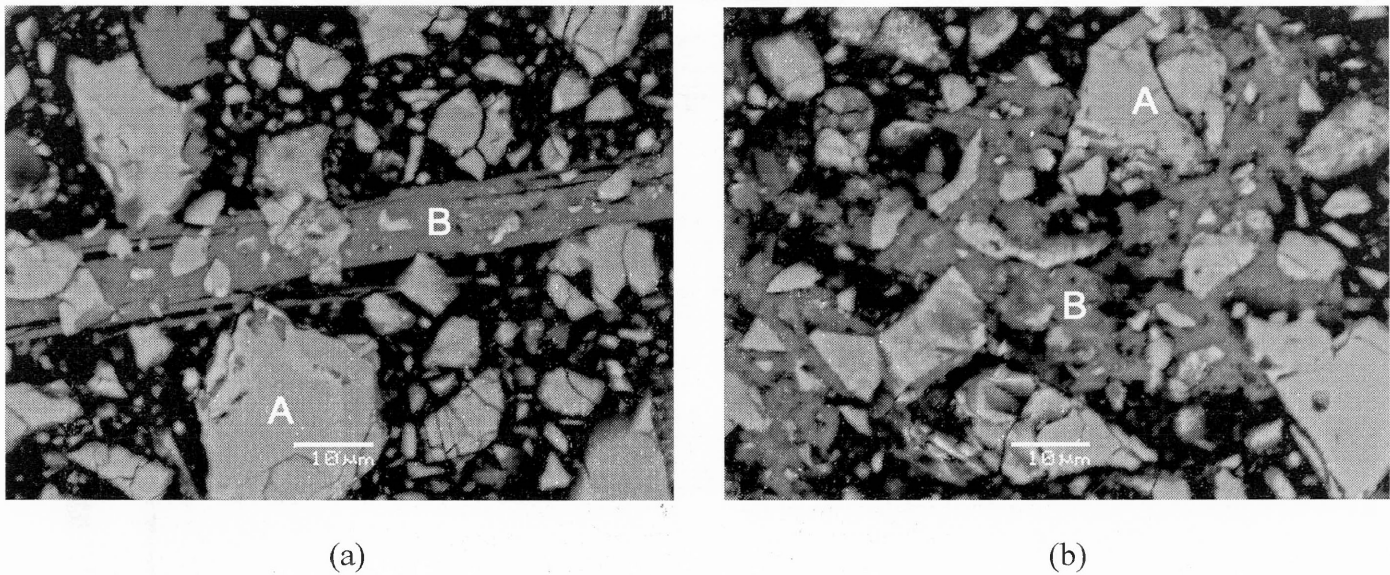
Figure 4-11 Backscattered electron images of (a) Sucrose-low and (b) Sorbitol samples at day 1 showing the (A) unhydrated C_3S phase and (B) CH.

When sucrose or sorbitol was added to cement in combination with Pb and Zn (Sucrose-low M, Sucrose-high M, Sorbitol M), the first hydration phase to appear consisted of platy Al-rich crystals (with cracks that were probably caused by drying; Figures 4-12a-c).
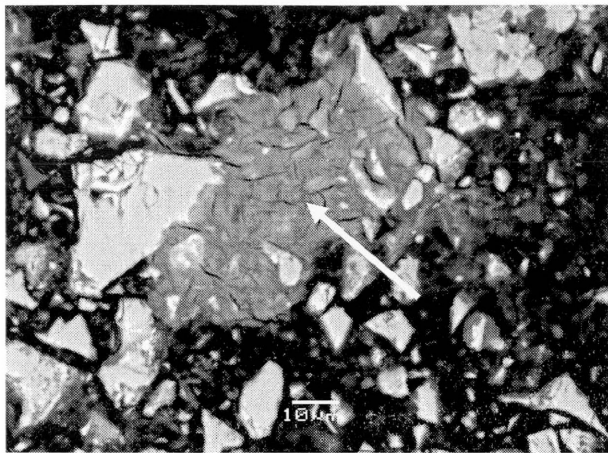
(a)
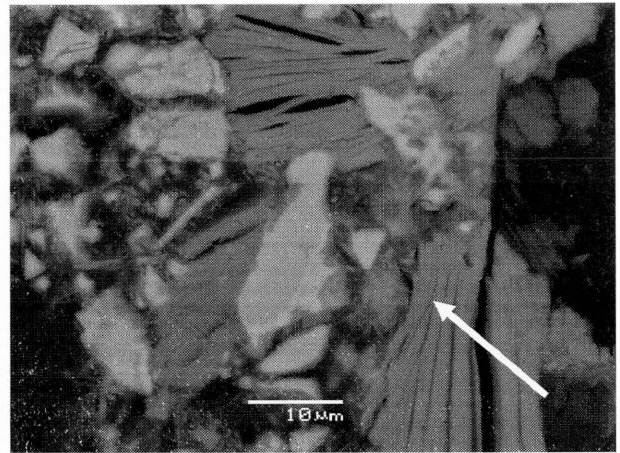
(b)
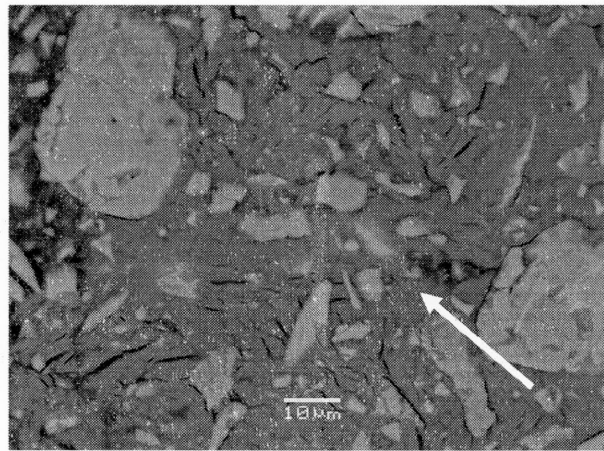
(c)

Figure 4-12 Backscattered electron images of (a) Sorbitol M, (b) Sucrose-low M and (c)

Sucrose-high M at day 7. The Al-rich phase is indicated by arrows. Bright areas are

unhydrated cement consisting mainly of C_3S. None of these samples were set by day 7.

It was identified by X-ray diffractometry as ettringite, $Ca_6Al_2(SO_4)_3(OH)_{12} \cdot 26H_2O$ (Figure

4-13)[8]. However, the average elemental composition determined by more than 50

independent EDS measurements – $Ca_{6.00} Al_{2.41} S_{0.45} O_{18.42} Fe_{0.11} Si_{0.57} Pb_{0.06} Zn_{0.11}$– indicates

_____

[8] The XRD diffractograms for the Sucrose-low M and Sucrose-high M samples are displayed in Appendix K.

a much lower S/Ca ratio than that of ettringite[9]. Therefore, it is likely that ettringite was intermixed with unhydrated C_3A, which would account for the low sulfur content. The presence of Fe, Si, Pb and Zn indicates that the ettringite contains impurities. As mentioned already, ettringite was also found in the absence of sucrose and sorbitol (Control M), but in much smaller amounts and coexisting with CH and CSH (Figures 4-10 and 4-14).

As the samples containing metal and sucrose or sorbitol began to set, the amounts of calcium hydroxide and CSH increased (Table 4-2). Figure 4-15 shows a backscattered electron image of the Sucrose-high M sample at day 56, by which time partial setting had occurred. The image depicts ettringite coexisting with CSH (characterized by Ca/Si = 2.5-3.0:1) and a transition product which contains a significant concentration of Al (Ca/Al = 3-5:1) and a lower Si concentration than CSH (Ca/Si = 3-8:1).
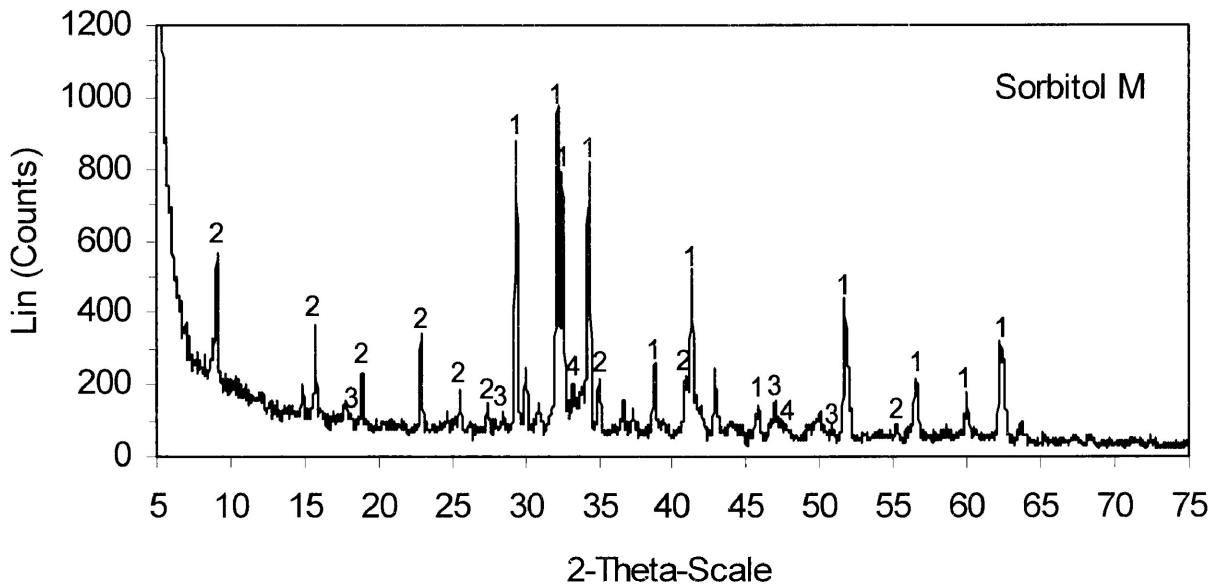
Figure 4-13 X-ray diffractogram of the Sorbitol M sample at day 7, showing (1) C_3S or C_2S, (2) ettringite, (3) portlandite (CH), and (4) C_3A.

---

[9] Due to the space limitation, only selected SEM-EDS results are displayed in this Chapter. More SEM-EDS results are shown in Appendix L.
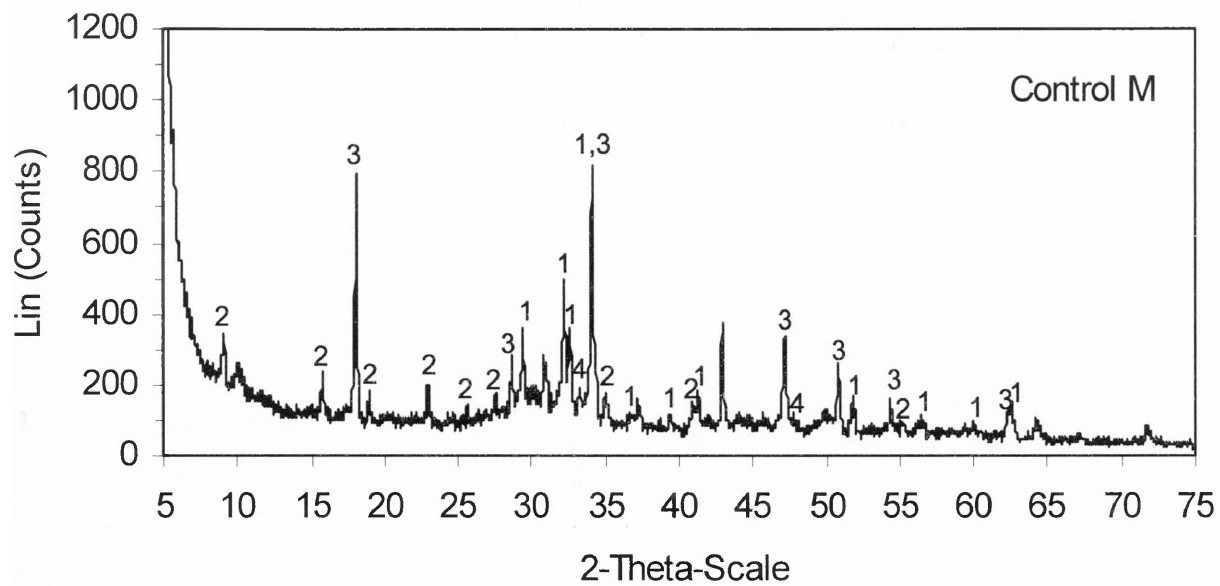
Figure 4-14 X-ray diffractogram of the Control M sample at day 7, showing (1) C_3S or C_2S,

(2) ettringite, (3) portlandite (CH), and (4) C_3A.
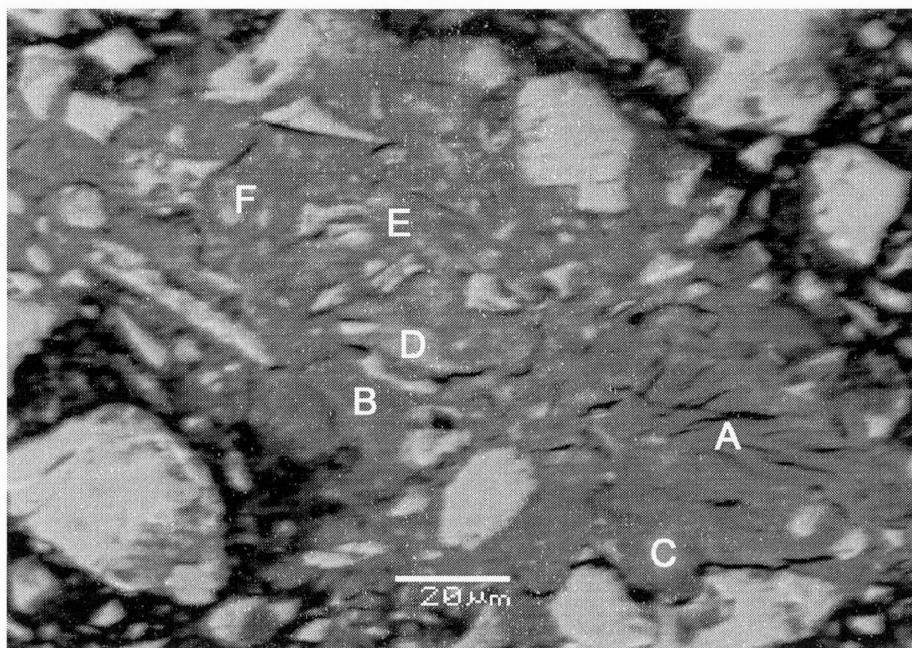
Figure 4-15 Backscattered electron image of the Sucrose-high M sample at day 56, showing

(A and B) ettringite, (C and D) CSH, and (E and F) transitional product.

The elemental composition at several points within the ettringite, CSH and

transition product was measured by EDS on several backscattered electron images of the

Sucrose-high M sample at day 56 and plotted in Figures 4-16 and 4-17. Three regions

corresponding to CSH (low Al content), ettringite (high Al content) and the transitional

product (intermediate Al content) are superimposed on the graphs. Similar results were

obtained for the Sorbitol M sample (data not shown). The Si concentration increases almost

linearly as the Al concentration decreases (Figure 4-16), representing the transition from

ettringite to CSH. Figure 4-17 indicates that Pb and Zn concentrations vary widely, from 1

to 6 wt%, in CSH (corresponding to low Al concentration). By contrast, the range of Pb and

Zn concentrations is relatively limited, less than 2 wt%, in ettringite. The larger capacity of
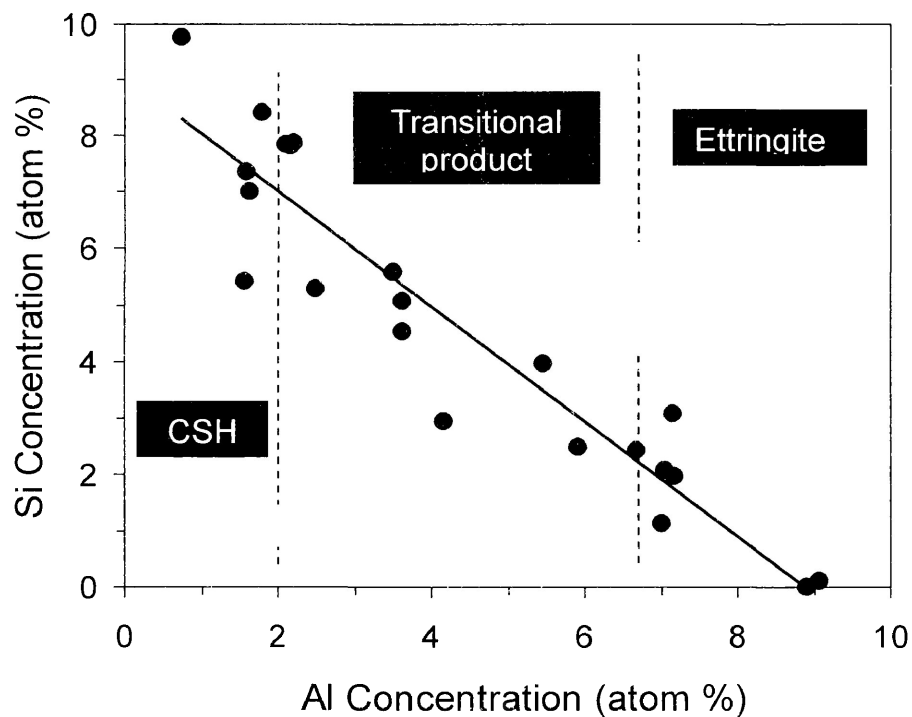
Figure 4-16 Concentration of Si as a function of Al concentration in the Sucrose-high M
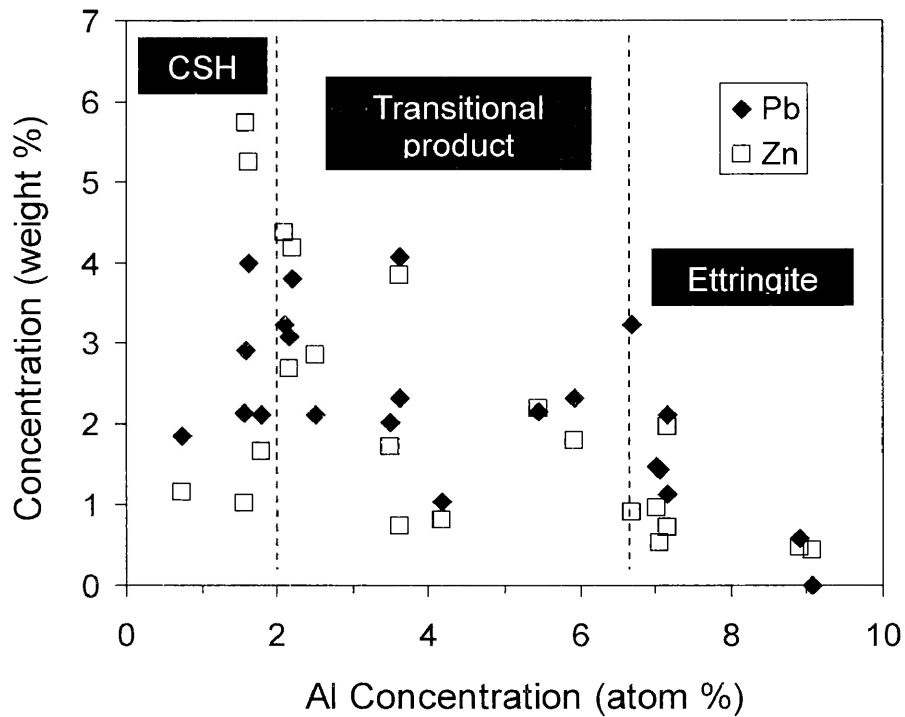
sample at day 56.

Figure 4-17 Concentrations of Pb and Zn as a function of Al concentration in the Sucrose-

high M sample at day 56.

CSH for immobilizing Pb and Zn is likely explained by structural differences: ettringite

forms hexagonal prismatic or acicular crystals in which ion substitutions are the only

significant immobilization mechanism [3], whereas CSH is an amorphous gel which allows

Pb and Zn atoms to be immobilized through a variety of mechanisms such as sorption,

coprecipitation, and formation of metallosilicates [3-7].

4.4. Conclusions

The presence of 1 wt% Pb and 1 wt% Zn significantly shortens the time at which

maximum hydration of Portland cement is achieved, but has relatively little effect

on the final compressive strength.

2. The addition of 0.15 wt% sucrose or 0.40 wt% sorbitol to metal-free Portland cement retards hydration and strength development for 3 to 7 days.

. The retardation effect of sucrose and sorbitol are considerably enhanced when Pb and Zn are present. Controlled sucrose or sorbitol addition to metal-cement mixtures can retard setting for up to 28 days without affecting the 56-day strength, thus adding flexibility to the handling of S/S-treated waste.

4. The long-term TCLP-based leachability of Pb may be somewhat reduced by the addition of sucrose or sorbitol; however, the long-term leachability of Zn is not significantly affected.

5. Cement setting correlates with the precipitation of CSH gel. Precipitation of ettringite was favored and the formation of CSH and CH were delayed when sorbitol or sucrose was added to metal-cement mixtures.

6. The ability of ettringite to immobilize Pb and Zn is inferior to that of CSH.

7. Sorbitol conferred a slightly higher degree of hydration and compressive strength than sucrose to Portland cement after 56 days.

4.5. Acknowledgement

4.6. References

[1]   J.R. Conner, S.L. Hoeffner, A critical review of stabilization/solidification technology,

Environ. Sci. Technol. 28 (1998) 397-462.

[2] S. Mindess, J.F. Young, Concrete, Prentice-Hall, Inc., Englewood Cliffs, NJ, 1981.

[3] M.L.D. Gougar, B.E. Scheetz, D.M. Roy, Ettringite and C-S-H Portland cement phases for waste ion immobilization: a review, Waste Manage. 16 (1996) 295-303.

[4] F.K. Cartledge, L.G. Butler, Devi Chaiasani, H.C. Eaton, F.P. Frey, Esteban Herrera, M.E. Tittlebaum, S.-L. Yang, Immobilization mechanisms in solidification/stabilization of Cd and Pb salts using Portland cement fixing agents, Environ. Sci. Technol. 24 (1990), 867-873.

[5] F. Ziegler, R. Giere, C.A. Johnson, Sorption mechanisms of zinc to calcium silicate hydrate: sorption and microscopic investigations, Environ. Sci. Technol. 35 (2001) 4556-4561.

[6] I. Moulin, W.E.E. Stone, J. Sanz, J.-Y. Bottero, F. Mosnier, C. Haehnel, Lead and zinc retention during hydration of tri-calcium silicate: a study by sorption isotherms and ^{29}Si nuclear magnetic resonance spectroscopy, Langmuir 15 (1999) 2829-2835.

[7] F. Ziegler, A.M. Scheidegger, C.A. Johnson, R. Dahn, E. Wieland, Sorption mechanisms of zinc to calcium silicate hydrate: X-ray absorption fine structure (XAFS) investigation, Environ. Sci. Technol. 35 (2001) 1550-1555.

[8] J.D. Birchall, N.L. Thomas, The mechanism of retardation of setting of OPC by sugars, Brit. Ceram. Proc. 35 (1984) 305-315.

[9] J.F. Young, A review of the mechanisms of set-retardation in Portland cement pastes containing organic admixtures, Cem. Concr. Res. 2 (1972) 415-433.

[10] P.F.G. Banfill, D.C. Saunders, The relationship between the sorption of organic compounds on cement and the retardation of hydration, Cem. Concr. Res. 16 (1986)

399-410.

[11] V.S. Ramachandran, M.S. Lowery, Conduction calorimetric investigation of the effect of retarders on the hydration of Portland cement, Thermochim. Acta 195 (1992) 373-387.

[12] N.L. Thomas, J.D. Birchall, The retardation action of sugars on cement hydration, Cem. Concr. Res. 13 (1983) 830-842.

[13] K. Luke, G. Luke, Effect of sucrose on retardation of Portland cement, Adv. Cem. Res. 12 (2000) 9-18.

[14] S.D. Kinrade, J.W. Del Nin, A.S. Schach, T.A. Sloan, K.L. Wilson, C.T.G. Knight, Stable five- and six-coordinated silicate anions in aqueous solution, Science 285 (1999) 1542-1545.

[15] M.C.G. Juenger, H.M. Jennings, New insights into the effects of sugar on the hydration and microstructure of cement pastes, Cem. Concr. Res. 32 (2002) 393-399.

[16] Patent: Use of particular polysaccharides as admixtures for mineral materials, http://www.freshpatents.com/Use-of-particular-polysaccharides-as-admixtures-for-mineral-materials-dt20060316ptan20060054062.php?type=description (accessed January 2007).

[17] http://en.wikipedia.org/wiki/Plasticizer (accessed January 2007).

[18] http://www.epa.gov/waterscience/criteria/wqcriteria.html#priority (accessed January 2007).

[19] Standard practice for capping cylindrical concrete specimens, ASTM C617-98 (2003).

[20] Standard test method for compressive strength of hydraulic cement mortars (using 2-in. or [50-mm] cube specimens), ASTM C109/C109M-98 (1998).

[21]   M.C.G Juenger, H.M. Jennings, Examining the relationship between the

microstructure of calcium silicate hydrate and drying shrinkage of cement pastes,

Cem. Concr. Res. 32 (2002) 289-296.

[22]   Toxicity Characteristic Leaching Procedure, http://www.epa.gov/sw-

846/pdfs/1311.pdf (accessed January 2007).

[23]   K.O. Kjellsen, R.J. Detwiler, O. E. Gjørv, Backscattered electron image analysis of

cement paste specimens: specimen preparation and analytical methods, Cem. Concr.

Res. 21 (1991) 388-390.

[24]   K.L. Scrivener, Backscattered electron imaging of cementitious microstructures:

understanding and quantification, Cem. Concr. Composites 26 (2004) 935-945.

[25]   K.L. Scrivener, Analysis of phases in cement paste using backscattered electron

images, methanol adsorption and thermogravimetric analysis, Mater. Res. Soc. Symp.

Proc. 85 (1987) 67-76.

[26]   S.K. Ouki, C.D. Hills, Microstructure of Portland cement pastes containing metal

nitrate salts, Waste Manage. 22 (2002) 147-151.

[27]   S. Igarashi, M. Kawamura, A. Watanabe, Analysis of cement pastes and mortars by a

combination of backscattered-based SEM image analysis and calculation based on the

Powers model, Cem. Concr. Composites 26 (2004) 977-985.

[28]   S. Asavapisit, G. Fowler, C. R. Cheeseman, Solution chemistry during cement

hydration in the presence of metal hydroxide wastes, Cem. Concr. Res. 27 (1997)

1249-1260.

[29]   J. D. Ortego, S. Jackson, G.-S. Yu, H. McWhinney, D. L. Cocke, Solidification of

hazardous substances- a TGA and FTIR study of Portland cement containing metal

nitrates, J. Environ. Sci. Health A 24 (6) (1989) 589-602.

[30]   N. L. Thomas, D. A. Jameson, D. D. Double, The effect of lead nitrate on the early hydration of Portland cement. Cem. Concr. Res. 11 (1981) 143-153.

[31]   N. Pannetier, A. Khoukh, J. François, Physico-chemical study of sucrose and calcium ions interactions in alkaline aqueous solutions, Macromol. Symp. 166 (2001) 203-208.

[32]   J.K. Beattie, M.T. Kelso, Equilibrium and dynamics of the binding of calcium ion to sorbitol (D-glucitol), Aust. J. Chem. 34 (1981) 2563 – 2568.

[33]   C. Tashiro, H. Takahashi, M. Kanaya, I. Hirakida, R. Yoshida, Hardening property of cement mortar adding heavy metal compound and solubility of heavy metal from hardened mortar, Cem. Concr. Res. 7 (1977) 283-290.

[34]   S. Diamond, The microstructure of cement paste and concrete — a visual primer, Cem. Concr. Composites 26 (2004) 919-933.

[35]   H.F.W. Taylor, Nanostructure of C-S-H: current status, Adv. Cem. Based Mater. 1 (1993) 38-46.

CHAPTER 5

CONCLUSIONS AND RECOMMENDED FUTURE WORK

5.1. Summary and Conclusions

This thesis deals with a series of laboratory experiments to investigate the effects of sugars and sugar derivatives (represented by sucrose and sorbitol) on the hydration and microstructure of tricalcium silicate (C_3S), white Portland cement (WPC) and ordinary Portland cement (OPC), in order of increasing compositional complexity.. The hydration and microstructure of C_3S, WPC and OPC without admixtures were first investigated to better understand the potential contribution of individual phase in the clinker to the overall hydration and microstructure of hydrated pastes (Chapter 2). As an environmental engineering application, the effects of sucrose and sorbitol on OPC-stabilized toxic metal wastes containing lead nitrate and zinc nitrate were also evaluated.

The ratios of non-evaporable water content in fully hydrated OPC and WPC were found to be $0.234_9 \pm 0.005_7$ and $0.208_6 \pm 0.003_2$, respectively. C_3S had a higher degree of hydration than OPC and WPC at any given time. WPC hydrated faster than OPC during the first day, but both reached the same degree of hydration (80%) at day 56. The early rate of hydration was positively correlated with the C_3S and C_3A contents.

Pure C_3S, upon hydration, formed dense CH-rich islands, containing large amounts of unhydrated C_3S, in a porous matrix composed mainly of CSH and residual C_3S. The number and size of the CH-rich islands increased from day 1 to day 7. Past day

7, hydration was only accompanied by precipitation of CSH and minor CH in the porous region.

Hydrated OPC contained CH-rich islands at day 1, but these islands were much smaller than in pure C_3S. As curing time increased, the distinction between CH-rich islands and the rest of the paste progressively disappeared owing to hydration of C_3S grains embedded in the islands and precipitation of irregularly textured CSH in the porous regions.

The evolution of microstructure in hydrated WPC was similar to that of OPC, except that the C_3S grains embedded in the CH-rich islands had thicker CSH rims than those in hydrated OPC at day 1, consistent with the larger degree of hydration of WPC at early times. Separated hydration shells (Hadley grains) were more prevalent in OPC and WPC than in pure C_3S.

The overall hydration stoichiometries for C_3S, OPC and WPC were not constant over time; the initial hydration products were CH and CSH, but after several days CH production almost ceased while CSH precipitation continued.

Sucrose and sorbitol addition delayed the hydration of C_3S, OPC and WPC by interfering with the precipitation of CSH and CH at early curing times. The delaying effect of sucrose (0.037 or 0.15 wt%) or sorbitol (0.40 wt%) only lasted a few days, except for the combination of C_3S with 0.15 wt% sucrose, which did not set even after 56 days. For the above concentrations of sucrose or sorbitol, the retardation period was longer in OPC (3-7 days) than in WPC (1-3 days). Calcium hydroxide appeared before

CSH at the earliest stages of hydration, and eventually formed into dense CH-rich islands that contained unhydrated grains of C_3S. These islands persisted in the paste microstructure even after CSH had started precipitating and the samples had set, but they were more prominent in pure C_3S than in OPC or WPC.

Sucrose affected the initial hydration and microstructure of C_3S much more than that of OPC and WPC. By contrast, the effect of sorbitol was similar for all three cements, and less than that of sucrose in the case of pure C_3S. After 56 days, all the cements attained nearly 80% hydration and 27.6-34.5 MPa (4000-5000 psi) compressive strength, except for OPC containing 0.40 wt% sorbitol which exhibited slightly higher strength and degree of hydration with statistical reliability.

The presence of 1 wt% Pb and 1 wt% Zn significantly shortened the time at which maximum hydration of Portland cement was achieved, but had relatively little effect on the final compressive strength. The retardation effect of sucrose and sorbitol were considerably enhanced when Pb and Zn were present. The controlled sucrose (0.15 wt%) or sorbitol (0.40 wt%) addition to metal-cement mixtures could retard setting for up to 28 days without affecting the 56-day strength, thus adding flexibility to the handling of S/S-treated waste. The amount of sucrose addition required to achieve a given delaying effect was always found to be lower than that of sorbitol. Furthermore, sucrose is cheaper than sorbitol. As a result, sucrose is recommended as an admixture to control the setting of cement-stabilized wastes.

Cement setting correlated with the precipitation of CSH gel. Precipitation of ettringite was favoured and the formation of CSH and CH were delayed when sorbitol or sucrose was added to metal-cement mixtures.

The long-term TCLP-based leachability of Pb may be somewhat reduced by the addition of sucrose (0.15 wt% or 0.38%) or sorbitol (0.40%); however, the long-term leachability of Zn was not significantly affected. The ability of ettringite to immobilize Pb and Zn was found to be inferior to that of CSH.

5.2. Recommendations for Future Work

The focus of this research was to investigate the effect of sucrose and sorbitol on the hydration and microstructure of cement as well as on the properties of heavy metal wastes stabilized/solidified by Portland cement. Although the results provide valuable insights, the exact mechanisms by which the microstructure is affected by the presence of sorbitol, sucrose, metals, and combinations thereof remain largely unexplained. Following are recommendations for further research which may help bridge these gaps in knowledge:

- Study the solution chemistry at early hydration times with sucrose, sorbitol, heavy metals and combinations thereof;
- Examine the effect of sucrose, sorbitol, heavy metals and combinations thereof on the porosity and surface area of the treated waste;
- Explore the impact of sucrose or sorbitol on the zeta potential of the hydrating cement particles;

- Investigate the interactions between sucrose or sorbitol and heavy metals by nuclear magnetic resonance (NMR) spectroscopy.

- Study how the microstructure of cement-based materials correlates with their physical properties such as strength, consistency, workability, etc.

Moreover, this work could be expanded by using a wider range of S/S agents, organic admixtures, contaminants, curing conditions and leaching procedures, such as:

- cement-fly ash admixtures with different cement-to-fly ash ratios;

- organic compounds such as lignosulfonates, which are byproducts of the pulp and paper industry and already used commercially as cement admixtures;

- toxic metal anions, such as chromate and arsenic, whose leachability in cement-stabilized waste may be more affected than the cations (Pb and Zn) used in this study;

  real industrial wastes containing a variety of inorganic contaminants;

- different water-to-solid ratios during sample preparation;

- different curing conditions, such as various curing temperatures (see preliminary tests in Appendix E);

- dynamic leaching tests to more accurately simulate leaching conditions of cement-stabilized waste in the field.

APPENDIX A

EFFECT OF PARTICLE SIZE ON THE RESULTS OF LOSS-ON-IGNITION TESTS

This appendix compares the degree of hydration values obtained with the same sample using different particle size ranges for loss-on-ignition testing. The results show that as long as particles are less than 2000 μm in size, their size distribution does not influence the hydration results significantly (Table A-1).

Table A-1 Degree of hydration of Control (pure OPC) sample with different particle size (samples were made from the same batch)

Particle size	Degree of hydration
850 ~ 2000 μm	68.33%
425~850 μm	67.91%
< 425 μm	67.65%

APPENDIX B

EFFECT OF ARABITOL ON THE DEGREE OF HYDRATION OF ORDINARY PORTLAND CEMENT

This appendix depicts how the addition of 2 wt% arabitol affects the degree of hydration of OPC. (The water-to-cement ratio was 0.40:1.) As displayed in Figure B-1, adding 2 wt% retards the hydration of OPC for at least 56 days.
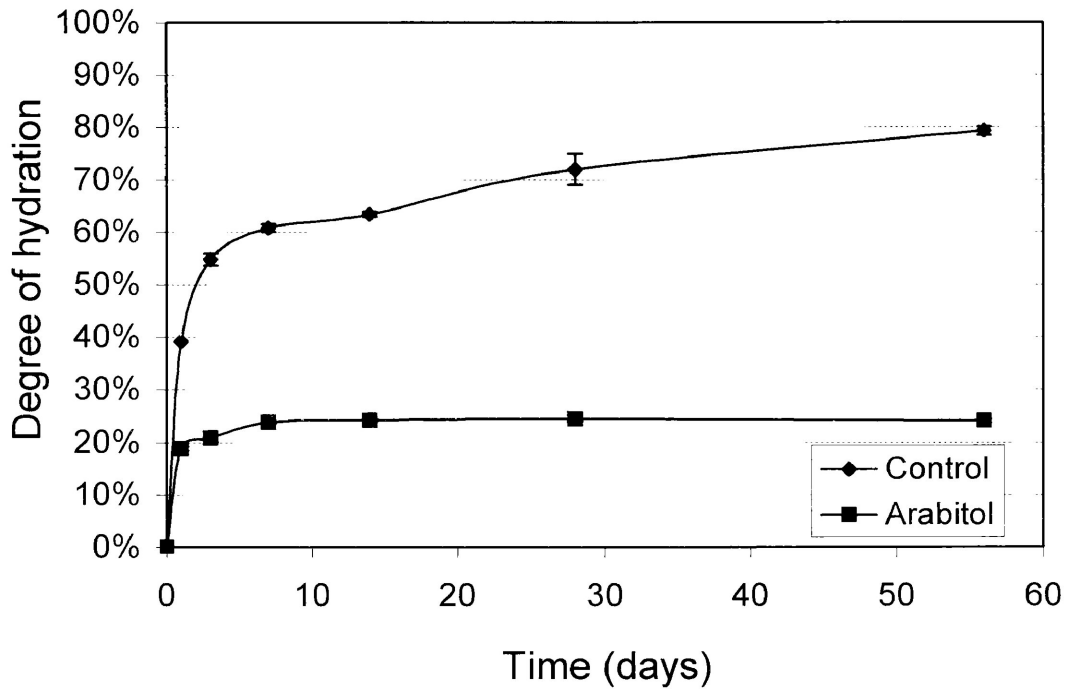
Figure B-1 Effect of 2 wt% arabitol on the degree of hydration of OPC.

APPENDIX C

BACKSCATTERED ELECTRON IMAGES OF TRICALCIUM
SILICATE CONTAINING ARABITOL

This appendix presents BSE images of C_3S samples containing 2 wt% arabitol after 1, 7, and 56 days of curing. (The water-to-cement ratio was 0.60:1.)
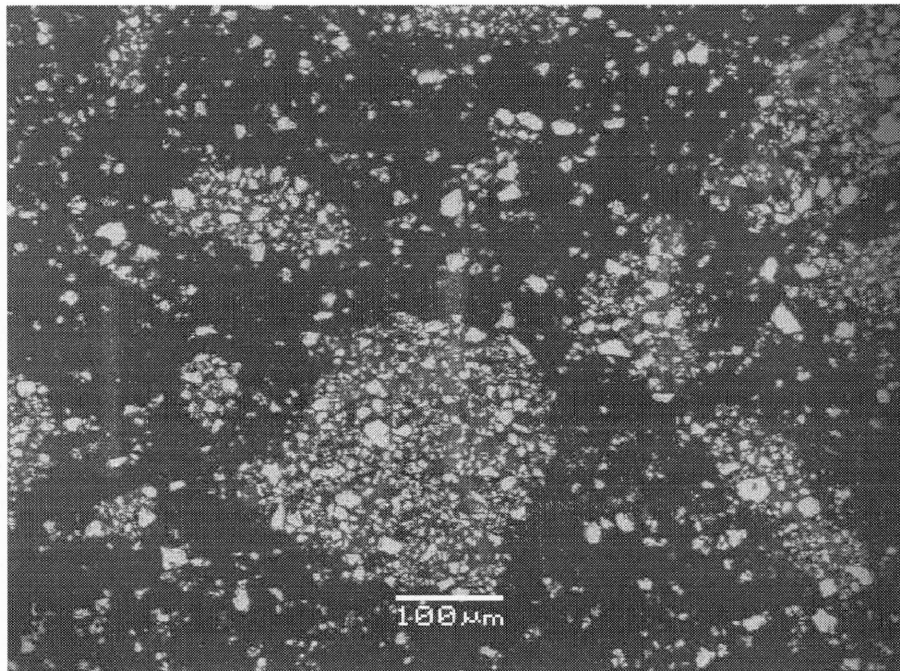
(a)
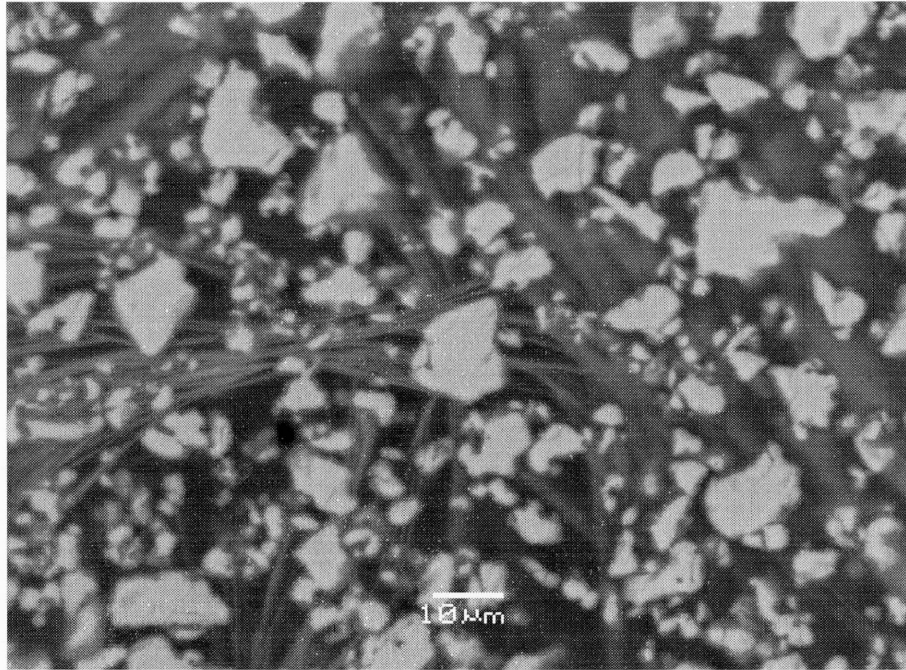
(b)

Figure C-1 Backscattered electron images of C_3S arabitol samples at day 1, (a) overview

and (b) magnified image. The bright grains are unhydrated C_3S particles and the

elongated crystals are calcium hydroxide.

Figure C-2 Backscattered electron image of C_3S arabitol samples at day 7.

Figure C-3 Backscattered electron image of C_3S arabitol samples at day 56.

APPENDIX D

EFFECT OF SUCROSE, SORBITOL, AND ARABITOL ON STRENGTH DEVELOPMENT OF ORDINARY PORTLAND CEMENT
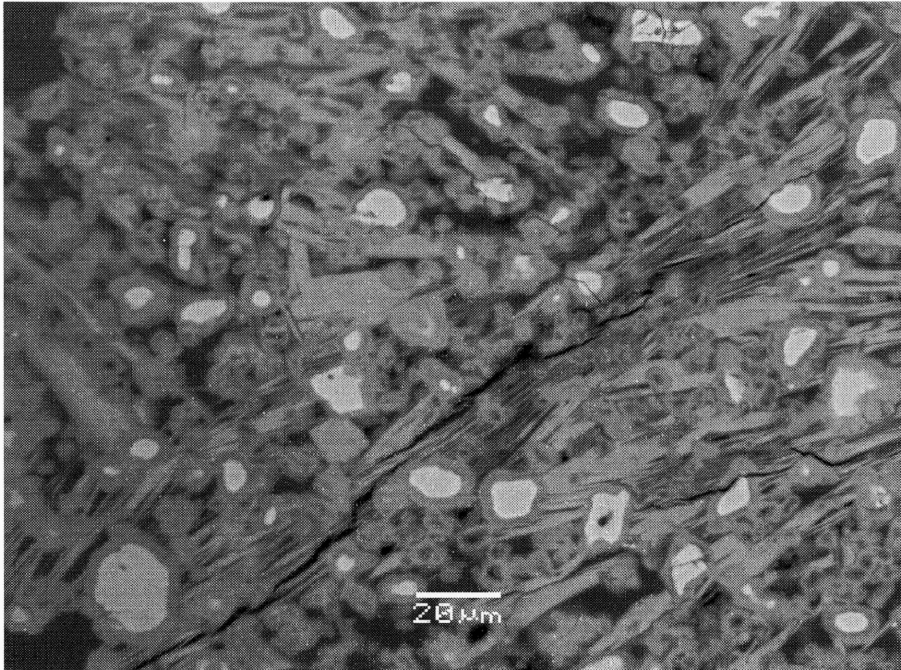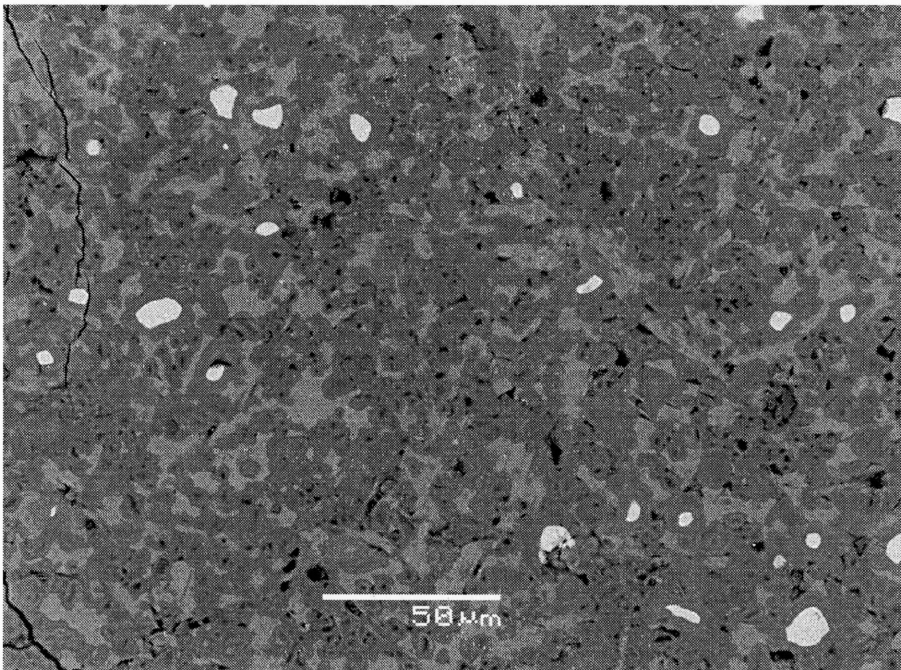
This appendix shows the strength data for OPC samples as a function of time with and without addition of sucrose, sorbitol, or arabitol. All the samples were in triple sealed plastic bags under water at room temperature. The data show that:

The addition of 2 wt% arabitol inhibits the strength development of OPC for at least 56 days.

Adding 0.40 wt% sorbitol or 0.15 wt% sucrose delays the strength development of OPC for less than 7 days.

Sorbitol improves the strength of OPC after 56 days of curing (with 81% confidence level by Student T-test).

Sucrose seems to slightly reduce the final strength of OPC. However, considering the experimental uncertainties, the effect is not significant.
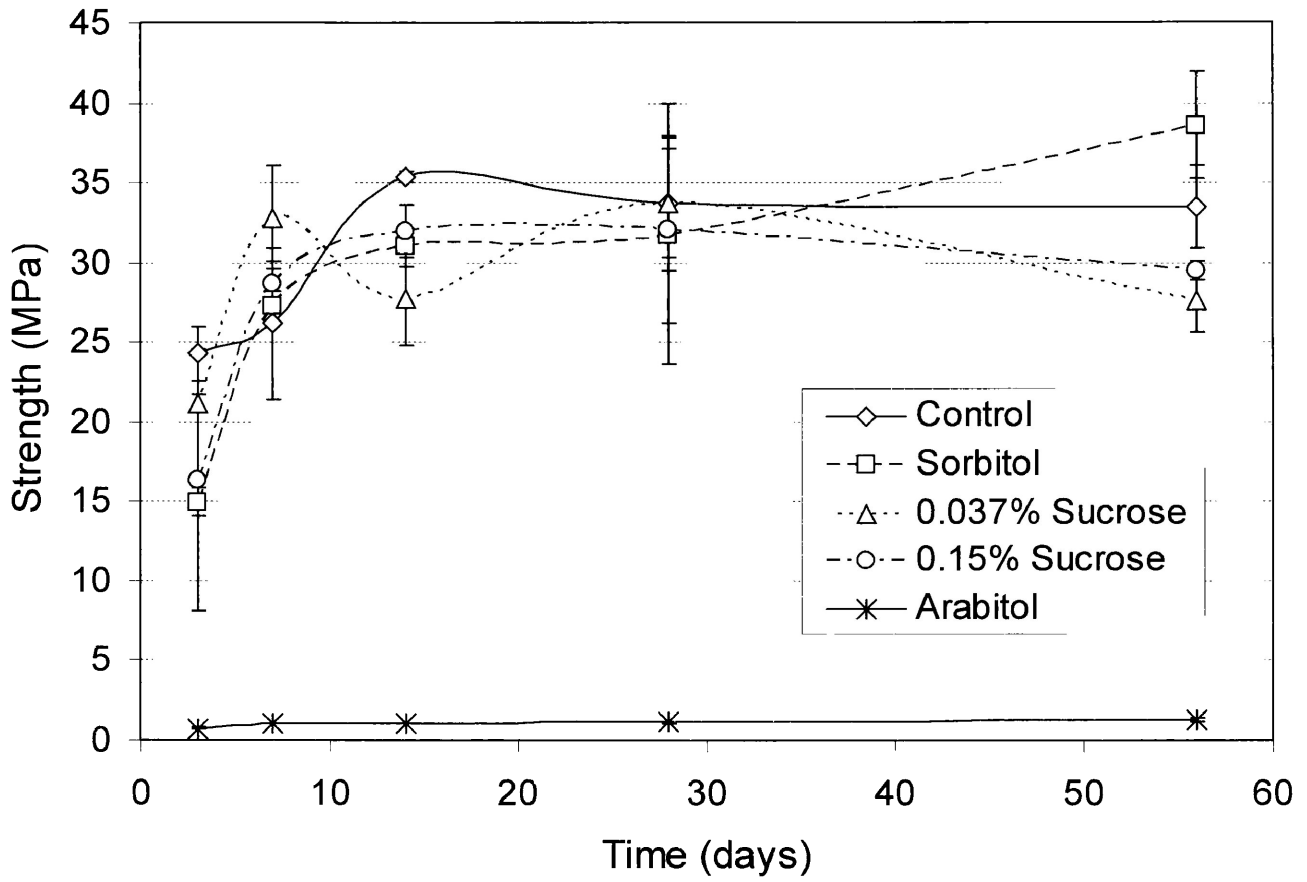
Figure D-1 Strength development in OPC samples with and without addition of sucrose, sorbitol or arabitol.

APPENDIX E

EFFECT OF TEMPERATURE ON THE PROPERTIES OF OPC-SUGAR-TREATED HEAVY METAL WASTE

This appendix demonstrates the effect of elevated curing temperature (40 °C) on the leachability, hydration rate, and the microstructure of OPC-treated waste containing 1 % Pb and 1% Zn. Samples containing small amount of sucrose or sorbitol were also evaluated.

The samples cured at 40 °C were kept in sealed plastic bags in an environmental chamber at a temperature of 40 °C and humidity of 99 %. Samples cured at 20 °C were kept in triple-sealed plastic bags under water at room temperature, Sucrose-high and sucrose-low samples contain 0.38 wt% and 0.15 wt% sucrose respectively. Sorbitol samples contain 0.40 wt% sorbitol. TCLP 1311, with an initial pH of the extraction fluid equal to 2.88, was used to evaluate the leachability of Pb and Zn. The degree of hydration was determined by loss-on-ignition test.

Conclusions:

. The higher curing temperature increases the leachability of Pb but does not significantly affect the leachability of Zn (Figure E-1).

2. The higher curing temperature accelerates the hydration process. For control samples, higher temperature leads to a higher degree of hydration by comparison with the sample cured at room temperature (Figure E-2). Higher curing

temperature also speeds up significantly the commencement of cement set when sucrose or sorbitol is added (Figure E-3).

3. Samples cured at higher temperature are more porous than the ones cured at lower temperature (Figure E-4).
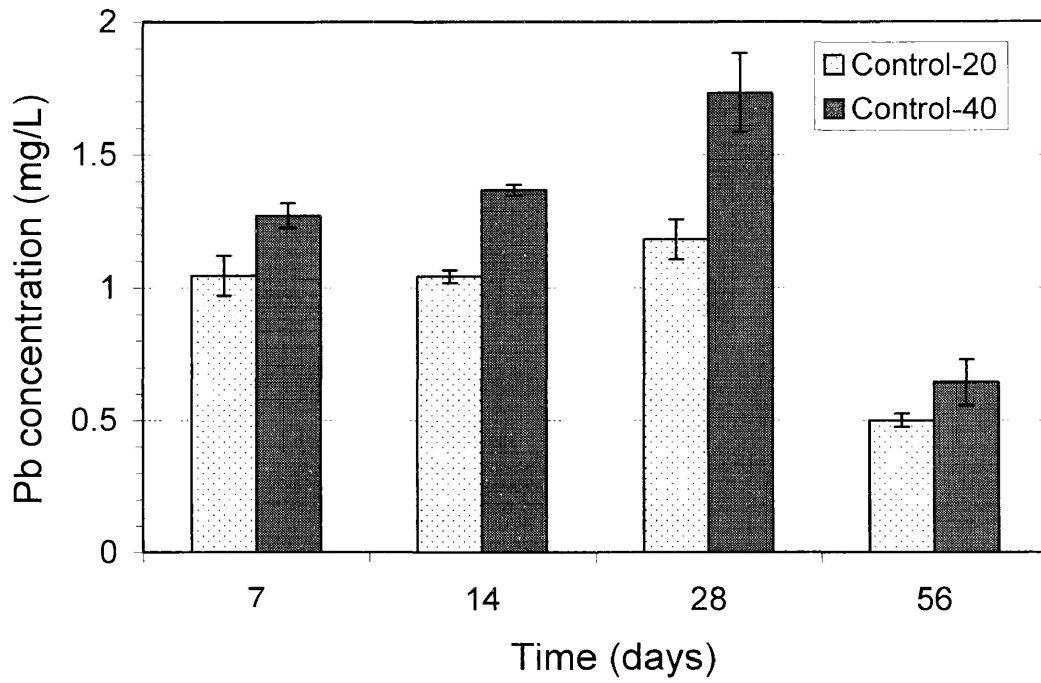
(a)
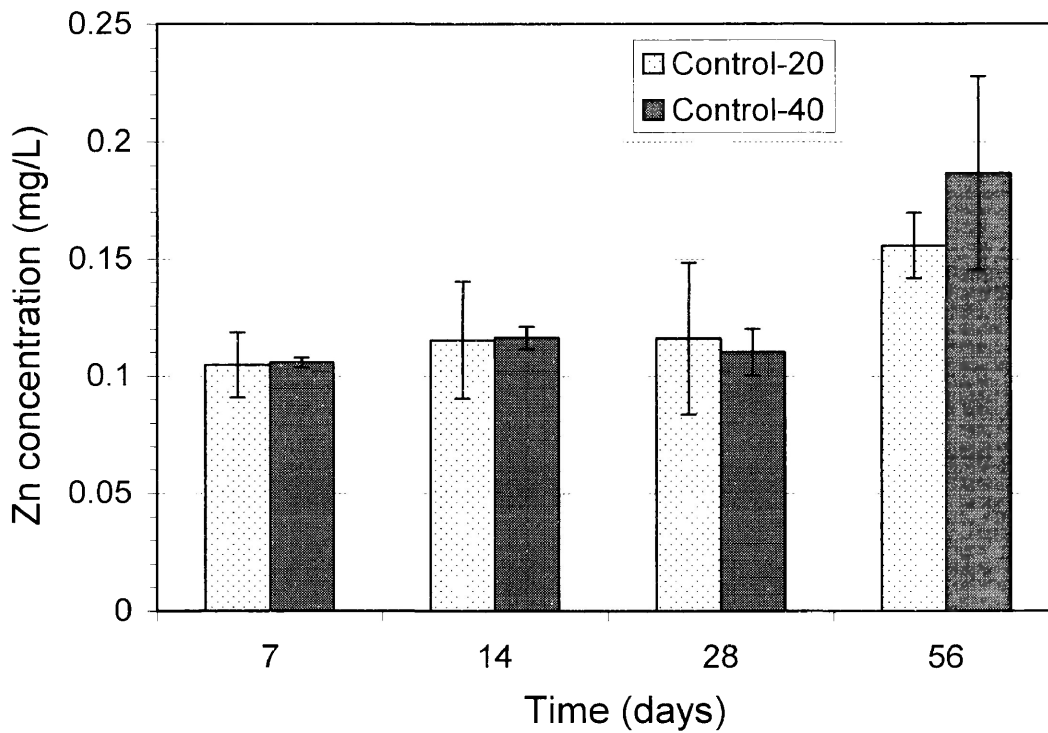
(b)

Figure E-1 Dissolved concentration of (a) Pb and (b) Zn in the extraction fluid after the

leaching tests when samples were cured at 20 or 40 °C.

Figure E-2 Effect of temperature on the degree of hydration of OPC metal samples.

Figure E-3 Effect of temperature on the degree of hydration of OPC metal samples

containing sorbitol or sucrose.

(a)
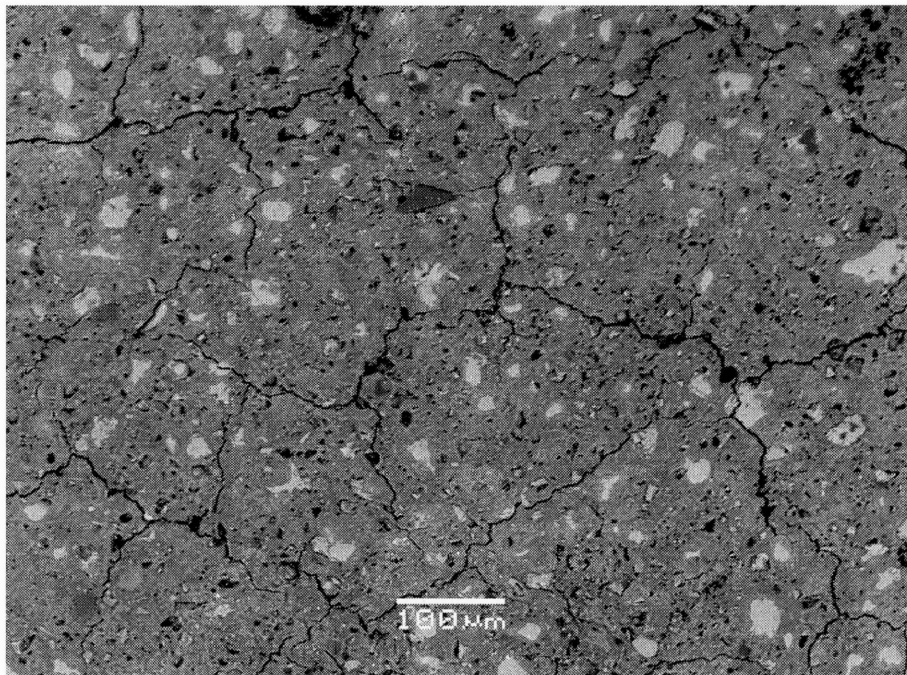
Figure E

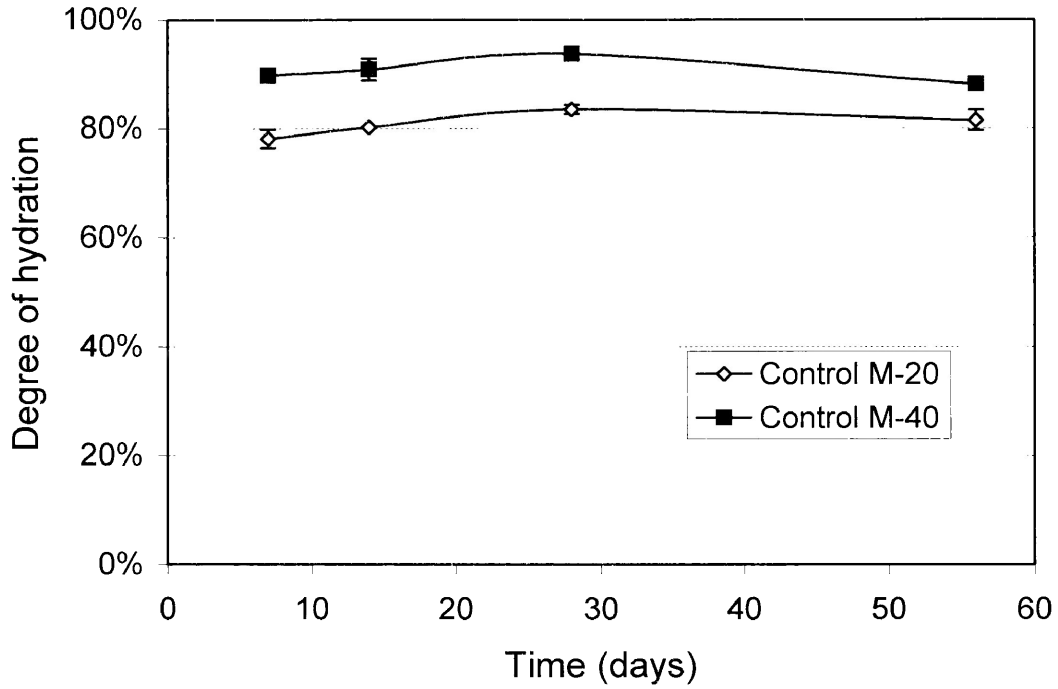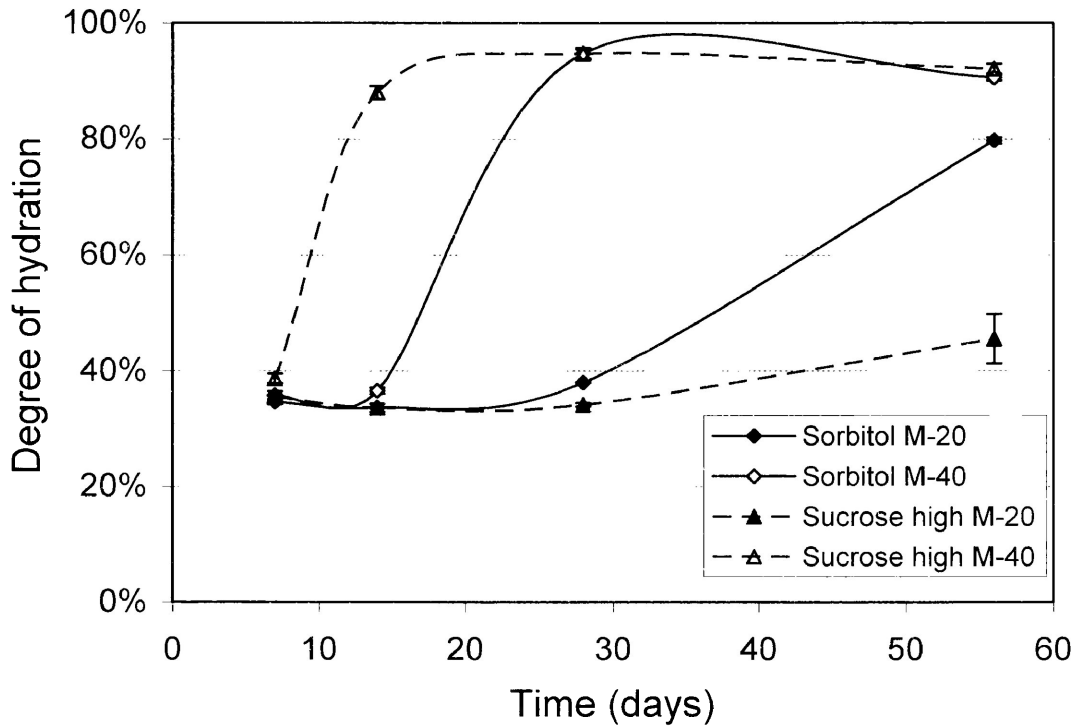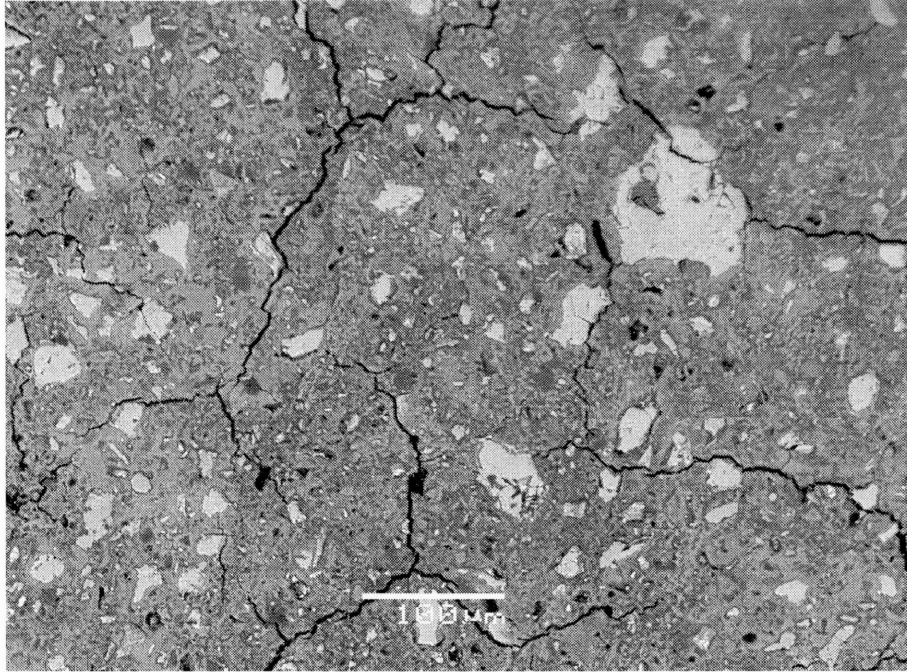(a) cured at 20°C and (b) cured at 40 °C.

APPENDIX F

EVALUATION OF THE FINAL PH OF PURE OPC AFTER LEACHING TESTS WITH EXTRACTION FLUIDS OF VARYING INITIAL ACIDITIES

This appendix shows the relationship between the initial acidity of the extraction fluid and its final pH value after 18 hours of static leaching test (TCLP 1311). Pure hydrated OPC was selected for the test. This result can be employed in choosing the proper extraction fluid for an aggressive leaching test.

Experimental procedure description: Mix 20 ml solid (hydrated OPC sample with the particle size: 425 ~ 850 μm) with 400 mL extraction fluid consisting of a solution of dilute acetic acid. (The acidity of each solution is listed in Table F-1). Rotate the mixture at 30 rpm for 18 hours and monitor the final pH of the extraction fluid after the leaching test.

Table F-1 The acidity of each extraction fluid before the leaching test and the final pH value after the leaching test

Volume of CH_3COOH added to make 1 L solution	5.7	11.4	22.8	34.2	45.6	57
Eq H^+/kg solid (20 solid + 400 ml liquid)	2^a	4	8	12	16	20
pH of the solution after the leaching test	12.29	12.04	11.4	9.65	6.45	5.25

[a]The solution that has an acidity of 2 H^+/kg solid has an initial pH of 2.88.

The pH of each extraction fluid after the leaching test was plotted as a function of the acidity of the solution before the leaching test. Figure F-1 depicts that as the acidity increases, the pH decreases; there is a smooth decrease at beginning followed by a sharp drop and then again a slow decrease. The steepest pH drop occurs when the acidity is in the range of 12 to 16 H^+/kg solid.

This graph can be used in the aggressive leaching test to determine the initial acidity of the extraction fluid to achieve the desired final pH after the leaching test.
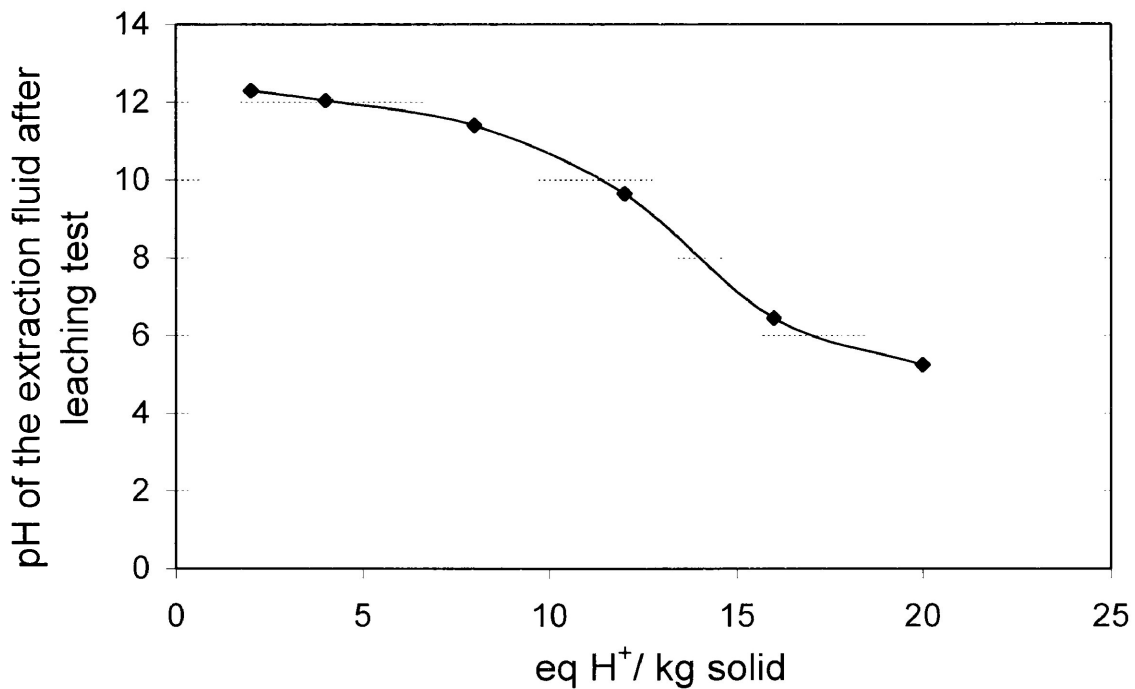

Figure F-1 pH of the extraction fluid after the leaching test as a function of the initial acidity of the fluid.

APPENDIX G

INFLUENCE OF METAL ADDITION ON THE EARLY HYDRATION RATE OF ORDINARY PORTLAND CEMENT

This appendix deals with the effect of Pb and Zn on the early hydration rate of OPC. As described in Chapter 4, metals were found to shorten the time to attain the maximum degree of hydration of OPC. To support this statement, several batches of samples were tested, and the results are reported in this appendix.

When 1 wt% Pb and 1 wt% Zn were added to OPC, the hydration process was delayed for several days at the beginning and then accelarated quickly to surpass the control sample. Three batches of samples have been made to confirm this pattern. Because the first data point for the Control M sample in the first batch was obtained on day 7, the sample had already set, and there were no data points to show the initial delaying effect of metals. The initial delay periods vary from batch to batch, which may be caused by the minor difference in the composition of OPC. However, the trends for all three batches were the same (Figure G-1).
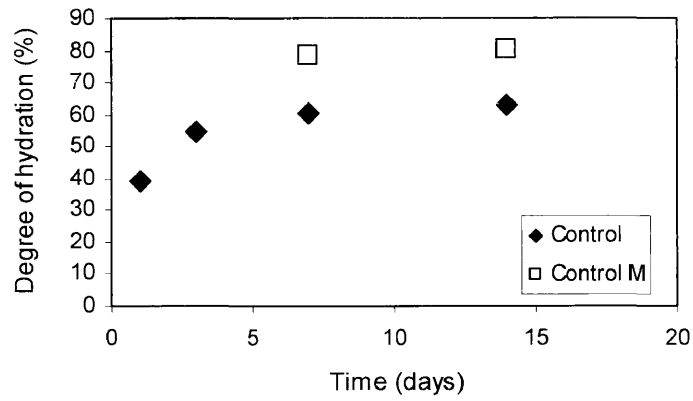
(a)
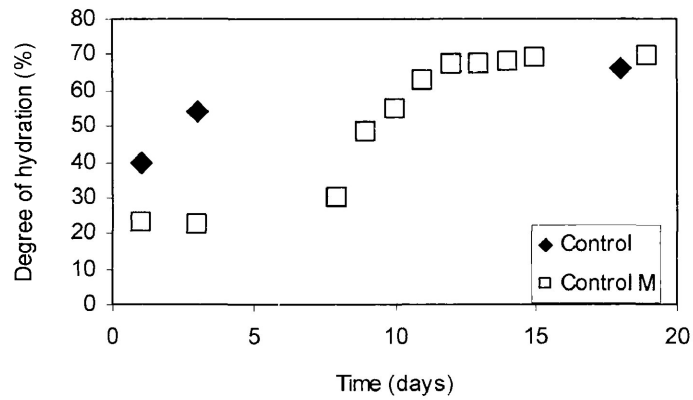
(b)
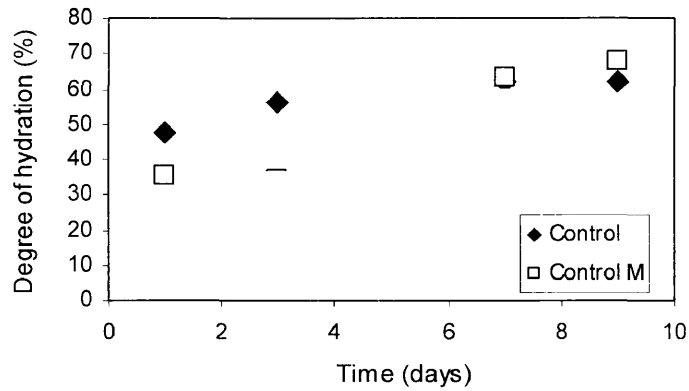
(c)

Figure G-1 Degree of hydration of OPC and OPC-metal samples showing that metals

delay the early hydration but later accelerate hydration (a) first batch, (b) second batch,

and (c) third batch.

APPENDIX H

RELATIONSHIP BETWEEN STRENGTH AND THE DEGREE OF HYDRATION OF OPC-SUGAR SAMPLES WITH AND WITHOUT METALS

This appendix analyzes how the strength data correlates to the degree of hydration of sugar-containing OPC samples and OPC-metal mixtures.

As shown in Figure H-1, samples with and without metals need a minimum degree of hydration of approximately 20% (without metals) and 33% (with metals), respectively, to develop any strength. In addition, for a given degree of hydration, samples with metals have a lower strength than samples without metals. Lastly, for samples without metals, there is a consistent and linear relations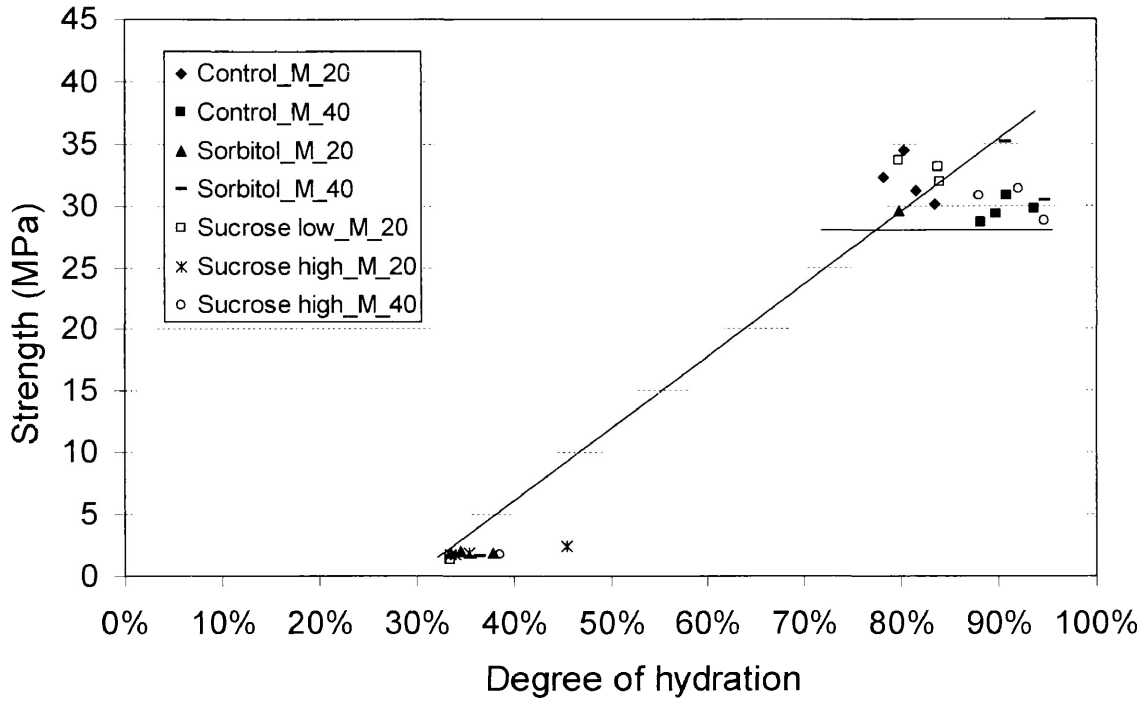hip between degree of hydration and strength for all samples up to a degree of hydration of about 65%; at higher degrees of hydration, the strength stabilizes between 27.6 and 34.5 MPa (4000 and 5000 psi), except perhaps for sorbitol that seems to have a more extended linear range and may reach higher strengths. However, for samples with metals, the available data is not sufficient to demonstrate the existence of a linear range, although it may exist. It can still be concluded that the strength of metal-containing samples stabilizes at values between 27.6 and 34.5 MPa (4000 and 5000 psi) at degrees of hydration higher than 80%, which is a much higher degree of hydration than that of metal-free samples.
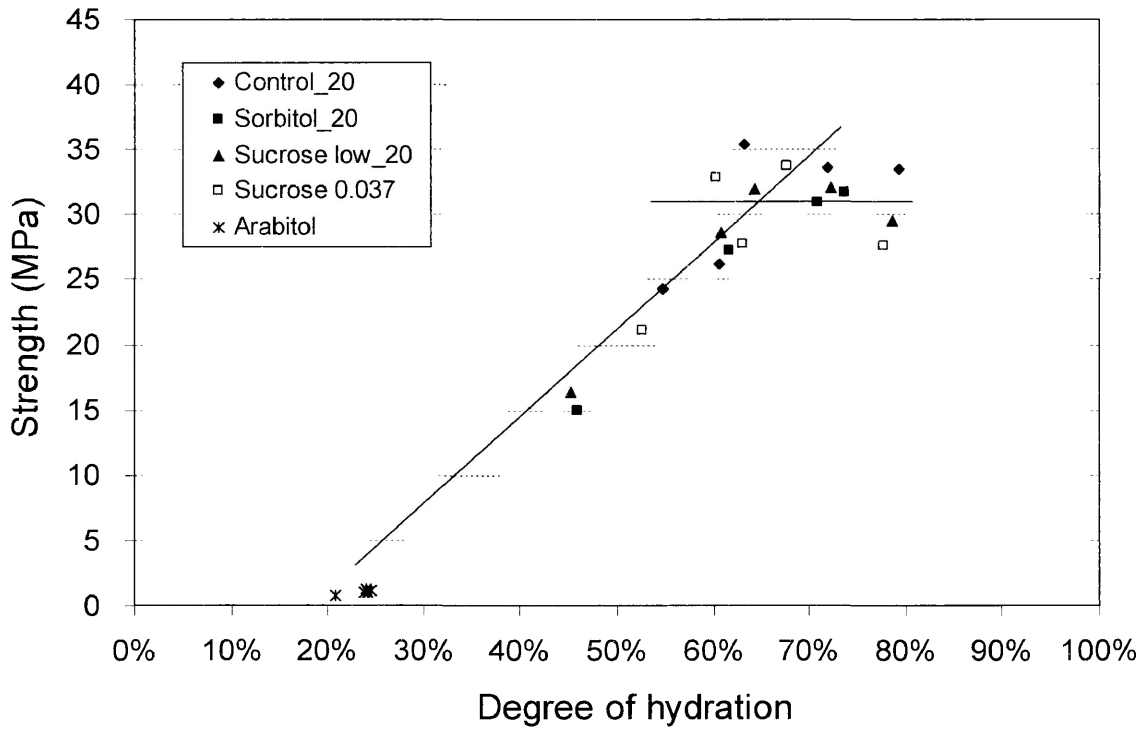
Figure H-1 Relationship between strength and the degree of hydration for OPC sugar

samples (a) with metals and (b) without metals.

APPENDIX I

EFFECT OF LIGNOSULFONATE ACID ON THE LEACHABILITY OF LEAD

This appendix examines the effect of lignosulfonate acid on the leachability of Pb from cement-teated samples. Two types of extraction fluid with different initial acidities were employed in the leaching test. Lignosulfonates are contained in some wastes from the pulp and paper industry that also contain sugars and sugar derivatives. Therefore, this study was relevant to assess the potential of these wastes as additives to cement used in stabilization/solidification processes.

All the samples contained 1 wt% Pb. Samples contained either no lignosulfonate or 1 or 2 wt% lignosulfonate acid labelled as Lig low and Lig high, respectively.

The effect of lignosulfonate acid on the leachability of Pb depends on the leaching test that is used. When the extraction fluid had an acidity of 14 eq H^+/kg solid, adding 1 wt% lignosulfonate acid greatly increased the leachability of Pb (Figure I-1). However, when the extraction fluid had an initial pH of 2.88 (2 eq H^+/kg solid), Figure I-2 shows that both 1 wt% and 2 wt% lignosulfonate acid did not affect the leachability of Pb.

The different effects may be due to complexation reactions between Pb and lignosulfonate acid. Once a Pb-lignosulfonate complex is formed, the Pb is transformed into a more soluble form, which increases its leachability. However, this is just an assumption without any experimental confirmation. More work to understand the underlying mechanisms is needed.
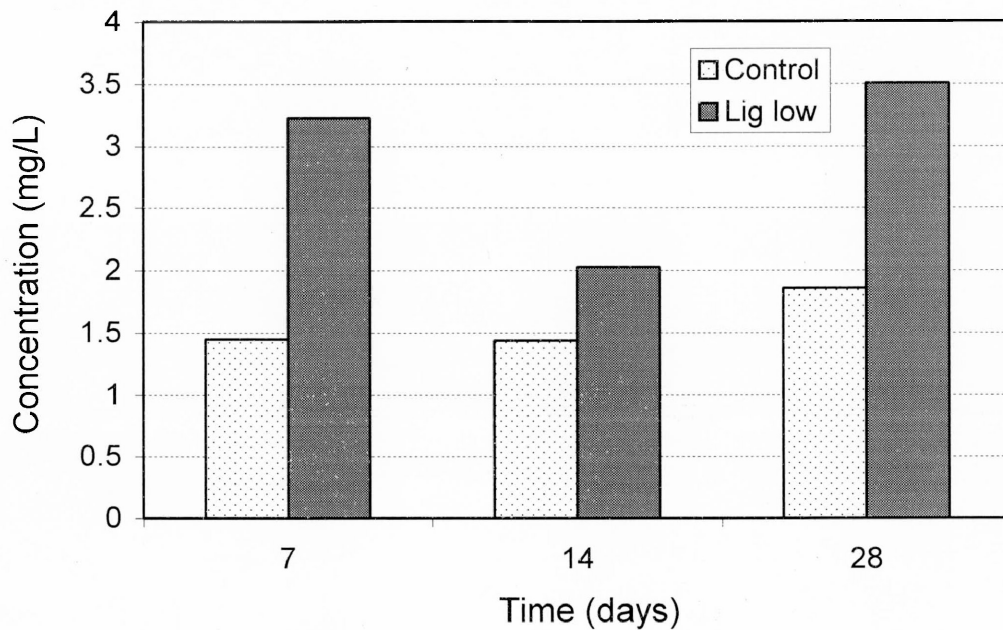
Figure I-1 Leachability of Pb with and without the addition of lignosulfonate acid using

the extraction fluid having an acidity of 14 eq H$^+$/kg solid.
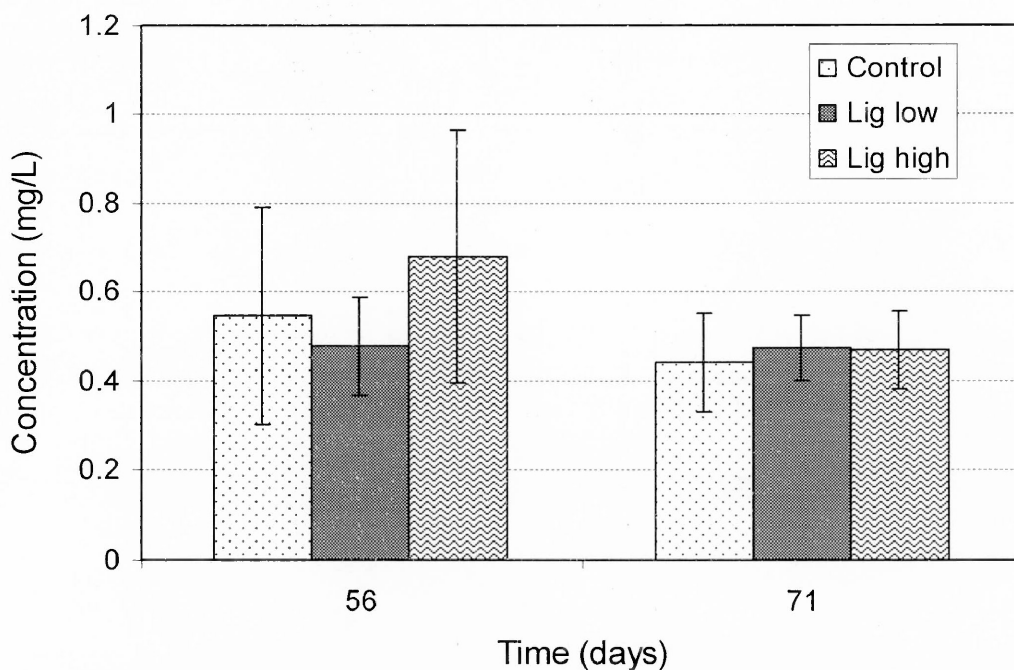
Figure I-2 Leachability of Pb with and without the addition of lignosulfonate acid using

the extraction fluid having an acidity of 2 eq H$^+$/kg solid (pH=2.88).

APPENDIX J

EFFECT OF SUCROSE AND SORBITOL ON THE LEACHABILITY
OF LEAD AND ZINC AS A FUNCTION OF TIME

This appendix shows the complete results of the leaching tests with and without the addition of sucrose or sorbitol at day 7, 14, 28, 56 and 71. Only 56 and 71 days data were provided in Chapter 4.
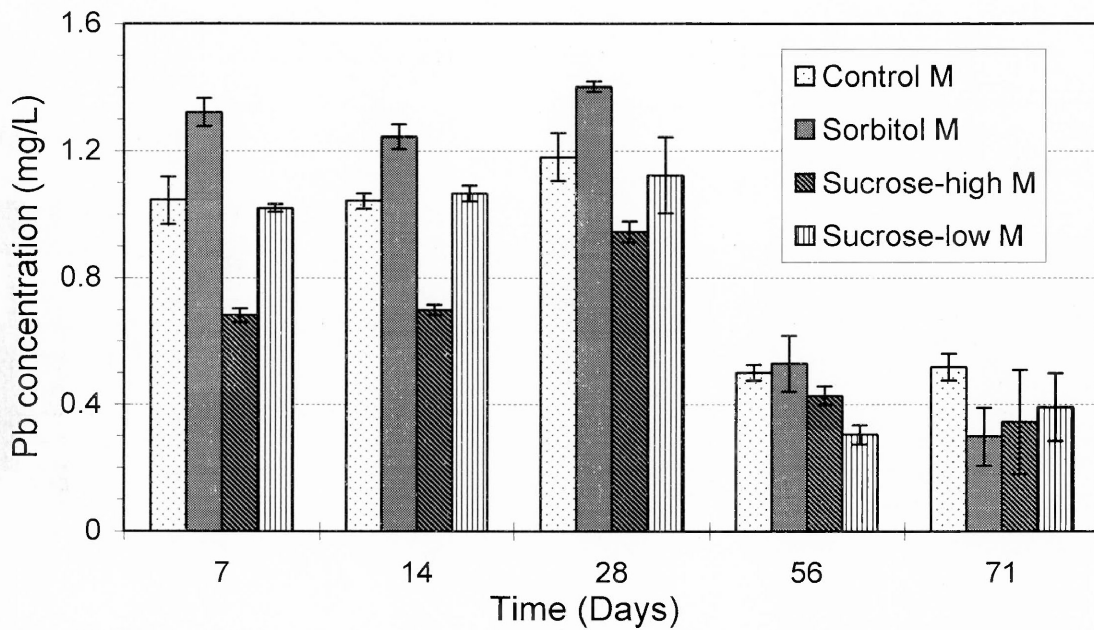
(a)
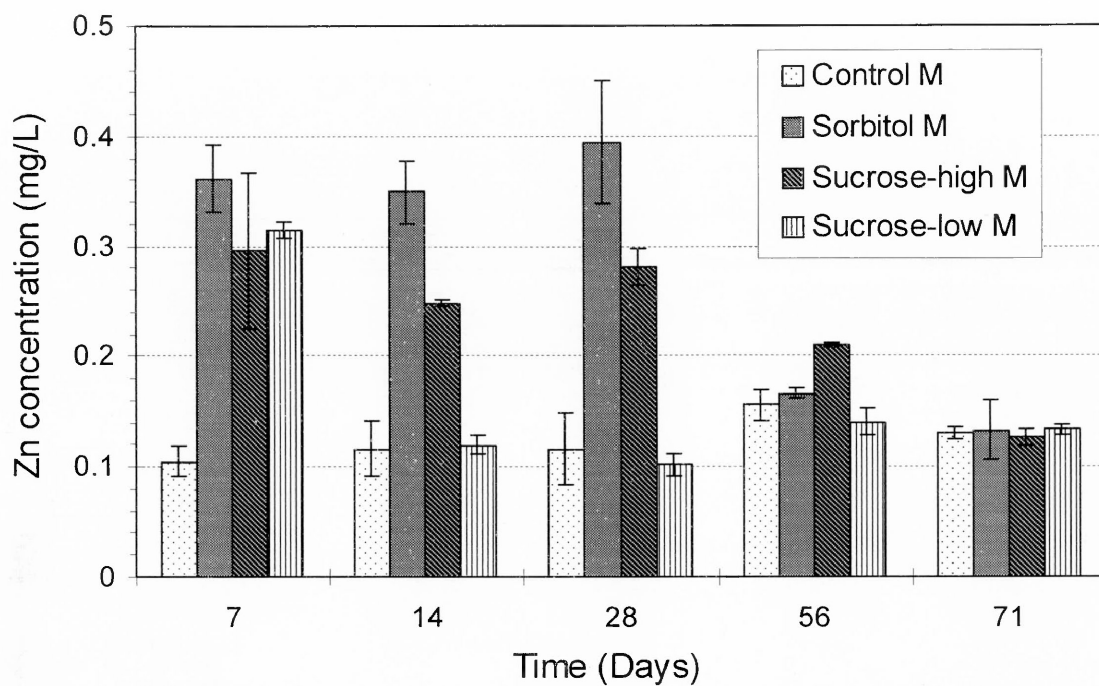
(b)

Figure J-1 Leachability of (a) Pb and (b) Zn with and without the addition of sucrose or

sorbitol at day 7, 14, 28, 56 and 71.

APPENDIX K

X-RAY DIFFRACTOGRAMS OF CONTROL M, SORBITOL M, SUCROSE-HIGH M, AND SUCROSE-LOW M SAMPLES AT DAY 7

This appendix displays the XRD diagrams of some OPC-metal samples with and without sucrose or sorbitol addition at early hydration times (day 7) in order to demonstrate that the addition of sucrose or sorbitol inhibits the hydration of OPC but facilitates the formation of ettringite.

All the samples contain 1 wt% Pb and 1 wt% Zn. The Sorbitol M sample contains 0.40 wt% sorbitol, the while Sucrose-high M and Sucrose-low M samples have 0.38 wt% and 0.15 wt% sucrose, respectively. Except for Control M, all the other three samples did not set on day 7. Comparison of the XRD diagrams for these four samples shows that Control M has samller peaks for ettringite and unhydrated phases (C_3S and C_2S) but much larger peaks for calcium hydroxide. By contrast, sugar-containing samples exhibit relatively high concentration of ettringite and little calcium hydroxide.
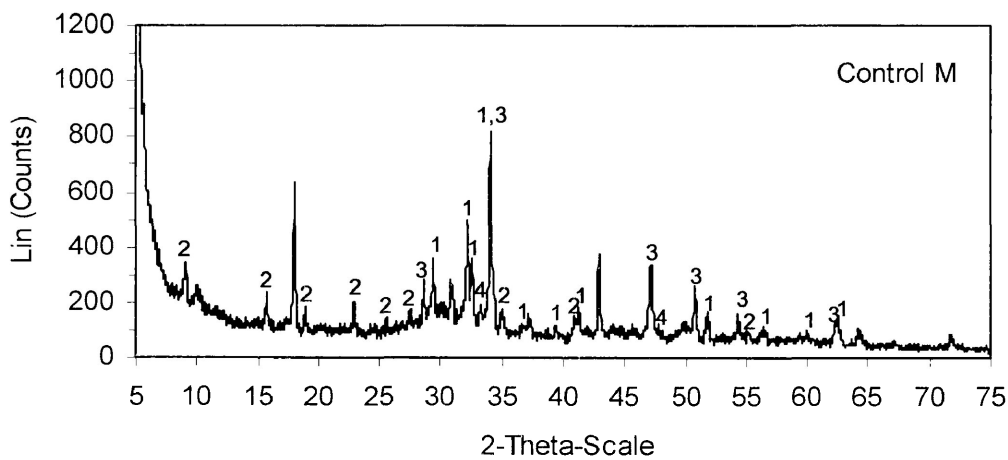
(a)
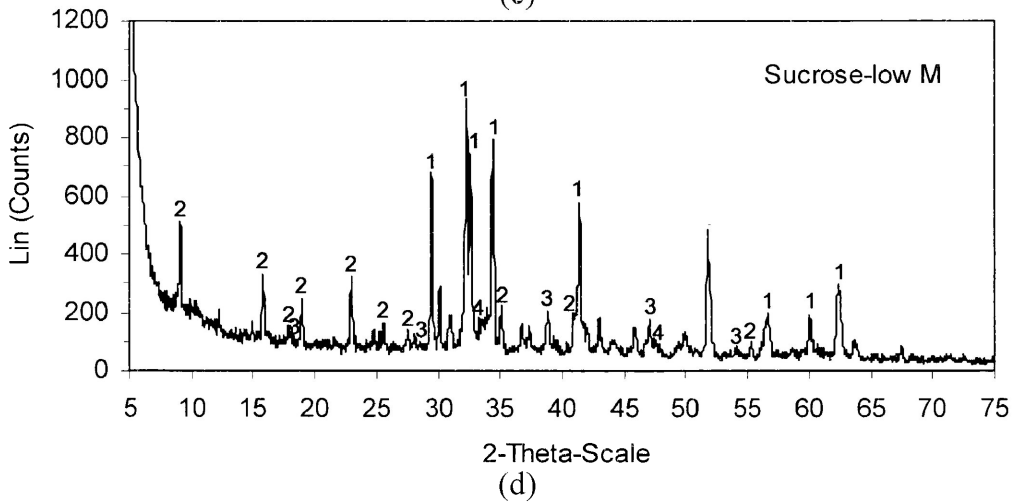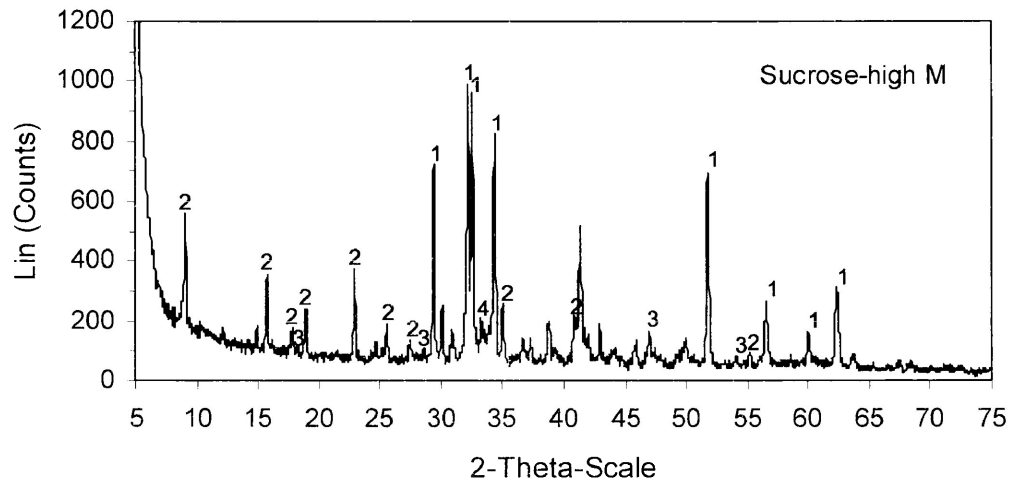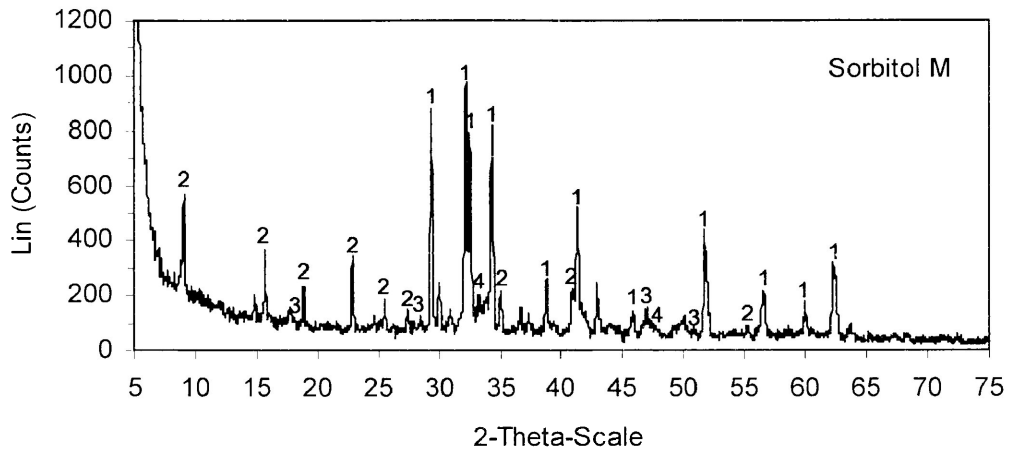
Figure K-1 XRD diagrams of (a) Control M, (b) Sorbitol M, (c) Sucrose-high M, and

(d) Sucrose-low M samples at day 7, showing

(1) C_3S or C_2S, (2) ettringite, (3) portlandite (CH), and (4) C_3A.

APPENDIX L

SEM-EDS ANALYSES OF OPC METAL SAMPLES WITH AND WITHOUT SUGAR ADDITION

This appendix lists SEM-EDS analysis results of OPC metal samples that were not presented in Chapter 4.

Figures A12-3, 5, and 7 show that adding metals (Pb and Zn) and sucrose or sorbitol together delayed cement hydration at 7 days. A certain amount of ettringite exhibiting different morphologies was the only hydration product. As hydration continued, calcium hydroxide and CSH started to precipitate, while ettringite was still visible at 28 or 56 days (Figures L-4, L-6 and L-8 to L-11). However, ettringite can also form without the addition of sucrose or sorbitol (Figure L-1).

Figures L-9 to L-11 demonstrate the existence of a transitional phase during the hydration process of sugar-containing metal-cement mixture. This transitional phase has an intermediate concentration of both Si and Al.

Figures L-1(b), L-2(b), L-3, and L-9 to L-11 and Tables L1-L6 reveal the elemental compositions of typical CH, CSH, and ettringite. These results also show that CSH has a higher capacity to immobilize heavy metals than ettringite.
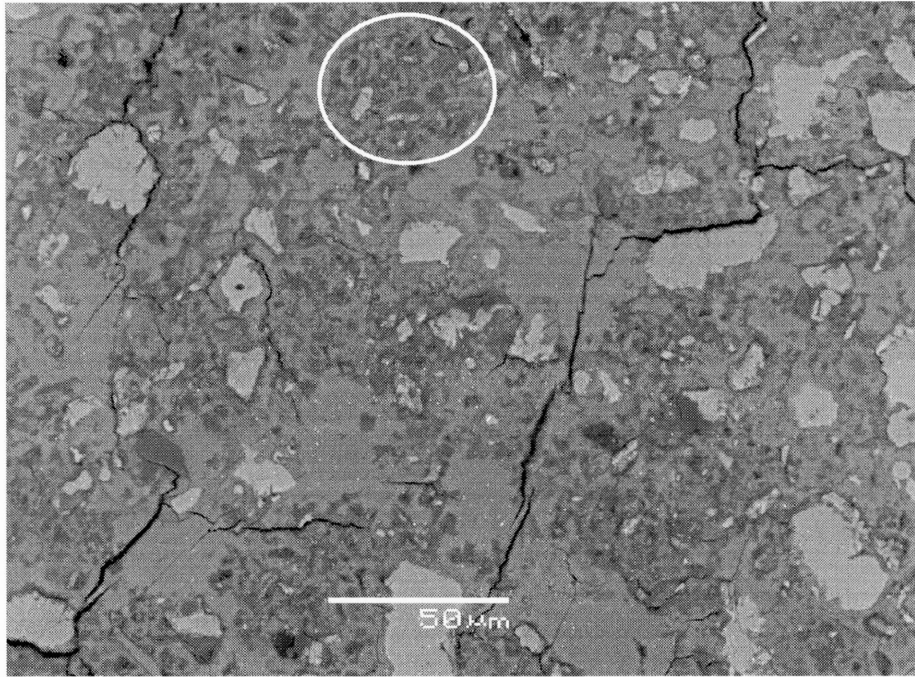
(a)
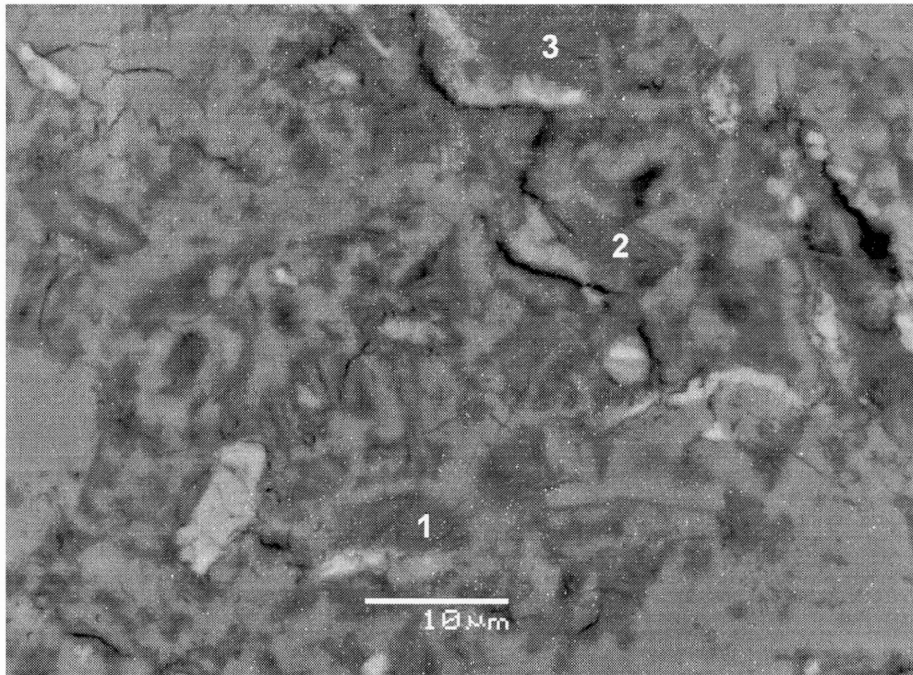
(b)

Figure L-1 Backscattered electron images of Control M sample at day 7, (a) overview

and (b) the magnified image of the circled area in image (a).

Table L-1 X-ray analysis of the points marked in Figure L-1 (b)

	Ca (atom%)	Al (atom%)	Si (atom%)	S (atom%)	Pb (wt%)	Zn (wt%)
1	20.04	8.67	2.06	1.95	1.15	0.10*
2	23.32	8.45	2.59	2.46	0.88	0.38
3	21.96	7.62	4.49	1.89	1.49	1.1

Note: all the three points are ettringite
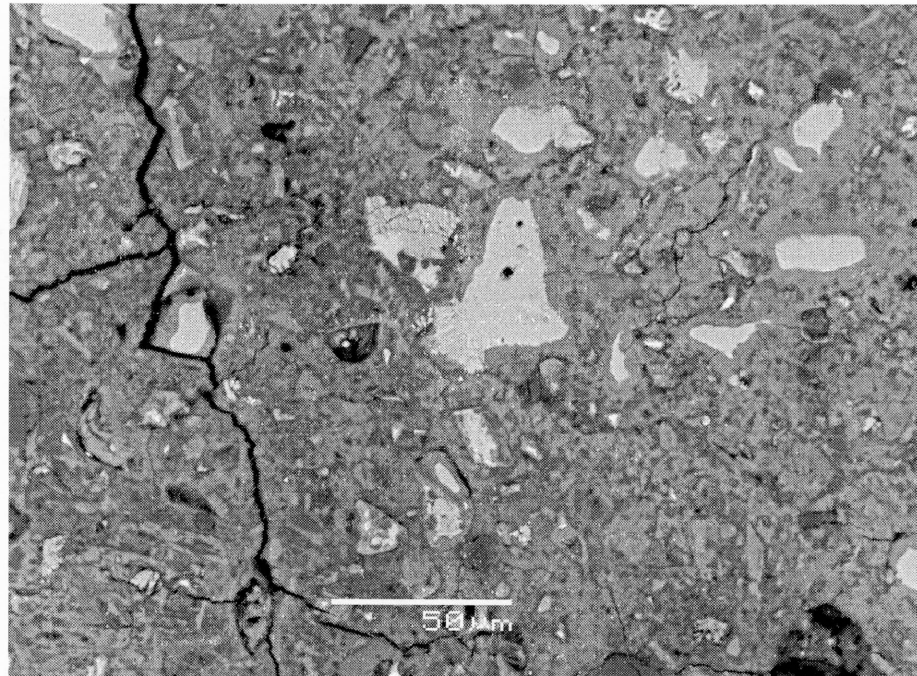
(a)
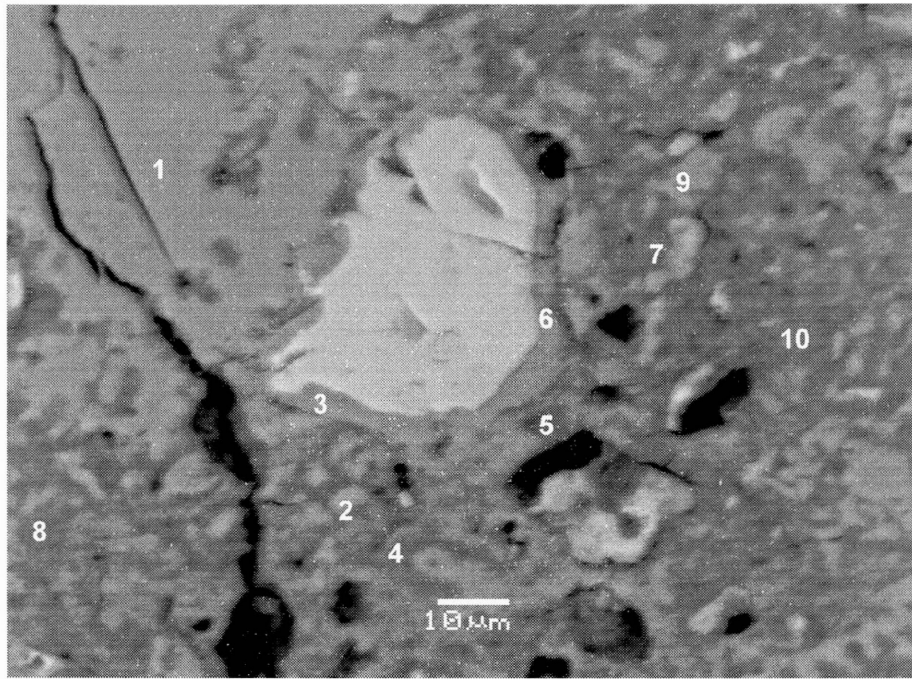
(b)

Figure L-2 Backscattered electron images of Control M sample at day 56, (a)

overview and (b) a magnified image.

Table L-2 X-ray analysis of the points marked in Figure L-2 (b)

	Ca (atom%)	Al (atom%)	Si (atom%)	S (atom%)	Pb (wt%)	Zn (wt%)
1	32.16	-0.02*	0.33	0.02*	0.22*	0.72
2	23.76	1.05	3.74	0.62	0.85	0.73
3	26.07	0.68	8	0.39	1.47	0.86
4	21.98	1.48	9.6	0.83	1.17	1.2
5	17.78	6.56	2.07	1.88	0.83	0.17*
6	29.54	1.1	10.12	0.55	1.56	1.27
7	18.85	3.07	6.68	1.29	1.09	1.15
8	23.54	1.32	8.14	0.85	1.62	1.2
9	30.11	0.23	1.23	0.19	0.44	0.44
10	21.08	1.92	8.23	1.26	1.82	1.28

Note:

1. Points 1, 2 and 9 are CH

2. Points 3, 4, 6, 8, and 10 are CSH

3. Point 5 is ettringite

4. Point 7 corresponds to medium concentrations of Al and Si.(maybe a transitional

   product)
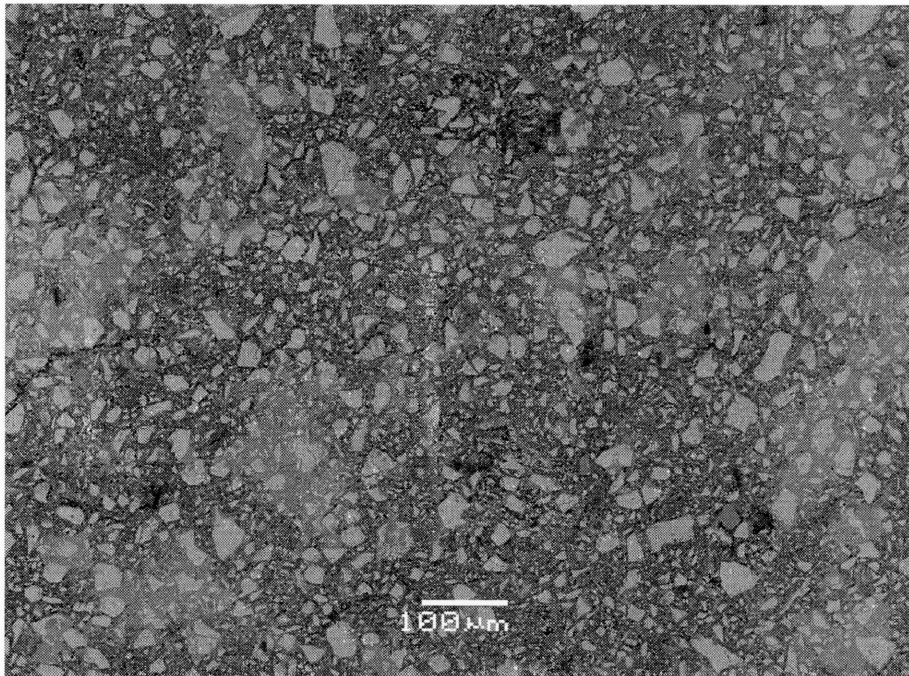
(a)
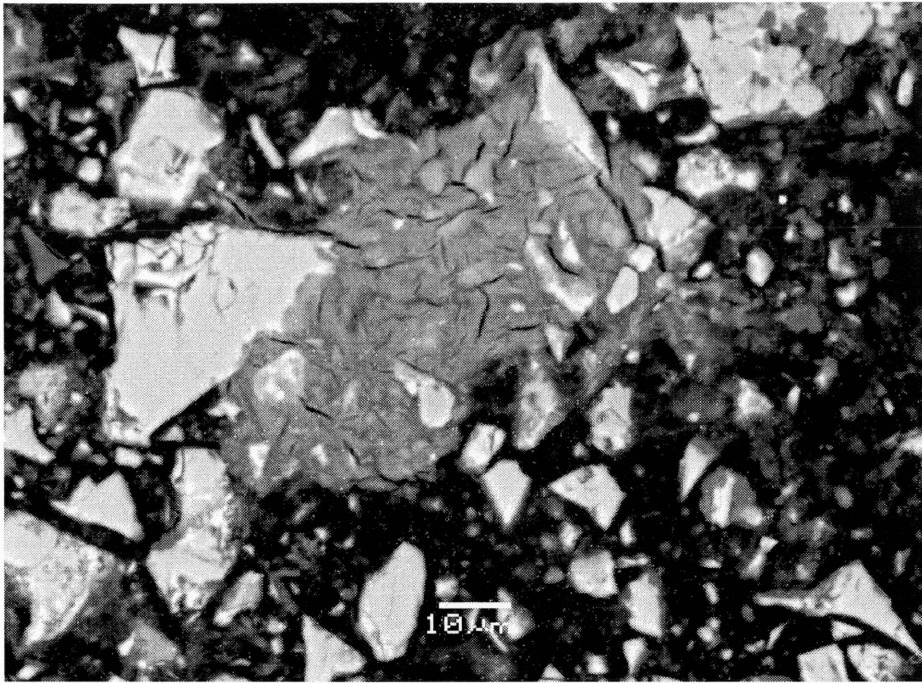
(b)
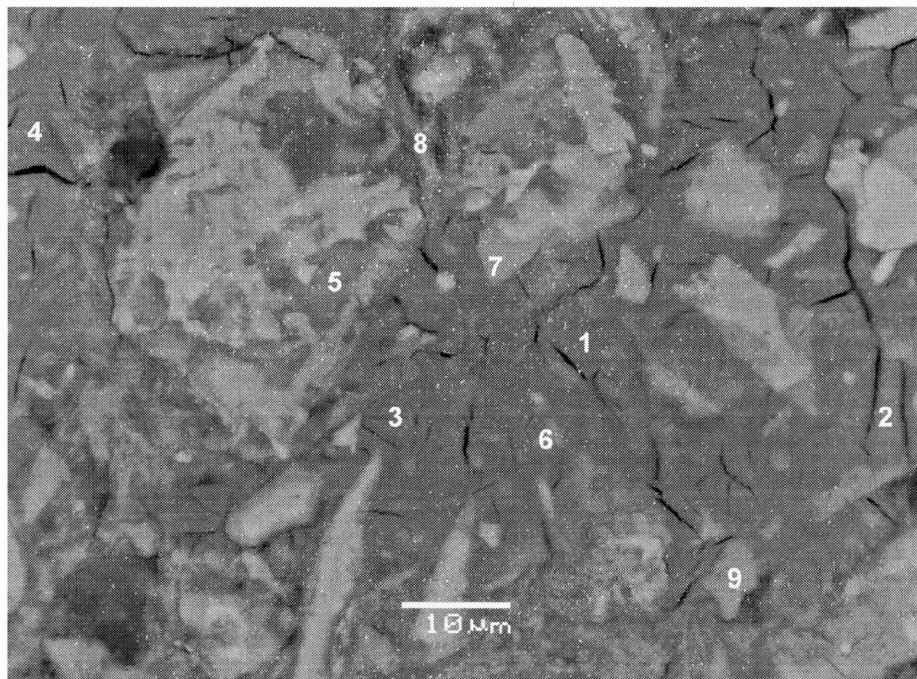
(c)

Figure L-3 Backscattered electron images of Sorbitol M sample at day 7.

Table L-3 X-ray analysis of the points marked in Figure L-3 (c)

	Ca (atom%)	Al (atom%)	Si (atom%)	S (atom%)	Pb (wt%)	Zn (wt%)
1	21.5	6.45	4.23	0.77	1.39	1.98
2	20.3	8.02	3.11	0.9	1.38	1.7
3	20.66	7.85	3.11	0.93	1.83	2.01
4	21.53	6.07	4.18	1.31	2.19	2.1
5	19	5.65	4.66	0.37	2.18	1.63
6	19.68	3.76	5.77	0.55	2.52	3.17
7	29.94	1.03	10.83	0.21	4.04	4.59
8	26.43	1.72	1.95	1.84	2.12	0.61
9	20.86	1.47	8.07	0.24	3.64	3.8

Note:

1. Points 1-4: Al phase (However, all these four points contain higher Si compared to other Al phases).

2. Point 5 and 6: transitional product

3. Points 7 and 9: CSH

4. Point 8: CH
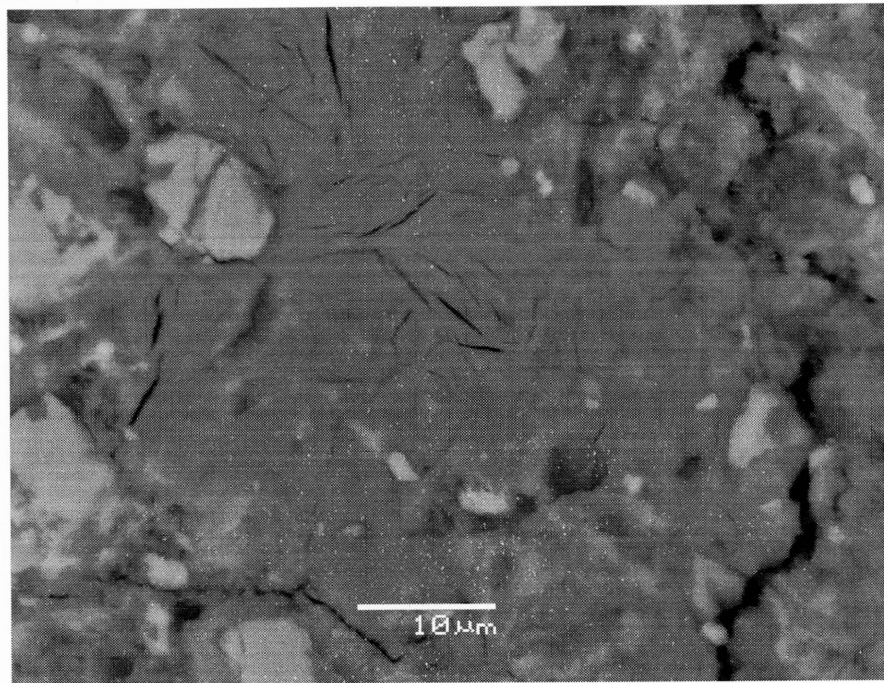
Figure L-4 Backscattered electron image of Sorbitol M sample at day 28.
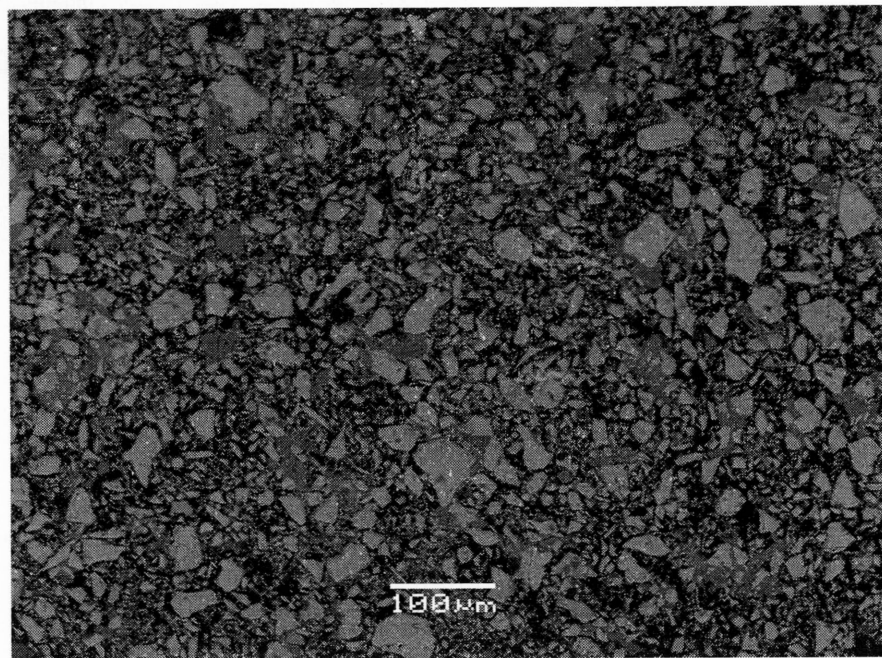
(a)
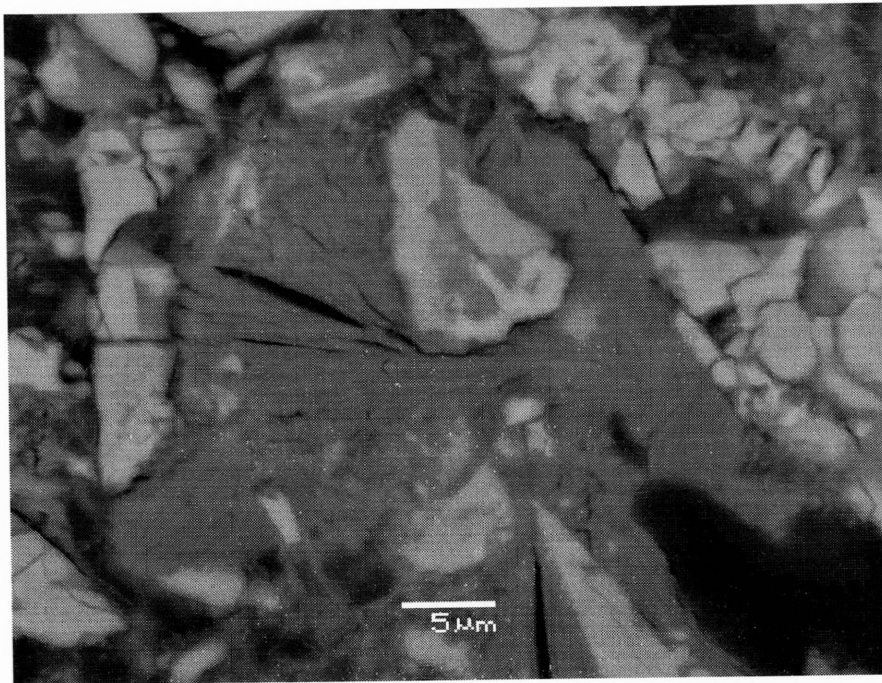
(b)
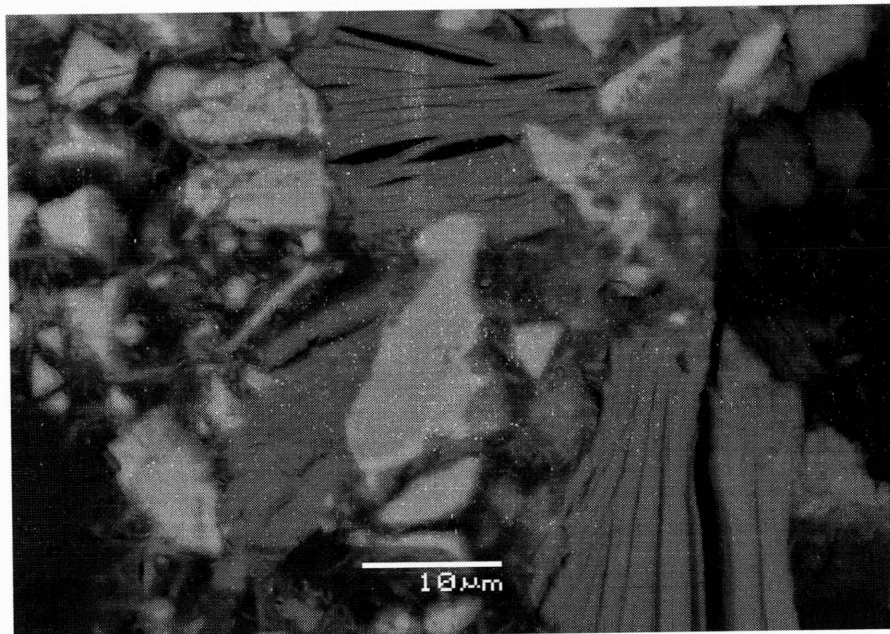
(c)

Figure L-5 Backscattered electron images of Sucrose-low M sample at day 7, the bright

grains are unhydrated cement, while the grey phase is ettringite.
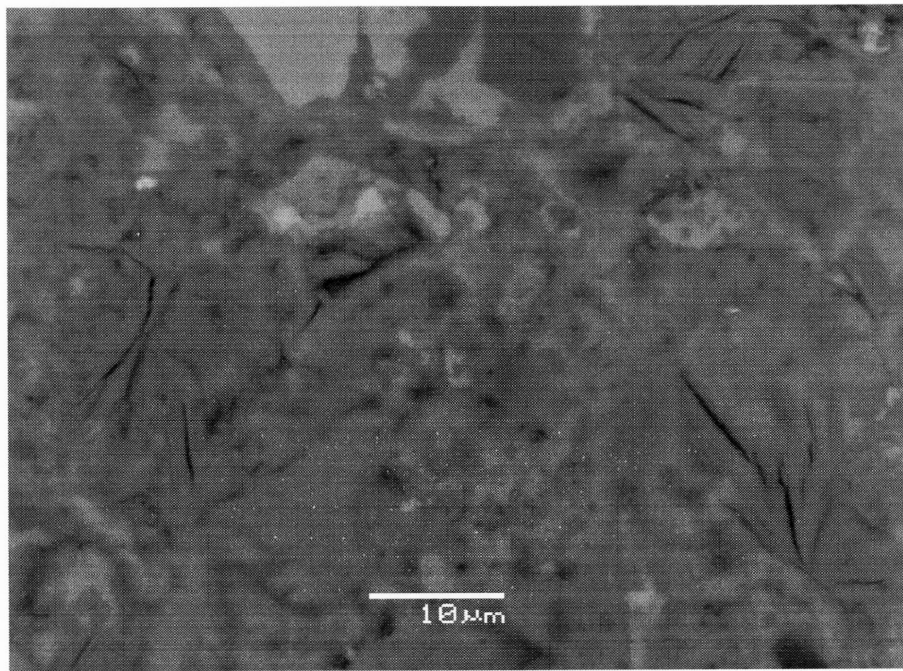
Figure L-6 Backscattered electron image of Sucrose-low M sample at day 28.
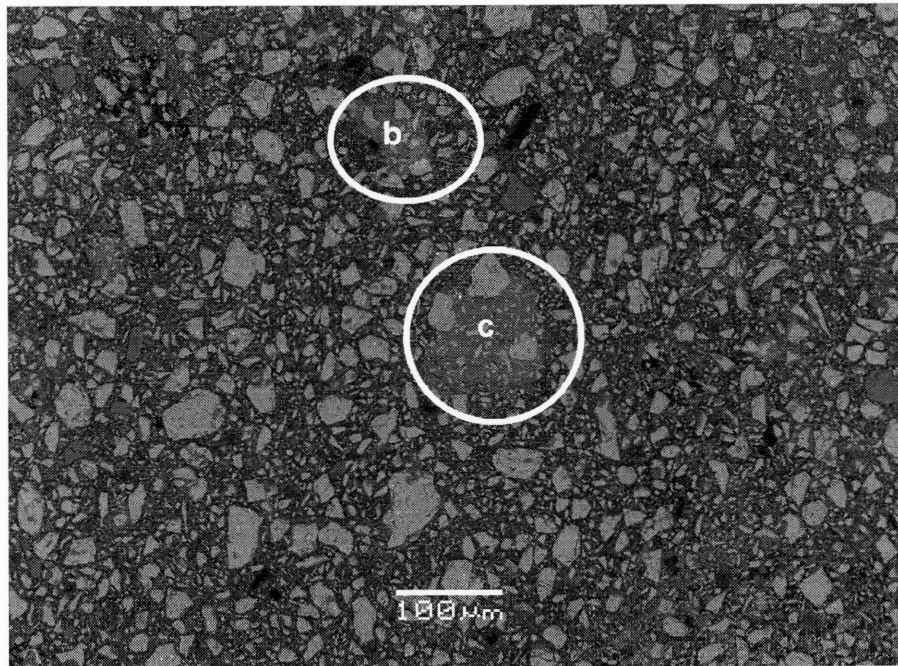
(a)
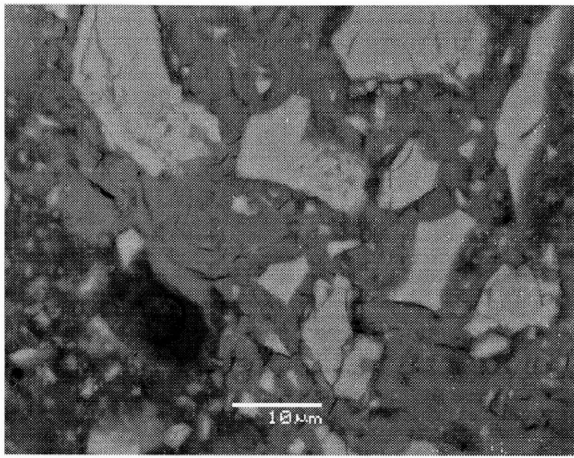
(b)
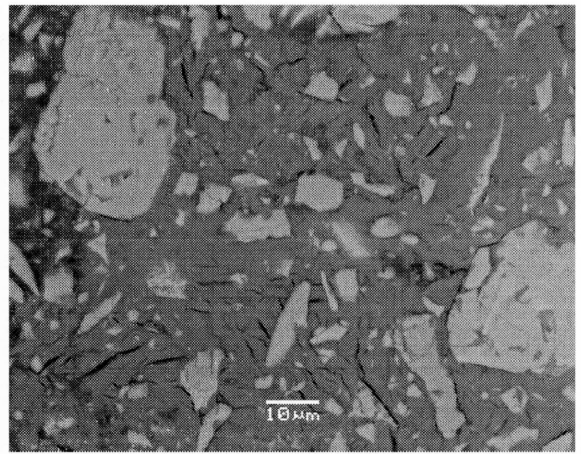
(c)

Figure L-7 Backscattered electron images of Sucrose-high M sample at day 7. The grey masses in both (b) and (c) are ettringite.

(a)
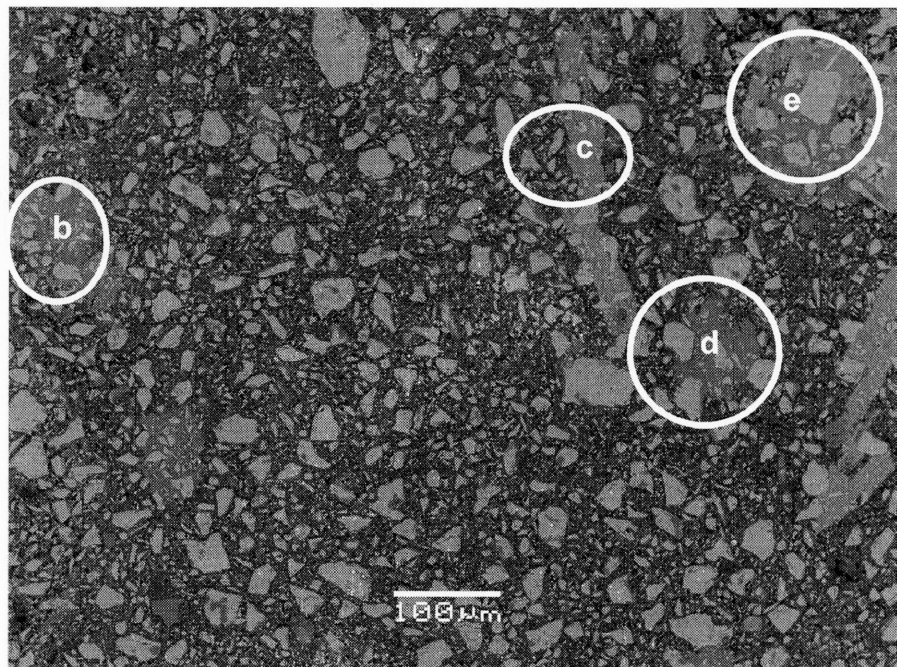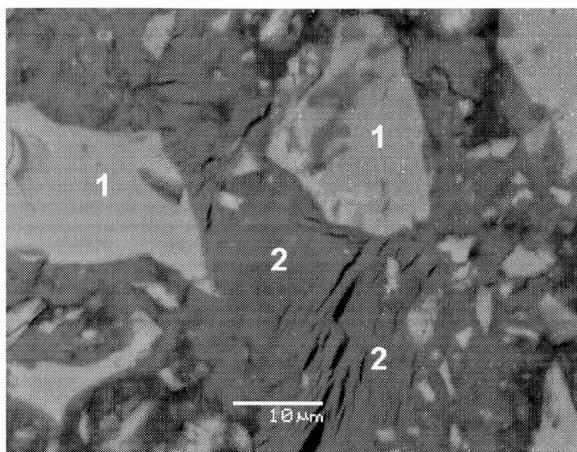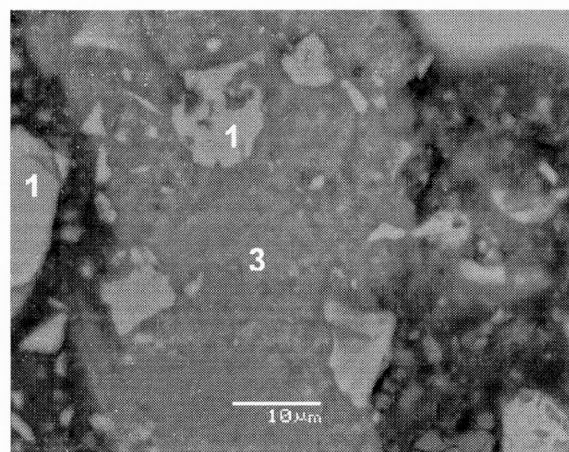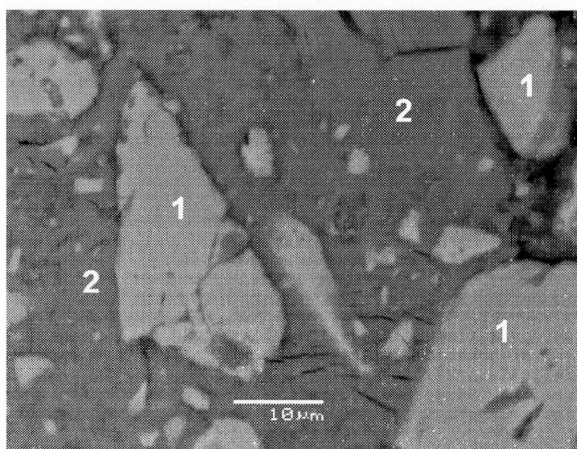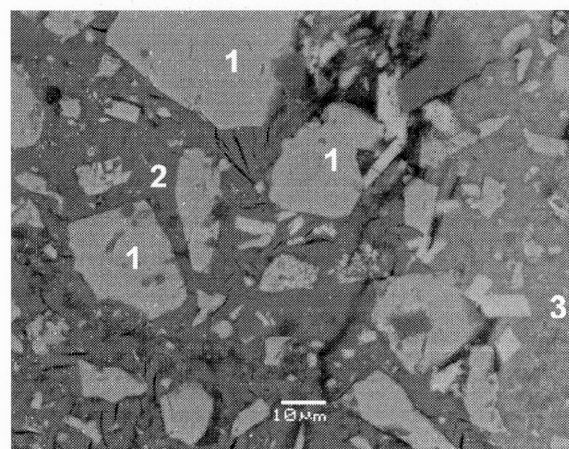
Figure L-8 Backscattered electron images of Sucrose-high M sample at day 28, showing

(1) unhydrated cement, (2) ettringite, and (3) calcium hydroxide.
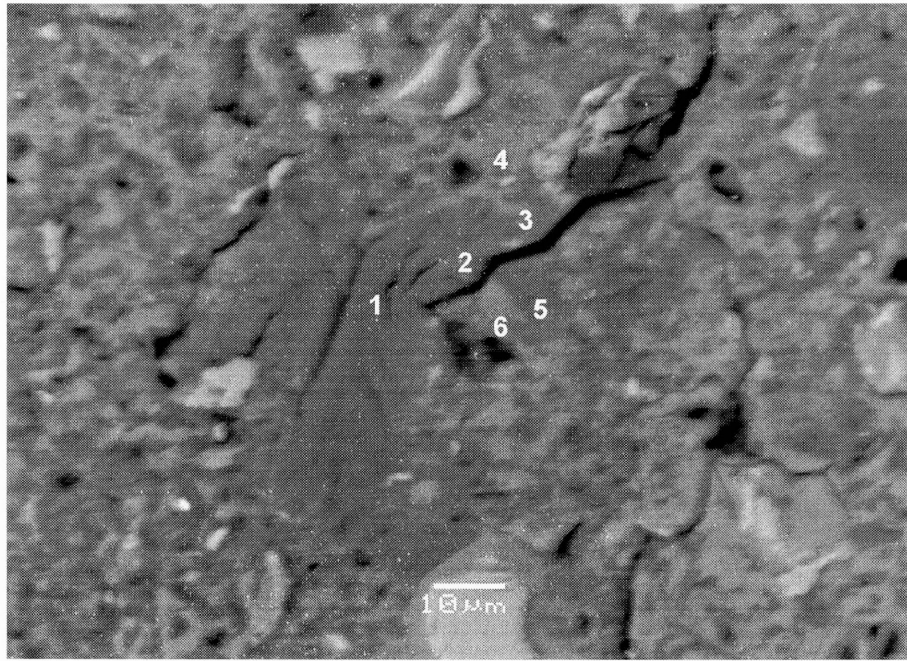
Figure L-9 Backscattered electron image of Sucrose-high M sample at day 56_1.

Table L-4 X-ray analysis of the chosen points marked in Figure L-9

	Ca (atom%)	Al (atom%)	Si (atom%)	S (atom%)	Pb (wt%)	Zn (wt%)
1	19.41	9.08	0.1	1.65	0.52*	0.43
2	19.26	7.17	1.96	1.78	1.13	0.72
3	20.25	4.17	2.94	1.04	1.05	0.82
4	18.74	1.8	8.41	0.76	2.11	1.67
5	17.41	7.06	2.08	1.47	1.44	0.53
6	17.37	3.5	5.57	1.17	2.02	1.73

Note: Figure A 12-9 combined with Table A 12-4 illustrates the change of the concentrations of Ca, Al, Si, Pb and Zn from point 1 to point 4, and from point 5 to point 6.
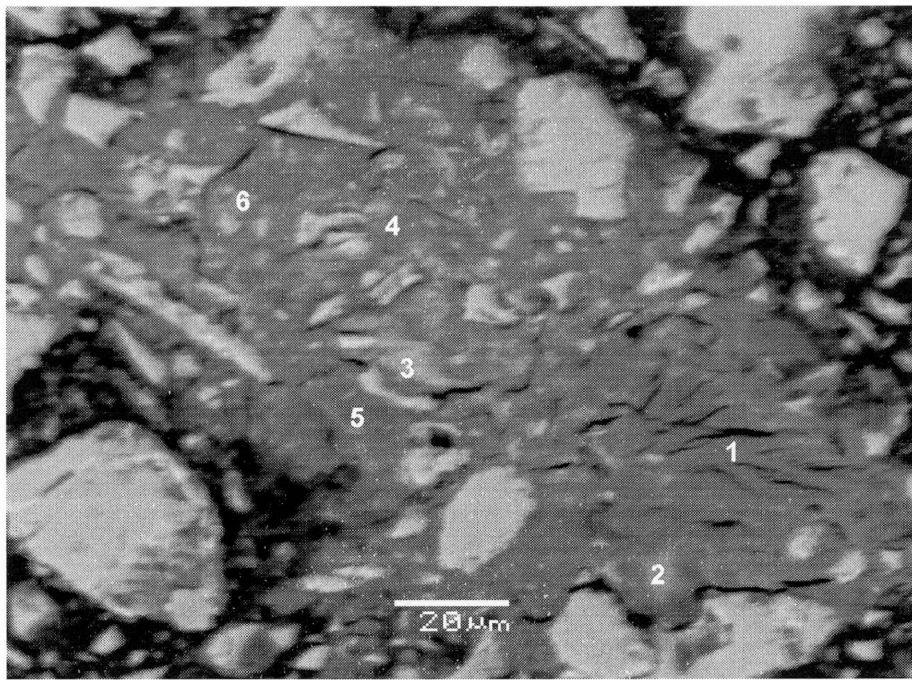
Figure L-10 Backscattered electron image of Sucrose-high M sample at day 56_2.

Table L-5 X-ray analysis of the chosen points marked in Figure L-10

	Ca (atom%)	Al (atom%)	Si (atom%)	S (atom%)	Pb (wt%)	Zn (wt%)
1	17.05	8.91	0.03*	1.29	0.59	0.48
2	18.59	1.59	7.37	0.33	2.91	5.74
3	19.41	1.63	7.02	1.32	3.99	5.24
4	19.03	5.92	2.47	2.17	2.32	1.79
5	18.32	7.01	1.13	1.59	1.47	0.96
6	17.97	3.62	5.06	1.43	2.32	3.84

Note:

1. Points 1 and 5: ettringite

2. Points 2 and 3: CSH

3. Points 4 and 6: transitional product
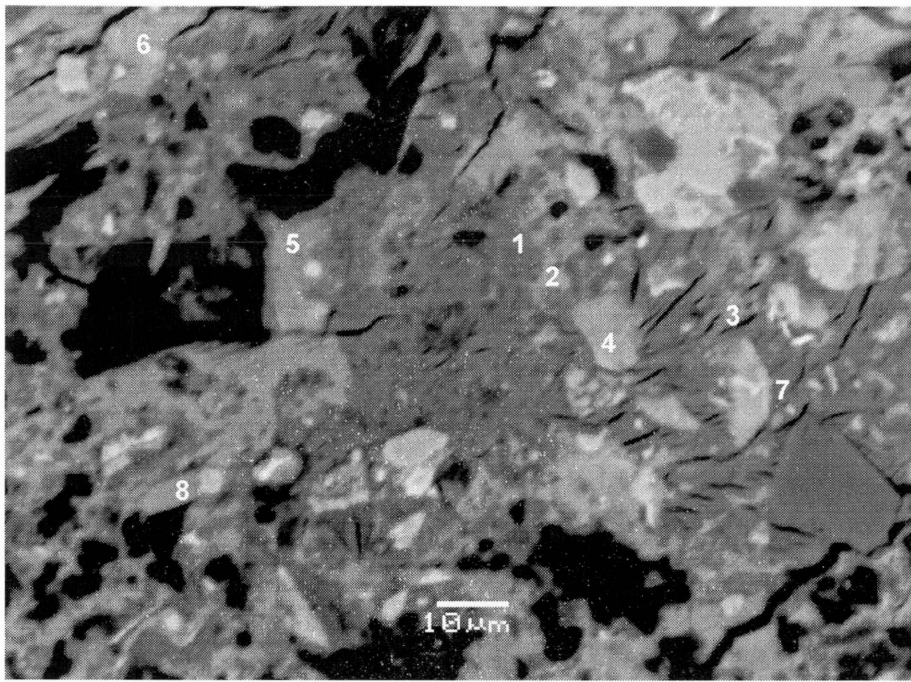
Figure L-11 Backscattered electron image of Sucrose-high M sample at day 56_3.

Table L-6 X-ray analysis of the chosen points marked in Figure L-11

	Ca (atom%)	Al (atom%)	Si (atom%)	S (atom%)	Pb (wt%)	Zn (wt%)
1	18.67	8.62	0.44	1.48	0.26*	0.47
2	18.94	1.25	7.1	0.79	2.86	5.16
3	13.52	5.28	4.07	1.17	2.31	1.9
4	19.11	0.96	9.7	0.15	3.91	3.68
5	18.2	1.26	9.11	0.35	2.98	2.9
6	25.18	0.77	9.18	0.17	2.14	1.55
7	18.45	8.32	0.79	1.6	0.85	0.77
8	32.35	0.36	1.88	0.23	0.77	0.72

Note:

1. Points 1 and 7: ettringite

2. Points 2, 4, 5, and 6: CSH

3. Point 8: CH

4. Point 3: the transitional product

APPENDIX M

EFFECT OF SUCROSE AND SORBITOL ON CEMENT-BASED STABILIZATION/SOLIDIFICATION OF TOXIC METAL WASTE

ELSEVIER

Effects of sucrose and sorbitol on cement-based stabilization/solidification of toxic metal waste

Linghong Zhang [a], Lionel J.J. Catalan [a,*], Andrew C. Larsen [b], Stephen D. Kinrade [b]

[a] *Department of Chemical Engineering, Lakehead University, 955 Oliver Road, Thunder Bay, Ontario P7B 5E1, Canada*
[b] *Department of Chemistry, Lakehead University, 955 Oliver Road, Thunder Bay, Ontario P7B 5E1, Canada*

Abstract

The effects of sucrose or sorbitol addition on the hydration, unconfined compressive strength and leachability of Portland cement pastes containing 1% Pb and 1% Zn were studied as a function of time. Whereas Pb and Zn were found to shorten the time to achieve maximum hydration of Portland cement, the combination of these metals with 0.15 wt% sucrose or 0.40 wt% sorbitol retarded the setting of cement by at least 7 and 28 days, respectively, without affecting the strength at 56 days. The leachability of Pb and Zn evaluated by the TCLP 1311 protocol at 56 and 71 days was slightly reduced or unchanged by the addition of sucrose or sorbitol. SEM-EDS and XRD analyses revealed that ettringite precipitation was favored whereas the formation of CSH gel, which accounts for most of the strength of hydrated cement, was delayed in cement pastes containing both metals and sucrose or sorbitol. These results indicate that controlled additions of sucrose or sorbitol can add flexibility to the handling of cement-treated metal waste, particularly when it needs to be transported by truck or pipeline between the treatment plant and the disposal site, without affecting its long-term performance.
© 2007 Elsevier B.V. All rights reserved.

Keywords: Stabilization/solidification (S/S); Cement; Sucrose; Sorbitol; Heavy metals

1. Introduction

Stabilization/solidification (S/S) is a widely used technique for immobilizing toxic metal ions in industrial waste prior to landfilling. The binder of choice is most often Portland cement, owing to its ready availability, high strength and amply documented performance [1]. The main components of Portland cement are tricalcium silicate (C_3S), dicalcium silicate (C_2S), tricalcium aluminate (C_3A), tetracalcium aluminoferrite (C_4AF) and calcium sulfate (gypsum or anhydrite, 10% max). During cement hydration, C_3A reacts with sulfate ions coming from the dissolution of calcium sulfate to form crystals of ettringite (AFt) and monosulfate (AFm), thus preventing the flash set of Portland cement. C_3S and C_2S undergo hydration to form calcium hydroxide (CH) and calcium silicate hydrate (CSH), which is the principal contributor to cement strength [2]. The CSH plays a key role in immobilizing adventitious metal ions by means

of physical adsorption [3], coprecipitation [4] and formation of metallosilicates [5–7]. Further metal uptake is provided via ion substitution in ettringite crystals [3].

Sugars and their derivatives are found in many industrial wastes and byproducts, either as individual molecules or as the repeating units in long-chain compounds. For example, wood sugars and oligosaccharides mixed with lignosulfonates are byproducts from the manufacture of pulp and paper. They are widely used as retarders to control the setting of cement [8–13]. There has been no study published, however, on the effects of sugars as additives in cement-based S/S processes. The retarding influence of sugars could be advantageous when the waste-cement mixture needs to be transported for some distance between the S/S treatment plant and the disposal site. In these situations, early hardening of the cement in the truck box or pipeline could result in severe operational difficulties and limited flexibility. In the present research, a sugar (sucrose) and a sugar alcohol (sorbitol) were investigated. Both additives are highly resistant to alkali attack but differ in their affinity toward silicon: sorbitol is a silicon binder [14], whereas sucrose is not [8,12]. As a result, these two additives are expected to interfere differently

* Corresponding author. Tel.: +1 807 343 8573; fax: +1 807 343 8928.
  E-mail address: lionel.catalan@lakeheadu.ca (L.J.J. Catalan).

with the cement hydration reactions. Sucrose is one of the most effective and commonly used retarders for cement setting. The addition of 0.075 wt% sucrose increases the induction period of the hydration process from 2.5 to 31 h [11]. Moreover, sucrose has been shown to enhance the specific surface area of hydrated cement pastes by increasing the number of small (1–2 nm) pores at the expense of medium-sized (4–20 nm) pores [15]. Sorbitol is often employed as a water-reducing plasticizer (superplasticizer) in cement admixtures, that is, it decreases the water needed to make the cement workable which, in turn, enhances its strength [16,17].

The objective of this study was to explore the effects of small additions of sucrose or sorbitol on metal leachability and strength development for specimens of metal waste treated by cement-based stabilization/solidification. Synthetic Pb and Zn waste solutions were used because both metals are common to industrial waste streams and have been identified as priority metallic pollutants by the US Environmental Protection Agency [18]. To aid in the interpretation of the results, the degree of cement hydration and the microstructure of the treated waste matrix were also assessed as a function of time.

2. Materials and methods

2.1. Sample preparation

Synthetic waste solutions containing 25.0 g/L of each Pb and Zn were prepared by dissolving 40.0 g $Pb(NO_3)_2$ and 114 g $Zn(NO_3)_2 \cdot 6H_2O$ per litre of distilled-deionized water. Sucrose and sorbitol were dissolved in these solutions at concentrations ranging between 0 and 10 g/L; equivalent metal-free solutions were also prepared. The solutions were pre-cooled to 10 °C and then mixed with normal Portland cement Type 10 (ASTM Type I) at a liquid-to-cement ratio of 0.40:1 in a plastic bowl over an ice-water bath. (Temperature control was necessary because certain mixtures – most notably those containing sorbitol – released more heat than others.) The mixtures were stirred with a plastic spoon until they were homogeneous, i.e., for about 7 min or, in the case of those which contained synthetic waste, about 12 min because of their higher viscosity. They were then poured into cylindrical PVC molds measuring 2 inches in diameter and 4 inches in height. To minimize the entrapment of air bubbles, the cylinders were filled in two successive layers and each layer tamped 50 times. Cylinders were placed in triple-sealed, air-tight polyethylene bags and immersed in a room temperature (20–22 °C) water bath to cure.

Table 1 provides the compositions of all sample mixtures. The Pb and Zn concentrations were each either 0 or 1.00 wt% of cement (i.e., 0.01 g of metal per gram of cement). Sucrose and sorbitol ranged from 0 to 0.40 wt%. Two types of control sample were prepared. The first ("Control") consisted only of hydrated Portland cement; the second ("Control M") additionally contained Pb and Zn but no sorbitol or sucrose. At least 12 test cylinders were prepared of each mixture, which allowed the strength, leachability and loss on ignition to be determined in triplicate after four different curing periods: 7, 14, 28, and 56

Table 1
Sample compositions

Batch name	Pb content (wt% of cement)	Zn content (wt% of cement)	Sorbitol/sucrose content (wt% of cement)
Control	0	0	0
Sorbitol	0	0	0.40
Sucrose-low	0	0	0.15
Control M	1.00	1.00	0
Sorbitol M	1.00	1.00	0.40
Sucrose-low M	1.00	1.00	0.15
Sucrose-high M	1.00	1.00	0.38

days. Additional tests were performed for the metal-free mixtures after curing 1 day (loss on ignition) and 3 days (loss on ignition and strength), and for the waste-containing mixtures after 71 days (leachability).

2.2. Strength testing

Immediately after they were removed from the molds, sample cylinders were capped top and bottom with sulfur according to ASTM C617-98 [19] and the unconfined compressive strength was measured according to ASTM C109 [20].

2.3. Loss on ignition testing

A small portion of each sample was crushed and ca. 1.5 g of the 850–2000 μm fraction oven-heated for 24 h at 105 °C to find the evaporable water-free weight, W_{105}, and again for 2 h at 1005 °C to determine the fully dehydrated weight, W_{1005}. The degree of hydration α_{LI} is given by the equation

$$\alpha_{LI} = \frac{W_{105} - W_{1005}}{0.24 W_{1005}} \tag{1}$$

in which 0.24 is the reported fraction of non-evaporable water in fully hydrated Portland cement [2,21].

2.4. Standard leaching procedure

The mobility of Pb and Zn in treated waste samples was determined using the regulatory Toxicity Characteristic Leaching Procedure (TCLP) [22]. 20.0 g of sample with particle size 425–850 μm was combined with 400 mL 0.100 M acetic acid (pH 2.88) in a 500 mL polypropylene bottle and rotated end-over-end at 30 rpm for 18 h at room temperature. The extract was passed through a 0.7 μm borosilicate microfiber filter, and its pH measured using a Metrohm 6.0233.100 combination glass electrode. It was then acidified to pH 2 with concentrated nitric acid and analyzed by inductively coupled plasma-atomic emission spectroscopy (ICP-AES) using a Varian Vista Pro ICAP Radial spectrometer. The detection limits for Pb and Zn were 0.025 and 0.05 mg/L, respectively.

Although the TCLP is a static batch test and does not simulate actual field conditions, it remains the standard regulatory method for monitoring the performance of full-scale cement-based stabilization/solidification operations in North America and for

laboratory studies of the leaching behavior of cement-stabilized waste.

2.5. Microstructure analyses

After reaching the desired curing time, a small slice (*ca.* 0.5 g) was removed from the inner part of the sample cylinder, immersed for 24 h in acetone to halt hydration [23], dried at 105 °C for 15 min, and then imbedded in epoxy resin. An oriented thin-section was cut, lapped and polished using oil-based media so as not to alter the water-soluble minerals. After carbon-coating, it was analyzed with a JEOL JSM 5900 scanning electron microscope in backscattered electron (BSE) mode to improve contrast between different mineral phases [24,25]. The elemental composition of mineral phases was determined by X-ray energy dispersive spectrometry (EDS) using an Oxford Link ISIS system (120 s live-time) calibrated with corundum for Al, barium sulfate for S and O, orthoclase for Si and K, periclase for Mg, wollastonite for Ca, and jadeite for Na. Pure metal standards were used to calibrate Fe, Pb and Zn. SEM-EDS analyses were carried out on days 7, 28, and 56 for the samples containing Pb and Zn. The metal-free samples were analyzed on days 1, 7, and 56.

2.6. Grey level analyses

Each BSE image consists of 1280×960 pixels having grey levels ranging from 0 (black) to 256 (white). The grey levels are directly related to the atomic number of the material, and thus can be used to distinguish between mineralogical phases: unhydrated cement grains are the brightest features, CH and other hydration products (abbreviated OHP, mainly composed of CSH) appear as two shades of grey, whereas pore space is black. These phases also appear as separate peaks in grey-scale histograms (Fig. 1), and the areas under these peaks can be used to calculate the percentage of individual phases [25,26]. For each sample, calculations were carried out on 15 adjacent BSE images and the results were averaged to obtain a representative phase distribution. Each image measured 254×190 μm, yield-

ing a resolution of 0.198 μm/pixel. The degree of hydration of a sample can also be calculated from the results of grey level analyses [27]:

$$\alpha_{GL} = 1 - \frac{UC_i}{UC_0} \tag{2}$$

in which UC_i and UC_0 are the area fractions of unhydrated cement particles at time t_i and the start of the hydration process, respectively. The value of UC_0 can be evaluated from the densities of Portland cement ($d_c = 3.14$ g/cm^3) and water ($d_w = 1.00$ g/cm^3) and the water-to-cement mass ratio ($R = 0.40$).

$$UC_0 = \frac{1/d_c}{(1/d_c) + (R/d_w)} \tag{3}$$

2.7. XRD analyses

The mineralogy of the metal-containing samples at day 7 was characterized by X-ray diffractometry using a Philips PW 1050-3710 diffractometer with Cu-Kα radiation. Scans were carried out in the range $5° < 2θ < 75°$ with a $0.04°$ step interval and a counting time of 2 s per step.

3. Results and discussion

3.1. Degree of hydration

Fig. 2 depicts degree of hydration as a function of time for pure cement (Control) and cement containing 1% Pb and 1% Zn (Control M). The curing of metal-free cement proceeded in two stages – a period of rapid hydration lasting about 3 days, followed by a slower reaction period exhibiting zeroth-order kinetics – and required 56 days to reach the maximum hydration level of 80%. The addition of Pb and Zn greatly accelerated the overall curing process, with maximum hydration being achieved in only 7 days. It would appear that added metal ions somehow interfere with the mechanistic step(s) responsible for terminating stage-1 of the hydration process.
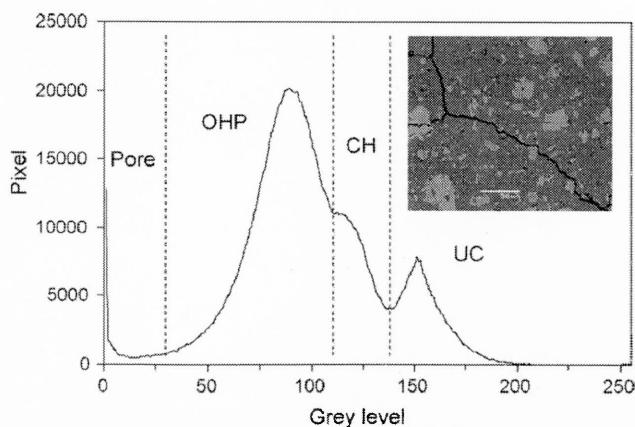

Fig. 1. BSE image of Control sample at day 7 and its grey level histogram obtained with the Image-Pro Plus 5.0 software (UC: unhydrated cement grains, OHP: other hydration products).
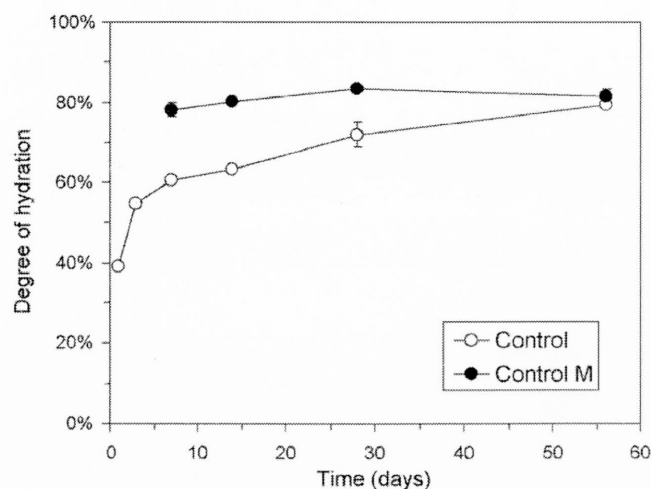

Fig. 2. Effect of 1% Pb + 1% Zn addition on cement hydration rate. Error bars correspond to the standard deviations over three measurements.
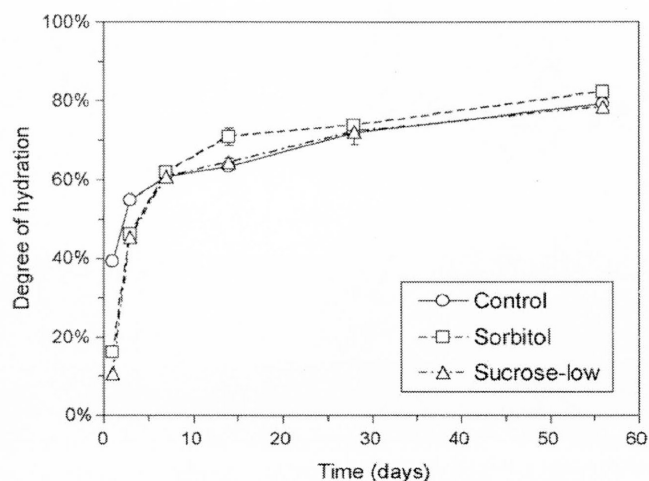
Fig. 3. Effect of sorbitol or sucrose addition on cement hydration rate.

Fig. 4. Effect of sorbitol or sucrose addition on cement hydration rate in samples containing 1% Pb + 1% Zn.

By contrast, previous studies of cement hydration in the presence of lead and zinc found that both metals retarded cement hydration. These studies, however, are not directly comparable to the present one because they were carried out with much larger metal concentrations [28,29] or were limited to early curing times of less than 17 h [30]. The retardation effect of Pb at early times has been explained by the rapid precipitation of colloidal lead hydroxide, sulfate, or hydroxysulfate as a protective membrane around unhydrated cement particles [29,30]. At high concentrations, Zn may precipitate as low permeability $CaZn_2(OH)_6 \cdot H_2O$ around unhydrated calcium silicate particles [28].

Fig. 3 reveals that, unlike added metal ions, sucrose and sorbitol did not radically alter the two-stage reaction profile that characterizes the hydration of pure Portland cement. However, the onset of stage-1 hydration was delayed by about 2 days in cements containing 0.15 wt% sucrose (Sucrose-low) or 0.40 wt% sorbitol (Sorbitol). Also, the sorbitol-containing mixture was slightly more hydrated after 7 days than either of the other two. The mechanisms by which certain sugars and sugar derivatives retard the hydration of cement are not fully understood. In the "half-salt" theory proposed by Thomas and Birchall [8,12], calcium ions react with sucrose in alkaline solution to form a soluble sucrose–calcium salt complex $Ca(OH)^+ \cdots R_{suc}^-$ (pK_{a1} of sucrose = 12.6). The pendant $Ca(OH)^+$ group in the half-salt is thought to adsorb onto growing calcium hydroxide (CH) nuclei and thus inhibit further precipitation of calcium and hydroxide ions on the poisoned surface. The precipitation of CSH gel, which relies on the deposition of silica on an existing CH lattice, is thought to be similarly inhibited by poisoning of the CH surface. Although published evidence supporting the existence of aqueous calcium-sucrose complexes is limited, Pannetier et al. [31] report formation of stable $Ca(OH)R_{suc}$ species in dilute alkaline solution and polymeric $[Ca(OH)R_{suc}]_n$ as the concentrations are increased. By contrast, no specific retardation mechanism has been proposed for sorbitol which, at best, interacts weakly with calcium ions ($pK_{a1} = 13.6$) [32]. Unlike sucrose, however, sorbitol is able to form $[HOSi(R_{sor})_2]^-$ and $[Si(R_{sor})_3]^{2-}$ complexes with aqueous silicon in high pH sur-

roundings [14]. These anionic complexes may play a role in delaying the hydration of cement (possibly through $Ca(OH)^+$ association) and contribute to the enhancement observed in the strength and final degree of hydration of cement mixtures containing sorbitol by crosslinking in the solid cement matrix.

When added together with the metal ions, sucrose and sorbitol countered the accelerating influence of Pb and Zn on cement hydration, as demonstrated in Fig. 4. Surprisingly, they were more effective at inhibiting hydration for the cement containing Pb and Zn than for pure cement. Addition of 0.15 wt% sucrose (Sucrose-low M) or 0.40 wt% sorbitol (Sorbitol M) limited the degree of hydration to 35% for at least 7 or 28 days, respectively. Thereafter, the reaction quickly went to completion (80% degree of hydration), that is, without going through stage-2 hydration. Addition of 0.38 wt% sucrose (Sucrose-high M) maintained hydration at 35–40% through the entire 56 day experiment.

3.2. Grey level analyses

Grey level analyses were carried out on Control and Control M samples at 7 days. The percentage of unhydrated cement was lower in the Control M sample ($10.2 \pm 1.9\%$) than in the Control sample ($15.1 \pm 2.6\%$) at a confidence level of 99.997% (Student t-test). The degrees of hydration calculated from grey level analysis using Eq. (2) ($\alpha_{GL} = 65.9 \pm 5.9\%$ for the Control sample and $77.0 \pm 4.3\%$ for the Control M sample) are consistent with those independently calculated by loss on ignition using Eq. (1) ($\alpha_{LI} = 60.7 \pm 0.7\%$ for the Control sample and $78.1 \pm 1.7\%$ for the Control M sample, see Fig. 2). Hence, both methods of measuring degree of hydration show that the presence of 1% Pb and 1% Zn improves hydration at 7 days. By contrast, grey level analyses reported by Ouki and Hills [26] found that the addition of 1% Pb or 1% Zn *decreased* hydration of Portland cement at 29 days by 29% and 11%, respectively.

Table 2
Summary of sample setting status and main hydration products found by SEM-EDS[a]

Sample	Day 1	Day 7	Day 28	Day 56
Control	CH, CSH	CH, CSH	na	CH, CSH
Control M	na	CH, CSH, ettringite[b]	CH, CSH, ettringite[b]	CH, CSH, ettringite[b]
Sorbitol	CH	CH, CSH	na	CH, CSH
Sucrose-low	CH	CH, CSH	na	CH, CSH
Sorbitol M	na	ettringite, CH[b], CSH[b]	ettringite, CH, CSH	ettringite, CH, CSH
Sucrose-low M	na	ettringite, CSH[b]	ettringite, CH, CSH	ettringite, CH, CSH
Sucrose-high M	na	ettringite	ettringite, CH	ettringite, CH, CSH

[a] Shading indicates that the cement was not set. Light shading indicates that the cement was partially set. No shading indicates that the cement was set. CH: calcium hydroxide; CSH: calcium silicate hydrate; na: not analyzed.
[b] Only a small amount of this phase was detected.

3.3. Strength tests

Table 2 indicates the setting status (unset, set, or partially set) of all the samples at various stages of curing. Several of the samples (e.g., samples containing both metals and sorbitol at day 1 and day 7) were poorly solidified and friable when removed from the molds, exhibiting less than 400 psi (2.76 MPa) compressive strength and under 35% degree of hydration. Hence, they were deemed to be unset. By contrast, cement was considered to be set when compressive strength exceeded 2000 psi (13.8 MPa) and the degree of hydration was over 45%. Two samples (Sorbitol M at day 28 and Sucrose-high M at day 56) were deemed to be only partly set. They consisted of millimetre-sized pebbles of cured cement within a poorly consolidated matrix, while exhibiting less than 400 psi compressive strength and 35–45% hydration.
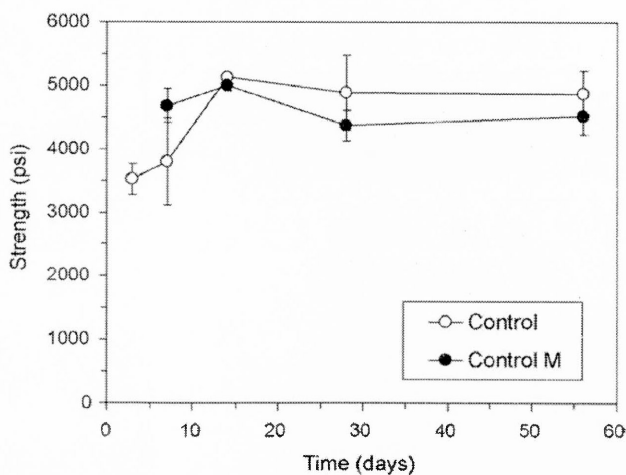

Fig. 5. Effect of 1% Pb and 1% Zn addition on cement strength. Error bars correspond to the standard deviations over three measurements.
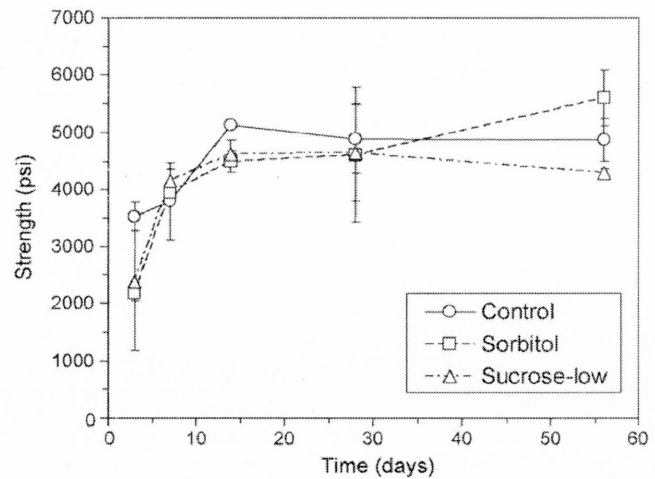

Fig. 6. Effect of sorbitol or sucrose addition on the development of cement strength.

Comparison between Figs. 5–7 and Figs. 2–4 reveals that evolution of compressive strength correlates closely with that of the degree of hydration.

Pure cement (Control) reached a maximum strength of ca. 5000 psi (34.5 MPa) after 14 days (Fig. 5). The addition of 1% Pb and 1% Zn (Control M) resulted in higher strength at day 7 compared to pure cement (86% confidence, based on Student t-test). This result reflects the higher degree of hydration for the Control M sample compared with the Control sample at day 7, and is also in accordance with the findings of Tashiro et al. [33] who reported increased strength for cement containing between 0.5% and 5% $PbO \cdot Pb(OH)_2$ or 0.5% $Zn(OH)_2$ at 3 days and 28 days. In the present study, however, there was statistically no difference between the strengths observed for pure and metal-containing cement from day 14 onwards.

The effect of low sucrose and sorbitol addition on the compressive strength of metal-free cement is shown in Fig. 6. Strength was reduced at day 3 for samples containing 0.15 wt% sucrose or 0.40 wt% sorbitol, but caught up with that of pure cement by day 7. At day 56, the sample containing sorbitol was slightly stronger (81% confidence level), which confirms previ-
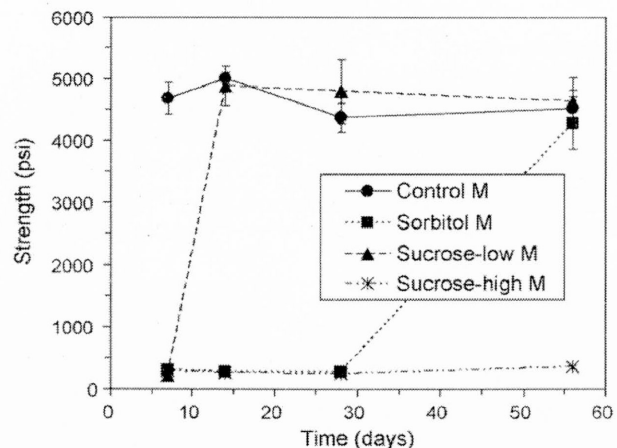

Fig. 7. Effect of sorbitol or sucrose addition on strength of samples containing 1% Pb + 1% Zn.

6   *L. Zhang et al. / Journal of Hazardous Materials xxx (2007) xxx–xxx*
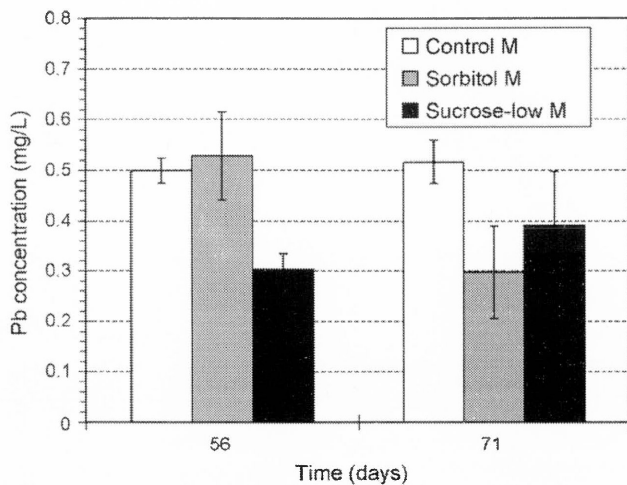

Fig. 8. Dissolved concentration of Pb in TCLP extracts. Error bars correspond to the standard deviations over three measurements.
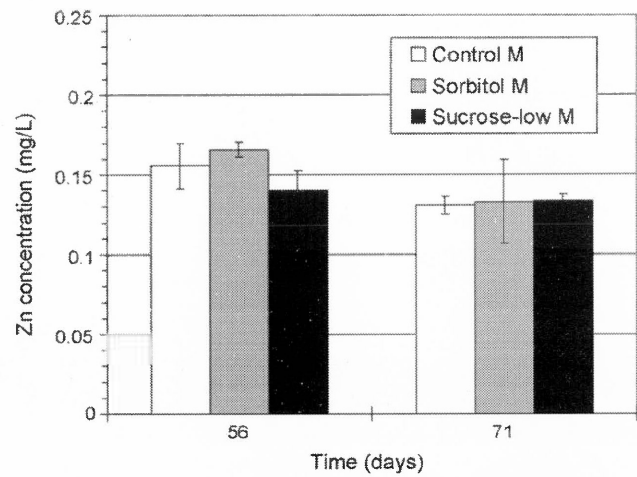

Fig. 9. Dissolved concentration of Zn in TCLP extracts.

ous reports that sorbitol improves the strength of OPC after 28 days [16]. These results parallel the influence that sucrose and sorbitol had on the degree of hydration (Fig. 3).

Similarly, the influence of added sucrose or sorbitol on the strength of cement containing Pb and Zn (Fig. 7) parallels their effect on the hydration of these samples (Fig. 4). The addition of 0.15 wt% sucrose (Sucrose-low M) or 0.4 wt% sorbitol (Sorbitol M) delayed cement setting for at least 7 and 28 days, respectively, with the strength of these samples rising to that of Control M immediately thereafter. These findings have practical importance because they demonstrate that controlled addition of sucrose or sorbitol can delay the setting of S/S-treated metal waste for several days, thus adding flexibility for transportation to the final disposal site without negatively impacting the final product strength. However, excessive sucrose addition (Sucrose-high M; 0.38 wt%) delays setting beyond 56 days with unknown effects on final strength.

3.4. Leaching tests

Fig. 8 shows the average concentrations and standard deviations of dissolved Pb in the TCLP extracts at day 56 and day 71 for the Control M, Sucrose-low M, and Sorbitol M samples, all of which were fully set by this time. The leachability of Pb from the cement containing sorbitol decreased between the two curing periods, but remained constant within experimental uncertainty for the other samples. On day 71, the average leachability of Pb for the control sample was 0.52 ± 0.04 mg/L. Sucrose or sorbitol addition significantly inhibited lead leachability, the final values being 0.30 ± 0.09 mg/L for 0.40 wt% sorbitol (leaching inhibited with 96% confidence) and 0.39 ± 0.11 mg/L for 0.15% sucrose (84% confidence). It is worth noting that differences in leachability were not caused by pH variations in the TCLP extracts; the final extract pH after 18 h agitation was 12.4 for all the samples.

Fig. 9 shows the concentration of Zn in the TCLP extracts. Between 56 and 71 days, the zinc leachability decreased for the control and sorbitol-containing samples (93% and 84% con-

fidence, respectively) but did not significantly change for the sample containing sucrose. Unlike the results obtained for lead, the addition of sucrose or sorbitol to cement had no significant effect on Zn leachability by day 71.

3.5. Microstructure analyses

Table 2 lists the hydration products identified in each cement sample at different curing times and indicates whether or not the samples were set.

In agreement with previous studies [24], calcium hydroxide and CSH were the main hydration products of pure Portland cement (Control). Cement containing 1% Pb and 1% Zn (Control M) had the same microstructure as metal-free cement (Fig. 10). Shells of smooth-textured CSH surrounded unhydrated cement grains (C_3S primarily), while irregularly textured CSH occupied much of the void space that was originally filled with water. These two different CSH phases respectively correspond to what Diamond [34] terms "inner" and "outer" CSH.
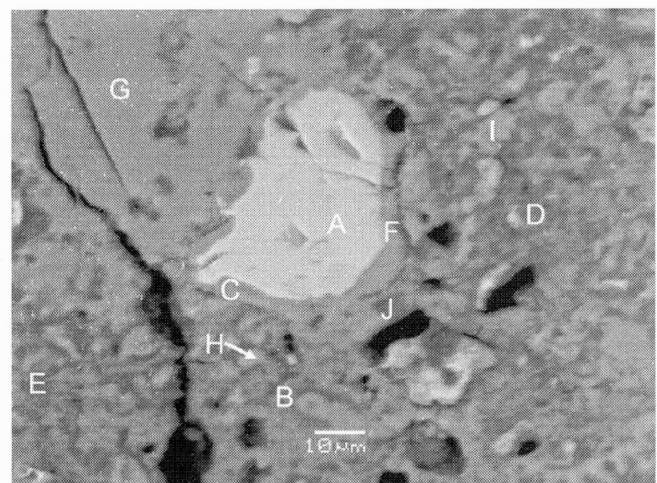

Fig. 10. Backscattered electron images of Control M sample (1% Pb + 1% Zn) at day 56 showing (A) C_3S, (C and F) inner CSH, (B, D, and E) outer CSH, (G, H and I) CH, and (J) ettringite.
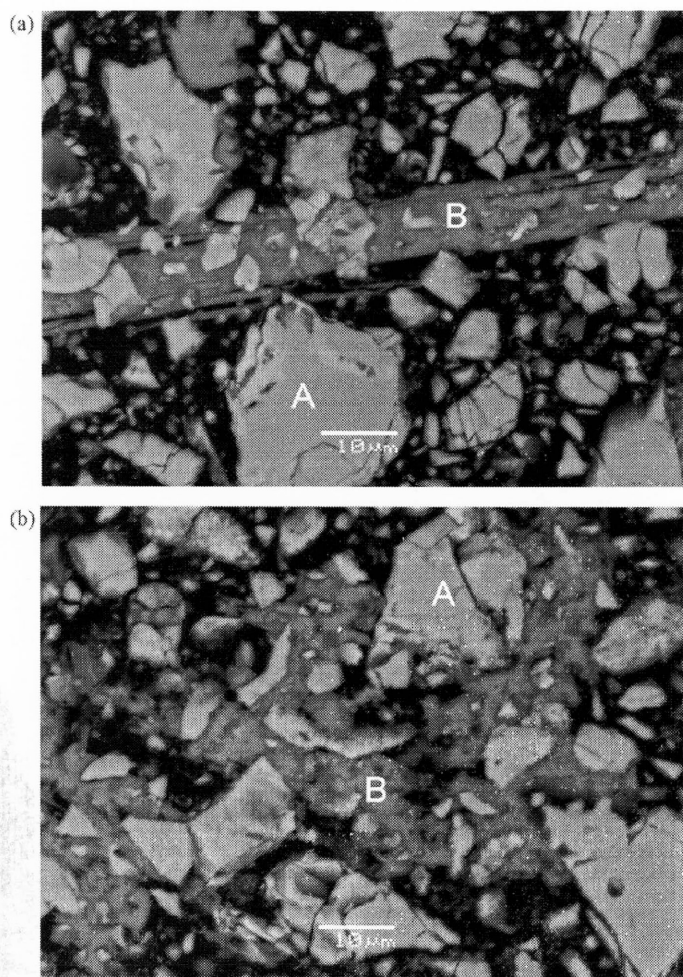
Fig. 11. Backscattered electron images of (a) Sucrose-low and (b) Sorbitol samples at day 1 showing the (A) unhydrated C_3S phase and (B) CH.

Small amounts of the Ca–Al-hydroxysulfate phases ettringite and monosulfate were disseminated throughout the sample and also might have been intermixed within the CSH as is suggested by the small amounts of Al and S detected in that phase (typically less than 2 atom%). Taylor [35] reports that Ca–Al-hydroxysulfate can intermix with CSH at the micrometer to single-layer scale which is too small to be resolved by SEM-EDS. Lead and zinc were mostly present in CSH at concentrations between 0.9 and 1.8 wt%. Ettringite and calcium hydroxide have much lower Pb and Zn concentrations (typically less than 0.8 wt%).

The addition of sorbitol or sucrose to metal-free cement delayed CSH formation. At day 1, CH was the only hydration product detected in the Sucrose-low and Sorbitol samples (Fig. 11). From day 7 onwards, however, these samples contained both CSH and CH.

When sucrose or sorbitol was added to cement in combination with Pb and Zn (Sucrose-low M, Sucrose-high M, Sorbitol M), the first hydration phase to appear consisted of platy Al-rich crystals (with cracks that were probably caused by drying; Figs. 12a–c). It was identified by X-ray diffractometry as ettringite, $Ca_6Al_2(SO_4)_3(OH)_{12} \cdot 26H_2O$ (Fig. 13). However, the average elemental composition deter-
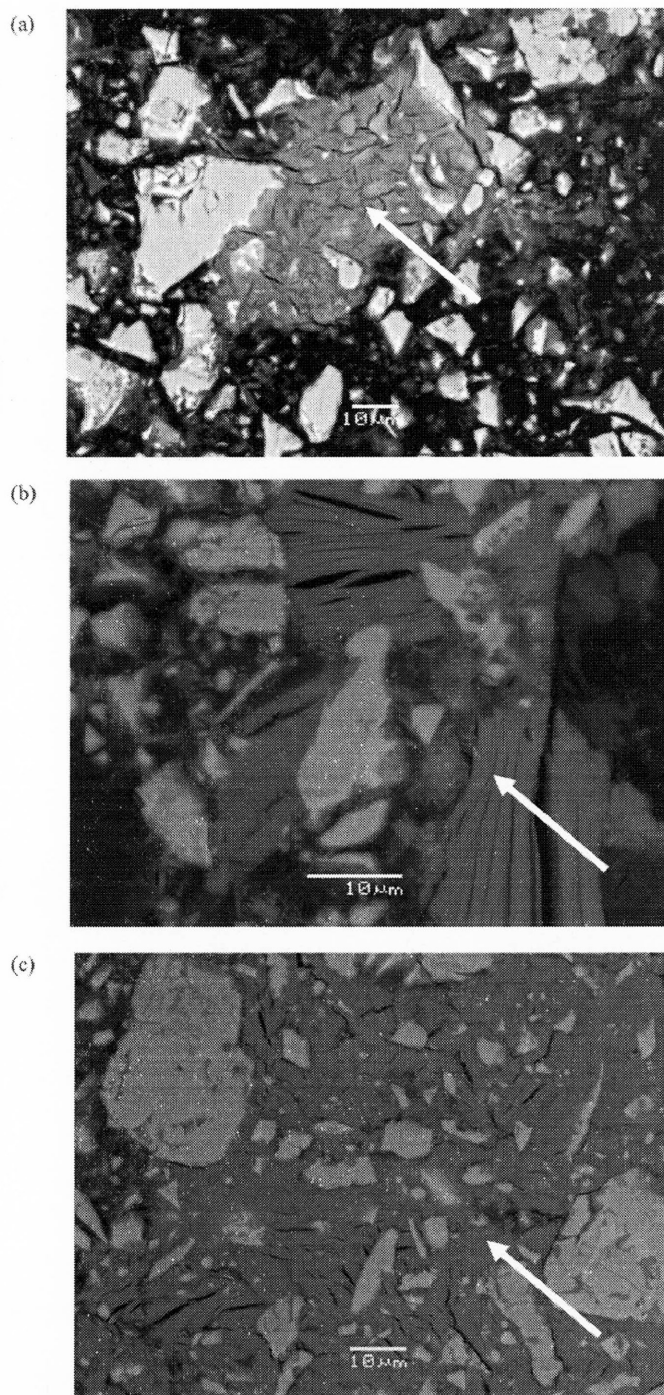

Fig. 12. Backscattered electron images of (a) Sorbitol M, (b) Sucrose-low M and (c) Sucrose-high M at day 7. The Al-rich phase is indicated by arrows. Bright areas are unhydrated cement consisting mainly of C_3S. None of these samples were set by day 7.

mined by more than 50 independent EDS measurements – $Ca_{6.00}Al_{2.41}S_{0.45}O_{18.42}Fe_{0.11}Si_{0.57}Pb_{0.06}Zn_{0.11}$– indicates a much lower S/Ca ratio than that of ettringite. Therefore, it is likely that ettringite was intermixed with unhydrated C_3A, which would account for the low sulfur content. The presence of Fe, Si, Pb and Zn indicates that the ettringite contains impurities. As mentioned already, ettringite was also found in the absence of sucrose and sorbitol (Control M), but in
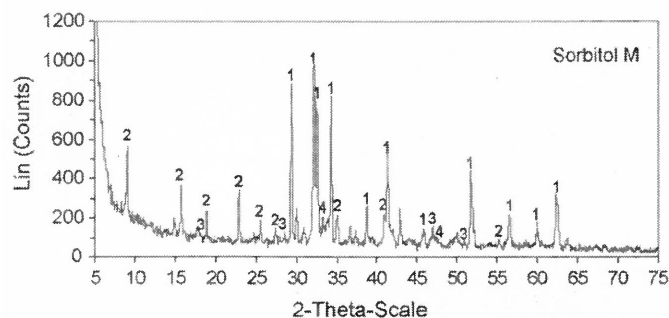
8   L. Zhang et al. / Journal of Hazardous Materials xxx (2007) xxx–xxx

Fig. 13. X-ray diffractogram of the Sorbitol M sample at day 7, showing (1) C_3S or C_2S, (2) ettringite, (3) portlandite (CH), and (4) C_3A.
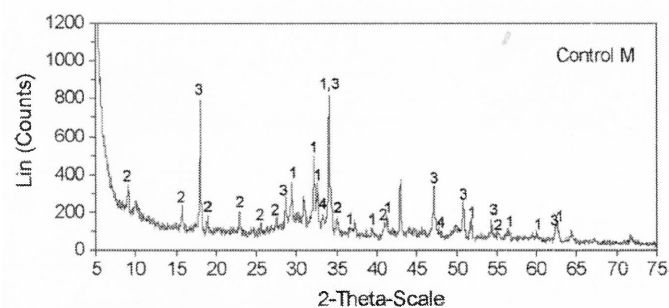

Fig. 14. X-ray diffractogram of the Control M sample at day 7, showing (1) C_3S or C_2S, (2) ettringite, (3) portlandite (CH), and (4) C_3A.

much smaller amounts and coexisting with CH and CSH (Figs. 10 and 14).

As the samples containing metal and sucrose or sorbitol began to set, the amounts of calcium hydroxide and CSH increased (Table 2). Fig. 15 shows a backscattered electron image of the Sucrose-high M sample at day 56, by which time partial setting had occurred. The image depicts ettringite coexisting with CSH (characterized by Ca/Si = 2.5–3.0:1) and a transition product which contains a significant concentration of Al (Ca/Al = 3–5:1) and a lower Si concentration than CSH (Ca/Si = 3–8:1).

The elemental composition at several points within the ettringite, CSH and transition product was measured by EDS on
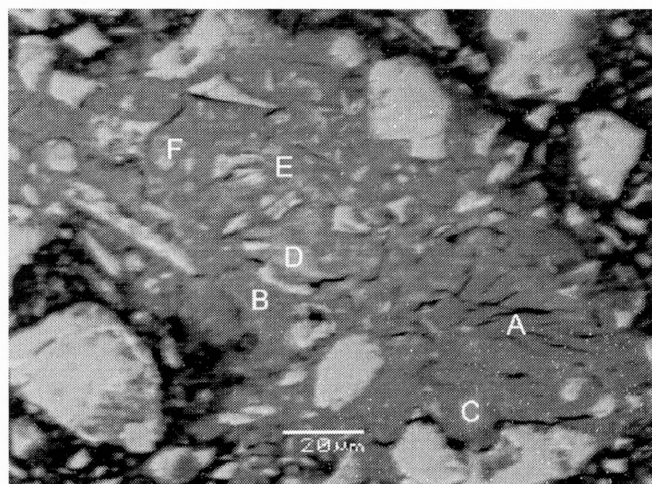

Fig. 15. Backscattered electron image of the Sucrose-high M sample at day 56, showing (A and B) ettringite, (C and D) CSH, and (E and F) transitional product.
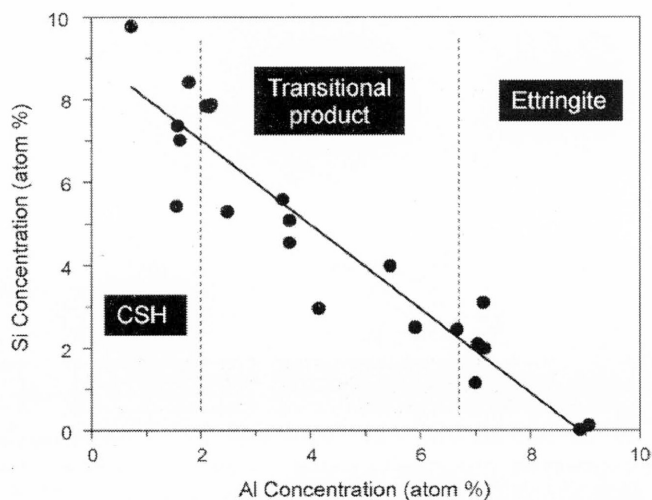

Fig. 16. Concentration of Si as a function of Al concentration in the Sucrose-high M sample at day 56.

several backscattered electron images of the Sucrose-high M sample at day 56 and plotted in Figs. 16 and 17. Three regions corresponding to CSH (low Al content), ettringite (high Al content) and the transitional product (intermediate Al content) are superimposed on the graphs. Similar results were obtained for the Sorbitol M sample (data not shown). The Si concentration increases almost linearly as the Al concentration decreases (Fig. 16), representing the transition from ettringite to CSH. Fig. 17 indicates that Pb and Zn concentrations vary widely, from 1 to 6 wt%, in CSH (corresponding to low Al concentration). By contrast, the range of Pb and Zn concentrations is relatively limited, less than 2 wt%, in ettringite. The larger capacity of CSH for immobilizing Pb and Zn is likely explained by structural differences: ettringite forms hexagonal prismatic or acicular crystals in which ion substitutions are the only significant immobilization mechanism [3], whereas CSH is an amorphous gel which allows Pb and Zn atoms to be immobilized through a variety of mechanisms such as sorption, coprecipitation, and formation of metallosilicates [3–7].
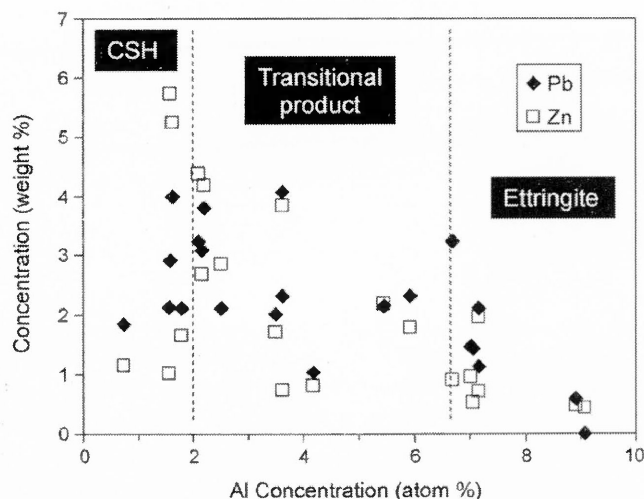

Fig. 17. Concentrations of Pb and Zn as a function of Al concentration in the Sucrose-high M sample at day 56.

4. Conclusions

1. The presence of 1 wt% Pb and 1 wt% Zn significantly shortens the time at which maximum hydration of Portland cement is achieved, but has relatively little effect on the final compressive strength.
2. The addition of 0.15 wt% sucrose or 0.40 wt% sorbitol to metal-free Portland cement retards hydration and strength development for 3 to 7 days.
3. The retardation effect of sucrose and sorbitol are considerably enhanced when Pb and Zn are present. Controlled sucrose or sorbitol addition to metal-cement mixtures can retard setting for up to 28 days without affecting the 56-day strength, thus adding flexibility to the handling of S/S-treated waste.
4. The long-term TCLP-based leachability of Pb may be somewhat reduced by the addition of sucrose or sorbitol; however, the long-term leachability of Zn is not significantly affected.
5. Cement setting correlates with the precipitation of CSH gel. Precipitation of ettringite was favored and the formation of CSH and CH were delayed when sorbitol or sucrose was added to metal-cement mixtures.
6. The ability of ettringite to immobilize Pb and Zn is inferior to that of CSH.
7. Sorbitol conferred a slightly higher degree of hydration and compressive strength than sucrose to Portland cement after 56 days.

Acknowledgement

References

[1] J.R. Conner, S.L. Hoeffner, A critical review of stabilization/solidification technology, Environ. Sci. Technol. 28 (1998) 397–462.
[2] S. Mindess, J.F. Young, Concrete, Prentice-Hall, Inc, Englewood Cliffs, NJ, 1981.
[3] M.L.D. Gougar, B.E. Scheetz, D.M. Roy, Ettringite and C-S-H Portland cement phases for waste ion immobilization: a review, Waste Manage. 16 (1996) 295–303.
[4] F.K. Cartledge, L.G. Butler, Devi Chaiasani, H.C. Eaton, F.P. Frey, Esteban Herrera, M.E. Tittlebaum, S.-L. Yang, Immobilization mechanisms in solidification/stabilization of Cd and Pb salts using Portland cement fixing agents, Environ. Sci. Technol. 24 (1990) 867–873.
[5] F. Ziegler, R. Giere, C.A. Johnson, Sorption mechanisms of zinc to calcium silicate hydrate: sorption and microscopic investigations, Environ. Sci. Technol. 35 (2001) 4556–4561.
[6] I. Moulin, W.E.E. Stone, J. Sanz, J.-Y. Bottero, F. Mosnier, C. Haehnel, Lead and zinc retention during hydration of tri-calcium silicate: a study by sorption isotherms and ^{29}Si nuclear magnetic resonance spectroscopy, Langmuir 15 (1999) 2829–2835.
[7] F. Ziegler, A.M. Scheidegger, C.A. Johnson, R. Dahn, E. Wieland, Sorption mechanisms of zinc to calcium silicate hydrate: X-ray absorption fine structure (XAFS) investigation, Environ. Sci. Technol. 35 (2001) 1550–1555.
[8] J.D. Birchall, N.L. Thomas, The mechanism of retardation of setting of OPC by sugars, Br. Ceram. Proc. 35 (1984) 305–315.
[9] J.F. Young, A review of the mechanisms of set-retardation in Portland cement pastes containing organic admixtures, Cem. Concr. Res. 2 (1972) 415–433.
[10] P.F.G. Banfill, D.C. Saunders, The relationship between the sorption of organic compounds on cement and the retardation of hydration, Cem. Concr. Res. 16 (1986) 399–410.
[11] V.S. Ramachandran, M.S. Lowery, Conduction calorimetric investigation of the effect of retarders on the hydration of Portland cement, Thermochim. Acta 195 (1992) 373–387.
[12] N.L. Thomas, J.D. Birchall, The retardation action of sugars on cement hydration, Cem. Concr. Res. 13 (1983) 830–842.
[13] K. Luke, G. Luke, Effect of sucrose on retardation of Portland cement, Adv. Cem. Res. 12 (2000) 9–18.
[14] S.D. Kinrade, J.W. Del Nin, A.S. Schach, T.A. Sloan, K.L. Wilson, C.T.G. Knight, Stable five- and six-coordinated silicate anions in aqueous solution, Science 285 (1999) 1542–1545.
[15] M.C.G. Juenger, H.M. Jennings, New insights into the effects of sugar on the hydration and microstructure of cement pastes, Cem. Concr. Res. 32 (2002) 393–399.
[16] Patent: Use of particular polysaccharides as admixtures for mineral materials, http://www.freshpatents.com/Use-of-particular-polysaccharides-as-admixtures-for-mineral-materials-dt20060316ptan20060054062.php?type=description (accessed January 2007).
[17] http://en.wikipedia.org/wiki/Plasticizer (accessed January 2007).
[18] http://www.epa.gov/waterscience/criteria/wqcriteria.html#priority (accessed January 2007).
[19] Standard practice for capping cylindrical concrete specimens, ASTM C617-98 (2003).
[20] Standard test method for compressive strength of hydraulic cement mortars (using 2-in. or [50-mm] cube specimens), ASTM C109/C109M-98 (1998).
[21] M.C.G. Juenger, H.M. Jennings, Examining the relationship between the microstructure of calcium silicate hydrate and drying shrinkage of cement pastes, Cem. Concr. Res. 32 (2002) 289–296.
[22] Toxicity Characteristic Leaching Procedure, http://www.epa.gov/sw-846/pdfs/1311.pdf (accessed January 2007).
[23] K.O. Kjellsen, R.J. Detwiler, O.E. Gjørv, Backscattered electron image analysis of cement paste specimens: specimen preparation and analytical methods, Cem. Concr. Res. 21 (1991) 388–390.
[24] K.L. Scrivener, Backscattered electron imaging of cementitious microstructures: understanding and quantification, Cem. Concr. Composites 26 (2004) 935–945.
[25] K.L. Scrivener, Analysis of phases in cement paste using backscattered electron images, methanol adsorption and thermogravimetric analysis, Mater. Res. Soc. Symp. Proc. 85 (1987) 67–76.
[26] S.K. Ouki, C.D. Hills, Microstructure of Portland cement pastes containing metal nitrate salts, Waste Manage. 22 (2002) 147–151.
[27] S. Igarashi, M. Kawamura, A. Watanabe, Analysis of cement pastes and mortars by a combination of backscattered-based SEM image analysis and calculation based on the Powers model, Cem. Concr. Composites 26 (2004) 977–985.
[28] S. Asavapisit, G. Fowler, C.R. Cheeseman, Solution chemistry during cement hydration in the presence of metal hydroxide wastes, Cem. Concr. Res. 27 (1997) 1249–1260.
[29] J.D. Ortego, S. Jackson, G.-S. Yu, H. McWhinney, D.L. Cocke, Solidification of hazardous substances—a TGA and FTIR study of Portland cement containing metal nitrates, J. Environ. Sci. Health A 24 (6) (1989) 589–602.
[30] N.L. Thomas, D.A. Jameson, D.D. Double, The effect of lead nitrate on the early hydration of Portland cement, Cem. Concr. Res. 11 (1981) 143–153.
[31] N. Pannetier, A. Khoukh, J. François, Physico-chemical study of sucrose and calcium ions interactions in alkaline aqueous solutions, Macromol. Symp. 166 (2001) 203–208.
[32] J.K. Beattie, M.T. Kelso, Equilibrium and dynamics of the binding of calcium ion to sorbitol (D-glucitol), Aust. J. Chem. 34 (1981) 2563–2568.
[33] C. Tashiro, H. Takahashi, M. Kanaya, I. Hirakida, R. Yoshida, Hardening property of cement mortar adding heavy metal compound and solubility of heavy metal from hardened mortar, Cem. Concr. Res. 7 (1977) 283–290.
[34] S. Diamond, The microstructure of cement paste and concrete a visual primer, Cem. Concr. Composites 26 (2004) 919–933.
[35] H.F.W. Taylor, Nanostructure of C-S-H: current status, Adv. Cem. Based Mater. 1 (1993) 38–46.